UNIVERSITY OF MÁLAGA
FACULTY OF SCIENCES
Department of Organic Chemistry

Tripodal *p*-phenylene molecules: synthesis and immobilization on gold and silicon surfaces

Moléculas tripodales de *p*-fenileno: síntesis e inmovilización sobre superficies de oro y silicio

Memoria para optar al grado de **Doctor en Química** con Mención Internacional por la Universidad de Málaga presentada por

María Sánchez Molina

Málaga, 2019

AUTOR: María Sánchez Molina

http://orcid.org/0000-0003-0073-1375

EDITA: Publicaciones y Divulgación Científica. Universidad de Málaga

D. JUAN MANUEL LÓPEZ ROMERO, CATEDRÁTICO DE QUÍMICA ORGÁNICA Y Dª. AMELIA DÍAZ MORILLA, PROFESORA TITULAR DE QUÍMICA ORGÁNICA DE LA FACULTAD DE CIENCIAS DE LA UNIVERSIDAD DE MÁLAGA

CERTIFICAN:

Que la memoria adjunta, titulada "TRIPODAL *P*-PHENYLENE MOLECULES: SYNTHESIS AND IMMOBILIZATION ON GOLD AND SILICON SURFACES", que para optar al grado de Doctor en Química (Mención Internacional) presenta Dª. María Sánchez Molina, ha sido realizada bajo nuestra dirección en los laboratorios del Departamento de Química Orgánica de la Universidad de Málaga.

Considerando que constituye trabajo de Tesis Doctoral, autorizamos su presentación en la Facultad de Ciencias de la Universidad de Málaga.

Y para que así conste, firmamos el presente certificado en Málaga a 30 de Enero de 2019.

Fdo: J. Manuel López Romero Fdo: A. Díaz

AGRADECIMIENTOS

A lo largo de todos estos años, muchas han sido las personas que queriéndolo o no han aportado su granito de arena para que esta Tesis pudiera hacerse realidad. Espero no dejarme a nadie atrás, la lista es extensa ☺

En primer lugar, a mis directores de Tesis, Juan Manuel López y Amelia Díaz:

Manolo, agradecerte la dedicación en este proyecto de tesis, la confianza depositada en mí, enseñarme a ser prácticos en la ciencia y encontrar siempre una aplicabilidad a lo que se hace, para darle sentido a la investigación. Gracias por tu apoyo y comprensión. Amelia, gracias por confiar y apostar por mi desde el principio. Me has enseñado a ser metódica y bien organizada. Agradecerte, además tu apoyo y cariño en los momentos buenos y no tan buenos, compartidos a lo largo de estos años.

A María Valpuesta, quien fue mi directora del Trabajo Fin de Master y prácticamente co-directora de esta tesis. Gracias a ti he aprendido valores como la disciplina, el tesón y el amor por la ciencia. Gracias también por tus sabios consejos y tu cariño.

A los profesores del Departamento de Química Orgánica, en especial a Marisol, Francis, y Gregorio. A mis compañeros del Departamento, tanto los del pasado (Carmen, Manuela, Rafa), como los del presente (Rafa C., Iván, Carlos, Cris y Alicia). Muy especialmente a mi amigo y compañero Jesús, del cual he heredado estos trípodes que aquí presento. Quiero agradecerte todos tus consejos, nuestros paseos y nuestras confesiones. A mis gemelas Ana y Cristina, vosotras sois las que más habéis disfrutado y sufrido conmigo el día a día de esta Tesis. Gracias por vuestros consejos dentro y fuera del lab, por vuestro cariño y disposición incondicional y ¡cómo olvidarlo!, nuestras merienditas en plena faena -esos breaks en la tarde eran muy necesarios-.

A Inma, Nuri y Mónica, por poner un punto diferente en la vida académica y enseñarme que la humildad y el respeto son más importantes que cualquier otro valor jerárquico. Inma, gracias por tu amistad y por poner un puntito de realidad en el día a día.

Al Prof. Michael Zharnikov y a mis compañeros Eric, Tobi, Can y Mustafa, por hacer posible mi estancia de seis meses en sus laboratorios de Heidelberg, Alemania. Gracias por enseñarme a conocer el otro lado de mi Tesis, la Química en superficie.

No puedo olvidarme de mis compañeros de la Licenciatura: María, Elena, Marta, Pedro y David, con los que he dedicado tantas horas a la Química (y a lo que no es la Química…). Tampoco dejo atrás a mi familia escogida, el “Malaguitaun”, un pilar fundamental en mi vida. En este apartado quiero agradecerles a las supernenas, Sandrita y Lucía, que hayan creído en mí de la forma en que lo han hecho. Gracias por vuestros consejos, por los audios infinitos y las risas maravillosas.

Por último, a mi familia en general, y en particular a mi tía Miss y mi tío Varo, a Sissi y Arturo. Especialmente a mi cuñi, gracias por tu cariño, tu calma en los momentos más necesarios, tu generosidad y tus buenos consejos, los llevo en mi corazón.

A mi hermana, Almudena. Somos el Yin y el Yang, tan opuestas y a la vez tan complementarias. Gracias por enseñarme a ver la vida desde tu punto de vista ;), por escucharme, aconsejarme en las dudas más fundamentales y quererme a tu manera.

A mi madre, el ejemplo de lucha más bonito que existe. Gracias mamá por tanto, por enseñarme que el esfuerzo siempre es motivo de recompensa, porque tirar la toalla no te hace avanzar, por confiar en mí de una manera distinta al resto, como solo una madre sabe. Por tus sabias palabras y tu amor infinito, gracias a ti estoy donde estoy y soy lo que soy.

A mi padre, mi tierna debilidad. Gracias papá porque con tu carisma y simpatía nos enseñas a disfrutar de la vida de otra manera, a superar los miedos y las dificultades con una sonrisa y un “dimite tú”. El amor y entrega a tus hijas son, desde luego, de los mayores tesoros que alguien puede tener.

Finalmente, quiero agradecerle a mi compañero de vida, mi marido Armando. Gracias a ti entiendo la Ciencia y la Investigación desde otro punto de vista; muy sacrificada, pero a la vez apasionante. La finalización de esta Tesis no solo supone el resultado de tantos años de trabajo, para nosotros dos también significa el comienzo de la etapa más dulce e importante de nuestras vidas. Gracias por tu apoyo incondicional, tus tan necesarios consejos y tu infinito amor.

A la generación que fue, mis abuelas

Y a la que está por venir, mis hijas

Table of Contents

List of abbreviations

Å	angstrom
Ac	acetyl
AcO	acetate
AcOH	acetic acid
AFM	atomic force microscopy
AIBN	azobisisobutyronitrile
Aq	aqueous
AT	alkanethiolate
a.u.	arbitrary units
BE	binding energy
Boc	*tert*-butyloxycarbonyl
br	broad
BSA	bovine serum albumin
Bu	butyl
ºC	degrees Celsius
4CDNA	4-chloro-2,6-dinitroaniline
^{13}C NMR	carbon nuclear magnetic resonance
δ	NMR chemical shift in parts per million downfield from a standard
d	doublet
DFT	density functional theory
DHB	dihydroxybenzoic acid
DIAD	diisopropyl azodicarboxylate
DIPEA	diisopropyl ethyl amine
DMABI	2-(*N,N*-dimethylamino)benzyliden-1,3-indandione
DMAP	4-dimethylaminopyridine
DME	dimethoxyethane
DMF	*N,N*-dimethylformamide
DMS	dimethylsilyl
DMSO	dimethyl sulfoxide
EI	electron impact

eq. or equiv	equivalent
ESI	electrospray ionization
Et	ethyl
et al.	and others
etc	and so forth
eV	electronvolt
g	gram(s)
h	hour(s)
^{1}H NMR	proton nuclear magnetic resonance
Hz	hertz
J	coupling constant
L	litre
LD	limit of detection
m	multiplet, mili or meter
m-	meta
μ	micro
M	molar
MALDI-TOF	matrix-assisted laser desorption ionization time-of-flight
MHz	megahertz
min	minute(s)
mol	mole(s)
mp	melting point
MS	mass spectroscopy
m/z	mass-to-charge ratio
NBS	*N*-bromosuccinimide
n-BuLi	*n*-Butyllithium
n	nano
NEXAFS	near-edge x-ray absorption fine structure
NMR	nuclear magnetic resonance
o-	ortho
OEG	oligoethylene glycol
p-	para

PBS	phosphate buffered saline
PEG	poly-ethylene glycol
PMDTA	*N*,*N*,*N*′,*N*″,*N*″-pentamethyldiethylenetriamine
ppm	parts per million
pyr	pyridine
QY	Quantum yield
RSD	relative standard deviation
rt	room temperature
s	singlet
SA	streptavidin
SAM(s)	Self-assembled Monolayer(s)
t	triplet
TBAF	tetrabutylammonium fluoride
TBDMS	*tert*-butyldimethylsilyl
t-Bu	*tert*-butyl
t-BuLi	*tert*-Butyllithium
TEA	triethylamine
THF	tetrahydrofuran
TLC	thin layer cromatography
TMG	trimethylgermanyl
TMS	trimethylsilyl
TOA	takeoff angle
UV	ultraviolet
XPS	x-ray photoelectron spectroscopy

1. INTRODUCTION

Everything in our environment is formed by matter and energy, from basic materials which are used in our daily routine (clothes, tableware, cosmetics products), to more complex systems such as smartphones and computers. There is no doubt that we live in a technological age and it is fundamental for us to understand and control the development of new materials and its properties.

In this sense, the area of molecular materials and electronics has become a very important branch of condensed matter research. Although the field of molecular electronic is far from maturity, the variety of systems is enormous, and due to the synthetic capabilities of organic chemistry there is hardly any limitation on the creation of new materials. The main objective of molecular electronics is to use molecules as functional building blocks and integrate them in electric circuits by assembly of terminal anchoring groups, thus creating a strong binding between these groups and the metal electrode. Only by this way, the control over the electronic properties of single-molecule devices will become possible. In addition to the effect of the anchoring groups, an accurate measurement of the molecular conductance is crucial to fulfill requirements for molecular electronic devices.

The term self-assembly is now a very common term and in a general sense it is defined as the spontaneous formation of complex hierarchical structures from pre-designed building blocks. In a more concrete manner, self-assembled monolayers (SAMs) are ordered molecular assemblies that are formed spontaneously by the adsorption of a surfactant with a specific affinity of its anchoring groups (or headgroups) to a substrate. The main constituents of a SAM are shown in figure 1.1, which includes the headgroup, chain or backbone and the endgroup, also named tail group.

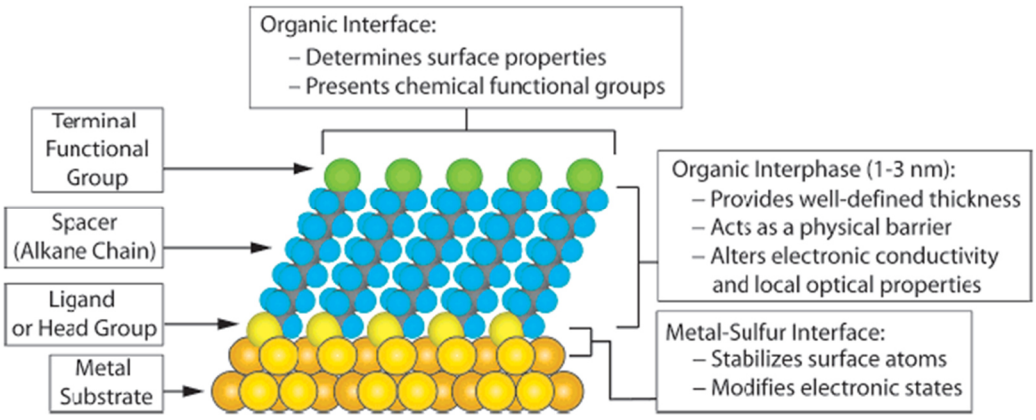

Figure 1.1 Schemtatic diagram of a typical SAM.

Popular examples of headgroups, from now and before, are thiols (R–SH, where R means the rest of the molecule) on Au(111)[1] or silane-based systems on SiO_2. [2] The discovery of SAMs, in particular the identification of the thiol/Au route, has valuably turned around the way of understanding the surface chemistry, opening a new area of study of well defined inorganic surfaces and organic species. Furthermore, the great flexibility of the SAM concept due to the wide variety of headgroups -which can be anchored to the substrate- has led to a large number of applications of SAMs in the area of biotechnology. These headgroups, are expected to provide well-defined and reproducible binding, a strong anchoring between the molecule and metal substrate, and should maintain an adecuate electron density,[3] (if the goal of the work is related to electronic devices).

During the last years the development of molecularly ordered surfaces to be applied in research fields as protein adsorption, clinical diagnostics or cellular adhesion, has been extensively reported.[4] A great number of approaches are currently investigated to generate ordered arrangements at the molecular level with the aim to replicate biochemical reactions on solid supports. Among a vast number of procedures for surface functionalization as electron-beam lithography,[5] assembly of supramolecular aggregates,[6] nanoparticles as templates,[7] or molecular modification of AFM tip for ligand-receptor AFM force spectroscopy,[8] the generation of SAMs has been widely employed for the fabrication of functionalized thin films on a wide range of surfaces. By this approach, the incorporation of active functional moieties can be easily performed at the molecular level in a controllable and reproducible way. Indeed, by this method it is possible to tune the space between grafted functional groups on surfaces, which offers the possibility to fabricate interfacial architectures in bio-devices with molecular precision for the interaction with cells or certain biomolecules in a highly specific manner.

[1] Nuzzo, R. G.; Allara, D. L. *J. Am. Chem. Soc.* **1983**, *105*, 4481.
[2] Sagiv, J. *J. Am. Chem. Soc.* **1980**, *102*, 92.
[3] Valasek, M.; Lindner, M.; Mayor, M. *Beilstein J. Nanotechnol*. **2016**, *7*, 374.
[4] a) Pertsin, A.J.; Grunze, M.; Kreuzer, H.J.; Wang, R.L.C. *Phys. Chem. Chem. Phys*. **2000,** *2*, 1729; b) Frommer, J.; Luthi, R.; Meyer, E.; Anselmetti, D.; Dreier, M.; Overney, R.; Guntherodt, H.J.; Fujihira, M. *Nature* **1993**, *364*, 198; c) Roberts, C.; Chen, C.S.; Mrksich, M.; Martichonok, V.; Ingber, D.E.; Whitesides, G.M. *J. Am. Chem. Soc*. **1998,** *120*, 6548; d) Sigal, G.B.; Bamdad, C.; Barberis, A.; Strominger, J.; Whitesides, G.M. *Anal. Chem.* **1996**, *68*, 490; e) López, G.P.; Albers, M.W.; Schreiber, S.L.; Carroll, R.; Peralta, E.; Whitesides, G.M. *J. Am. Chem. Soc.* **1993**, 115, 5877; (f) Pirrung, M.C. *Angew. Chem. Int. Ed*. **2002**, *41*, 1276; g) Wilson, D.S.; Nock, S. *Angew. Chem. Int. Ed*. **2003**, *42,* 494.
[5] Schmitt, S.W.; Schechtel, F.; Amkreutz, D.; Bashouti, M.; Srivastava, S.K.; Hoffmann, B.; Dieker, C.; Spiecker, E.; Rech, B.; Christiansen, S.H. *Nano Lett.* **2012**, *12,* 4050.
[6] Yokoyama, T.; Yokoyama, S.; Kamikado, T.; Okuno, Y.; Mashiko, S. *Nature*, **2001,** *413*, 619.
[7] Paraschiv, V.; Zapotoczny, S.; De Jong, M.R.; Vancso, G.J.; Huskens, J.; Reinhoudt, D.N. *Adv. Mater*. **2002**, *14*, 722.
[8] Drew, M.E.; Chworos, A.; Oroudjev, E.; Hansma, H.; Yamakoshi, Y. *Langmuir* **2010,** *26,* 7117.

The formation of SAMs redefines the properties of the substrates giving them new identity according to the specific terminal chemical groups (tail groups), so that the functionalized substrates can serve as advanced electrodes,[9] biosensors,[10] or components of electronics devices.[11] As we mentioned before, one of the most popular types of SAMs is based on the strong covalent bond between sulfur and gold, being therefore the most extensively used and investigated.[12] There are several advantages in using gold as the substrate since it possesses a variety of useful properties; gold forms a reasonable clean, inert and atomically flat surface, which makes it suitable for different studies and handling under ambient conditions before functionalization. This metal is not prone to impurities by reaction with oxygen and can be easily handled under ambient conditions before its surface functionalization with thiol-based compounds.

The adsorption mechanism that generates the covalent bond between sulfur and gold is still unknown, but it is considered that the hydrogen of the thiol group is removed in contact with gold and then, a covalent Au–S bond is formed.[12,13] This bond has a dissociation energy of around 2.1 eV (ca. 50 kcal·mol−1), which is large enough to ensure the thermal stability of thiol monolayers up to 80 °C, [14] and stronger than the Au-Au bond with a dissociation energy of around 0.8 eV.[15]

On the other hand, the second most popular type of SAM is the silane-based system,[16] which in terms of mechanisms is quite different from thiols on gold. The typical example presents as headgroup a trichlorosilane or similar, which is attached to a hydroxylated surface (e.g., silicon oxide) obtaining a strongly bound network of the headgroups, when the sidegroup is removed. This process of absorption differs substantially from the formation of sulfur-gold bond, and endows the new surface with strong sensitivity to temperature, pH, and water content in solution.[17]

The main differences with respect thiol-based SAMs is that Si-based SAMs present a lower defined structure, in a physical sense, and therefore a low mobility of the monolayer molecules on the surface. The latter is also due to the strong and localized

[9] Gooding, J.J.; Mearns, F.; Yang, W.; Liu, J. *Electroanalysis* **2003,** *15,* 81.
[10] Chaki, N.K.; Vijayamohanan, K. *Biosens. Bioelectron*. **2002**, *17*, 1.
[11] Tour, J.M. Molecular Electronics, World Scientific, Singapore, 2003.
[12] Love, J.C.; Estroff, L.A.; Kriebel, J.K.; Nuzzo, R.G.; Whitesides, G.M. *Chem. Rev*. **2005**, *105,* 1103.
[13] Kankate, L.; Turchanin, A.; Gölzhäuser, A. *Langmuir* **2009**, *25*, 10435.
[14] Delamarche, E.; Michel, B.; Kang, H.; Gerber, C. *Langmuir* **1994,** *10,* 4103.
[15] Huang, Z.; Chen, F.; Bennett, P. A.; Tao, N. *J. Am. Chem. Soc.* **2007,** *129,* 13225.
[16] Sagiv, J. *J. Am. Chem. Soc.* **1980**, *102*, 92.
[17] a) Schreiber, F. *Prog. Surf. Sci.* **2000,** *65*,151; b) Schwartz, D.K. *Annu. Rev. Phys. Chem.* **2001**, *52*,107.

binding of the Si-O-Si network, what makes it a more robust structure that can not be easily changed by annealing.

The Schwartz group[18] has deeply investigated the growth, the nucleation dynamics and the associated correlation functions, and features such as adsorption, diffusion, grafting, and cross-linking, have to be taken into consideration.[19] More recently a new methodology (alternative to the Si-O strategy) for the preparation of SAMs is based on the hydrosilylation of 1-alkenes on hydrogen-terminated silicon surfaces.[20] The new class of thin films produced well-ordered and densely packed monolayers that bind to the silicon substrates by strong Si-C bonds. This strategy have found applications in sensors, nonlinear optics, and opto-electronics.[21]

However, everything has its pros and cons and for many of these potential applications, it is desirable or necessary to control the orientation and density of the functional groups in the films. The principal drawbacks of any aliphatic monolayer are the inclined molecular plane that is formed with respect to the surface and the close spatial arrangement of the molecules that frequently appeares in systems that form densely packed SAMs. This usually promotes significant steric and/or electrostatic repulsions. Moreover, in the particular case of thiol-based SAMS, the intermolecular linking of bifunctional dithiols due to disulfide brigdes formation may cause multilayer formation. To overcome this problem the in situ formation of thiols from thioacetates with a deprotection agent can significantly reduce the risk of multilayer formation. [22]

Researchers have explored other ways to prevent these disadvantages being one of the most employed method the use of mixed SAMs. This SAMs are composed of two or more different molecules, where one has a longer alkyl chain than the others and carries the functional group. This strategy may be useful for molecules that form well-ordered and densely packed monolayers but nevertheless, it is not possible to avoid nonrandomized mixing on the nanoscale that prevents controlling the spacing between the functional groups on the surface.

[18] Schwartz, D.K. *Annu. Rev. Phys. Chem.* **2001**, *52*, 107.
[19] Bautista, R.; Hartmann, N.; Hasselbrink, E. *Langmuir* **2003**, *19*, 6590.
[20] Deng, X.; Cai, C. *Tetrahedron Letters*, **2003**, *44*, 815.
[21] a) Strother, T.; Cai, W.; Zhao, X. S.; Hamers, R. J.; Smith, L. M. *J. Am. Chem. Soc.* **2000**, *122*, 1205; b) Stewart, M. P.; Buriak, J. M. *Adv. Mater*. **2000**, *12*, 859; c) Lopinski, G. P.; Wayner, D. D. M.; Wolkow, R.A. *Nature* **2000**, *406*, 48.
[22] Azzam, W.; Wehner, B. I.; Fischer, R. A.; Terfort, A.; Wöll, C. *Langmuir* **2002,** *18,* 7766.

1.1 Multipodal molecules in SAM formation

For all the aboved mentioned, new protocols to create free volume around the functional molecules in the monolayers have been studied recently. In this sense, it is highly desirable to obtain an optimal spacing between the functional moieties that may be perpendicularly oriented on the film surface for maximizing the binding strength and density of target molecules.

To date, several architectures based on either bulk spacer molecules or large multipodal structures have been deeply investigated to provide functional molecular platforms to be used as templates for different applications ranging from tissue engineering,[23] medicine,[24] cell biology,[25] immunology[26] and marine biofouling.[27] The multipodal architecture not only provides control on the spatial arrangement of the molecules but also increases the binding stability on metal surfaces when compared to single molecules, since these molecules present multiple anchor groups (figure 1.2).

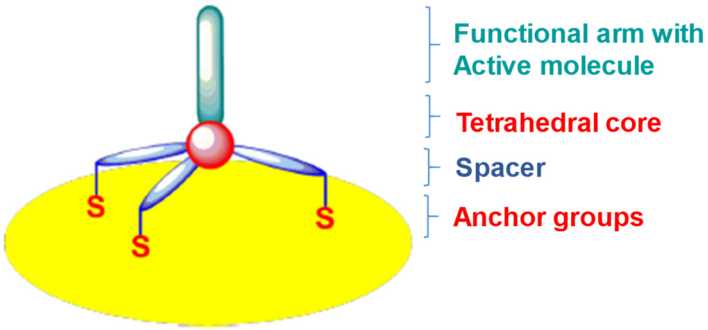

Figure 1.2 Schematic drawing of an example molecule with tripodal structure attached to a metal surface by three anchoring groups.

Concerning 2D arrangements, an useful strategy is the use of tripodal molecules as binding units, which can cover a specific area and control lateral spacing after being attached on different surfaces. Depending on the tripod size, they will be able to significantly guarantee the spatial arrangement between the selfstanding functional arms that protrudes from the surface, (in blue, see figure 1.3). These molecules usually consist of a tetrahedral core structure with an active tail group positioned perpendicular to the

[23] Chang, H.I.; Wang, Y. in: D. Eberli (Ed.), Regenerative Medicine and Tissue Engineering-Cells and Biomaterials, vol. 1, first ed., InTech, Rijeka, Croatia, **2011**, pp. 569.
[24] Thomas Parsons, J.; Horwitz, A.R.; Schwartz, M.A. *Nat. Rev. Mol. Cell Biol*. **2010**, *11*, 633.
[25] Abedin, M.; King, N. *Trends Cell Biol*. **2010**, *20,* 734
[26] Cannons, J.L.; Qi, H.; Lu, K.T.; Dutta, M.; Gomez-Rodriguez, J.; Cheng, J.; Wakeland, E.K.; Germain, R.N.; Schwartzberg, P.L., *Immunity* **2010**, *32*, 253.
[27] Callow, J.A.; Callow, M.E. *Nat. Commun*. **2011,** *2*, 1.

surface. The remaining three legs are comprised of oligophenylene or oligophenylacetylene spacer of a desired length and the terminal anchor groups, such as thiol or derivatives in the case of the noble metal substrates.

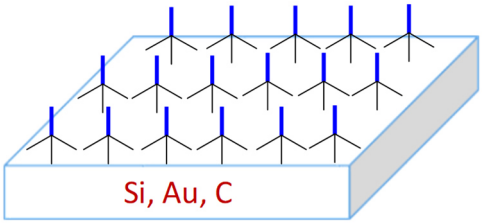

Figure 1.3 Nanostructured surface with tripodal organic adsorbates

The generated thin films should resist the nonspecific adsorption of proteins (if they have been designed for that purpose) and should ideally be readily functionalized by using bio-orthogonal chemistry, such as click or Suzuki reactions. In addition, once the SAM is formed, the stepwise strategy most frequently applied is a further derivatization of the functionalized substrate, creating versatile assemblies for a specific application. A suitable experimental tool in this regard is the so-called click reaction.[28] By this approach, components that cannot be directly attached to the surface upon the SAM formation can be incorporated by an additional step. This is carried out by the reaction between the predefined, click-reaction capable terminal groups of the SAMs and the selected component bearing a complementary group for the reaction.[29]

[28] Kolb, H.C.; Finn, M.; Sharpless, K.B. *Angew Chem. Int. Ed*. **2001**, *40*, 2004.
[29] a) Ciampi, S.; Böking, T.; Kilian, K.A.; James, M.; Harper, J.B. Gooding, J.J. *Langmuir* **2007**, *23,* 9320; b) Chelmowski, R.; Käfer, D.; Köster, S.D.; Klasen, T.; Winkler, T.; Terfort, A.; Metzler-Nolte, N.; Wöll, C. *Langmuir* **2009**, *25,* 11480; c) Darlatt, E.; Traulsen, C.H.-H.; Poppenberg, J.; Richter, S.; Kühn, J.; Schalley, C.A.; Unger, W.E.S. *J. Electron Spectr. Relat. Phenom.* **2012**, *185*, 85; d) Yan, R.; Le Pleux, L.; Mayor, M.; Zharnikov, M. *J. Phys. Chem. C* **2016**, 120, 25967.

1.2 Specific protein adsorption as an application of these films

The possibility to generate a surface with biologically relevant functionalities is undoubtedly one of the most exciting applications SAMs can exhibit. To this end, SAM should be terminated with a specific functional group (as shown in figure 4), to which e.g. a receptor can be immobilized, thus generating a lock–key pair to specifically bind a biomolecule of interest. This concept has been firstly described by Whitesides and coworkers,[30] and since then, many other biorelated applications of SAMs have been studied.

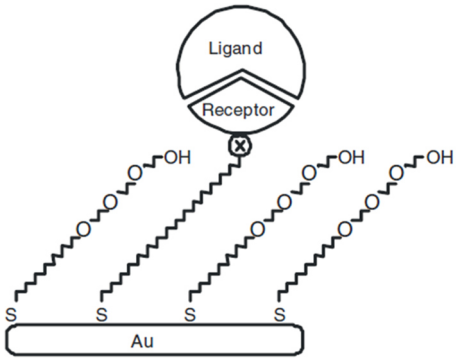

Figure 1.4 Example of a SAM prepared for the specific adsorption of protein components. The SAM also presents components to avoid unspecific adsorption (using oligo-ethyleneglycol termination).

As pointed out above, to create a surface for biological purposes which resists non-specific adsorption of proteins, the employment of oligoethylene-terminted SAMs (OEG-SAMs) has become a powerful tool. [31] In this context, the study of the protein resistance in terms of chain lenght is also interesting. Although it is well-known that OEGs prevent non-specific absorption of proteins, it seems unclear what really drives the resistance of OEG-SAMs to protein adsorption.

[30] Prime, K.L.; Whitesides G.M. *Science,* **1991**, 252, 1164.
[31] a) Harder, P.; Grunze, M.; Dahint, R.; Whitesides, G.M.; Laibinis, P.E *J. Phys. Chem.* B. **1998,** *102*, 426; b) Qin, G. T.; Yam, C. M.; Kumar, A.; Lopez-Romero, J. M.; Li, S.; Huynh, T.; Li, Y.; Contreras-Caceres, R.; Cai, C. Z*RSC Adv.* **2017**, *7*, 14466–14476. c) Contreras-Caceres, R.; Santos, C. M.; Li, S. H.; Kumar, A.; Zhu, Z. L.; Kolar, S. S.; Casado-Rodriguez, M. A.; Huang, Y. K.; DcDermott, A.; Lopez-Romero, J. M.; Cai, C. Z. *J. Colloid Interf. Sci.* **2015**, *458*, 112; d) Qin, G.; Gu, J.; Liu, K.; Xiao, Z.; Yam, C. M.; Cai, C. Z. *Langmuir* **2011**, *27*, 6987; e) Lopez-Romero, J. M.; Rico, R.; Martinez-Mallorquin, R.; Hierrezuelo, J.; Guillen, E.; Cai, C. Z.; Otero, J. C.; Lopez-Tocon, I. *Tetrahedron Lett.* **2007**, *48,* 6075; f) Yam, C. M.; Deluge, M.; Tang, D.; Cai, C. Z. *J. Colloid Interface Sci.* **2006**, *296*, 118–130; g). Deng, X.; Cai, C. Z. *Tetrahedron Lett.* **2003**, *44*, 815.

Despite the fact that there is a large number of already synthesized and investigated multipodal molecules and different fashions to modify and functionalize surfaces by forming SAMs, the design of the ideal molecule for a particular application still has to be found.

This Doctoral Thesis is based on two fundamental aspects of the applied organic chemistry. On one hand, the synthesis of macromolecules derived from oligo-*p*-phenylenes with possible applications in the nanostructuration and modification of surfaces and, on the other hand, the study of the modification of different metallic surfaces with these molecules to further test them for specific protein adsorption.

2. HYPOTHESIS & OBJECTIVES

The starting hypothesis of this thesis is that the maximum effectiveness of any device will be achieved with the suitable structuration of the surfaces at the molecular level. This structuration must fullfil several requirements, being these the biocompatibility, a high coating density, adequate molecular orientation and minimum spacing between functional groups or active molecules. In addition, it is necessary to have different methods to chemically modify these surfaces and provide them with other properties or applications. Thus, the first objective of this thesis is the preparation of molecules that are capable to accomplish all these features by modifying the surface. And, the second, the study of the modification of different metallic surfaces with these molecules.
Therefore, the thesis is going to be structured in two fundamental objectives:

Objective 1. “SYNTHESIS OF ORGANIC ADSORBATES WITH TRIPODAL SHAPE INCLUDING ACTIVE-MOLECULES”.

In particular, the following specific objectives have been considered:

- Synthesis of tripod-shaped oligo-*p*-phenylenes having anchoring groups compatible with the different surfaces to be modified (azide for alkynyl-terminated silicon surfaces, thiols or thioderivatives in the case of gold surfaces).
- Synthesis of tripods with lateral ethylene glycols units joining the three "arms", to provide rigidity for their attachment to the surface.
- Synthesis of tripods with chromophore groups, thus obtaining fluorescent properties.
- As active molecules we propose theophylline derivatives; the synthesis of adequately substituted theophyllines will be carried out for their immobilization on the different surfaces previously structured with the corresponding tripods.

Objective 2. “MODIFICATION OF METALLIC SURFACES”.

In this objective we propose several types of surface modification:

- Modification of silicon surfaces with organic molecules derived from alkynes and immobilization via copper-catalyzed click reaction of the tripodal adsorbates bearing azides as anchoring groups, synthesized in Objetive 1.

Hypothesis & Objectives

- Modification of gold substrates by preparing Self-Assembled Monolayers (SAMs) with tripodal adsorbates bearing thiols (or derivatives) as anchoring groups.
- Study of the functionality of the fabricated tripod SAMs as a platform for subsequent chemical reactions and biosensor fabrication. With this purpose, the covalent incorporation of theophylline active molecules, also by click reaction, and subsequent behavioral test of theses surfaces for protein immobilization will be carried out.

3. RESULTS & DISCUSSION

CHAPTER I. SYNTHESIS OF TRIPOD-SHAPED ADSORBATES AND ACTIVE MOLECULES

CHAPTER I. Synthesis of tripod-shaped adsorbates and active molecules

In this chapter, we describe the background and the obtained results of the synthesis of tripod-shaped oligo(p-phenylene)s. The chapter is divided in a background -which includes bibliographic information about the methods of synthesis of tripodal molecules-, and synthesis of tripod-shaped molecules -which includes synthesis of tripods having azide groups as anchors, tripods with thioacetate groups as anchors, tripods laterally substituted with ethyleneglycols and biphenyls, tripods with chromophore groups and, finally, the synthesis of spacers for silicon substrate modification and theophylline derivatives as active molecules for protein adhesion study-.

I.1 Background

In order to control the spacial arrangement of functional groups in nanostructured organic thin films, the synthetic strategy to develop new molecules capable to fulfill this goal has been focused on the preparation of large and rigid multipodal architectures.[1]

These multipodal platforms are intended to considerably increase the binding stability on metal surfaces, when compared to single binding units, since they have multiple anchor groups, and to guarantee the orientation of the molecule at a fixed distance from the surface. Although a large variety of macromolecules with defined structure have been constructed from different types of rigid chain oligomers,[2] very few have been published with tripodal structure. The tripod framework usually consists of a tetrahedral molecule, characterized by the presence of at least three anchoring groups that are not in a line, while the fourth bond is positioned perpendicular to the surface. The remaining three substituents of the tetrahedral core should be as rigid as possible to form a stable contact to the surface. Hence, these legs usually contain aromatic units or ethylene species with the desired length.

[1] Chinwangso, P.; Jamison, C. A.; Lee, T. R. *Acc. Chem. Res.* **2011,** *44,* 511.
[2] a) Schwab, P. F. H.; Levin, M. D.; Michl, J. *Chem. Rev.* **1999**, *99*, 1863; b) Tour, J. T. *Chem Rev.* **1996**, *96*, 537; c) Moore, J. S. *Acc. Chem. Res.* **1997**, *30*, 402; d) Navak, J. P.; Feldheim, D. L. *J. Am. Chem. Soc.* **2000**, *122*, 3979; e) Hensel, V.; Schlüter, A. D. *Chem. Eur. J.* **1999**, *5*, 421; f) Keegstra, M. A.; de Feyter, S.; de Schryver, F. C.; Müllen, K. *Angew. Chem., Int. Ed. Engl.* **1996**, *35*, 774; g) Lewis, P.; Strongin, R. M. *J. Org. Chem.* **1998,** *63*, 6065; h) Mongin, O.; Gossauern A. *Tetrahedron* **1997**, *53*, 6835. (i) Rukavishnikov, A. V.; Phadke, A.; Lee. M. D.; LaMunyon, D. H.; Petukhov, P. A.; Keana, J. F. W. *Tetrahedron Lett.* **1999**, *40*, 6353.

So far, a number of large, shape-persistent and self-standing molecules whose core can incorporate a silicon atom,[3] a carbon atom,[4] or an adamantane structure,[5] have been developed to be used as "molecular caltrops" for the functionalization of different metal and metal-oxide surfaces. As examples of these structures, we can highlight those with four phenylacetylene legs extending from either a tetrahedral silicon core (**IV**) or an adamantane core (**III**), conically shaped dendron adsorbates with a functional group at the core (**I**),[6] and tripod-shaped oligo(*p*-phenylene)s joined together by a single silicon atom (**II**)[7] (figure I.1).

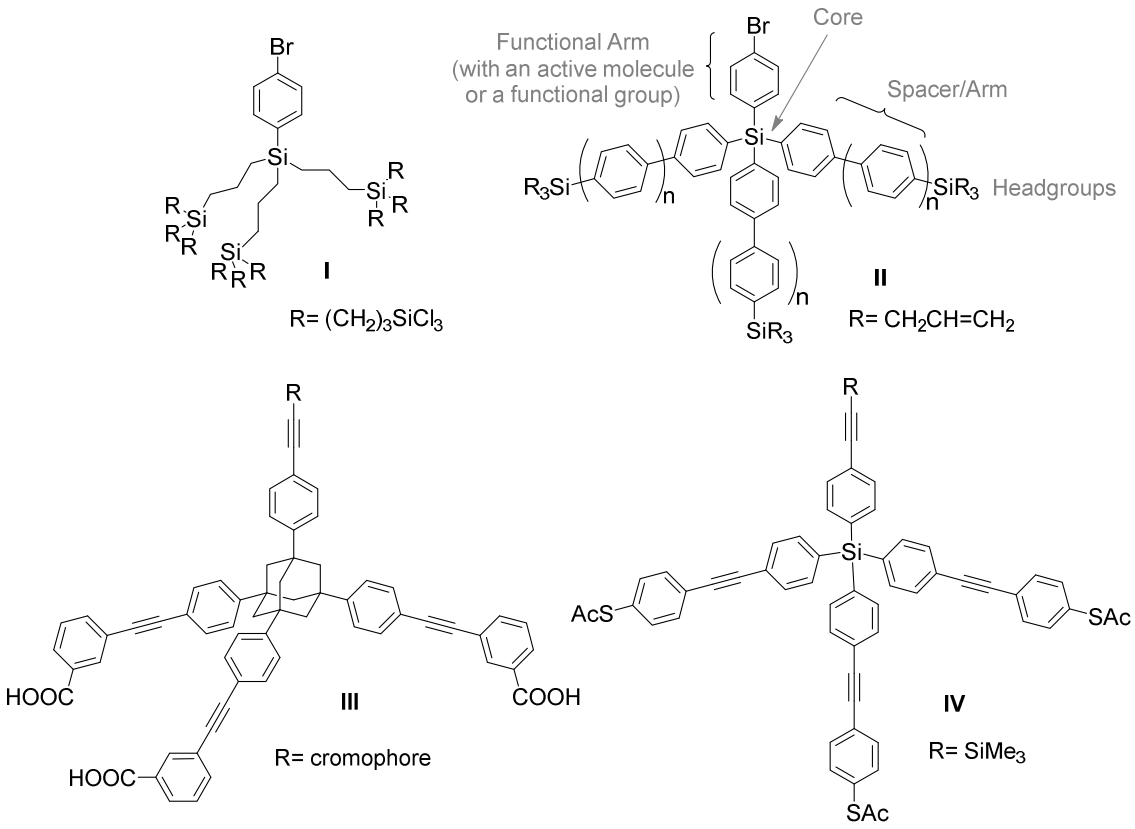

Figure I.1 Rigid macromolecules for the nanostructuration of surfaces.

[3] a) Yao, Y.; Tour, J. M. *J. Org. Chem.* **1999,** *64,* 1968; b) Jian, H.; Tour, J. M. *J. Org. Chem.* **2003,** *68,* 5091; c) Shirai, Y.; Guerrero, J. M.; Sasaki, T.; He, T.; Ding, H.; Vives, G.; Yu, B.-C.; Cheng, L.; Flatt, A. K.; Taylor, P. G.; Gao, Y.; Tour, J. M. *J. Org. Chem.* **2009,** *74,* 7885; d) Ramachandra, S.; Schuermann, K. C.; Edafe, F.; Belser, P.; Nijhuis, C. A.; Reus, W. F.; Whitesides, G. M.; De Cola, L. *Inorg. Chem.* **2011,** *50,* 1581. f) Deng, X.; Cai, C. *Tetrahedron Lett*. **2003**, *44*, 815.

[4] a) Ie, Y.; Hirose, T.; Yao, A.; Yamada, T.; Takagi, N.; Kawai, M.; Aso, Y. *Phys. Chem. Chem. Phys.* **2009,** *11,* 4949; b) Ie, Y.; Hirose, T.; Nakamura, H.; Kiguchi, M.; Takagi, N.; Kawai, M.; Aso, Y. *J. Am. Chem. Soc.* **2011,** *133,* 3014.

[5] a) Thyagarajan, S.; Liu, A.; Famoyin, O. A.; Lamberto, M.; Galoppini, E. *Tetrahedron* **2007**, *63*, 7550; b) Lamberto, M.; Pagba, C.; Piotrowiak, P.; Galoppini, E. *Tetrahedron Lett*. **2005**, *46*, 4895; c) Lee, C.-H.; Zhang, Y.; Romayanantakit, A.; Galoppini, E. *Tetrahedron* **2010**, *66*, 3897; d) Kitagawa, T.; Matsubara, H.; Komatsu, K.; Hirai, K.; Okazaki, T.; Hase, T. *Langmuir* **2013,** *29,* 4275.

[6] a) Choi, S.; Yoon, C. W.; Lee, H. D.; Park, M.; Park, J. W. *Chem. Commun*. **2004**, 1316; b) Deluge, M.; Cai, C. *Langmuir* **2005**, *21*, 1917; c) Yam, C. M.; Cai, C. *Langmuir* **2004**, *20*, 1228; d) Yam, C. M.; Cho, J.; Cai, C. *Langmuir* **2003**, *19*, 6862.

[7] a) Hierrezuelo, J.; Guillén, E.; López-Romero, J. M.; Rico, R.; López-Ramírez, M. R.; Otero, J. C.; Cai, C. *Eur. J. Org. Chem*. **2010**, 5672; b) Hierrezuelo, J.; Rico, R.; Valpuesta, M.; Díaz, A.; López-Romero, J. M.; Rutkis, M.; Kreigberga, J.; Kampars, V.; Algarra, M. *Tetrahedron* **2013**, *69*, 3465.

As can be seen in figure I.1, all the molecules present headgroups at the end of the spacer or arms, to be properly attached to the different surfaces, and an active molecule or functional group in the fourth arm. Molecule **III** in this figure presents a cromophore as tail group and was firstly described by Galoppini and coworkers in 2007.[5a] This tripod also has COOH anchoring groups in *meta* position, which the authors reported that enhances the binding of the molecule to TiO_2 anatase (001) by all three legs of the tripods, because of the more favorable angle for surface anchoring (figure I.2).

The spacing of dyes on the surface of semiconductors, by using large tripods, could be useful to study excimer and monomer effects having the COOH anchoring groups in *meta* position, rather than in *para*. This compound exhibited spectral properties typical of phenylacetylene substituted pyrenes and its quenching of fluorescence on anatase TiO_2 films indicates efficient electron injection into the semiconductor.

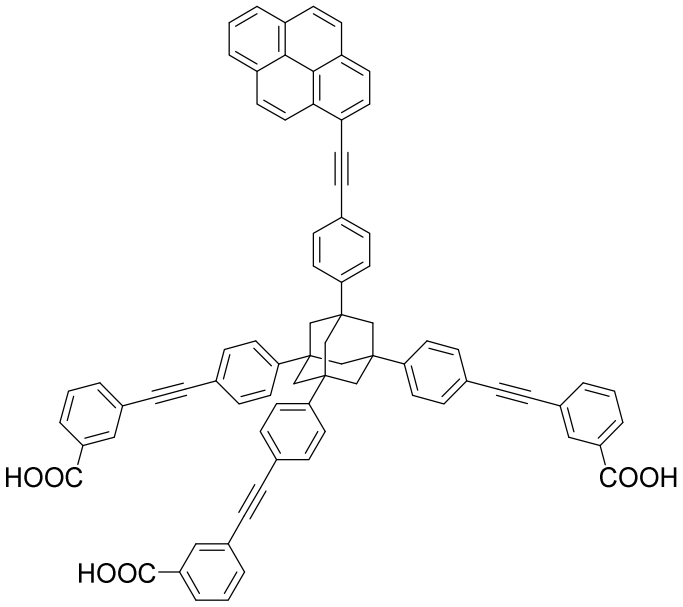

Figure I.2 Tripodal sensitizer molecule described by Galoppini.[5a]

In the case of dendron derivatives (molecule **I** in figure I.1), it is important to note that these are compounds now commercially available (NanoCones) as innovative surface coating.[8] However, these structures present several drawbacks, such as the lability towards chemical degradation, the lack of rigidity, and the limited chemical functionalities attached in the functional arm, which makes highly desirable the design of more stable molecules to be used as adsorbates in organic nanostructures for sensing purposes.

[8] Hong, B. J.; Oh, S. J.; Youn, T. O.; Kwon, S. H.; Park, J. W. *Langmuir* **2005**, *21*, 4257.

On the other hand, Tour[3a] proposed the use of phenylacetylene tripodal molecules (similar to molecule **IV** in figure I.1) for the modification of scanning probe microscopy tips. The author described the design and synthesis of "molecular caltrops" employing a silicon atom as tetrahedral core, which allowed the joint of four phenylacetylene arms, as observed in figure I.3a.

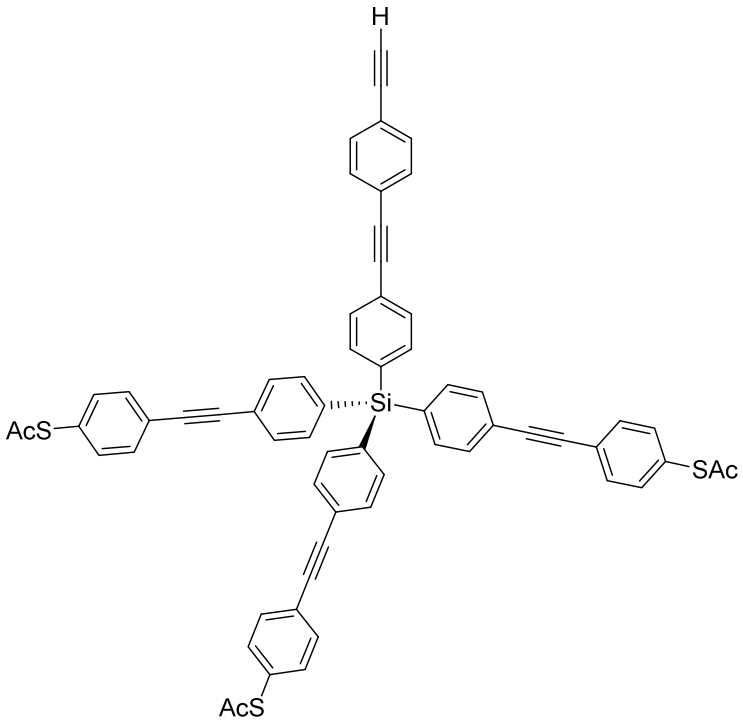

Figure I.3a Tripodal molecule derived from phenylacetylene synthesized by Yao and Tour in 1999.[3a]

The synthetic route was carried out in a convergent manner as shown in scheme I.2. In a first step, the synthesis of the ethoxytri(*p*-iodophenyl)silane **A**, was performed by addition of *p*-diiodobenzene to tetraethyl orthosilicate in ether and using *n*-BuLi. Then, lithiumhalogen exchange of 1-bromo-4-(trimethylsilylethynyl)-benzene with *t*-BuLi followed by quenching with **A** provided **B** (scheme I.1).

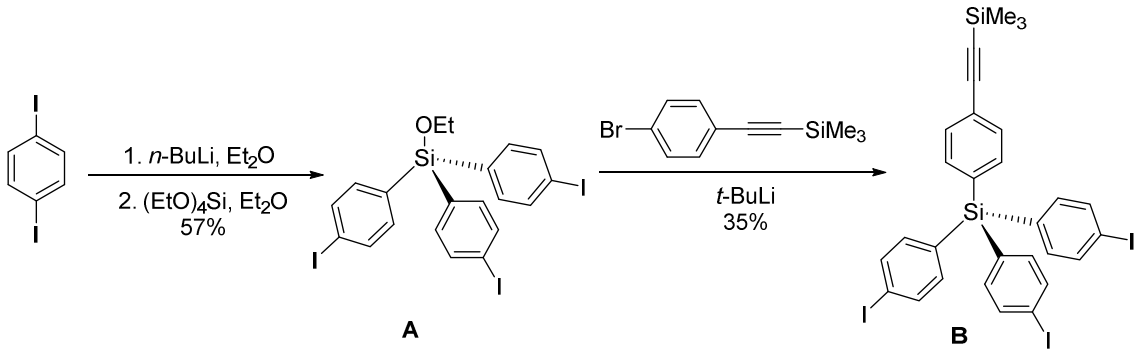

Scheme I.1 Synthesis of the silicon precursor **A** and silicon core **B**, in Yao and Tour´s work. [3a]

In order to perform the synthesis of the molecular caltrop **C**, the coupling between **B** and 1-ethynyl-4-(thioacetyl)benzene by using Pd/Cu as catalyst, was carried out (scheme I.2). Then, desilylation using tetra(*n*-butyl)ammonium fluoride (TBAF) in acetic anhydride and acetic acid gave the molecule **D**. Again, Pd/Cu-catalyzed coupling of **D** with 1-iodo-4-(trimethylsilylethynyl)benzene afforded **E** and, subsequent desilylation with TBAF, gave its counterpart **F** in good yield (71%), (see scheme I.2).

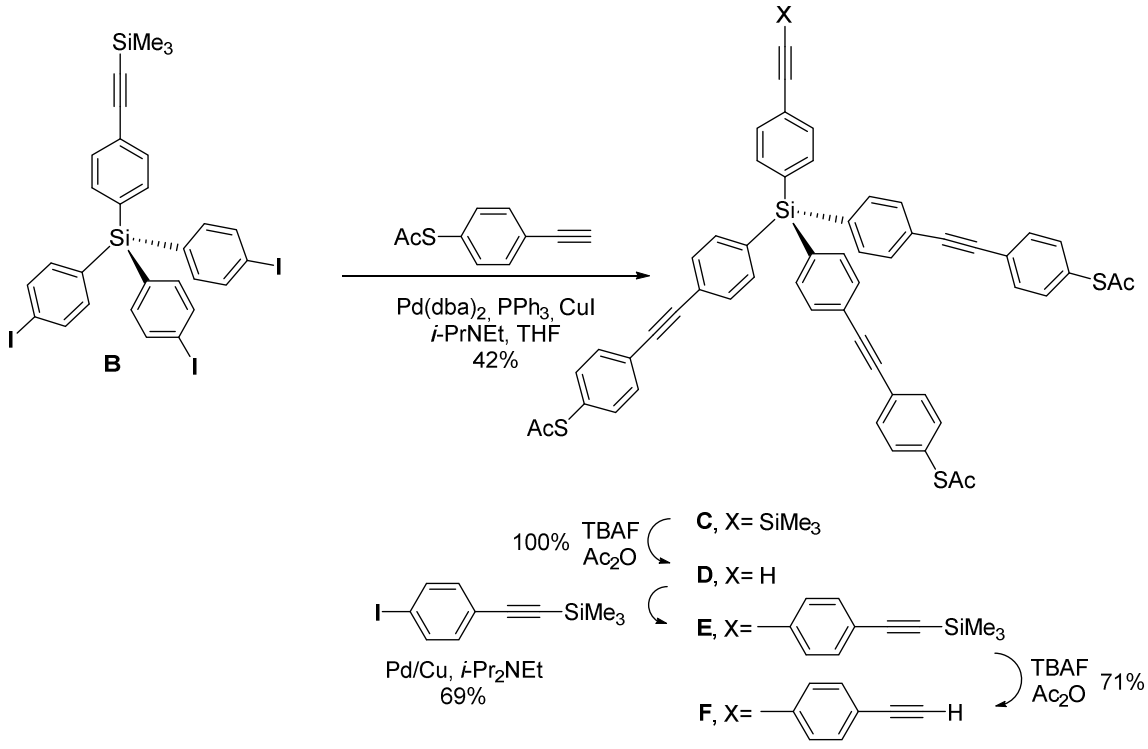

Scheme I.2. General procedure to obtain caltrops **C**-**F**.[3a]

Another example of molecular caltrops, also performed by Tour, is shown in the next figure, which also has a silicon atom as tetrahedral core and thioacetate groups as binding units for the modification of gold substrates.[3b]

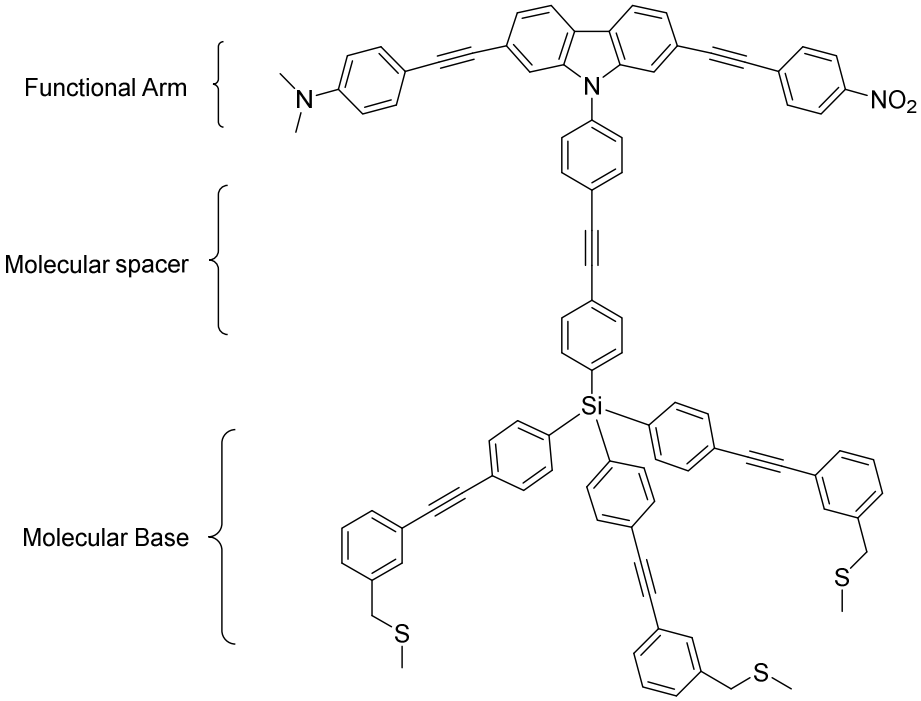

Figure I.3b Tripodal molecular caltrop designed by Tour for it assembly on gold surfaces.[3b]

Tour also described[3a] that some of this molecular caltrops could be useful as molecules for the modification of AFM tips, increasing the resolution up to molecular level. Nevertheless, in this study, they demonstrated that the tripods with *p*-phenylenethiol groups as anchors were tilted when attached to the gold surface because only two of the three potential Au-S bonds could form. In the following work,[3b] they modified the molecular tripod base, using benzylic thiols at *m*-positions relative to the ethynylene groups, thus permitting the proper orientation for assembly in gold substrates. The functional arm in this molecule posseses a strong dipole net moment, with donor-acceptor funcionality, thereby influencing the control of the rotation when is subjected to oscillating electric fields.

The same strategy was used by Cai and coworkers[9] for the synthesis of a tripod-shaped molecule constituted, in this case, by three chains of hepta-*p*-phenylene, connected in a silicon atom that acts as core (figure I.4). This is the first antecedent that describes a tripodal molecule derived from oligo-*p*-phenylene.

This molecule is characterized by having at the ends of the oligo-*p*-phenylene legs dendrons derived from triallylsilane as indicated in figure I.4. These groups are included

[9] Deng, X.; Mayeux, A.; Cai, C. *J. Org. Chem.* **2002**, *67*, 5279.

in the structure to be used as attachment points to a silicon surface (Si-H) by means the formation of a Si-C covalent bond via a hydrosilylation reaction. At the apical end, it also presents a bromine atom in order to allow its subsequent derivatization by the incorporation of active molecules. These active molecules can include biotin, theophylline, different chromophore groups, etc.

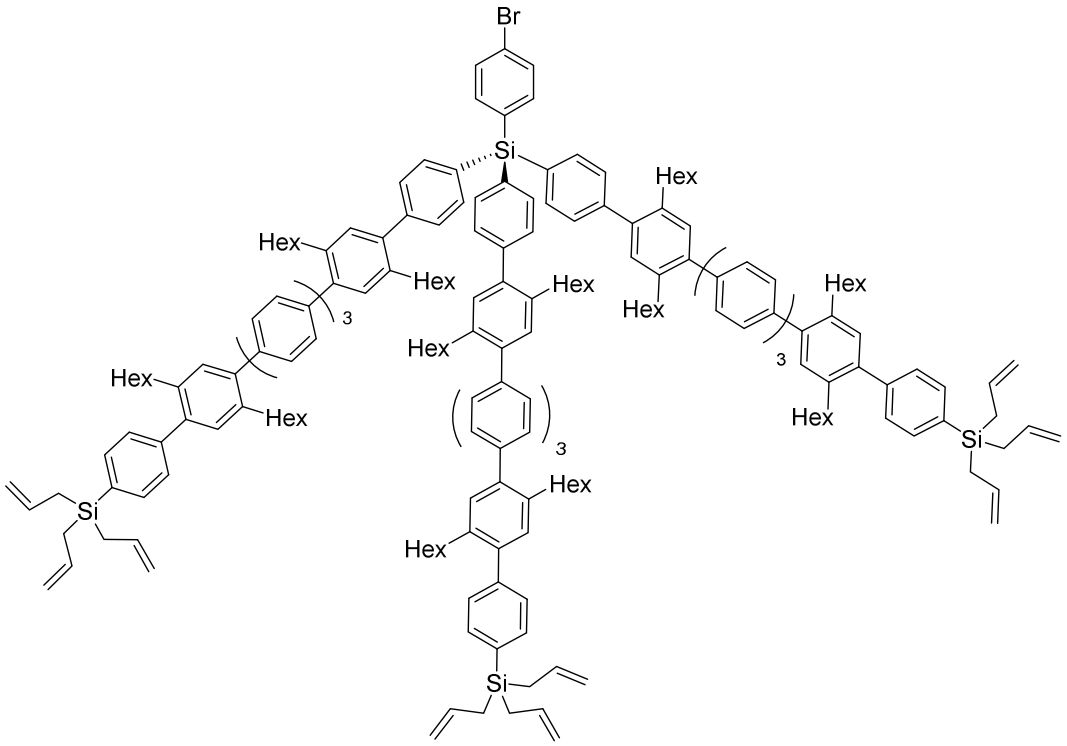

Figure I.4 Tripodal molecule that comprises oligo-*p*-phenylene units as legs, first time described by Cai.[9]

The synthesis of this compound, represented as **I** in scheme I.3, was carried out according to the presented retrosynthetic pathway. Although in the preparation, the key step is the coupling between the *p*-phenylene (**II**) derivative and the silicon core (**III**), performed by a Suzuki type reaction, the synthesis can be differentiated in several parts. The first one consists of the preparation of the *p*-phenylene unit (**II**) with the desired length and functionalized at the terminal position with R, that will constitute the anchor position to the surface. The second one is the preparation of the molecule derived from silicon (**III**) that is used as core and the third is the coupling between both molecules.

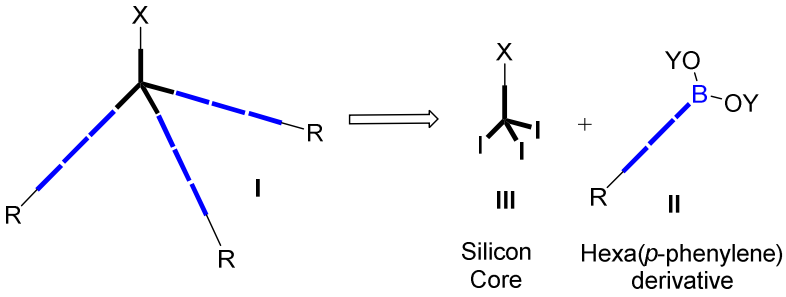

Scheme I.3 Retrosynthetic pathway to carried out the synthesis of a tripod-shaped molecule.

Scheme I.4 summarizes the steps followed to obtain the *p*-phenylene derivative **II**. The synthesis was first carried out by coupling of *p*-diiodoterphenyl with 2,5-dihexyl-4-bromo-phenylboronic acid, using $Pd(PPh_3)_4$ as catalyst. The reaction proceeded at room temperature and the product was obtained in 83% yield. Then, treatment with *t*-BuLi, subsequent iodination and incorporation of the boronic group by treatment with boron bispinacolate, gave the intermediate molecule, taking advantage of the greater reactivity of the aryl iodide in comparison with that of the bromide. However, in this step the yield only reached 25%, being this fact explained by the isolation of the bis-substituted product in 36% (scheme I.4).

Finally, the incorporation of the triallylsilyl group to the oligo-*p*-phenylene chain was performed by Suzuki coupling with *p*-triallylsilyl phenyl boronic acid, obtaining hexa-*p*-phenylene in 98% yield in the last stage, and an overall yield of 21%.

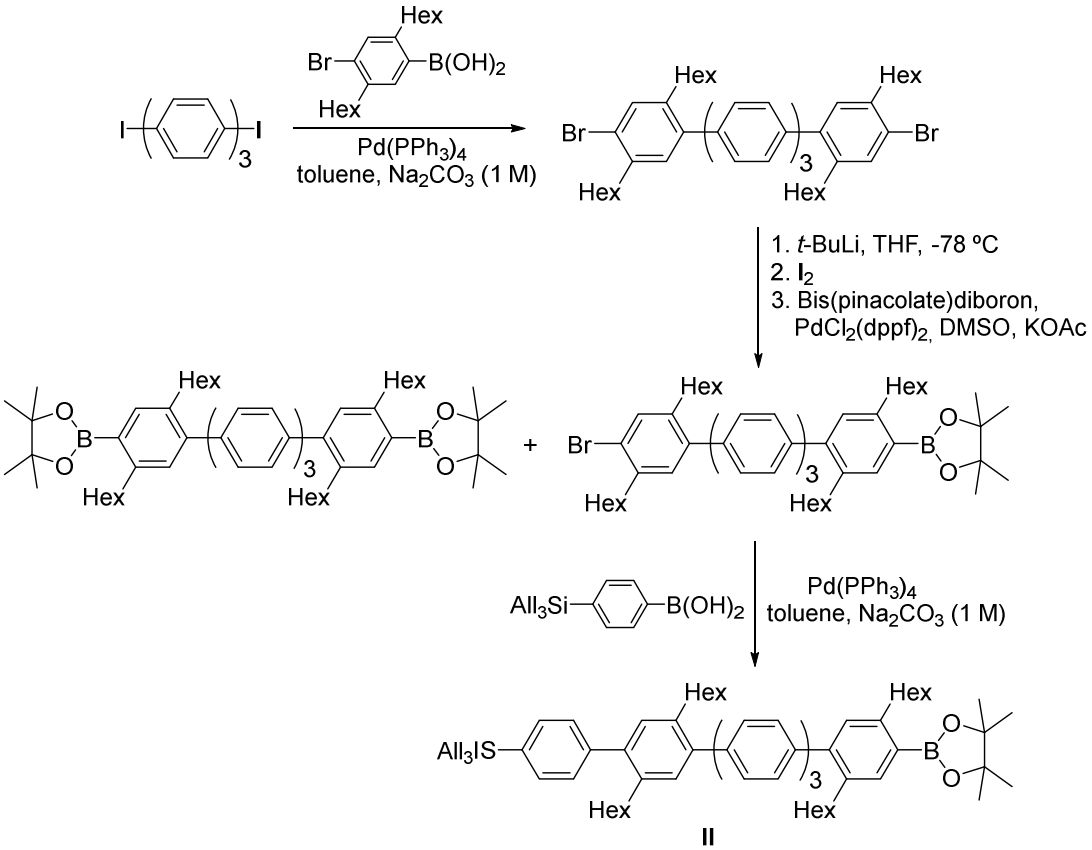

Scheme I.4 Preparation of the hexa-*p*-phenylene derivative.

The molecule derived from silicon and used as core was (4-bromophenyl)tris(4-iodophenyl)silane. It was prepared in 32% yield from the reaction of trichlorosilane with *p*-diiodobenzene, using *n*-BuLi as a base, (scheme I.5). This yield is in agreement to others obtained in similar reactions.[3a]

A first coupling attempt between the core and the hexa-*p*-phenylene under Suzuki coupling reaction conditions $Pd(PPh_3)_4$, toluene/water, Na_2CO_3, at 85 °C, during 12 h did not lead to the expected molecule, and only a complex mixture of products was obtained. This was attributed to a low reactivity, due to the steric hindrance presented in the boronate derivative by the presence of the hexyl substituents. Therefore, when the reaction was carried out using aqueous KOH as base and *n*-Bu_4NBr as a phase transfer catalyst, the tripodal molecule was obtained with a yield of 78% prior to purification (scheme I.5).

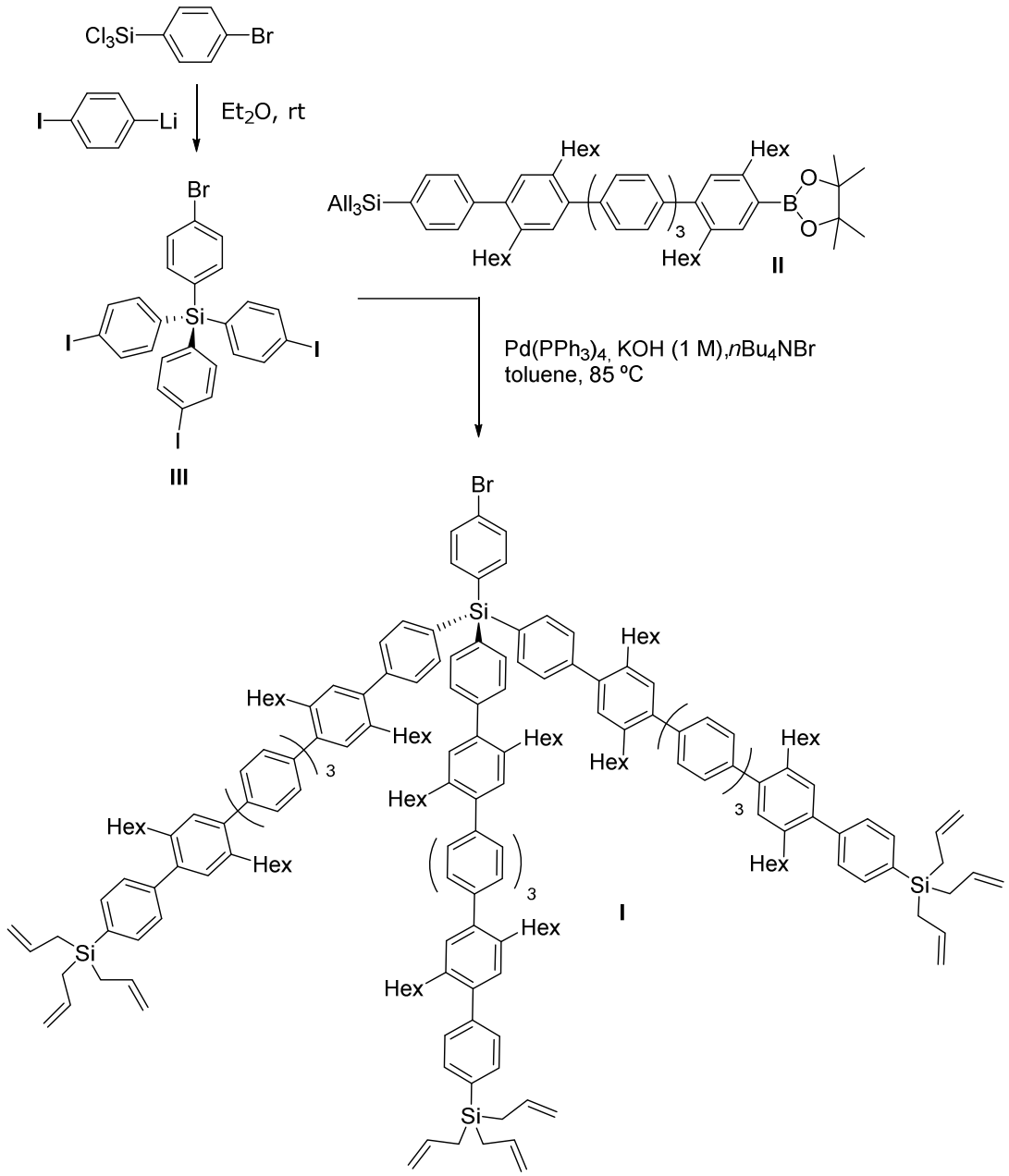

Scheme I.5 Procedure to synthesize tripod **I**.[9]

The reported tripod derivative **I** cannot be used to study multivalent and multi-component interactions in biological systems when attached to silicon surfaces, since both the hydrophobic tripod framework and its hexyl side chains are well known to interact non-specifically with protein molecules, thus interfering the specific interaction of target molecules with the ligand on the focal point of the tripod. To overcome this problem, novel tripod molecules, modified with side chains that do not interact nonspecifically with

protein molecules, must be develop. The most common materials for resisting non-specific interaction with proteins are poly- or oligo(ethylene glycol) (PEG or OEG).[10]

Our research group reported[11] then an efficient synthesis of a series of penta-*p*-phenylene derivatives with four side chains of various lengths, including deca(ethylene glycol) groups. The main feature of the synthesis is that the side chains are properly introduced in the last step, facilitating a good optimization for different applications. For instance, the deca(ethylene glycol) substituted penta-*p*-phenylene derivatives are versatile building blocks for construction of tripod-shaped adsorbates for biological applications (figure I.5).

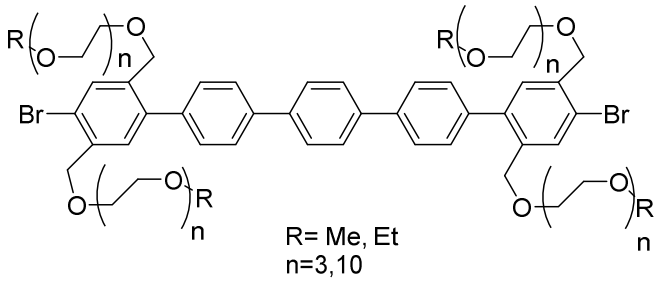

Figure I.5 Penta-*p*-phenylenes with OEG side chains: Key building blocks for the preparation of tripod molecules.

With this background, we chose tripodal oligo(*p*-phenylene)s as the ideal anisotropic adsorbates for surface modification and carried out the synthesis of several tripod-shaped molecules, as will be explained next. The synthesis of tripod-shaped oligo(*p*-phenylene)s molecules with legs composed of three phenylene units was first reported by Hierrezuelo *et al*.[7a] Each leg was end-capped with an iodine atom or a TMS group, an ethoxy group was presented composing the functional arm and the methyl tri(ethylene glycol) side chains were introduced for biological applications. Note that, the ethoxy group on the functional arm would allow further functionalization of the tripod, which will define the applications of the tripod-nanostructured surfaces (see figure I.6).

[10] a) Yam, C. M.; López-Romero, J. M.; Gu, J.; Cai, C. *Chem. Commun*. **2004**, 2510; b) Sharma, S.; Johnson, R. W.; Desay, T. A. *Appl. Surf. Sci*. **2003**, *206*, 218; c) Lee, S.-W.; Laibinis, P. E. *Biomaterials* **1998**, *19*, 1669; d) Papra, A.; Gadegaard, N.; Larsen, N. B. *Langmuir* **2001**, *17*, 1457; e) Leoni, L.; Attiah, D.; Desai, T. A. *Sensors* **2002**, *2*, 111. f) Zhu, X.-Y.; Jun, Y.; Staarup, D. R.; Major, R. C.; Danielson, S.; Boiadjiev, V.; Gladfelter, W. L.; Bunker, B.C.; Guo, A. *Langmuir* **2001**, *17*, 7798.

[11] López-Romero, J. M.; Rico, R.; Martínez-Mallorquín, R.; Hierrezuelo, J.; Guillén, E.; Cai, C.; Otero, J.C.; López-Tocón, I. *Tetrahedron Letters* **2007**, *48*, 6075.

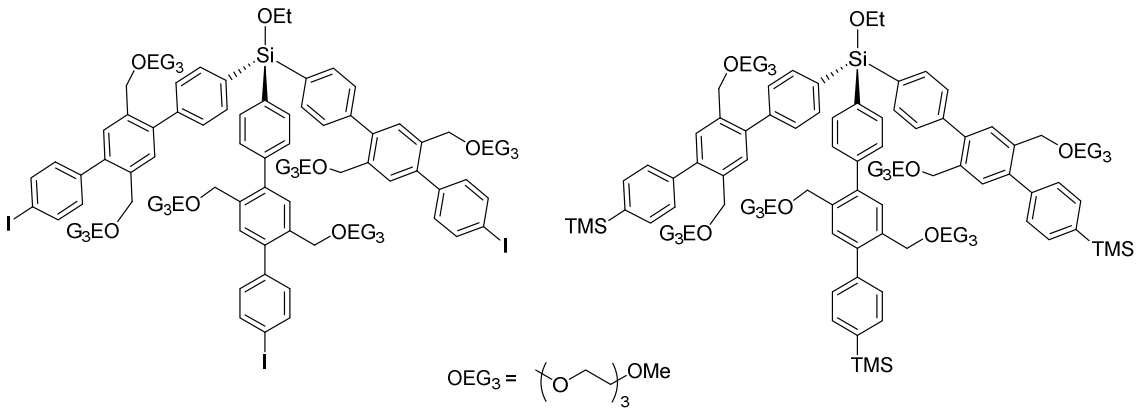

Figure I.6 Tripod-shaped molecules with OEG_3 side chains designed for biological applications.

The key step in the synthesis was the Pd-catalyzed Suzuki cross-coupling reaction between the silicon molecule (acting as the core) and the appropriately substituted *p*-biphenyl moiety. The authors reported this synthesis as a new strategy of iterative coupling so that the first-generation tripods would allow the homologation of the tripod legs to obtain giant tripod-shaped oligo(*p*-phenylene)s. To carried out the synthesis, they followed an approach (Route B, scheme I.6) that is conceptually different to that previously mentioned.[9]

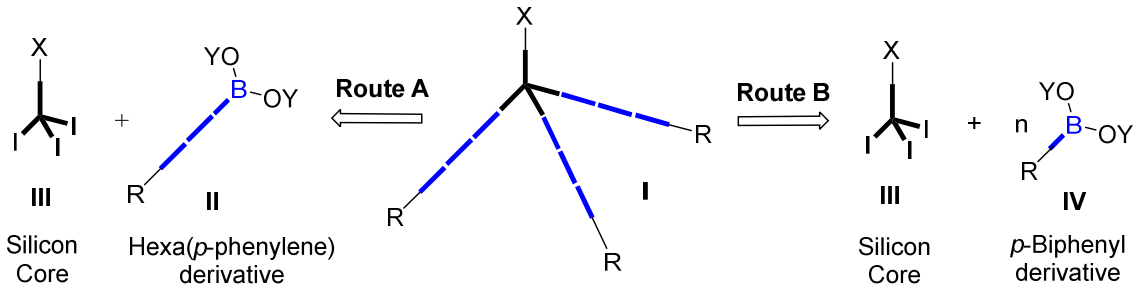

Scheme I.6 Retrosynthetic analysis.

Due to the presence of the iodine atom, the three tripod legs can be end-capped with a variety of functional groups for surface immobilization, such as carboxylic acid groups for attachment onto amino-terminated surfaces.

Another example, carried out in our laboratories, was the synthesis of azobenzene substituted tripod-shaped bi(*p*-phenylene)s for the modification of gold and quantum-dots surfaces (figure I.7).[7b] In this study, tripods with two phenylene units in each leg, end-capped with thioacetate goups and azobenzene chromophore groups on the functional arm were synthesized. Due to the thioacetate functional group located in each leg, fluorescent nanoparticles, such as CdS quantum-dots (CdS QDs), were capped by

the tripods, obtaining an adequate platform for the solubilization of this system in aqueous media.

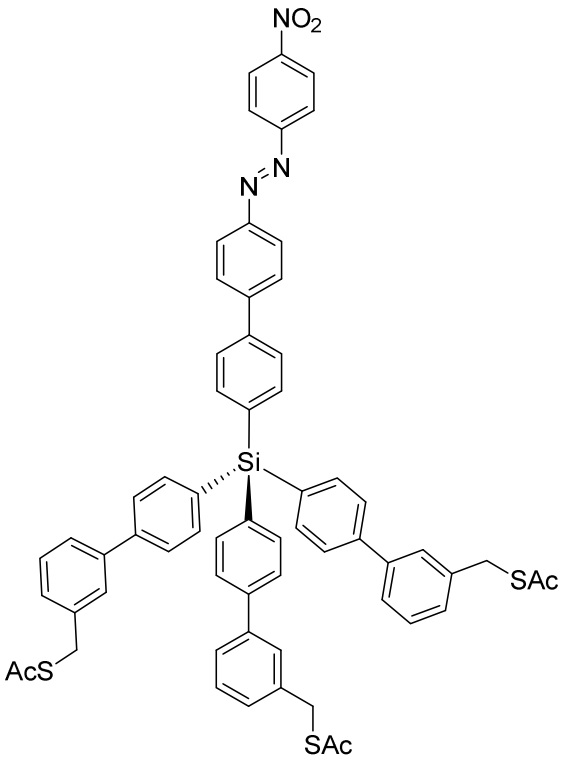

Figure I.7 Oligo(*p*-phenylene) tripod substituted by azoderivative chromophore.

The synthetic route that yielded this target tripod was achieved in several steps. First of all, from the corresponding comercial pinacolate by treatment with *t*-butyldimethylsilyl chloride in the presence of DMAP (a) in scheme I.7). On the other hand, the preparation of the silicon core was performed according to the reaction sequence indicated in scheme I.7 b). Then, coupling between these two molecules, under Suzuki reaction conditions, employing Pd(0) as catalyst, KOH as base, in the presence of *n*-Bu_4NBr and in a mixture of toluene/water as solvent, afforded the biphenylene derivative tripod in 54% yield (c) scheme I.7).

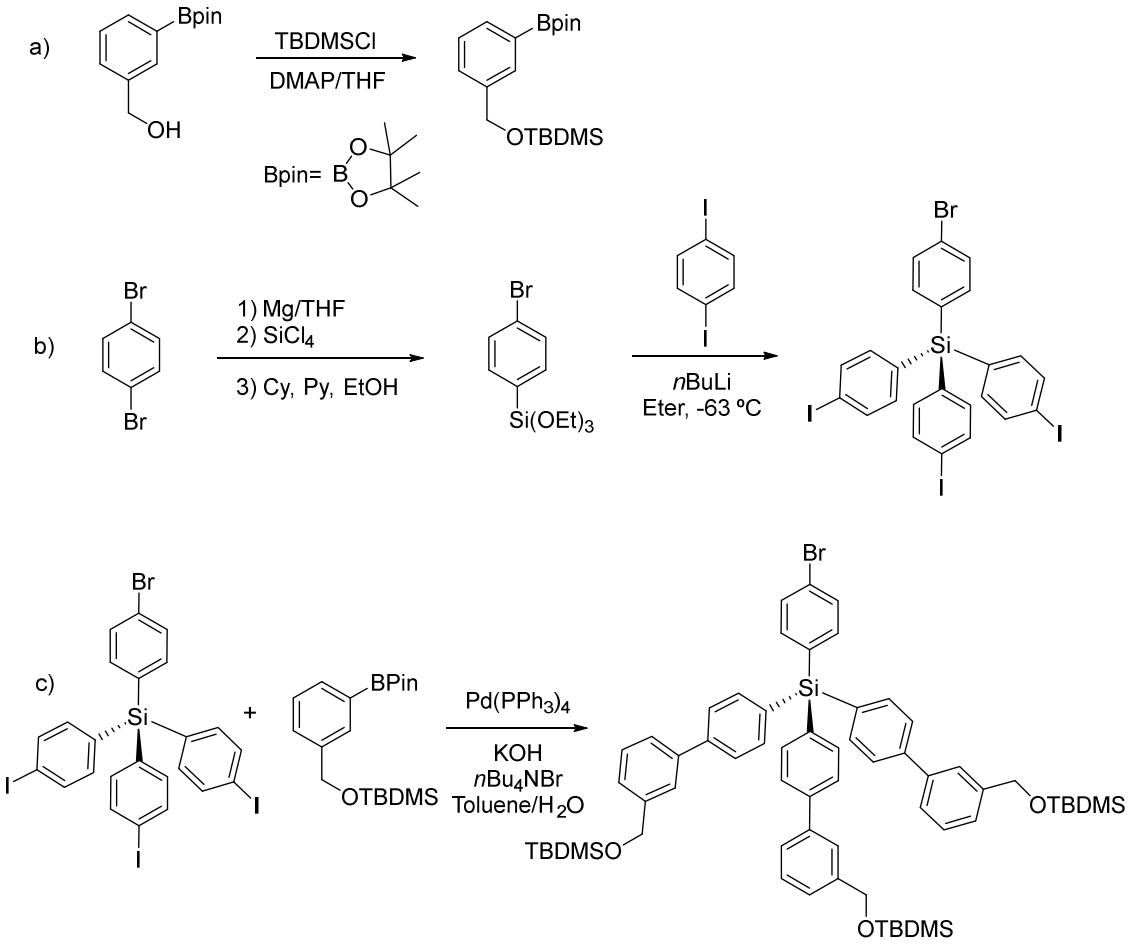

Scheme I.7 First steps to form precursor tripod with TBDMS protecting groups in each leg and bromine atom on the functional arm.

As can be observed in figure I.7, the target tripod presents as active group a cromophore molecule which also incorporates a nitro group, that is an electron withdrawing. The incorporation of the cromophore in the tripod was made by using the azoderivative shown in scheme I.8, which was obtained from the corresponding brominated azo-compound by treatment with bis(pinacolate)diboron in the presence of Pd(0) (scheme I.8).

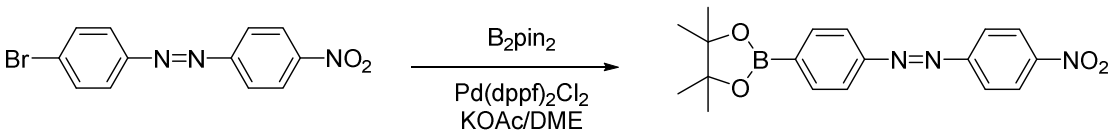

Scheme I.8 Synthesis of the cromophore molecule, which will be part of the functional arm.

The introduction of the chromophore group in the tripod-shaped molecule was carried out in the next step of the synthesis, by reaction between the pinacolate and precursor tripod (scheme I.9), in the presence of $Pd(PPh_3)_4$ and Na_2CO_3, using ethanol and toluene as solvents. According to this procedure, final azobenzene substituted tripod was obtained in 55% yield. Deprotection of the *t*-butyldimethylsilyl protecting group to release OH groups, was carried out by treatment with TBAF in the presence of AcOH and THF as solvent. Subsequent Mitsunobu reaction with PPh_3 and DIAD followed by thioacetic acid in THF gave the trithioacetate derivative tripod in 17% yield.

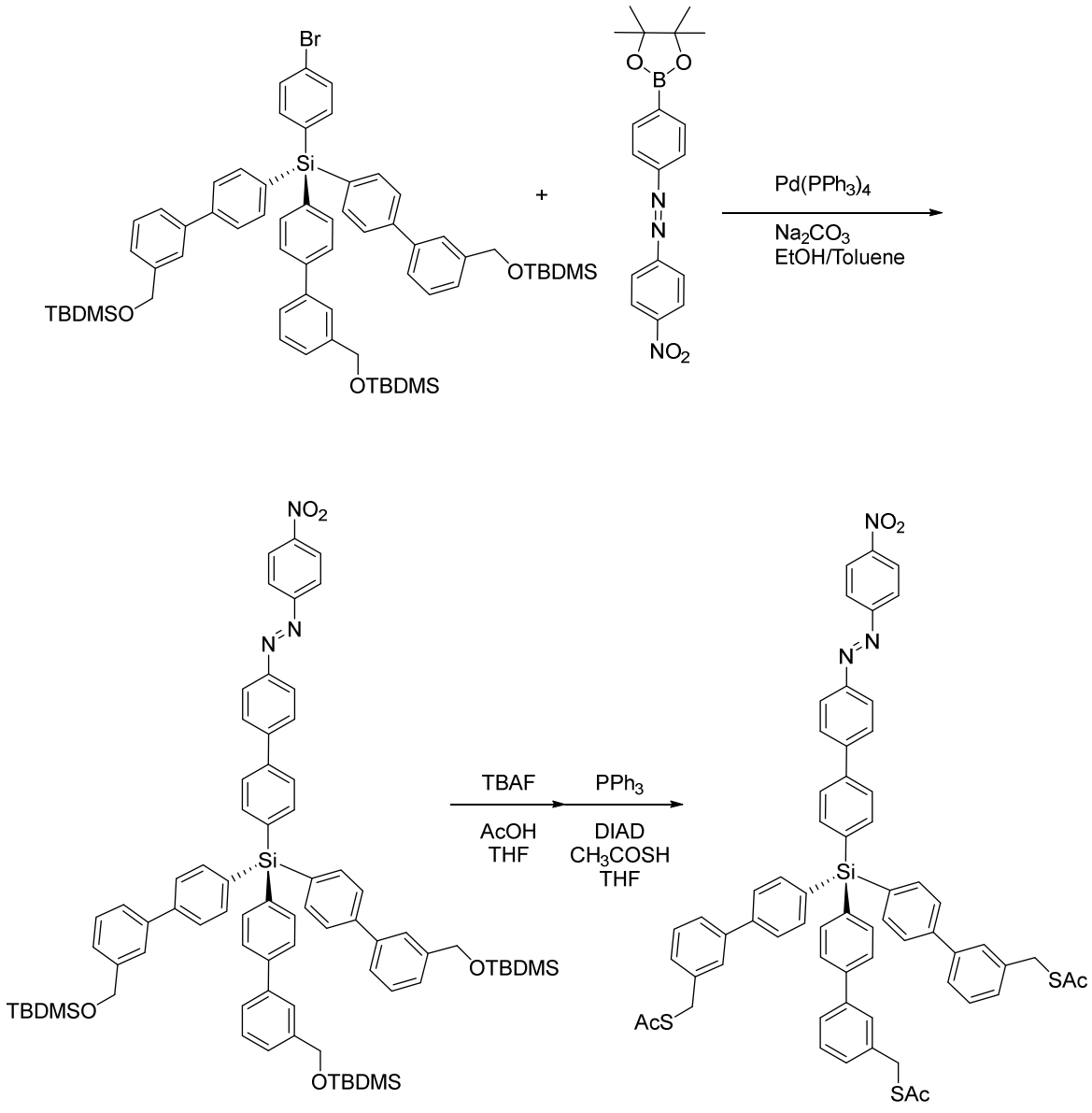

Scheme I.9 Synthesis of the final tripod reported by Hierrezuelo *et al.*[7b]

Coming up next, our results obtained for the synthesis of tripod-shaped molecules are described. These include the results obtained during the preparation of derivatives that present azide or thioacetate as anchor groups, the fir st designed for the attachment on modified silicon surfaces and the second, for their attachment on gold substrates. Also the synthesis of the active molecules employed, such as theophylline, and the spacer molecules to obtain silicon functionalized surfaces are described.

I.2 Synthesis of tripods with azide groups as headgroups

The synthetic strategy detailed below, provided ready access to a set of tripods end-capped with azide groups (**12**, **14** and **21**, figure I.8) for their incorporation to previously modified silicon substrates.

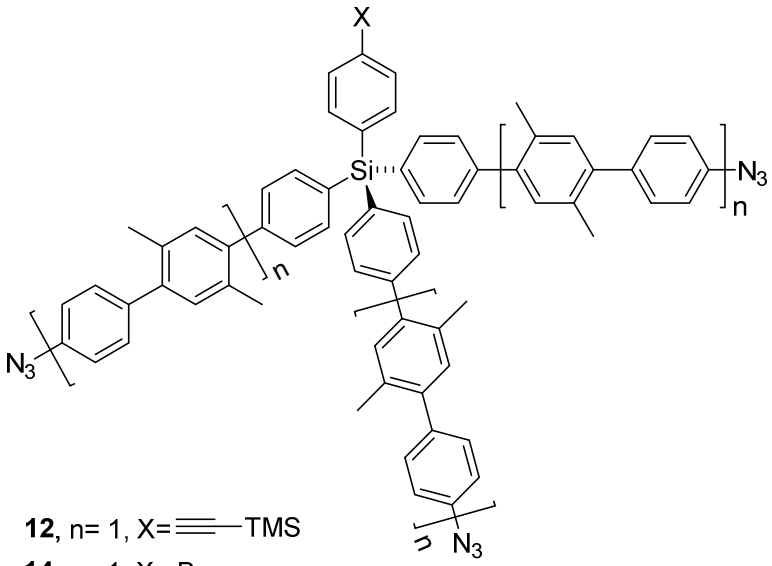

12, n= 1, X= TMS
14, n= 1, X= Br
21, n= 2, X= TMS

Figure I.8 Target molecules with azide anchor groups.

In order to carry out the synthesis of these three tripods, we firstly prepared the precursors (**1, 3**) and the silicon cores **2** and **4**. This was achieved in two differentiated steps (scheme I.10), in a similar way to the previously reported method.[3a]

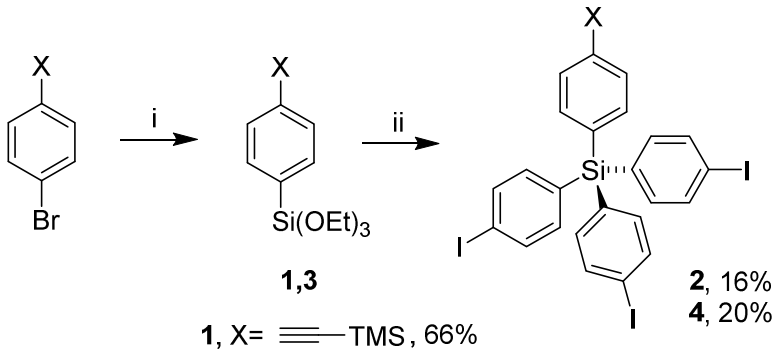

i) 1) Mg/THF 2) $SiCl_4$ 3) EtOH/Cyclohexane/Py
ii) 1) *p*-Diiodobenzene/*n*-BuLi/Et_2O 2) **1,3**/Et_2O

Scheme I.10 Preparation of precursors **1, 3** and silicon cores **2**, **4**.

First, *p*-chlorophenylmagnesium was generated at -78 ºC; then, it was treated with tetrachlorosilane producing a trichlorosilane derivative that in presence of ethanol, produced the exchange of chlorine atoms by ethoxy groups to give **1** and **3** in 66% and 31% yield, respectively. Secondly, the treatment of **1** and **3** with the monolithium salt of *p*-diiodobenzene afforded the corresponding silicon cores **2** and **4** in 16 % and 20% yield, respectively. This procedure avoids the isolation of the trichlorosilane derivative, since this specie decomposes by reaction with moisture.

Tripods **12, 14** and **21** were all planned to be synthesized by preparation of an oligo(*p*-phenylene) with the appropriate length and then, perform the Suzuki cross-coupling reaction with the respective silicon cores (**2** or **4**). Considering this approach and, to obtain tripods with three phenylene units (**12** and **14**), we initially arranged the synthesis of biphenyl **8** through the intermediate **7**, which already has the azide functionality present in the molecule (scheme I.11).

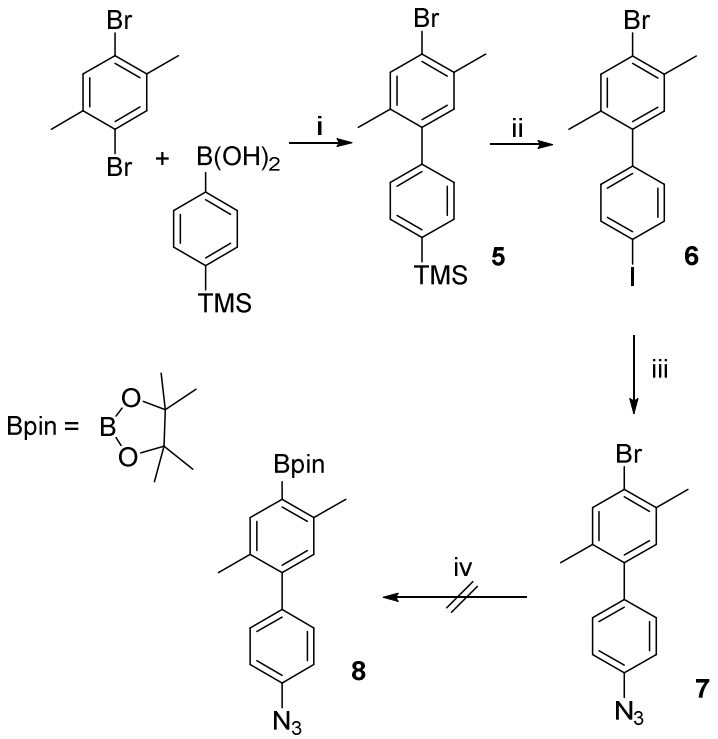

i) $Pd(PPh_3)_4$,Cs_2CO_3, toluene/H_2O, 98%
ii) ICl, CH_2Cl_2, 90%
iii) NaN_3, Cu, Ascorbic acid, *L*-Proline, *i*-$Propyl_2NH$/DMSO, 80 ºC, 43%
iv) B_2pin_2, $Pd(dppf)_2Cl_2$, KOAc, DME

Scheme I.11 Preparation of biphenyls building blocks.

The construction of the biphenyl building blocks started with the coupling of 1,4-dibromo-2,5-dimethylbenzene with *p*-trimethylsilyl phenylboronic acid to get biphenyl **5** in very good yield (98%). After this, exchange of the trimethyl silyl group in **5** was carried out by iodine, using iodine chloride as reagent and dichloromethane as solvent yielding compound **6** also in good yield (90%). Then, by following the procedure reported by Chen *et al*,[12] treatment with NaN_3 and metallic copper in the presence of ascorbic acid, afforded biphenyl derivative **7**. However, even when compound **7** was prepared in good yield (43%), only decomposition was observed during the transformation from bromine to pinacolate (scheme I.11).

Due to these negative results, we decided to carry out the synthesis of **10** through **9**, having the azide moiety protected (scheme I.12). Biphenyl **9** was prepared in good yield (50%) by following the procedure reported by Hierrezuelo *et al*.[7a] starting from 1,4-dibromo-2,5-dimethylbenzene and 4-(*N*-Boc-amino)phenylboronic acid, and the

[12] Chen, Y.; Zhuo, Z-J.; Cui, D.M.; Zhang, C. *J. Organomet. Chem.* **2014**, *749*, 215.

subsequent treatment of **9** with bis(pinacolate)diboron to exchange the bromine atom by the boropinacolate group yielded **10** in 77% (scheme I.12).

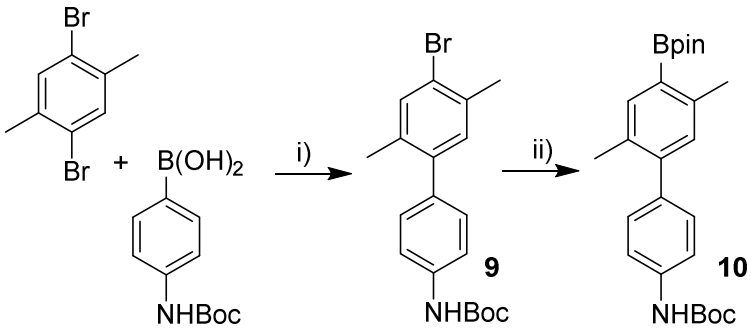

i) $Pd(PPh_3)_4$, $CsCO_3$, Toluene/H_2O, 50%
ii) B_2pin_2, $Pd(dppf)_2Cl_2$, KOAc, DME, 77%

Scheme I.12 Steps followed to obtain biphenyl **10**.

We have chosen a *N*-Boc moiety as the oligo(*p*-phenylene) tripod leg since the *N*-Boc protecting group can be easily deprotected and further converted into an azide group. Moreover, the presence of an amino or *N*-Boc group in the oligo(*p*-phenylene) guarantee the polarity of the molecule and therefore a good solubility.

As mentioned above, one of the key steps in the process of synthesis is the coupling of three units of **10** with **2** and **4**, under standard Suzuki conditions by using $Pd(PPh_3)_4$ as catalyst (scheme I.13). This reaction also allowed us to prepare the small tripods **11** and **13** in good yields (70%). Compound **11** was prepared using Ag_2CO_3 as the base, THF as solvent and the mixture was stirred during 12 h, while **13** was prepared without heating the mixture, by coupling **10** with **4** and using aqueous KOH as the base, toluene as the solvent and keeping the reaction overnight under reflux (scheme I.13).

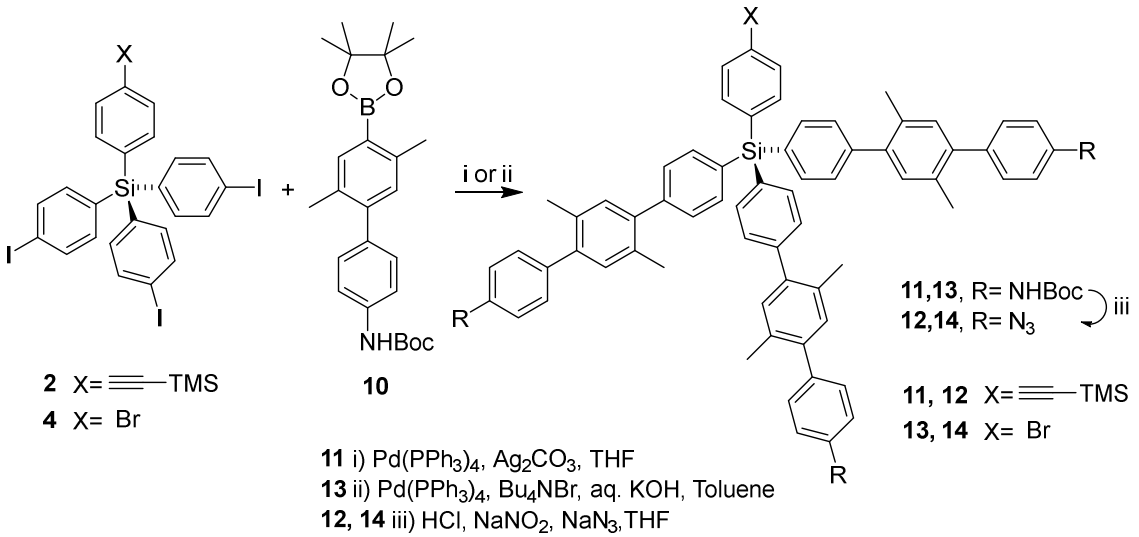

Scheme I.13 Synthesis of tripods **11**, **13** and **12**, **14** with azide-terminated groups.

As can be observed above, the three ends of the supporting legs in **12** and **14** are azide groups, which were generated in the last part of the synthesis. These compounds were prepared by treatment of **11** and **13**, respectively, with conc. HCl, $NaNO_2$ and NaN_3, as described in literature.[13] This is a one-pot reaction where HCl provides the deprotection of *N*-Boc moiety, to obtain the free amine groups, followed by their conversion into azide groups by using $NaNO_2$ and thereafter NaN_3. Both tripods **12** and **14** were obtained in good yields (50% and 65%, respectively).

Both tripods **12** and **14** were characterized based on their spectroscopic data. In the spectrum of ^{1}H NMR, performed in $CDCl_3$, of the precursor tripods **11** and **13** a singlet is observed around 1.54 ppm, which in both cases integrates by 27H, corresponding to the hydrogens of the 3 *t*-Bu groups of the *N*-Boc moiety, located in each leg. This group has its corresponding signal in the ^{13}C NMR spectrum at around 28 ppm on both tripods and an additional one at 80 ppm corresponding to the quaternary carbon of the *t*-Bu group. Chemical shifts from the *N*-Boc protecting group disappear in both the proton and carbon spectra for both tripods **12** and **14**, whose anchor groups are now azides (N_3). In addition, in the cases of tripods **11** and **12**, where the silicon core has a TMS group at the top, a signal is observed at 0.25 ppm corresponding to the three methyl groups on both tripods. In all cases, the singlets assigned to the six methyl groups present on the sides of the four molecules **11**, **12**, **13** and **14** are observed. For tripods **11** and **12**, two singlets are observed between 2.27 and 2.31 ppm, whereas in the case of tripods **13** and **14**, there are four singlets 2.26, 2.27, 2.31 and 2.34 ppm. However, these signals in ^{13}C NMR

[13] Lo, C.-N.; Hsu, C.-S. *J. Polym. Sci., Part A: Polym. Chem.* **2011**, *49*, 3355.

spectrum does not change, observing two chemical shifts 19.9 and 20.0 ppm in each spectrum.

On the other hand, in order to prepare tripod **21**, we carried out the homologation of the biphenyl **10** by reaction with **6** (scheme I.14) followed by the coupling with the silicon core **2** (scheme I.15). The amine protected quaterphenyl **15** was obtained in 41% yield, by coupling **10** with **6**; then boron bispinacolate substitution was readily achieved by treating **15** with bis(pinacolate)diboron in the presence of KOAc and $Pd(dppf)_2Cl_2$ as catalyst in DME to provide **16** in 50% yield (scheme I.14). Even when the solubility of quaterphenyls is limited,[7a] compounds **15** and **16** present a good solubility in organic solvents, which we attribute to the presence of *N*-Boc groups at one end of both molecules.

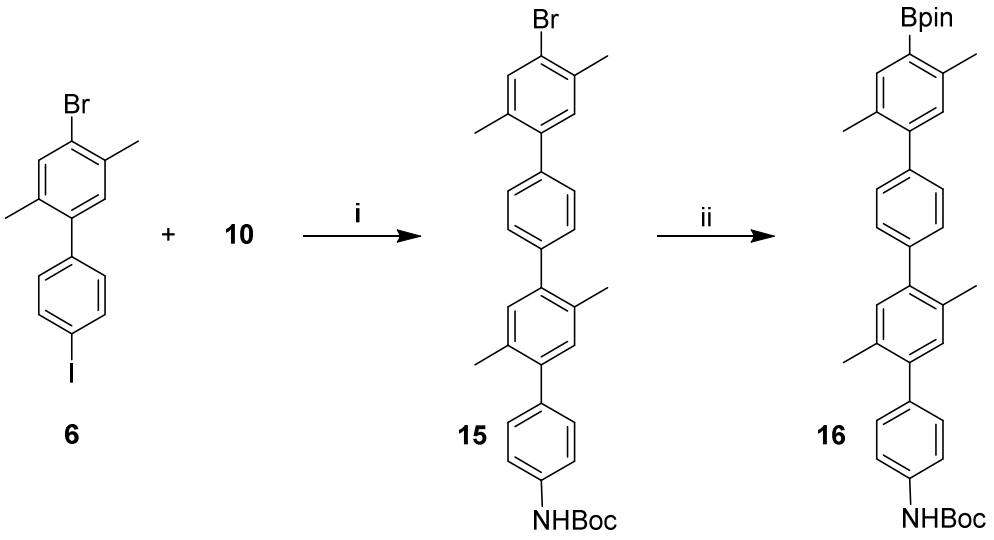

i) $Pd(PPh_3)_4$, Bu_4NBr, aq. KOH, Toluene, 41%
ii) B_2pin_2, $Pd(dppf)_2Cl_2$, KOAc, DME, 50%

Scheme I.14 Synthesis of quaterphenylenes **15** and **16**.

Coupling **16** with the triiodide **2** gave the TMS substituted and amine protected tripod **17** in 61% yield (scheme I.15). Furthermore, the TMS terminated functional arm in **17** could be used as substrate to perform click reaction for the incorporation of different architectures to be applied in several fields. As mentioned above, the designed tripod-shaped molecules with azide substitution were used as adsorbates in click reaction onto alkynyl modified silicon surfaces. For the synthesis of tripod-shaped oligo(*p*-phenylene) with five phenylene units, several attempts to deprotect *N*-Boc groups were carried out: by using from a stoichiometric amount to a large excess of concentrated HCl, and/or

from 0 ºC to refluxing the mixture from 48 to 72h. However, only a complex mixture of reaction was obtained, and unfortunately, compound **21** was not detected (scheme I.15).

We assumed that the increase of the legs length in **17** handicaps its reactivity sterically, and therefore, we decided to deprotect the amine group prior to the Suzuki coupling, when it is ubicated less sterically bulky.

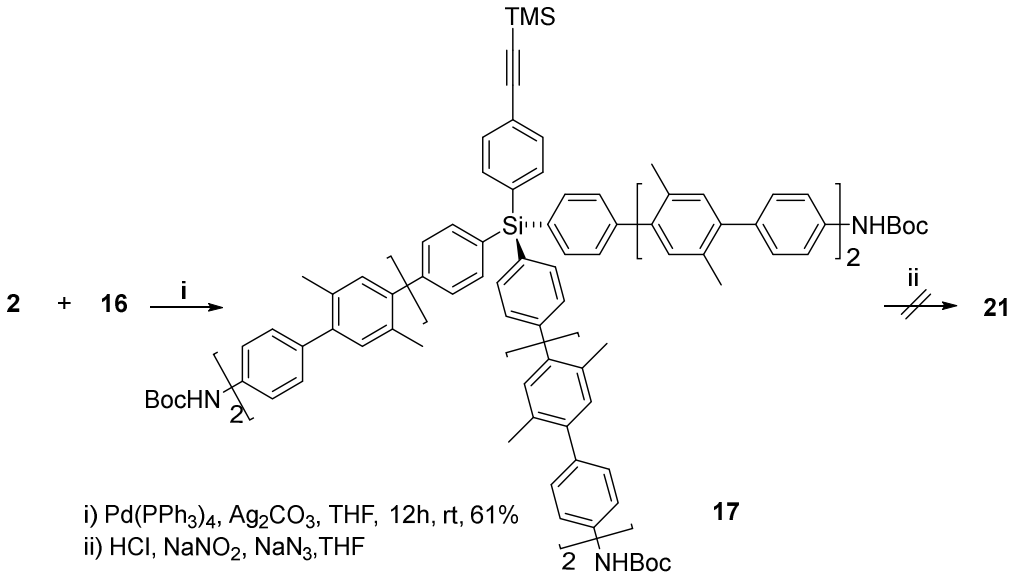

Scheme I.15 Synthesis of compound **17** and attempt of deprotection.

Therefore, when quaterphenyl **15** was treated with concentrated HCl, unprotected compound **18** was isolated. Subsequent reaction of **18** with bis(pinacolate)diboron in the presence of KOAc and $Pd(dppf)_2Cl_2$ as a catalyst in DME gave compound **19** (scheme I.16).

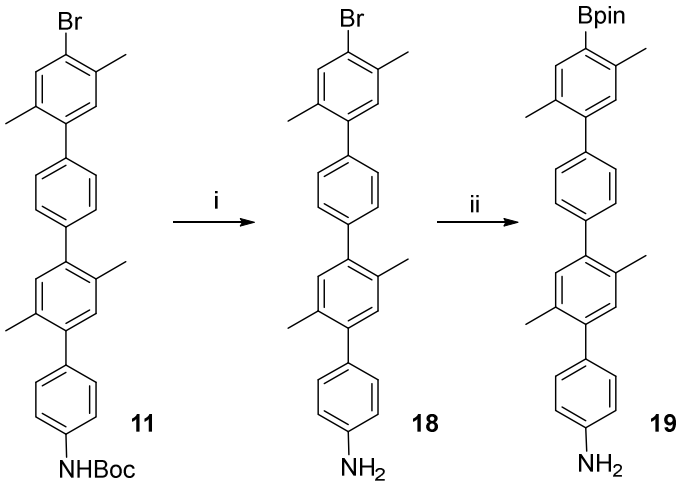

i) conc. HCl/THF, 88%
ii) B_2pin_2, $Pd(dppf)_2Cl_2$, KOAc, DME, 80%

Scheme I.16 Preparation of **19**.

As it is well known, amine functionality is compatible with both the Suzuki reaction with a bispinacolate derivative or a boronic acid.[14] Consequently, the coupling of **2** and **19** under standard Suzuki conditions provided the tripod-shaped molecule **20** (scheme I.17). Finally, amine group was successfully converted into azide by treatment with sodium azide and sodium nitrite in acidic THF, thus obtaining compound **21**.

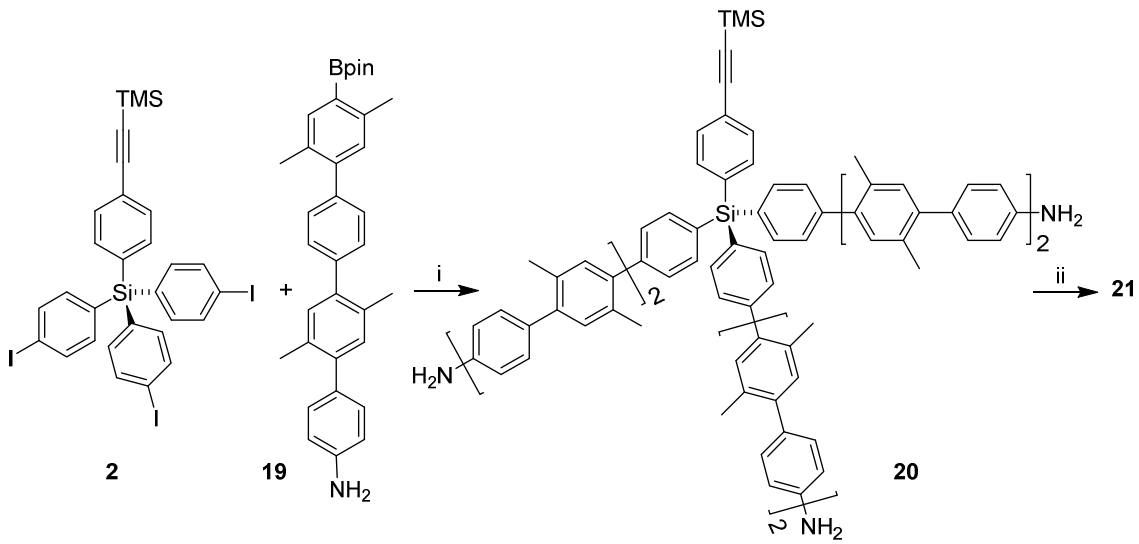

i) $Pd(PPh_3)_4$, Ag_2CO_3, THF, 12h, rt, 37%
ii) HCl, $NaNO_2$, NaN_3,THF, 54%

Scheme I.17 Synthesis of tripods **20** and **21**.

[14] Su, P.; Wang, J.; Shi, Y.; Pan, X.; Shao, R.; Zhang, J. *Bioorg. & Med. Chem* **2015**, 23, 3228.

Tripods **20** and **21** were characterized by their spectroscopic data. In the spectrum of ^{1}H NMR performed in $CDCl_3$, for both compounds, a singlet signal is observed at 0.30 ppm that integrates by 9H, corresponding to the TMS group in the silicon core. For both tripods, it can also be observed between 2.20-2.40 ppm four singlet signals that integrate by 36H, which are assigned to the six side methyl groups located on each leg. In addition, in tripod **20** spectra a broad singlet appears at 3.40 ppm, which integrates by 6H and which is assigned to the hydrogens of the free amino groups. The most significant thing to note is the chemical shift observed in the aromatic part. Where for **20** there is a doublet at 6.77 ppm that integrates by 6H, in **21** it moves up to 7.10 ppm, being the corresponding hydrogens in ortho position with respect to the amino and azido group. Because any change in the chemical environment will be translated into a change in the chemical shift in NMR spectra.

Likewise, in carbon spectrum for both molecules can be found the 26 signals corresponding to the carbon atoms present in the molecule. At 0.0 ppm we observe the signal assigned to the TMS group, between 19.9 and 20.0 ppm two signals corresponding to the side methyl groups and, in the aromatic part, the rest of carbons.

I.3 Synthesis of tripods with thioacetate groups as headgroups

The retrosynthetic strategy is displayed in figure I.9, and consists of the construction of the tetraphenylsilane tripod-shaped structure in two steps. First, the three identical oligo(*p*-phenylene) subunits (with the appropriate length: 1 or 3 phenyl gropus), bearing a substituent enabling the later introduction of the anchor group, are bonded by Suzuki cross-coupling reaction to the silicon core. The coupling partners are a boron derivative and an aryl halide, in the presence of a palladium complex as catalyst. The second step is the conversion of the protected hydroxyl end-capped group into the anchor group itself, by the well-known Mitsunobu reaction. It is necessary to use an acidic nucleophile to protonate one of the reagent (DIAD) to prevent from side reactions.

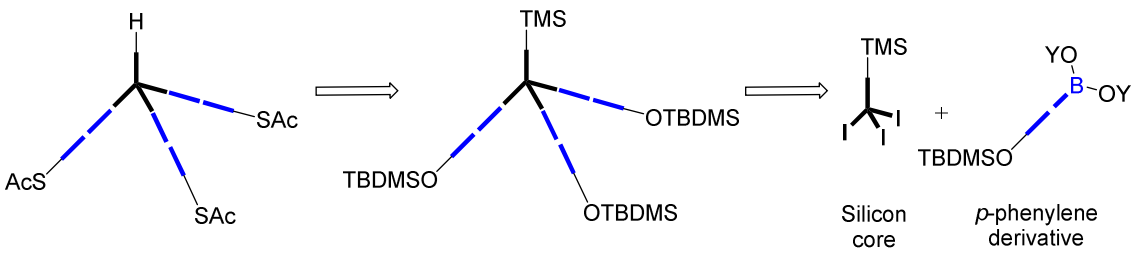

Figure I.9 Retrosynthetic analysis of tetraphenylsilane platforms.

This approach provides the corresponding tripods with the last phenyl substituent exposing an acetyl-protected thiol group in the *meta* position. Subsequent and *in situ* deprotection of this functional group, during the SAM preparation process, will allow its transformation into the thiol group to be attached onto gold substrates. Following this method, we carried out the synthesis of tripods **26** and **31** in good yields: **26** has two phenylene units in each leg, while **31** has four (figure I. 10). They have been designed in this way to test if there is noticeably difference of behaviour in the self-assembly process on gold substrates.

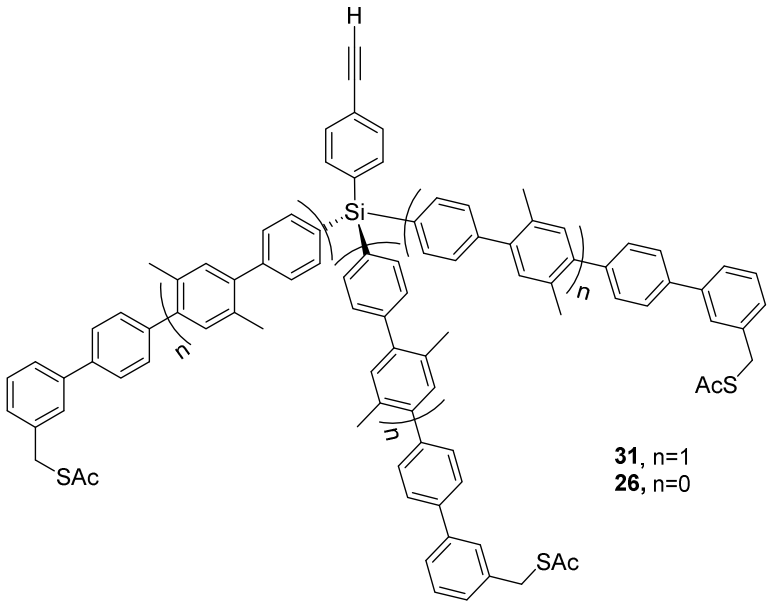

Figure I.10 Target molecules of this section, **26** and **31** with SAc groups.

In this section, we propose as silicon core **2**, (according to the reaction sequence indicated in scheme I.10) since it has a phenylacetylene group that can be further functionalized by click reaction with an azide moiety once it is deposited on the metal surface. Although at first, the preparation of **22** (scheme I.18) was carried out to use it as an anchor group in these molecules, its employment was discarded when treating S-(4-bromophenyl)ethanethioate with bis(pinacolate)diboron did not afforded the desired product **22** (scheme I.18). Therefore, it was decided to introduce the thioacetate group in the final part of the synthesis.

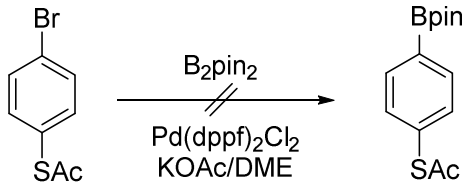

22

Scheme I.18 Unsuccessful synthesis of **22**

The preparation of tripod **26** started with the formation of the boronic ester **23**, derived from *t*-butyldimethylsilane (TBDMS). The synthesis was carried out from the commercial available pinacolate by treatment with *t*-butyldimethylsilane chloride, in the presence of DMAP.

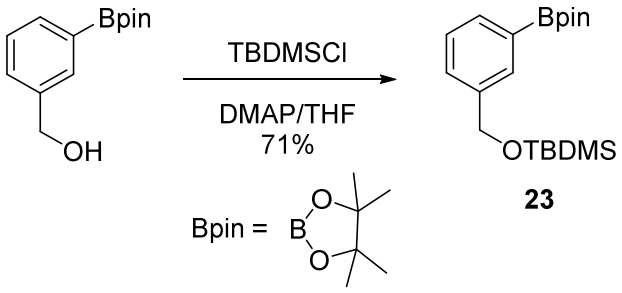

23

Scheme I. 19 Protection of hydroxyl group, obtaining molecule **23**.

Subsequent coupling between **2** and **23**, (scheme I.20) via Suzuki conditions, employing Pd(0) as catalyst, $AgCO_3$ as base and THF as solvent afforded tripod **24** end-capped with TBDMS groups.

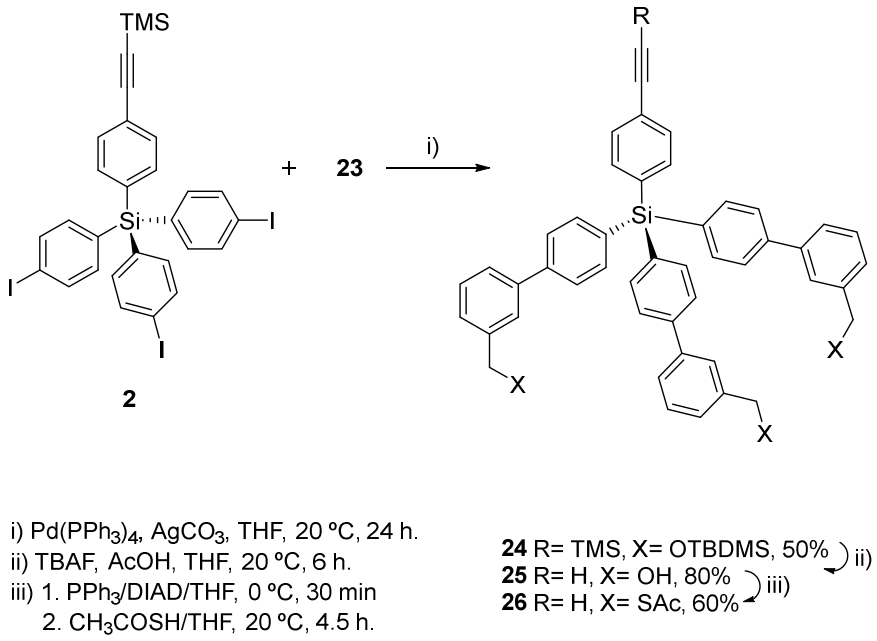

Scheme I.20 Synthesis of tripods **24**, **25** and **26**.

Later deprotection of **24** by means of a strong nucleophile such as TBAF in acetic acid, allowed the release of hydroxyl groups thus obtaining tripod **25**. Note that, in this strong conditions, the TMS-protected phenylacetylene group located at the top of the core, is also released. From this key intermediate, the final and interesting tripod **26** can be synthesized as described below. The triphenylphosphine is combined with DIAD to generate a phosphonium salt (intermediate) that binds to the alcohol oxygen, activating it as a leaving group. Substitution by the thioacetate derivative completes the Mitsunobu process.

Tripods **24**, **25** and **26** were characterized based on their spectroscopic data. The most important chemical shifts found in ^{1}H NMR and ^{13}C NMR spectra, between **24, 25** and **26**, are indicated in Table I.1:

Table I.1 Most relevant differences in chemical shifts for tripods **24**, **25** and **26**

Tripod (Functional group)	**24** ($CH_2OTBDMS$)	**25** (CH_2OH)	**26** (CH_2SAc)
^{1}H NMR δ (ppm)	4.69	4.76	4.17
^{13}C NMR δ (ppm)	65.1	65.4	33.5

Furthermore, is characteristic in tripods **25** and **26** the absence of the TMS group signal at 0.24 ppm for ^{1}H NMR and 0.0 ppm for ^{13}C NMR, which can be observed for tripod **24**, due to the double deprotection for both TMS and TBDMS groups when treating **24** with

TBAF. With respect to carbon spectra, in all cases we find the set of signals relative to all the non-equivalent carbons of the molecules. And for tripod **24**, the chemical shifts of dimethylsilyl (DMS) and *t*-Bu groups are found at 26.1 ppm (for C-**C**H_3, t-Bu), 18.5 ppm (**C**-CH_3, t-Bu) and -5.1 ppm (for DMS).

The biggest tripod structures, compounds **29**, **30** and **31**, were also obtained by coupling the conveniently substituted oligo(*p*-phenylene) **28** with the triiodotetraphenylsilane **2**. The synthetic sequence that yields the oligo(*p*-phenylene) **28** with the appropriate length is detailed in scheme I.21. The reaction between **23** and **6** under standard Suzuki conditions using $Pd(PPh_3)_4$ as catalyst and KOH_{aq} as the base in toluene produced compound **27** (90%). Boron bispinacolate substitution was readily achieved by treating **27** with bis(pinacolate) diboron in the presence of KOAc and $Pd(dppf)_2Cl_2$ as catalyst in 1,2-dimetoxyethane (DME) to provide **28** in 90% yield.

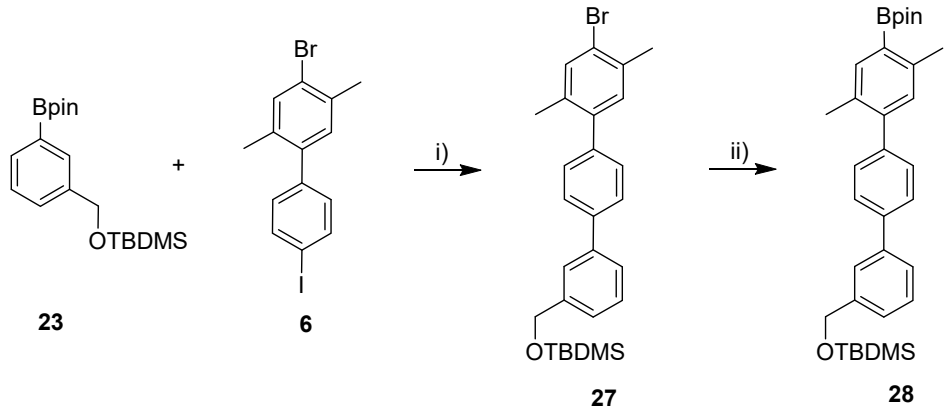

i) $Pd(PPh_3)_4$, KOH_{aq}, Bu_4NBr, toluene, 85 ºC; 90%
ii) B_2pin_2, $Pd(dppf)_2Cl_2$, KOAc, DME, reflux; 90%

Scheme I.21 Synthesis of compounds **27** and **28**.

Then, direct coupling of the silicon core **2** with **28** afforded protected tripod **29** in moderate yield (43%). After this, compound **29** was subjected to deprotection conditions by using TBAF and AcOH in THF providing compound **30** in 70% yield. Tripod **30** was then converted into **31** via Mitsunobu reation, by treatment with PPh_3 and DIAD followed by thioacetic acid in THF, giving the trithioacetate group in 81% yield (scheme I.22).

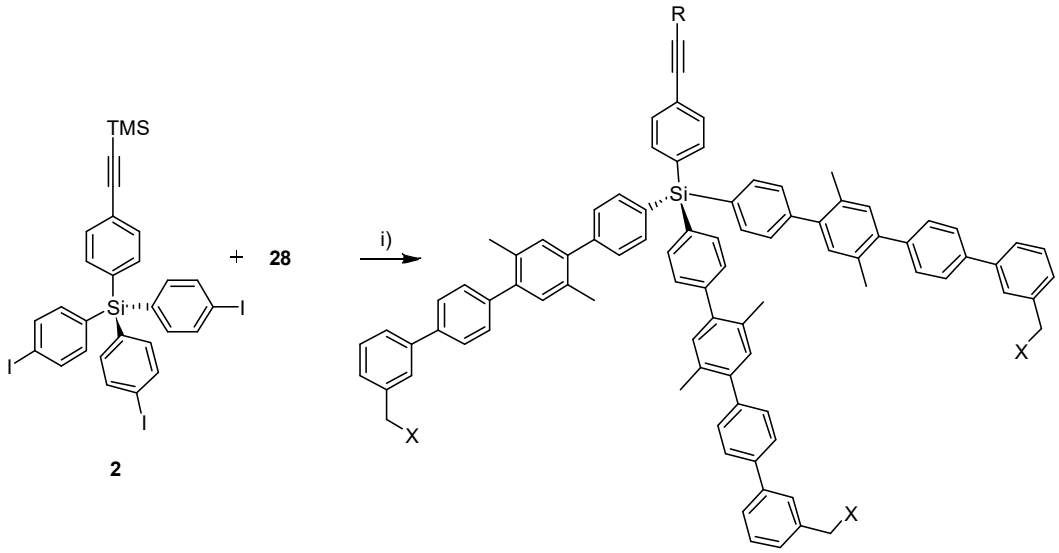

i) $Pd(PPh_3)_4$, $AgCO_3$, THF, 20 ºC, 24 h.
ii) TBAF, AcOH, THF, 20 ºC, 6 h.
iii) 1. PPh_3/DIAD/THF, 0 ºC, 30 min; 2. CH_3COSH/THF, 20 ºC, 4.5 h.

29, R= TMS, X= OTBDMS, 43% ii)
30, R= H, X= OH, 70% iii)
31, R= H, X= SAc, 81%

Scheme I.22 Synthesis of big tripod-shaped molecules **29**, **30** and **31**.

In this series of compounds, designed for gold substrates modification, the thioacetyl protecting group offers an improvement in the storage and handling of these molecules, preventing polymerization through intermolecular disulfide bonds. Tripod-shaped molecules **26** and **31** were used for the modification of gold substrates with *in situ* deprotection during the self-assembly process.

Compound **31** was characterized according to its spectroscopic data. In the ^{1}H NMR spectrum, it can be observed the corresponding signals to all hydrogen atoms present in the structure (80 H), including a singlet signal at 2.36 ppm, which integrates by nine protons, and is assigned to the three CH_3 groups in the tioacetate moities (SAc). Again here and for tripods **29**, **30** and **31**, the most important differences with respect chemical shifts found in ^{1}H NMR and ^{13}C NMR spectra, are shown in Table I.2:

Table I.2 Most relevant differences in chemical shifts for tripods **29**, **30** and **31**.

Tripod (Functional group)	**29** (CH_2OTBDMS)	**30** (CH_2OH)	**31** (CH_2SAc)
^{1}H NMR δ (ppm)	4.82	4.78	4.20
^{13}C NMR δ (ppm)	65.1	65.4	33.5

In the ^{13}C-NMR spectrum, the whole carbon atoms present in the molecule are assigned, highlighting as the most representative signals, the 30.3 ppm signal which corresponds to the three CH_3 from SAc groups, the signal at 33.5 ppm corresponding to the three methylene groups present in the molecule and the signal at 195.1 ppm assigned to the carbons of the three C=O groups.

I.4 Synthesis of tripods laterally substituted with ethylene glycols.

The purpose of this section is to prepare tripod-shaped molecules presenting the three legs connected with ethylene glycol groups. This goal is based in two fundamental objectives. The first of them is the fact that joining the legs, as shown in figure I.11, will provides a greater stabilization and rigidity of the structure desired upon immobilization onto the surface. In this way, the legs would have less freedom of movement and the effectiveness of the tripod attachment by three anchor points would increase. The second objective relies on the employment of ethylene glycols as joint molecules. We must develop modified tripod molecules with appropriate side chains to avoid non-specifically interaction with protein molecules, for biological application. Due to the hydrophobic tripod framework, in some cases are known to interact nonspecifically with protein molecules, thus interfering with the specific interaction of target molecules with the ligand on the focal point of the tripod. To overcome this problem, we have design a tripod-shaped molecule (figure I.11) with three phenylene units in each leg, TMS as end-capped groups and tetraethylene glycol (OEG_4) as joint molecules. Likewise, the radical X may be bromine or alkynyl-TMS, depending on the reaction conditions used (figure I.11).

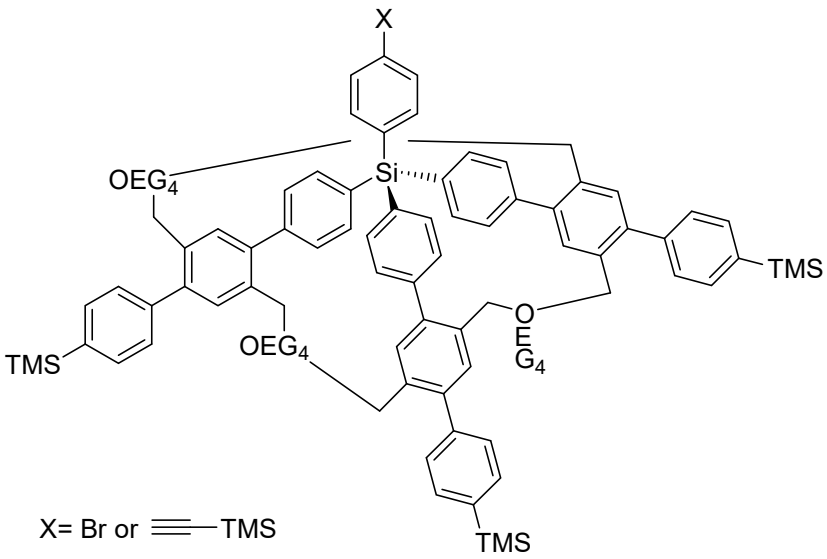

Figure I.11 Tripod-shaped molecules with the three legs joint by tetraethylenglycol units.

To carry out the synthesis of these molecules we first prepared the biphenyl **32** by following the same procedure outlined for molecule **10**. Thus, bromide **5** (previously prepared in section I.**2**) was treated with bis(pinacolate)diboron in the presence of

potassium acetate (KOAc) and $Pd(dppf)_2Cl_2$ as catalyst in DME to provide **32** in good yield, 80% (scheme I.23).

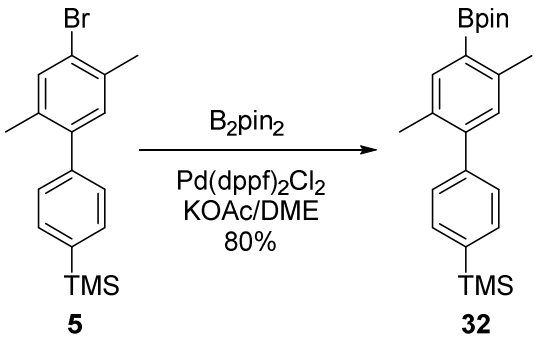

Scheme I.23 Preparation of biphenyl building block **32**.

Coupling **32** with triiodide **4** gave the tripod **33** in 40% yield, by using the same conditions as for tripod **13** (scheme I.24). We chose dimethylated *p*-biphenyl as the tripod leg since it can be easily brominated on the methylgroups, allowing further functionalization. Moreover, the TMS terminated *p*-phenylenes could be exchanged with an iodine atom that can be used to apply for various functionalities.

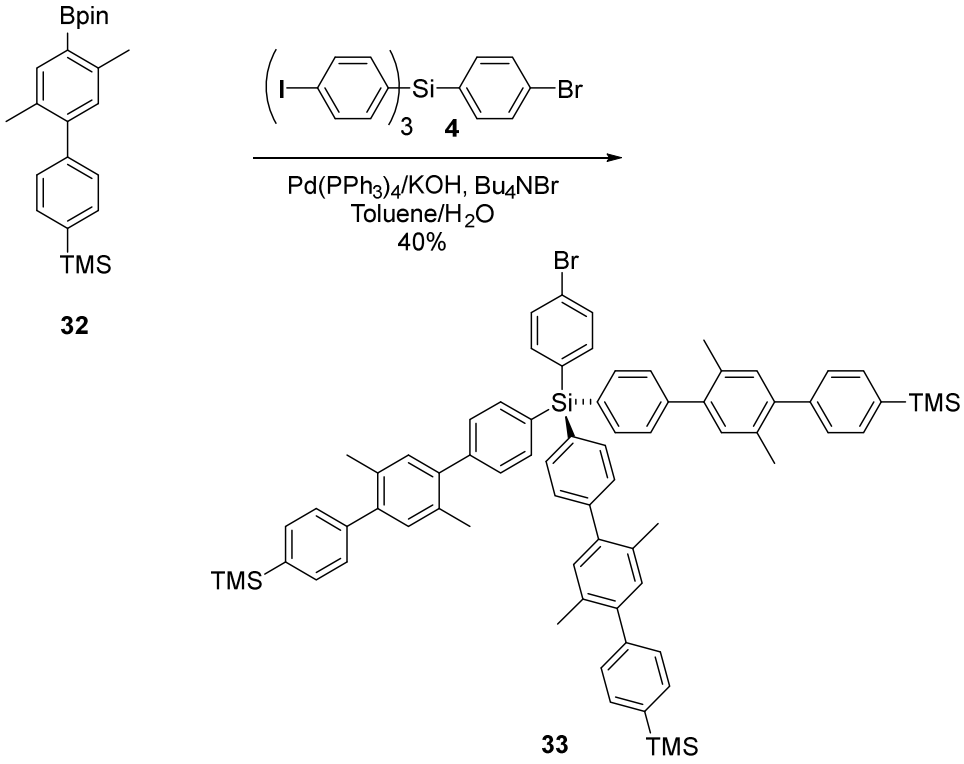

Scheme I.24 Synthesis of tripod **33**.

Derivatization of the methyl groups in tripod **33** was performed by benzylic bromination, catalyzed with AIBN, in the presence of NBS and refluxing in CCl_4, thus obtaining hexabromo derivative tripod **34** in moderate yield (40%, scheme I.25).

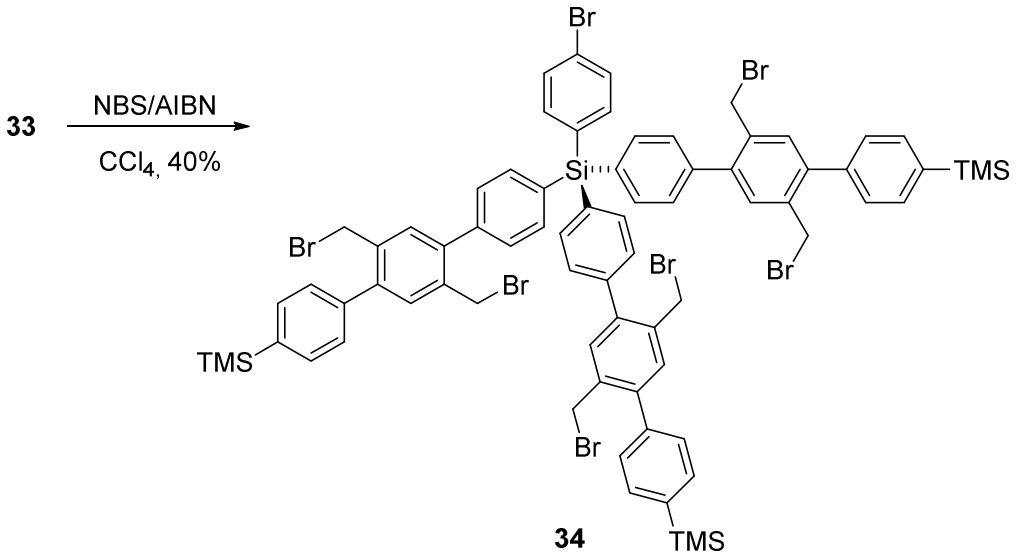

Scheme I.25 Synthesis of tripod **34**.

Therefore, the synthesis of OEG_4 substituted tripod was performed by coupling of **34** with comercial tetraethylene glycol (OEG_4). To carried out this synthesis, sodium salt was prepared first by mixing metallic sodium portions and OEG_4 in toluene at 0 ºC. Once the salt was formed, tripod **34** was then added to the mixture of reaction. However, not all the benzylic positions could be substituted and joint, thus obtaining **35** in 30% yield (scheme I.26).

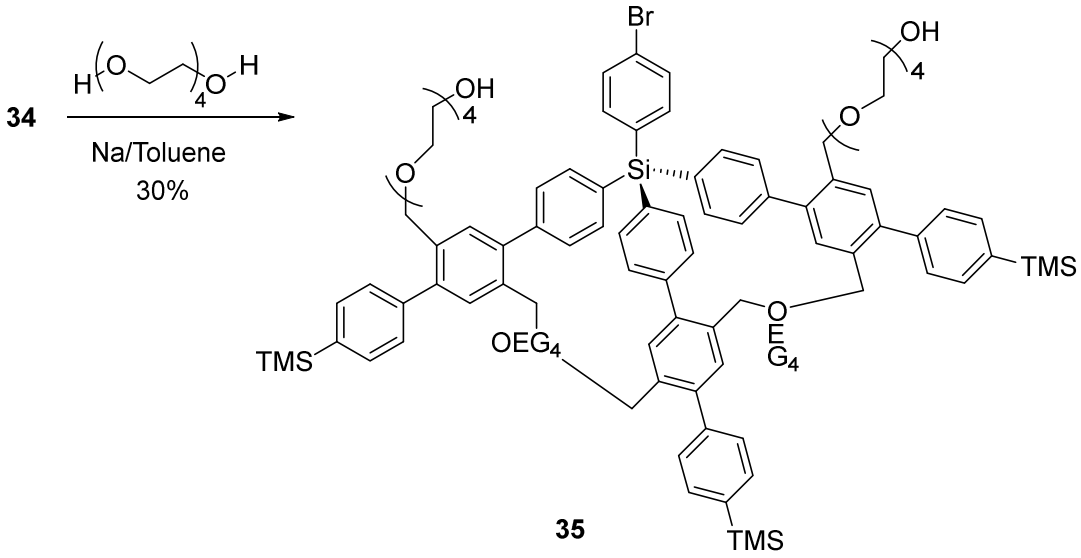

Scheme I.26 Synthesis of tripod **35**.

The synthetic sequence was then performed to prepare tripod-shaped molecule **38**, having an alkynyl-TMS group located on the core and the three legs joint by tetraethylene glycol molecules (figure I.11).

The synthethis was carried out in the same manner as for the tripod **35**, but in this case by using the silicon core **2** in the first step, where the coupling between the **2** and three units of **32** is already implement (scheme I.27). In this case, the Suzuki conditions employed for the coupling were those that have been previously described for tripod **17**.

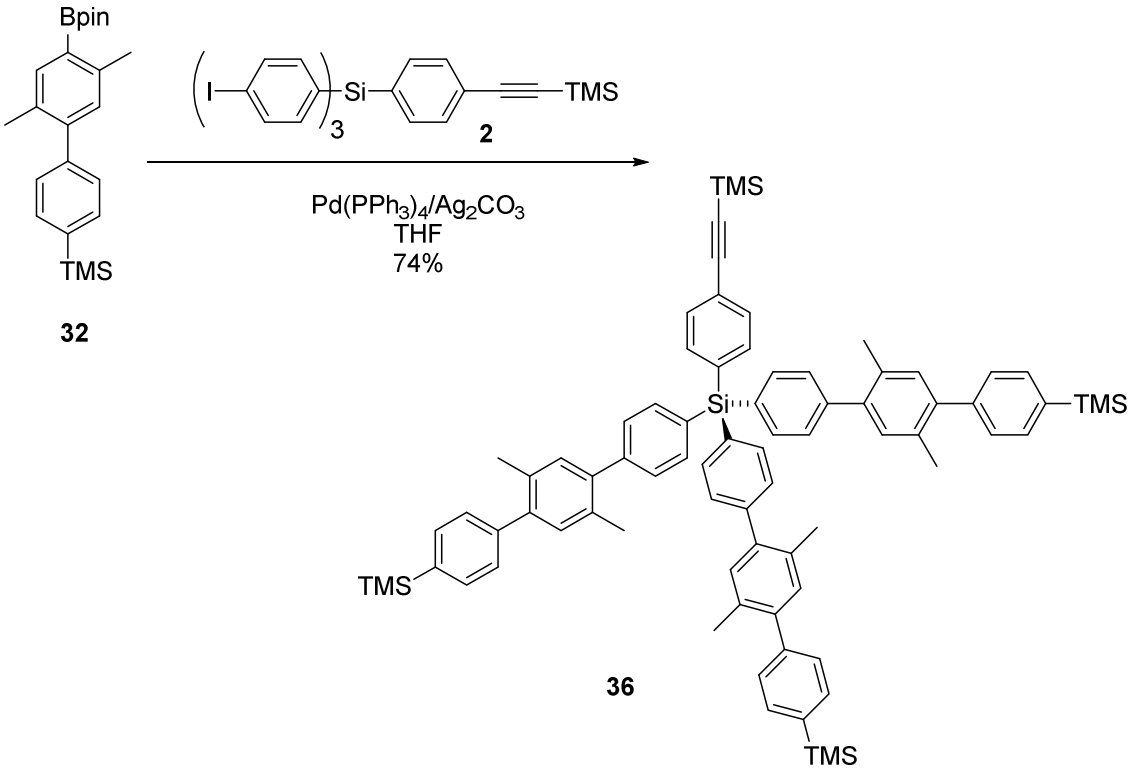

Scheme I.27 Synthesis of tripod **36**.

In this tripod, it can be observed two types of TMS groups, those located at the end of each leg and the one positioned on top of the silicon core. They can also be distinguished by ^{1}H NMR spectra, since TMS groups at the end of each leg have a singlet signal at 0.30 ppm which integrates by 27 H and, at 0.25 ppm, another singlet which integrates by 9 H corresponding to the one on top of the core.

Subsequent, treatment of **36** with NBS and AIBN in CCl_4, following the same conditions as for tripod **34**, afforded molecule **37** in good yield (65%, scheme I.28).

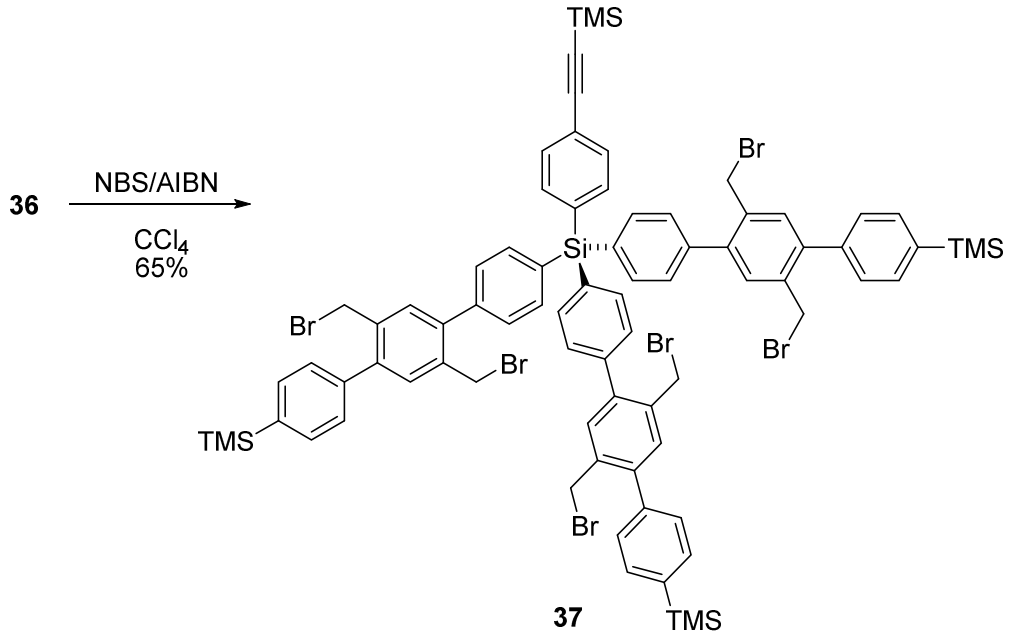

Scheme I.28 Synthesis of **37** by following the same procedure as for tripod **34**.

Finally, over this product **37** could be carried out, by treatment with sodium and tetraethylene glycol in toluene, the substitution and joint of the three legs with OEG_4, thus obtaining tripod **38** in moderate yield (30%, scheme I.29).

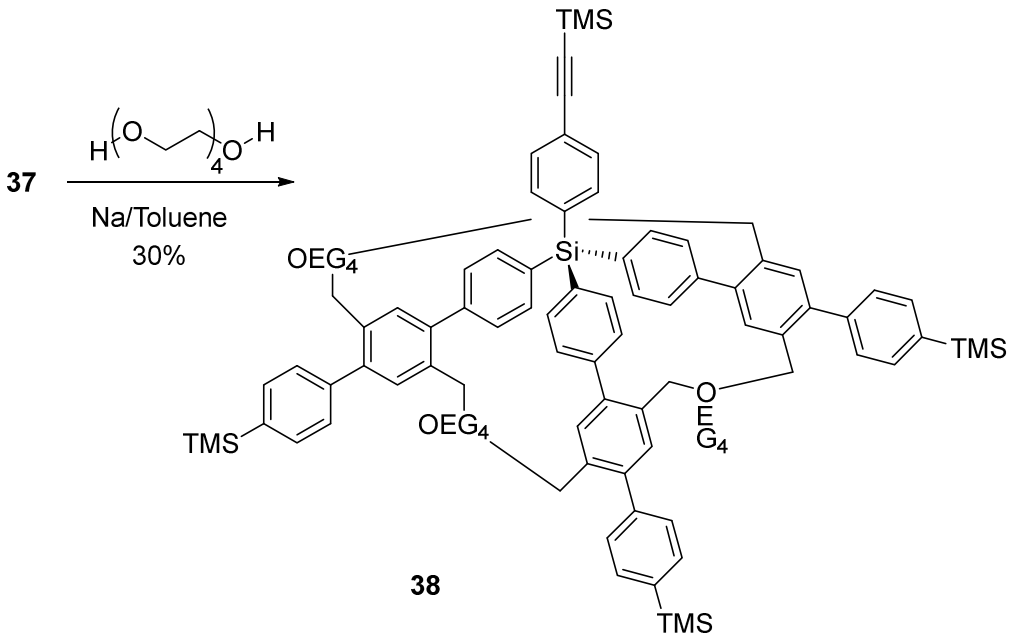

Scheme I.29 Synthesis of desired tripod **38**, with the three legs joint by OEG_4 molecules.

These tripods were characterized according to its spectroscopic data. First, the chemical change from **36** to **37** gave a characteristic shift in NMR signals (in both ^{1}H and ^{13}C NMR spectra) for the protons in CH_3 (2.31-2.29 ppm) which changed to CH_2Br groups (4.51-

4.48 ppm) in ^{1}H NMR, and from 20.0 ppm to 31.5 ppm for ^{13}C NMR spectra. Second, in the ^{1}H NMR spectrum for tripod **38**, performed in $CDCl_3$, all the signals corresponding to the hydrogen atoms present in the molecule are observed. The presence in the molecule of the TMS groups is confirmed when two singlet signals appear at 0.31 and 0.26 ppm, integrated by 27 and 9 protons respectively, corresponding to the trimethyl groups located at both the core and the legs. Also, singlet at 4.50 ppm, integrated by 12H, assigned to the six methylene groups of the benzylic positions ($-CH_2O-$) groups from the side chains. Finally, a mutiplet at 3.65-3.52 ppm, integrating by 48H, which corresponds to all the hydrogens from OEG_4. Although in the ^{13}C NMR we were not able to see every carbon signal, the molecular mass of the compound was confirmed by its MALDI-TOF spectrum by observing the molecular ion [$M+Na^+$] 1781.339 m/z.

I.5 Synthesis of tripods laterally substituted with biphenylenes.

In the previous section, it has been detailed the procedure of synthesis of tripod **38**, which has the three legs joint with ethylene glycol groups. In this section, we extend the methodology to the preparation of tripod **39**, which includes biphenylenes as leg-connecting groups, showing the versatility of the method.

On this ocassion, the synthesis was carried out by using *p,p'*-biphenyl derivative as binding molecule. We chose this molecule to give greater rigidity to the tripod when compared to that with ethylene glycols units (**38**), since OEGs have a conformationally unrestricted structure. The target tripod of this section is presented in figure I.12, compound **39**.

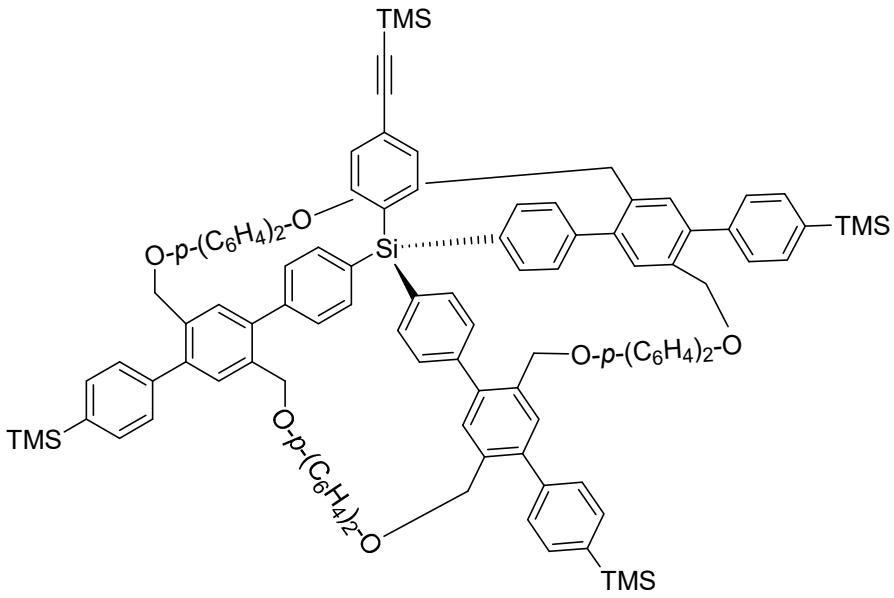

39

Figure I.12 Structure of tripod **39**.

The synthesis was accomplished by using tripod **36** as starting material. This compound was brominated at the benzilic positions (conditions referred in scheme I.28) and tripod **37** was obtained. Then, tripod **37** was treated with NaOH, [1,1'-biphenyl]-4,4'-diol, in a mixed solution of THF/etanol (1:1) (scheme I.30).[15]

[15] Wang, W.; Li, R.; Gokel, G. W. *Chem. Eur. J*. **2009**, *15*, 10543.

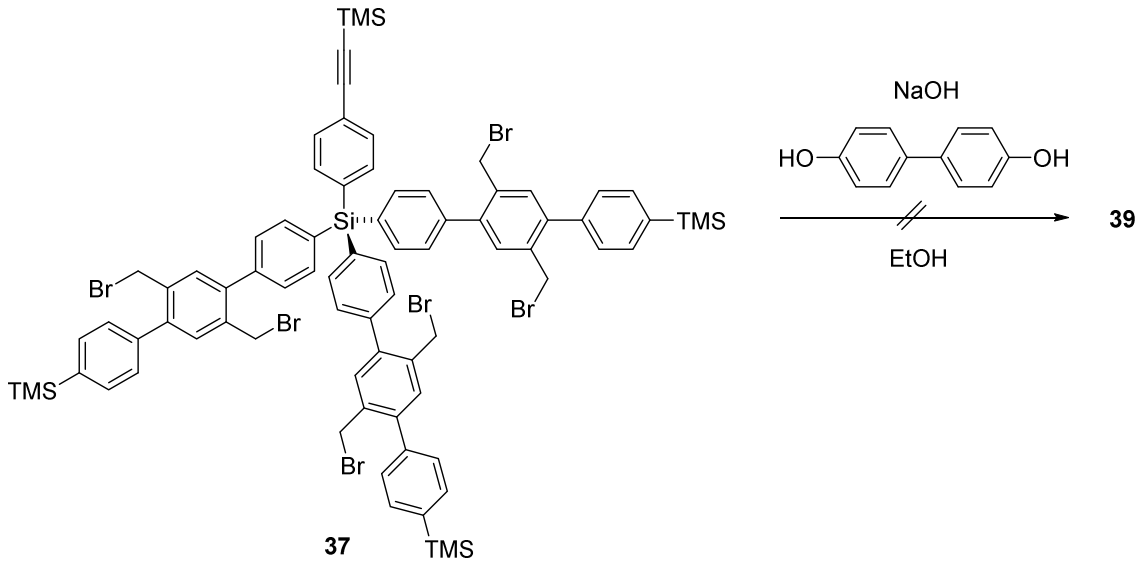

Scheme I.30 Failed synthesis of tripod **39**.

Unfortunately, tripod **39** was not isolated, since we could only corroborate by NMR data the degradation product after purification by column cromatography. We attribute this fact to the strong basic conditions of this reation.

I.6 Synthesis of tripods with cromophore groups.

In comparison with other organic or inorganic materials having fluorescence capabilities, 2-(*N,N*-dimethylamino)benzyliden-1,3-indandione (DMABI) derivatives are easy to synthesize (typically by aldol reaction). However, an important challenge is the improvement of its chemical and photochemical stability, which is one of the principal motivations for the widespread application of these chromophores in the development of optoelectronic devices with the aim to be implemented in biolabeling and biomedicine purposes.[16,17]

An alternative to improve the optical capabilities of these materials is the optimization of the chemical structure and spectroscopic properties of the chromophores. In the case of DMABI, the optical properties can be optimized by including different substituents in their structures or by the modulation of their 3D structures. It has also been reported that by increasing the molecular weight and the number of phenyl groups in a molecule a better thermal sustainability can be obtained.[18]

In this section, we accomplished the synthesis of the tripod-shaped molecule **47** having a DMABI chromophore in the structure. The retrosynthetic analysis of compound **47** is shown in figure I.13. By this analysis, we first envisioned the synthesis by using as starting materials: 1,3-indandione, the asymmetric tetraphenylsilane **4** and the boronic acid pinacol ester **43**.

[16] Grzibovskis, R.; Latvels J.; Muzikante, I. *Mater. Sci. Eng*. **2011**, *23*, 012021.
[17] Acharya, S.; Krief, P.; Khodorkovsky, V.; Kotler, Z.; Berkovic G; Klug J. T.; Efrima S. *New J. Chem.* **2005**, *29*, 1049.
[18] a) Tokmakovs, A.; Rutkis, M.; Traskovskis, K.; Zarins, E.; Laipniece, L.; Kokars V.; Kampars, V. *IOP Conf. Ser.: Mater. Sci. Eng.* **2012**, *38*, 012034; b) Traskovskis, K.; Mihailovs, I.; Tokmakovs, A.; Jurgis, A.; Kokars V.; Rutkis, M. *J. Mater. Chem. A* **2012**, *22*, 11268.

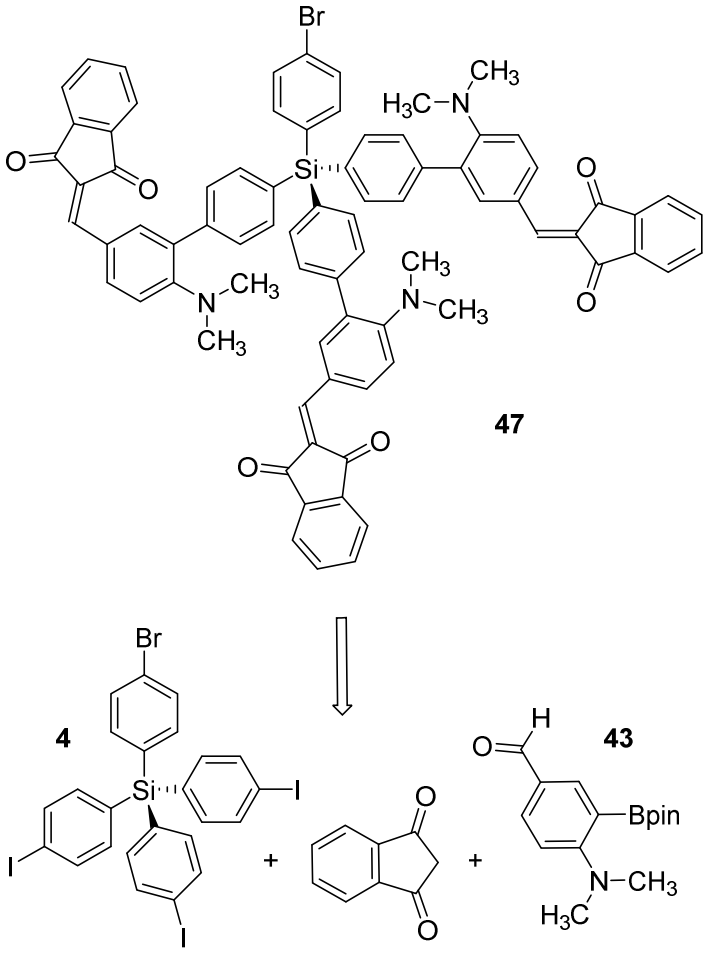

Figure I.13 Synthetic strategy to obtain tripod-shaped molecule **44**.

Firstly, we studied the preparation of compound **43** as the key product, analyzing its synthesis by following two different routes shown in scheme I.31. Both routes start from **40**, which was easily prepared by the bromination of commercial 4-(*N*,*N*-dimethylamino)benzaldehyde by treatment with NBS.

The first route (scheme I.31, Route I) presents as the first step the aldol condensation of 1,3-indandione with **40** to give **41**. This reaction gave **41** in 67% yield. However, the treatment of **41** with bis(pinacolate)diboron and $Pd(dppf)_2Cl_2$ as dcatalyst did not produce **42**, only the debromination product was isolated instead. As a second option (scheme I.31, Route II), the formation of the pinacolboronate **43** was planned as an alternative in the first step of the synthesis, followed by its aldol condensation with 1,3-indandione, likewise yielding **42**.

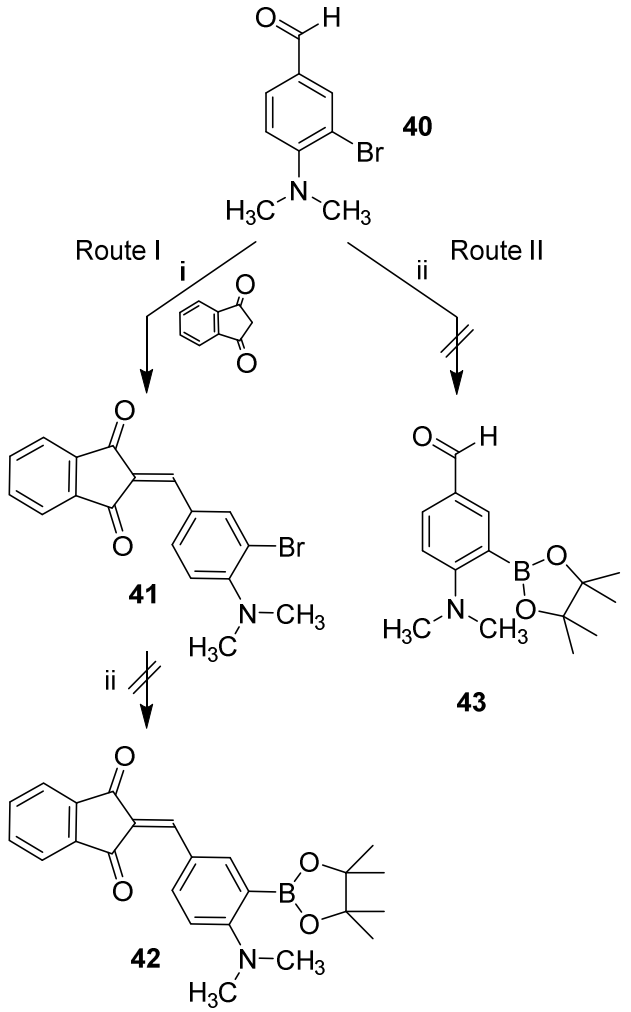

i. Piperidine/EtOH/reflux/3 h
ii. Bis(pinacolate)diboron, $Pd(dppf)_2Cl_2$, KOAc/DME / reflux / 18 h

Scheme I.31 Preparation of starting material through two unsuccessful routes.

Unfortunately, when **40** was treated with bis(pinacolate)diboron under the same conditions as above, only the debromination of this product was isolated. These results can be explained by the steric hindrance of the *N*,*N*-dimethylamino group present in **40** and also in **41**, which could avoid the bulky pinacolboronate substitution. Due to these negative results, we decided to prepare the boronic acid of 3-bromo-4-(*N*,*N*-dimethylamino)benzaldehyde (**45**, scheme I.32) where steric hindrances are not so strong. The successful synthesis of **45** was carried out by protecting the carbonyl group in **40** to obtain **44** (98% yield), followed by treatment with *n*-BuLi and trimethyl borate, as shown in scheme I.32.

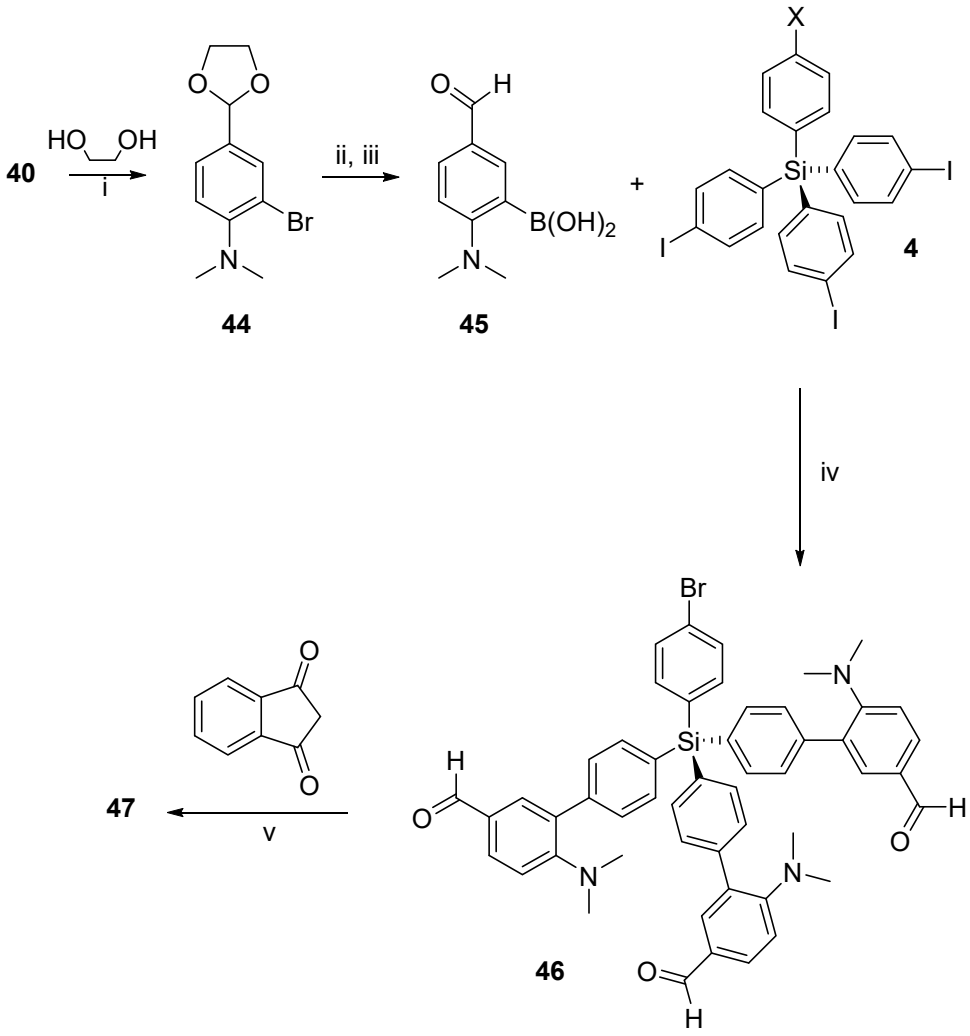

i. *p*-TsOH / toluene / reflux / 12 h, 98%
ii. 1) *n*-BuLi / THF / -78 ºC / 5 min; 2) trimethylborate / THF / -50 ºC / 2 h
iii. 1 M HCl / rt / 30 min
iv. $Pd(PPh_3)_4$, Cs_2CO_3 / toluene:methanol /reflux / 12 h, 87%
v. Piperidine / EtOH / reflux / 18 h, 29%

Scheme I.32 Synthesis of DMABI tripod **47**.

Compound **45** was obtained with a 97% overall yield. This aldehyde was then successfully coupled with compound **4** under Suzuki Miyaura reaction conditions, obtaining the tripod-shaped molecule **46** in 87% yield. The final reaction of **46** with 1,3-indandione, under aldol reaction conditions, in the presence of piperidine, afforded compound **47** in 29% yield. This compound presents three DMABI moieties in its structure. By following this strategy, the construction of the arms for the tripod and the chromophore derivative was achieved simultaneously.

Compound **47** is a solid that shows a strong absorption at 470 nm in the UV spectrum in AcOEt solution, which gives the compound a strong orange colour. It is also worth mentioning that chromophore **47** shows a high thermal stability with a melting point of 287 ºC without decomposition, which is much higher than that for pure DMABI molecules (231.7 ºC).

This new tripod was characterized by their spectroscopic data, highlighting in the ^{1}H NMR spectra, performed in $CDCl_3$, a singlet signal at 8.53 ppm integrating by three corresponding to the hydrogen atom from the vinyl system (multiplied by three legs). Several multiplets and doublets, located at the aromatic zone, integrate by all the aromatic hydrogens and, finally, at 2.79 ppm a big singlet, which integrates by 18H, corresponding to the NMe_2 groups in each leg. In the ^{13}C NMR spectrum, the whole carbon atoms present in the molecule are assigned, being the most representative those which correspond to the C=O groups at 190.1 and 190 ppm, also at 155.5 ppm the C-N signal appears and, at 42.7 ppm, the NMe_2 signal is observed. The molecular mass of the compound is confirmed by its HRMS spectrum by observing the molecular ion at 1239.3348 m/z.

I.6.1 Fluorescence measurements and 4CDNA sensing

Figure I.14 A shows the fluorescence spectra of tripod-shaped molecules **46** and **47**. Two maximum emission at about 543 nm for compound **47** and 470 nm for compound **46** were obtained, when excited at 470 and 343 nm, respectively.

Relevant information was obtained for compound **47** when a marked shift to red was observed (73 nm) in comparison to **46**, providing 0.43 eV of stabilization. The terminal 1,3-indandione moieties play an important role in tripod **47**, since it provides additional stabilization energy when compared to the starting molecule **46**. This additional stabilization is attributed to the close plane-to-plane distance between the neighbouring planar 1,3-indandione and benzene moieties, resulting in suitably strong intermolecular π^*–π^* interactions (providing a red-shift as observed in the absorption spectra in figure I.14 A). The quantum yields (QY) of the fluorescence in a dilute solution of ethyl acetate were calculated by using equation (1) (see Experimental section) and were 0.16 and 0.38 for compounds **46** and **47**, respectively. These data are in agreement with

previously reported studies, which suggest that an increase in QYs is favoured by the rigidity of the molecular structure.[19]

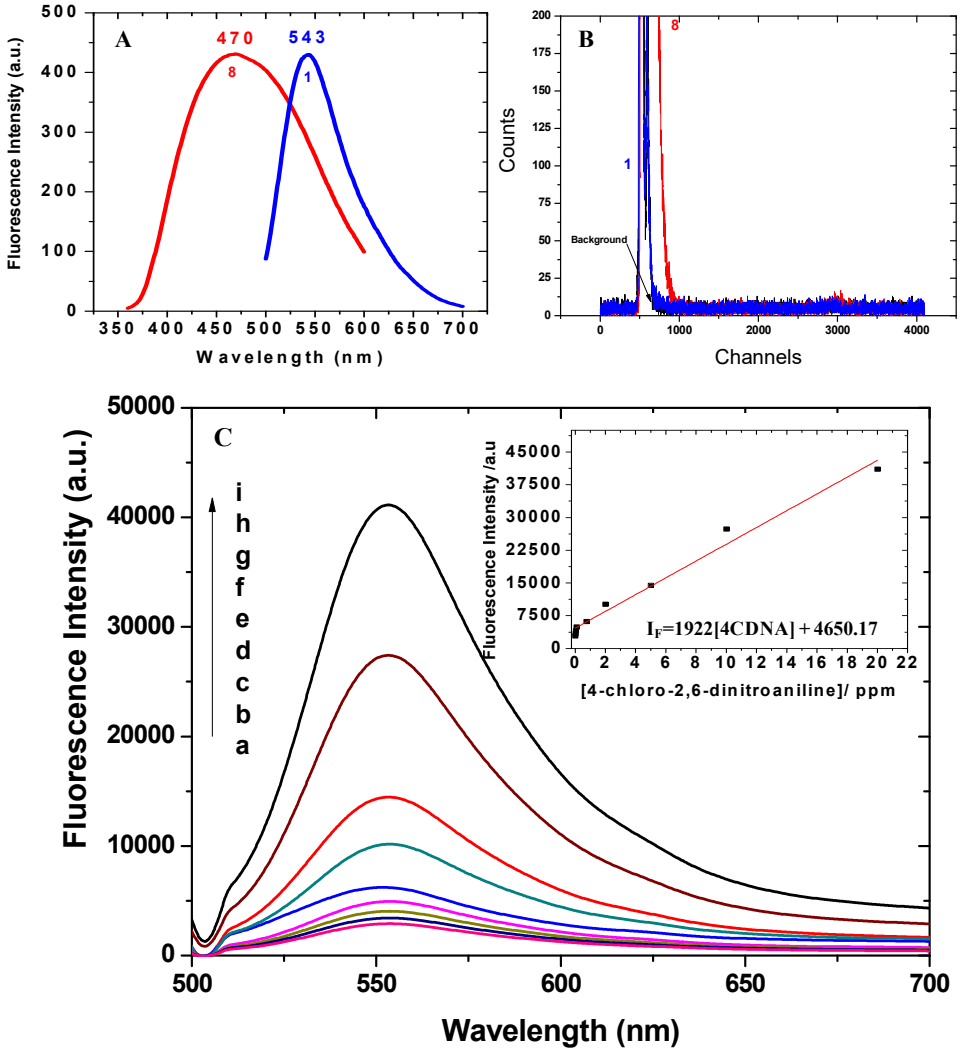

Figure I. 14 (A) Fluorescence intensity spectra of **46** (red line) and **47** (blue line) at 25 ºC in ethyl acetate (1:50). (B) Fluorescence decay curves of **47** and **46** (for compound **47**: λex=470 nm; λem=543 nm, slit widths: 5.5 nm). (C) Fluorescence spectra obtained when DMABI tripod **47** (200 mL, 0.1 M) was exposed to increasing concentrations of 4CDNA: (a) 0.001; (b) 0.01; (c) 0.05; (d) 0.1; (e) 0.75; (f) 2; (g) 5; (h) 10 and (i) 20 mg/ L, respectively. The inset shows the obtained calibration curve.

The photoluminescence features reveal typical characteristics of conjugated derivatives.[20] Intensity decay-time profiles of both tripods are shown in figure I.14 B, and

[19] Gulbinas, V.; Kodis, G.; Jursenas, S.; Valkunas, L.; Gruodis, A.; Mialocq, J. C.; Pommeret S.; Gustavsson, T. *J. Phys. Chem. A* **1999**, *103*, 3969.
[20] Wong, K. T.; Wang, C. F.; Chou, C. H.; Su, Y. O.; Lee G. H.; Peng, S. M. *Org. Lett.*, **2002**, *4*, 4439.

the corresponding measured lifetimes (τ_1 and τ_2) are shown in Table I.3. One and two component exponential-decay curves are detected for **47** and **46**, respectively, with lifetimes in the nanosecond range (parameters B_1, B_2, A and X^2 are fluorescence decay components in Table I.3). Furthermore, as a proof of concept, DMABI tripod **47** was assessed as a sensor probe for 4-chloro-2,6-dinitroaniline (4CDNA), a nitro-derivative compound which is used in the fabrication of explosive materials.[21]

Table I.3 Lifetime intensity decays corresponding to compounds **46** and **47**[a]

[a] In brackets the standard deviation of three measurements

	DMAB tripod **46**	DMABI tripod **47**
τ_1 (s)	5.74 x 10^{-10} (0.49)	1.48 x 10^{-10} (1.47)
τ_2 (s)	2.79 x 10^{-9} (0.07)	_
B_1	0.023 (3.32 x 10^{-4})	37.11 (0.08)
B_2	0.045 (3.30 x 10^{-4})	_
A	4.28 (0.025)	17.04 (0.34)
X^2	1.32	1.61

Figure I.14 C shows the emission spectra when DMABI tripod **47** (200 mL, 0.1 M) was exposed to increasing concentrations of 4CDNA, in the range from 0 to 20 mg/L. As can be observed, a remarkable fluorescence enhancement at about 553 nm is produced, reaching 15 times higher when a concentration of 20 mg/L of 4CDNA was used. A slightly small red shift (10 nm) was also observed, which can be explained by the polar micro-environment produced by -NO_2 substituents in 4CDNA. From the analysis of the fluorescence spectra (figure I.14 C), a linear dependence in the concentration range 0–20 mg/L was observed. The fluorescence enhancement versus 4CDNA concentration was successfully linearized (r = 0.98, the inset in figure I.14 C), with a limit of detection (LD) of 1.92 mg/L1 (8.82 x 10^{-6} M) and an accuracy (as Relative Standard Deviation) RSD = 1.92%. This fact opens up the possibility of sensing 4CDNA.

[21] Algarra, M.; Campos, B. B.; Miranda M. S.; Esteves da Silva, J. C. G. *Talanta*, **2011**, *83*, 1335.

I.7 Synthesis of spacers for the modification of silicon surfaces

In order to synthesize spacer compound **49** (scheme I.34), starting product **48** was employed. The synthesis of this compound **48** was carried out in a first step, by treatment of tetraethylen glycol with a 50% solution of NaOH to obtain the sodium salt at one end of the chain. Then, by substitution with 11-bromoundec-1-ene and heating during two hours, compound **48** was finally obtained with 83% yield (scheme I.33).

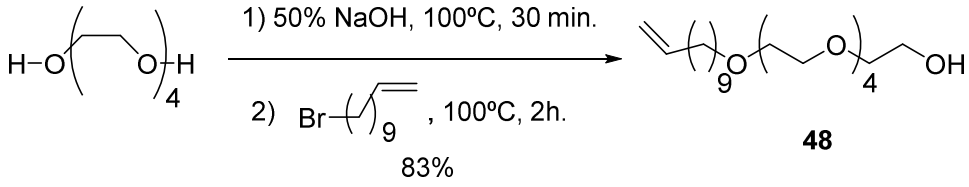

Scheme I.33 Synthesis of spacer precursor **48**.

The synthesis of spacer **49** was accomplished in two steps (scheme I.34). Firstly, treatment of **48** with sodium hydride as base to form the corresponding sodium salt. And, secondly substitution with propargyl bromide was readily achieved to get compound **49**, whose employment is explained in the next chapter for the modification of silicon surfaces.

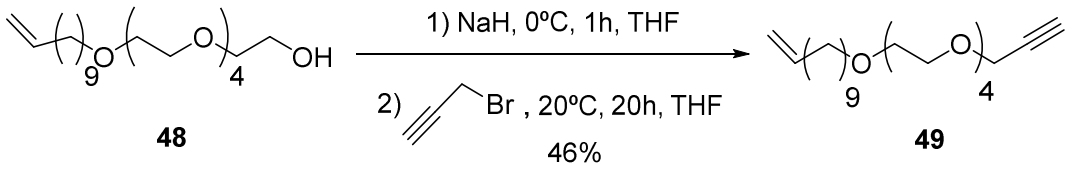

Scheme I.34 Synthesis of compound **49**

This molecule **49** is designed in order to be immobilized by photo-activated hydrosilylation reaction onto H-Si(111) substrates fabricating a clickable silicon surface. As the H-Si(111) surface is hydrophobic (water contact angle approx. 90 ºC; far from hydrophilic) the hydrosilylation reaction of compound **49** would be performed on the alkene edge, resulting in an alkynyl-terminated substrate, because the presence of four oligo(ethylene glycol) units is closer to the alkynyl groups.

I.8 Synthesis of theophylline derivatives

The target molecule in this section is theophylline **52** (scheme I.37), where a terminal azide group having a tetraethylene glycol spacer is incorporated at the position 7 of the theophylline moiety. Azide moiety can be used as a linking group to the tripod-shaped molucules having an alkyne residue as active tail group.

The preparation has been carried out in three steps detailed in schemes I.35-37. First, **50** was prepared in a substantially quantitative manner by ditosylation of tetraethylene glycol with excess of tosyl chloride and in the presence of DMAP (scheme I.35).

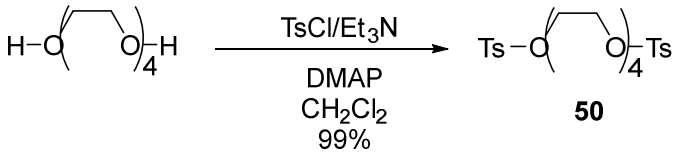

Scheme I.35 Synthesis of ditosylated derivative compound **50.**

Then, the theophylline reaction was carried out with **50** to obtain **51**. Thus, compound **50** was subjected to react with the sodium salt of theophylline obtained by treating it with NaH in DMF. Precursor theophylline **51** were obtained in moderate yield (50%, scheme I.36).

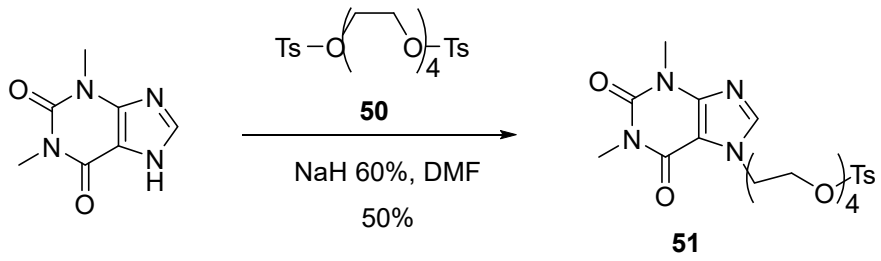

Scheme I.36 Synthesis of precursor theophylline **51**.

In the third step, the reaction of theophylline **51** with sodium azide was carried out, thus isolating compound **52** in 33% yield (scheme I.37).

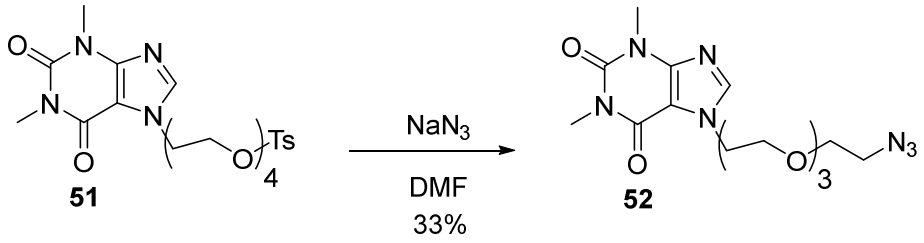

Scheme I.37 Synthesis of theophylline **52**.

Compound **52** is characterized based on its spectroscopic data. In the ^{1}H NMR spectrum, performed in $CDCl_3$, two singlets are observed at 3.39 and 3.62 ppm, which integrates by 3H each, corresponding to the hydrogens of the NMe groups. At 4.49-3.58 appears a multiplet signal, integrating by 16H, corresponding to the eight CH_2 groups of the tetraethylene glycol spacer. Finally, in the aromatic part a singlet appears at 7.69 ppm, which integrates by 1H and is assigned to the hydrogen atom in position 8 of theophylline.

In the ^{13}C NMR spectrum of **52** performed in $CDCl_3$, the signals corresponding to the carbon atoms of the NMe groups of theophylline are observed at 27.9 ppm and 29.8 ppm. At 46.8 ppm, the carbon of the ethylene glycol chain attached to the azide group is assigned. At 50.6 ppm, the carbon of the ethylene glycol chain attached to the nitrogen at position 7 of the theophylline is assigned. Between 69.4 ppm and 70.7 ppm, the rest of signals corresponding to carbon atoms of the ethylene glycol moiety are assigned. In the aromatic part of the spectrum, the signals due to the carbon atoms of the xanthine skeleton are observed and at 151.7 and 155.4 ppm appear the signals that correspond to the double bond of the carbonyls present in the molecule.

The molecular mass of the compound is confirmed by its HRMS spectrum by observing the molecular ion (M^{+}+Na) at 404.1667 m/z.

CHAPTER II. MODIFICATION OF METALLIC SURFACES

CHAPTER II. Modification of Metallic Surfaces

In this chapter, the most relevant methods for the modification of metallic surfaces, such as silicon and gold substrates, are described. Furthermore, our obtained results for the covalent grafting of the tripodal molecules synthesized in chapter I is discussed, including the optimization of the developed procedure. Finally, the modified nanostructured templates are modified by covalent incorporation of theophylline active molecules and the resulting films are tested for specific protein adsorption, verifying the validity and reliability of the presented concept, in terms of tripodal design and "activation" of the surface by click reaction.

Characterization of the prepared surfaces has been carried out by X-Ray Photoelectron Spectroscopy (XPS), Near-Edge X-Ray Absorption Fine structure (NEXAFS) Spectroscopy, Atomic Force Microscopy (AFM), Bright-Field Optical Transmission Microscopy (Confocal), including structural calculations by using the Density Functional Theory (DFT).

II.1 Background

As discussed in the objectives of this Thesis, this work aims to address the development of hybrid structures with enhanced biocompatibility and, therefore, use them in biological environments. Another aim is to perform an appropriate nanostructuring to achieve maximum effectiveness towards the monitorization of interactions and, finally, to achieve the surface functionalization that allows the analysis of defined biological interactions.

The preparation and characterization of new organic materials for the construction of nanoscale structures to properly modify different surfaces, constitutes one of the priority areas in the current research.[1] In case of surface modification by constructing monolayers of organic molecules, is fundamental to control the orientation and spacing between the functional groups -already adsorbed on the surfaces- and to have reliable methods for the derivatization of the organic surface. Among these methods, click and Suzuki reactions are often used.

[1] Bhushan, B., Ed.; Springer Handbook on Nanotechnology, Springer **2003**

Pristine surfaces of metals and metal oxides tend to adsorb adventitious organic materials easily.[2] The presence of adventitious organic materials on the surfaces also disturbs the interfacial properties, having a significant influence on the stability of nanostructures on metals and metal oxides. For instance, they can act as a physical or electrostatic barrier against aggregation; also act as an electrically insulating film or decreasing the reactivity of the surface atoms. Surfaces coated with adventitious materials are not well defined, do not present specific chemical functionalities and do not have reproducible physical properties such as conductivity, wettability, or corrosion resistance.[3]

Among a vast number of procedures for controlled surface functionalization, the generation of self-assembled monolayers (SAMs) has been extensively used for the fabrication of thin films in a wide range of surfaces such as Au, Ag, Cu, Al_2O_3, SiO_2, TiO_2 or Si.[4] SAMs have proof to provide a facile, flexible and simple system to module the interfacial properties of metals, metal oxides, and semiconductors.

SAMs are organic assemblies formed by the adsorption of molecular constituents from solution or the gas phase onto the surface of solids. The adsorbates that form SAMs organize themselves spontaneously into ordered domains. The ligands, also named "headgroups", are a part of the adsorbate structure that have a high specific affinity for the substrate, providing the displacement of the adsorbed adventitious organic materials from the surface. To date, the most common method for the preparation of functional organic layers, based on the self-assembly, is the incorporation of monodentate adsorbates having long alkyl chains, such as alkylsiloxanes on polar surfaces, alkene derivatives on silicon surfaces[5] or alkylthiolates on gold surfaces.[6] In these cases, the orientation of these flexible molecules is achieved by the high degree of packaging that exists in the monolayer, since the molecules are kept close together thanks to the Van der Waals forces among the alkyl residues. Furthermore, to prevent the non-specific

[2] Adamson, A. W.; Gast, A. P. *Physical Chemistry of Surfaces*, 6th ed.; Wiley-Interscience: New York, 1997.
[3] Love, J. C.; Estroff, L.A.; Kriebel, J.K.; Nuzzo, R.G.; Whitesides G.M. *Chem. Rev*. **2005,** *105*, 1103.
[4] a) Poirier, G. E.; Pylant, E. D. *Science (Washington, D.C.)* **1996**,*272*, 1145; b) Dubois, L. H.; Nuzzo, R. G. *Annu. Rev. Phys. Chem.* **1992**, *43*,437; c) Biebuyck, H. A.; Bain, C. D.; Whitesides, G. M. *Langmuir* **1994**, *10*, 1825; d) Dubois, L. H.; Zegarski, B. R.; Nuzzo, R. G. *J. Chem. Phys.* **1993**, *98*, 678; e) Fenter, P.; Eisenberger, P.; Li, J.; Camillone, N., III; Bernasek, S.; Scoles, G.; Ramanarayanan, T. A.; Liang, K. S. *Langmuir* **1991**, *7*, 2013.
[5] a) Yam, C. M.; López-Romero, J. M.; Gu, J.; Cai, C. *Chem. Commun.* **2004**, 2510; b) Sharma, S.; Johnson, R. W.; Desai, T. A. *Appl. Surf. Sci.* **2003**, 206, 218; c) Lee, S.-W.; Laibinis, P. E. *Biomaterials* **1998**, *19*, 1669; d) Papra, A.; Gadegaard, N.; Larsen, N. B. *Langmuir* **2001**, *17*, 1457; e) Leoni, L.; Attiah, D.; Desai, T. A. *Sensors* **2002**, 2, 111.
[6] a) Onclin, S.; Ravoo, B. J.; Reinhoudt, D. N. *Angew. Chem., Int. Ed.* **2005**, *44*, 6282; b) Love, J. C.; Estroff, L. A.; Kriebel, J. K.; Nuzzo, R. G.; Whitesides, G. M. *Chem. Rev.* **2005**, *105*, 1103.

adsorption of proteins, oligo(ethylene glycol)s (OEGs), which is a well-known building block for the modification this kind of films, are usually used.

For example, an approach based on hydrosilylation of α-OEG-ϖ-alkenes directly onto H-terminated silicon surfaces, was reported by Yam *et al.*,[5] which used this tool to form Si–C bonds that are more stable towards hydrolysis than Si–O bonds. This became a very useful approach that was not reported before, although hydrosilylation was widely used to prepare alkyl monolayers presenting a variety of surface functional groups.[7]
In this case, the employment of molecules having multiple ethylene glycol units raised the doubt since they might interfere with the reaction by trapping certain amount of water and could facilitate the oxidation of the H–Si surface. But, still, the main reason that prompted Yam and coworkers to carry out this study on flat silicon surfaces was the novelty and potentially utility for the development of silicon based biotechnology; using such monolayers as atomically flat, robust, and protein-resistant platforms for patterning single protein molecules on such surfaces.

Therefore, the study involved OEG layers grown by hydrosilylation of three alkenes with the general formula $CH_2=CH(CH_2)_9(OCH_2CH_2)_nOCH_3$ (n= 3,[8] 6,[9] and 9), named EG_3, EG_6 and EG_9, on atomically flat H–Si(111) surfaces. They developed a practical procedure for photo-induced surface hydrosilylation, in which only approx. 1 mg of the alkenes, without solvent, was used for coating a 1 x 1 cm^2 wafer under a 254 nm UV lamp. This procedure clearly improved the quality of the films, presumably due to the use of a small amount of ethylene glycol derivatives, which facilitated the removal of the trapped water even under a moderate vacuum (3 mTorr).

Another example, in which Si was used as substrate for surface modification, is the functionalization of acetylene-terminated monolayers on Si(000) by the click chemistry approach.[10] In this article, Ciampi *et al*. reported the functionalization of alkyne-terminated alkyl monolayers on Si(100) using the Cu(I)-catalyzed Huisgen 1,3-dipolar cycloaddition reaction of azides with alkyne terminated surfaces. As can be observed in figure II.1, the covalent attachement of terminal diyne derivatives was performed in a one-step procedure, providing structurally well-defined acetylene-terminated organic monolayers. Subsequent derivatization of the alkyne-terminated monolayers by click

[7] Buriak J. M. *Chem. Rev.*, **2002**, *102*, 1271.
[8] (a) Lee S.-W.; Laibinis, P. E. *Biomaterials* **1998**, *19*, 1669.
[9] Fischer, C. P.; Schmidt C.; Finkelmann, H. *Macromol. Rapid Commun*. **1995**, *16*, 435.
[10] Ciampi, S.; Böcking, T.; Kilian, K.A.; James, M.; Harper, J.B.; Gooding, J.J. *Langmuir* **2007**, *23*, 9320.

reaction in aqueous medium with azide molecules (**2a-c** in figure II.1) gave the disubstituted surface-bound [1,2,3]-triazole species.

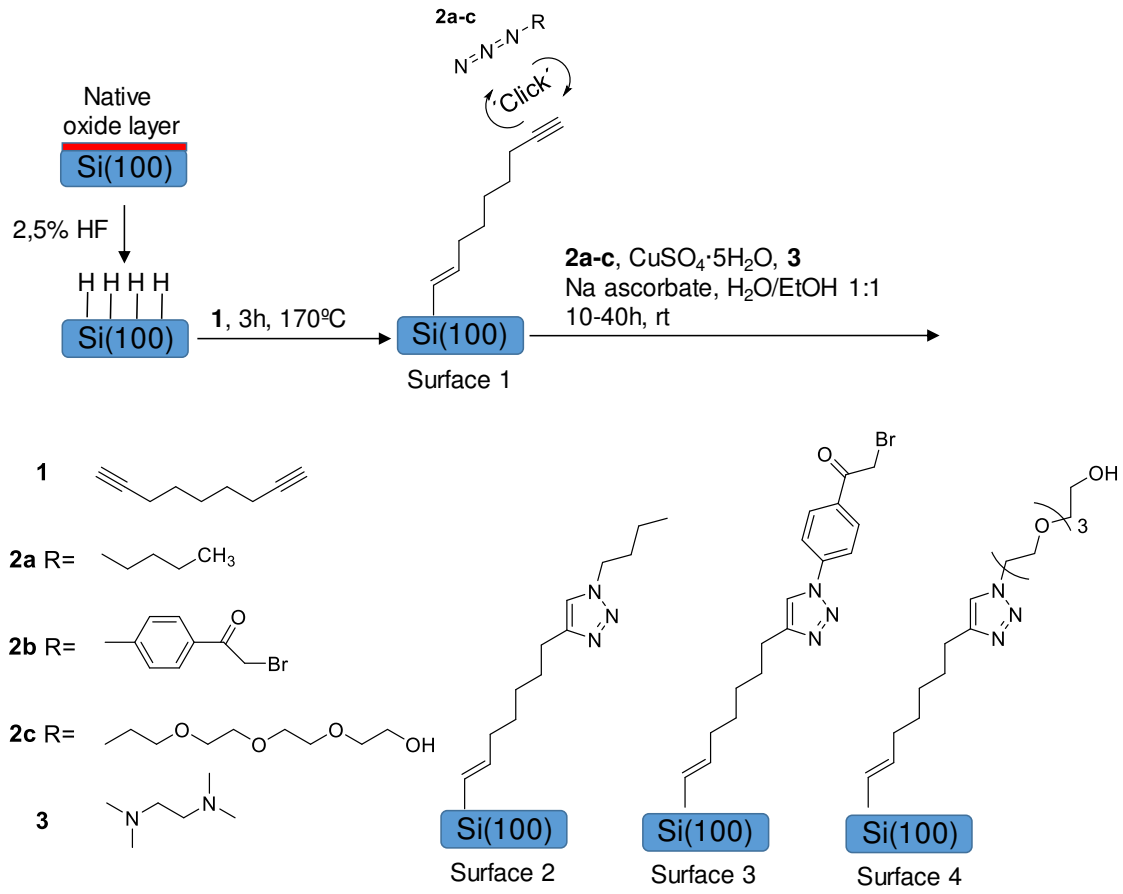

Figure II.1 Huisgen-Type Click Cycloaddition Reactions on Acetylene-Terminated Si(100) Surfaces.[10]

Characterization by X-ray photoelectron spectroscopy and X-ray reflectometry showed click reaction yields were found from moderate to high, providing surfaces with alkyl chains, OEG moieties or aromatic structures. These results evidenced that the immobilization by performing the click reaction can open a good way for a versatile and simple approach (in experimental terms) to produce modified silicon surfaces with potential application in biosensing, also having the electronic properties of the silicon substrate.

The "Click Chemistry" concept is a term that was first introduced by Sharpless in 2001,[11] and describes reactions that are high yielding, wide in scope, create only byproducts that

[11] a) Kolb, H. C.; Finn, M. G.; Sharpless, K. B. *Angew. Chem. Int. Ed.* **2001**, *40*, 2004; b) *Angew. Chem.* **2001**, *113*, 2056.

can be removed from the mixture of reaction without chromatography, that are stereospecific, simple to perform, and can be conducted in easily removable or green solvents. In this regard, click reactions in solution have become a successful tool for the functionalization of a wide range of metal surfaces that have been previously modified by alkynyl or azido groups.

A recent study, that used click chemistry for the biofunctionalization of alkylated Si(111) surfaces, was performed by Cai and coworkers[12] in 2010. In this work, they also grew "clickable" monolayers onto H-Si by photoactivated hydrosilylation with alkenynes, where the terminal alkynyl moiety was protected with trimethylgermanyl (TMG) group. This protecting group could be easily removed in the presence of copper aqueous solutions, which left the free alkyne group prepared to react with an azide residue. The strategy carried out by Cai combined in a single step both the deprotection and click reaction, with several azide molecules, as can be seen in figure II.2.

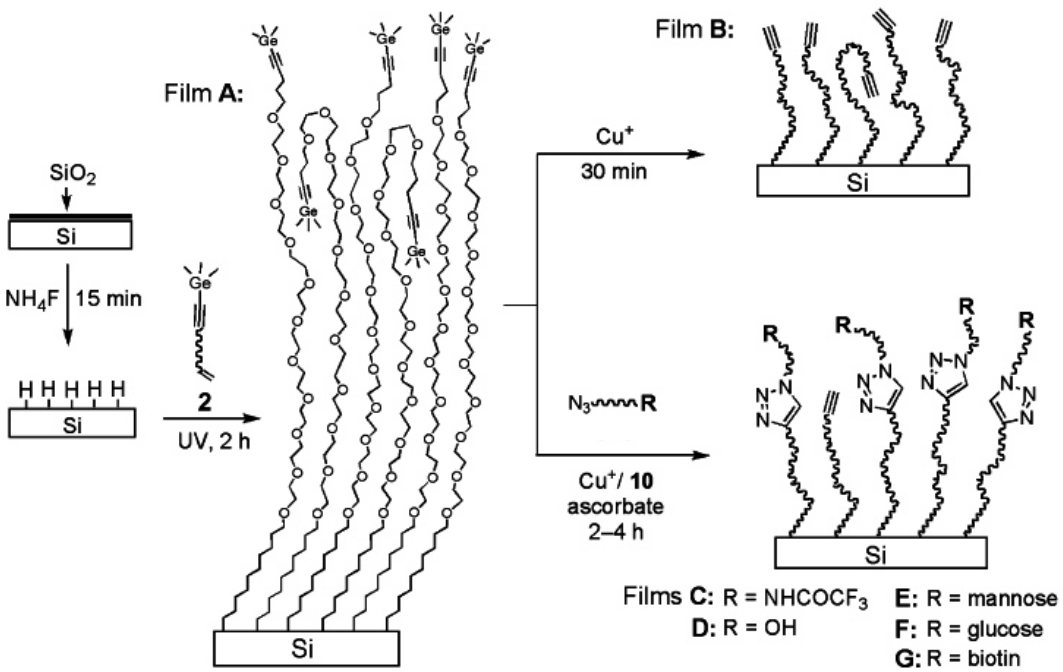

Figure II.2 Summary scheme for the preparation of the different films in Cai´s work.[12]

In this study, every azide molecule that is tagged (azides **3**-**7** in figure II.3) has an oligo(ethylene glycol) moiety, reducing the nonspecific adsorption of fibrinogen (the model protein used in this case) by >98%. They also demonstrated that the monolayer

[12] Quin, G.; Santos, C.; Zhang, W.; Lin, Y.; Kumar, A.; Erasquin, U.J.; Liu, K.; Muradov, P.; Wells Trautner, B.; Cai, C. *J. Am. Chem. Soc.* **2010**, *132*, 16432.

platform could be functionalized with mannose for highly specific capture of living targets (*Escherichia coli*) onto the silicon substrates.

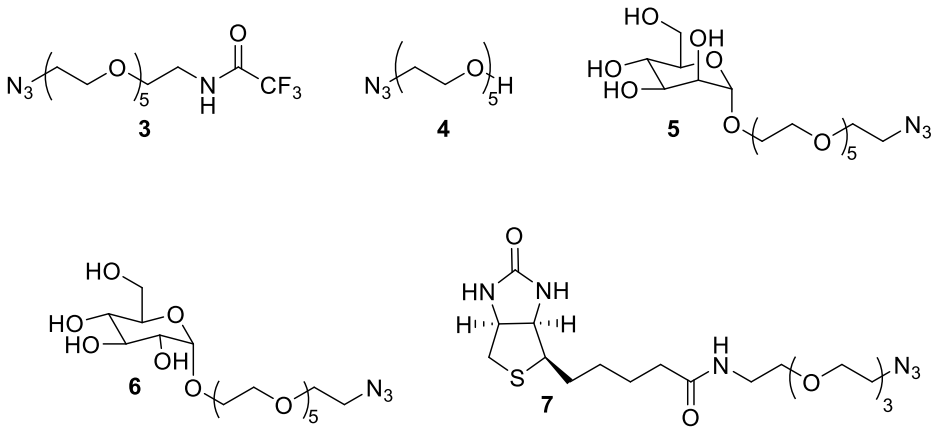

Figure II.3 Azides with OEG moieties employed by Cai for their immobilization on alkynyl-terminated Si(111) surfaces.[12]

On the other hand, one of the most popular types of SAMs is based on the strong covalent bond between sulfur and gold, being therefore the most extensively used and investigated.[13] There are several benefits in using gold as the substrate since it possesses a variety of useful properties, such as chemical inertness, self-cleaning ability, and well-defined morphology, which makes it suitable for different studies and handling under ambient conditions before functionalization.

The major advantage of these systems is the possibility to control the chemical composition of both surfaces and interfaces by selecting a proper terminal tail group, which is able to provide a dense molecular packing in the monolayer and has a contamination-free character. These are known to be single-component films, however, mixed monolayers comprising molecules with different terminal groups have various benefits as compared to the single-component ones. By this method, the chemical properties of the monolayers can be tuned to achieve a particular goal. The most common manner to prepare a mixed monolayer is by coadsorption starting from a mixed solution of both molecules, followed by the standard immersion procedure. Another way to form mixed monolayers is the use of electron irradiation of the primary single-

[13] a) Valasek, M.; Lindner, M.; Mayor, M. *Beilstein J. Nanotechnol*. **2016**, *7*, 374; b) Tour, J.M. *Molecular Electronics*, World Scientific, Singapore, **2003**; c) Chaki, N.K.; Vijayamohanan, K. *Biosens. Bioelectron*. **2002**, *17*, 1.

component SAM or by exposing it to UV light.[14] A recent example of this type of strategy was carried out by Yan *et al*. In this study, the promoted exchange reaction between alkanethiolate self-assembled monolayers and azide molecules was analyzed.[15] Herein, they described the employment of UV light to promote an exchange reaction between the primary alkanethiolate (AT) SAM films and an azide derivative ($C_{12}N_3$), which is capable of click reaction with ethynyl-bearing species. This reaction resulted in mixed AT/$C_{12}N_3$ monolayers and, as primary matrix, they used either nonsubstituted (C_{12}, figure II.4a) or OEG substituted (EG_3 and EG_6, figure II.4b) AT SAMs, obtaining mixed SAMs with chemical and biological applications.

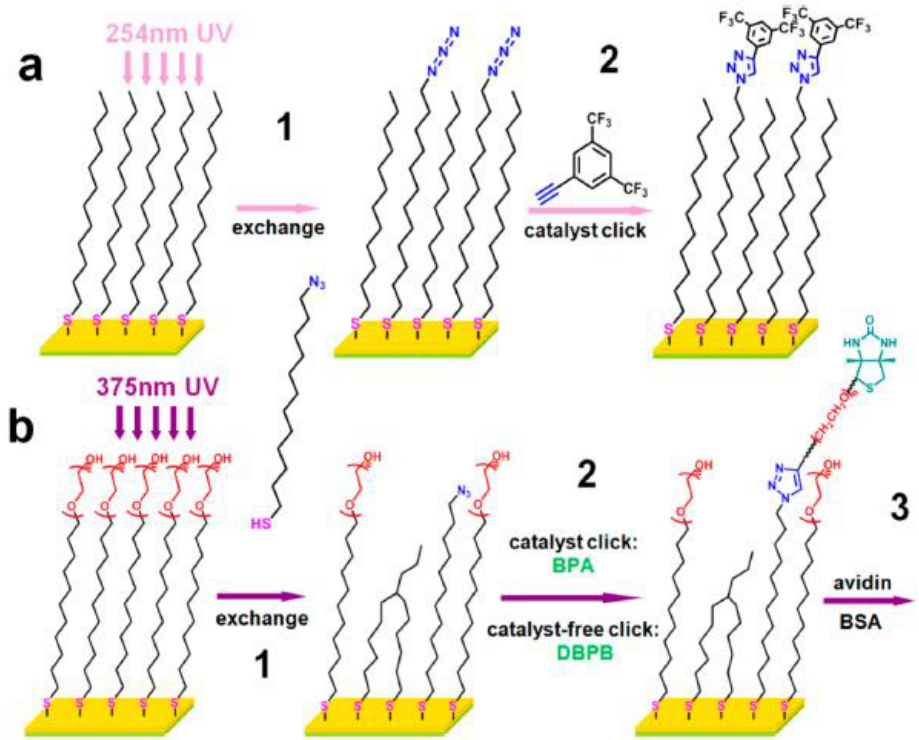

Figure II.4 Schematic of the experimental procedure carried out by Yan *et al*.[15]

The procedure involves the exposure of the primary C_{12} SAMs to UV light with a wavelength of 254 nm and the EGn SAMs (C_{12}) at 375 nm; then promoted exchange reaction with $C_{12}N_3$ under catalyst-mediated or catalyst free conditions; and finally test for nonspecific and specific protein adhesion (only for the EGn/$C_{12}N_3$ films). The templates exhibited much higher affinity to the specific protein (avidin) when compared to the nonspecific one (bovine serum albumin, BSA).

[14] a) Ballav, N.; Shaporenko, A.; Krakert, S.; Terfort, A.; Zharnikov, M. *J. Phys. Chem. C* **2007**, *111*, 7772; b) Jeyachandran, Y. L.; Terfort, A.; Zharnikov, M. *J. Phys. Chem. C* **2012**, *116*, 9019; c) Jeyachandran, Y. L.; Zharnikov, M. *J. Phys. Chem. C* **2012**, *116*, 14950.
[15] Yan, R.; Le Peux, L.; Mayor, M.; Zharnikov, M. *J. Phys. Chem. C* **2016**, *120*, 25967.

However, although the density of functional groups in these monolayers can be controlled by the co-deposition with analogous but inert adsorbates, it is not possible to prevent a random distribution of active groups in the monolayer. To avoid this problem several types of relatively rigid macromolecules with defined form and size have been deeply investigated to provide functional molecular platforms to be used as templates for different applications.[16]

Most recently, the strategy has evolved into the use of more complex binding units that cover a specific area that exceeds the functional unit present in the molecule.[17] Depending on the size of the binding unit, these SAMs can exhibit considerable rigidity and space separation between the grafted functional groups on a particular substrate, offering the possibility to fabricate interfacial architectures in bio-devices with molecular precision.

In this sense, the use of rigid, large multipodal architectures such as tripod-shaped molecules can potentially provide good and stable arrangement of the grafted molecules on the selected substrate. These molecules usually consist of a tetrahedral core having an active tail group positioned perpendicular to the surface. The remaining three legs include an aliphatic, oligophenylene or oligophenylacetylene spacer with the desired length, and the terminal anchor groups. The chemical properties of these groups depends on the nature of the substrates.[18]

To this end, tripodal binding units for the self-assembly on gold substrates were tested by Weidner *et al*.[19] in their study for the comparison between thiol and thioether groups as anchor groups. As tripodal ligands with thiol groups they used $PhSi(CH_2SH)_3$ (PTT) and *p*-Ph-$C_6H_4Si(CH_2SH)_3$ (BPTT), and compared these systems with $PhSi(CH_2SMe)_3$ (PTET) and *p*-Ph-$C_6H_4Si(CH_2SMe)_3$ (BPTET) which have thioether moieties (figure II.5).

[16] a) Parsons, J.T.; Horwitz, A.R.; Schwartz, M.A. *Nat. Rev. Mol. Cell Biol*. **2010**, *11*, 633; b) Abedin, M.; King, N. *Trends Cell Biol*. **2010**, *20*, 734; c) Callow, J.A.; Callow, M.E. *Nat. Commun*. **2011**, *2*, 1.
[17] Weidner, T.; Krämer, A.; Bruhn, C.; Zharnikov, M.; Shaporenko, A.; Siemeling, U.; Träger, F. *Dalton Trans.* **2006**, 2767.
[18] Hierrezuelo, J.; Rico, R.; Valpuesta, M.; Díaz, A.; López-Romero, J.M.; Rutkis, M.; Kreigberga, J.; Kampars, V.; Algarra, M. *Tetrahedron* **2013**, *69*, 3465.
[19] Weidner, T.; Ballav, N.; Siemeling, U.; Troegel, D.; Walter, T.; Tacke, R.; Castner, D.G.; Zharnikov, M. *J Phys Chem C Nanomater Interfaces* **2009**, *113*, 19609.

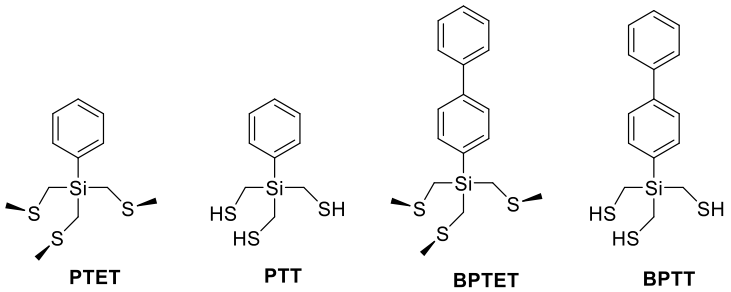

Figure II. 5 Structures of the tripod ligands adressed in the study carried out by Weidner *et al*.

The PTT and BPTT films were compared with the analogous systems prepared by using the same tripodal ligands but with thioether groups instead of thiol binding units (anchors). The results obtained by XPS suggest a better orientation order, higher packing density, and more uniform binding configuration for the films formed with thiol-based ligands as compared to their thioether counterparts. In addition, this study suggested that the rational design of tridentate anchors can overcome steric effects of bulky tail groups and be a viable route for the assembly of phenyl-based SAMs on metal substrates. In particular, the thiol-based tripod ligand PTT in this study yielded SAMs of significantly higher quality compared to its monodentate analogue, benzenethiol.

In the case of silicon substrates, a good example of thin films derived from tripod-shaped molecules is the study performed by Cai and coworkers.[20] They used, as tripod-shaped framework, a molecule (figure II.6) composed of three heptaphenylene legs end-capped with a triallylsilyl group joined at a Si atom with a bromophenyl group. Subsequent attachment onto hydrogen-terminated Si(111) surfaces was performed *via* thermally induced surface hydrosilylation.

[20] Yam, C.M.; Cai, C. *Journal of Colloids and Interface Science* **2006**, *301*, 441.

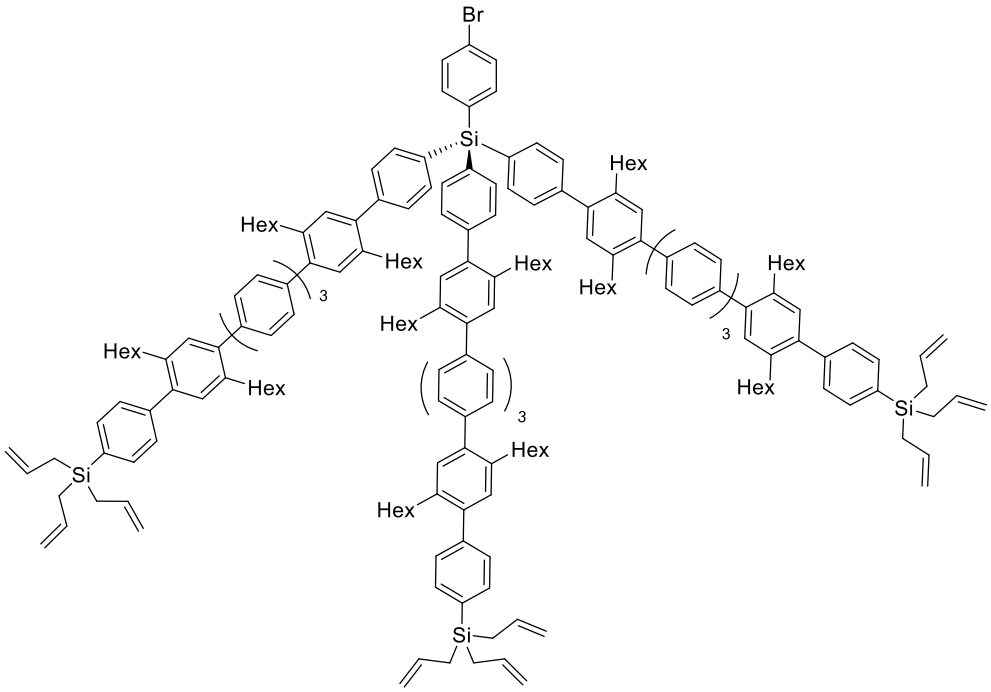

Figure II.6 Molecule employed by Cai and coworkers to be attached on H-Si substrates.[20]

Moreover, they demonstrated that the tripodal molecule was successfully adsorbed onto the surface adopting a tripodal orientation with the tail group perpendicular to the surface to effectively undergo further coupling reactions. Finally, Suzuki coupling reactions with arylboronic acid derivatives on the films was achieved with excellent yields (~90%), suggesting that the desired tripod orientation of such giant molecules helped to eliminate the steric hindrance for the reaction (figure II.7).

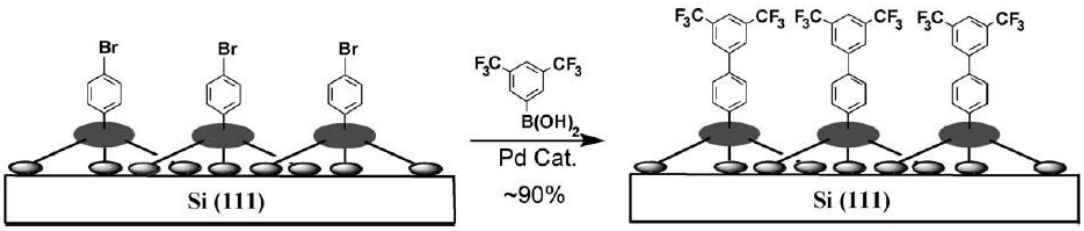

Figure II.7 Suzuki reaction carried out by Cai and coworkers to evidence the preferred orientation of tripod attachment.[20]

Most recently, molecules derived from tetraphenylmethane have been used as rigid molecular scaffolds for the metal surfaces.[21] These are the adsorbates studied by

[21] Lindner, M.; Valasek, M.; Homberg, J.; Edelmann, K.; Gerhard, L.; Wulfhekel, W.; Fuhr, O.; Wätcher, T.; Zharnikov, M.; Kolivoska, V.; Pospisil, L.; Meszaros, G.; Hromadova, M.; Mayor, M. *Chem. Eur. J.* **2016,** *22*, 13218.

Lindner *et al.* This author reported the synthesis of the tetraphenylmethane tripodal platforms (**7** and **21**, figure II.8) having three acetyl-protected thiol groups in either *meta* or *para* positions and the analysis of the deposition on Au (111) surfaces. These platforms are intended to provide a vertical arrangement of the substituent in position 4 of the phenyl ring perpendicular to the surface (CN group in figure II.8) and an electronic coupling to the gold substrate. The results of these experiments indicated that the *m*-derivative formed a better well-ordered monolayer, with most of the anchoring groups bound to the surface, in contrast to the *p*-derivative that formed multilayer films with physically adsorbed adlayers on the chemisorbed one.

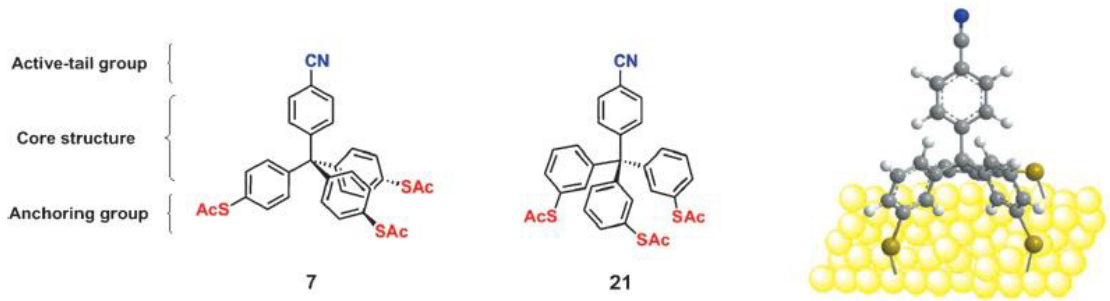

Figure II.8 Structure of the molecular tripods (**7** and **21**) used in the study performed by Lindner.

With this background, the modification of gold and silicon surfaces with the tripod-shaped molecules synthesized in the previous chapter was addressed. The obtained results for the covalent grafting of the tripodal molecules are described below.

II.2 Modification of silicon surfaces with tripods 12 and 21.

II.2.1 Modification with tripod 12.

In this section, we first present a preliminary study which involves the incorporation of compound **12** onto alkynyl modified H-Si(111) silicon wafers. The clickable silicon surfaces were prepared by an easy and reproducible photo-activated hydrosilylation reaction of 4,7,10,13,16-pentaoxaheptacos-26-en-1-yne (compound **49**) onto H-Si(111) substrates (Surface **A**), as described elsewhere.[22] Scheme II.1 represents the general procedure for the grafting of tripod **12** on alkynyl-terminated substrate thus resulting in Surface **B**.

[22] Lucena-Serrano, A.; Lucena-Serrano, C.; Contreras-Cáceres, R.; Díaz, A.; Valpuesta, M.; Cai, C.; López-Romero, J. M. *Appl. Surf. Sci.* **2016**, *360*, 419.

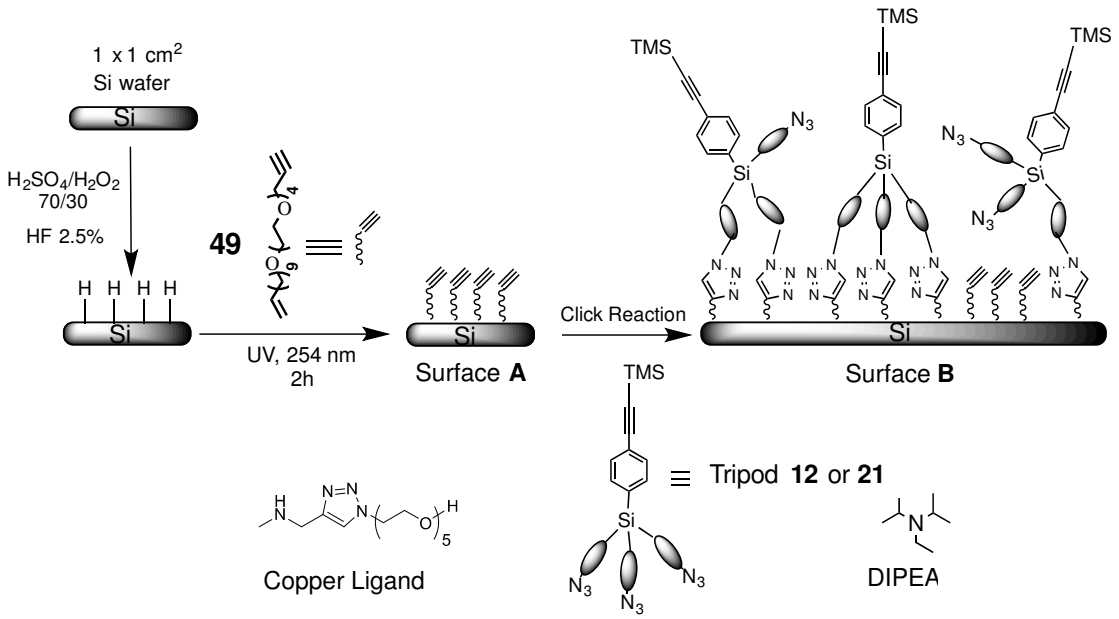

Scheme II.1 Schematic representation for the grafting of tripod **12** and **21** on alkynyl-modifed H-Si(111) substrates.

The click reaction conditions carried out with tripod **12** are detailed in the Experimental Section. In summary, $Cu(MeCN)_4PF_6$ was used as copper salt, the copper ligand indicated in scheme II.1 and a mixture of methanol/THF as solvent.

X-Ray photoelectron spectroscopy (XPS) and Atomic Force Microscopy (AFM) analysis were used to confirm the presence of the oligo(*p*-phenylene) tripod **12** on the silicon surface, and to study its structuration, respectively. The XPS survey scan (figure II.9) shows the first evidence for the presence of the tripod-shaped molecule by displaying the N1s peak at ~400 eV, which corresponds to the presence of the triazole group formed after the click reaction, suggesting the presence of **12** covalently attached to the alkynyl modified silicon surface.

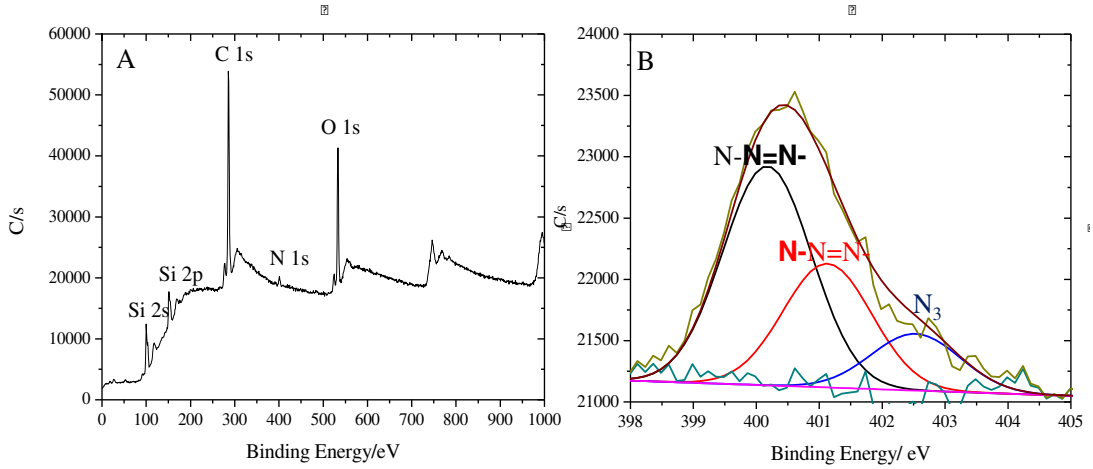

Figure II.9. A) Survey and B) XPS narrow scan of the N1s regions after click reaction.

Moreover, the yield of click reaction was calculated by following the same procedure previously reported.[22] In our particular case, this parameter yield was calculated from the next equation: $(C/N)_{xps}$= (22+71x%)/9x%, where $(C/N)_{xps}$ is the C/N ration extracted from XPS measurements, 22 is the number of C atoms before click reaction, and 71 and 9 correspond to the number of C and N after the grafting of tripod **12**. The yield (non-optimized) of the embedded tripods was 31.2%. This value is very close to those previously obtained for biomolecules and proteins incorporated on silicon substrates.[12,22]

The presence of the triazole group after click reaction was demonstrated by deconvolution of the N1s narrow scan (figure II.9 B). Three peaks were assigned to 400.5 eV (**N-**N=N**-**), 401.7 eV (N-**N=N**-) and 403 eV (corresponding to free azide group non-attached on the triple bond). The calculated ratio for the areas of both groups (**N-**N=N- and N-**N=N**-) presented in the triazole ring extracted from the N1s narrow scan was 2:1, in consistence with the stoichometric ratio.

The location of the incorporated tripod **12** was also demonstrated by tapping mode AFM analysis. Figure II.10 A shows AFM representative image of the H-Si(111) substrate before click reaction, as it is observed, a total flat surface was clearly displayed.

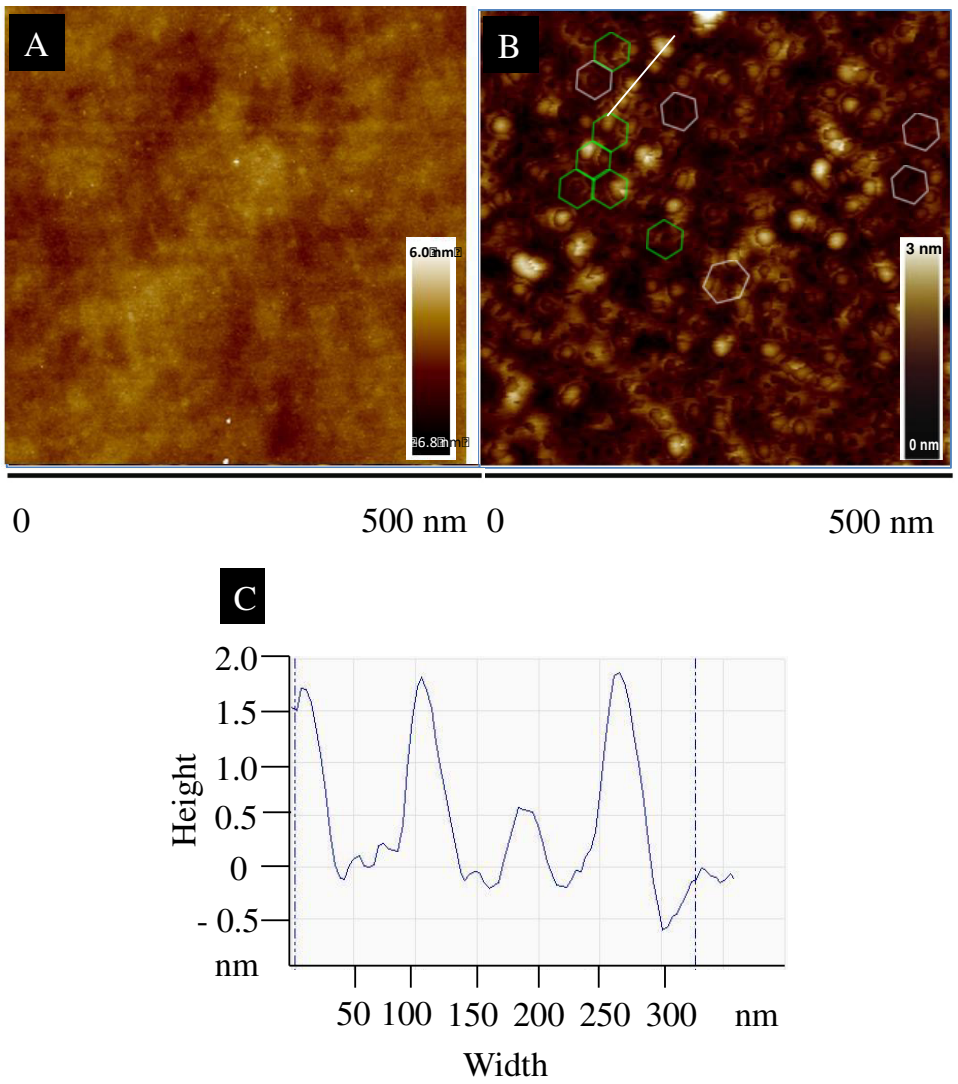

Figure II.10 Tapping mode AFM images (500 x 500 nm) of A) surface A, before click reaction B) surface B, after click reaction and C) Height profile of surface B.

On contrary, the AFM images corresponding to the surface after the incorporation of tripod **12**, (figure II.10 B) as well as the 2D height profile (figure II.10 C) confirms the presence of the tripodal oligo-*p*-phenylene compound **12**.

From the analysis of the AFM image shown in figure II.10 B, a highly ordered distribution of **12** on the surface can be induced. A more detailed observation shows how mono and bilayers of **12** draw a 50 nm hexagonal side pattern. The 2D height profile (figure II.10 C), extracted from white line in figure II.10 B, confirms the nanostructured surface showing constant heights of around 1.7 and 0.7 nm. This value is in good concordance with the reported calculated height of 6 Å (0.6 nm) of the silicon atom above the base,

when the tripod-shaped molecule has three phenylene units.[23] Moreover, from the 2D profile line, the distance among tripods is around 40 Å being also in concordance with the density functional theory (DFT) calculated in 33 Å.

It has been reported[24] that lower yields are obtained for the click reaction on surfaces containing alkynyl groups when compared to the surface functionalized with azide moieties, being the reasons still unclear. Even when the yield of the reaction is modest, the easy procedure for the preparation of the alkynyl modified surface and the good results in surface coverage can be taken as a proof showing that the method is useful for the modification of surfaces with organic molecules, specially when it is carried out with complex molecules. Moreover, secondary reactions are not observed.

II.2.2 Modification of silicon substrates with tripod 21

Since the preliminary study gave good results, this prompted us to study more in depth the optimum conditions for the click reaction with tripod **21**, (figure II.11) which has a larger size with five phenylene units in each leg.

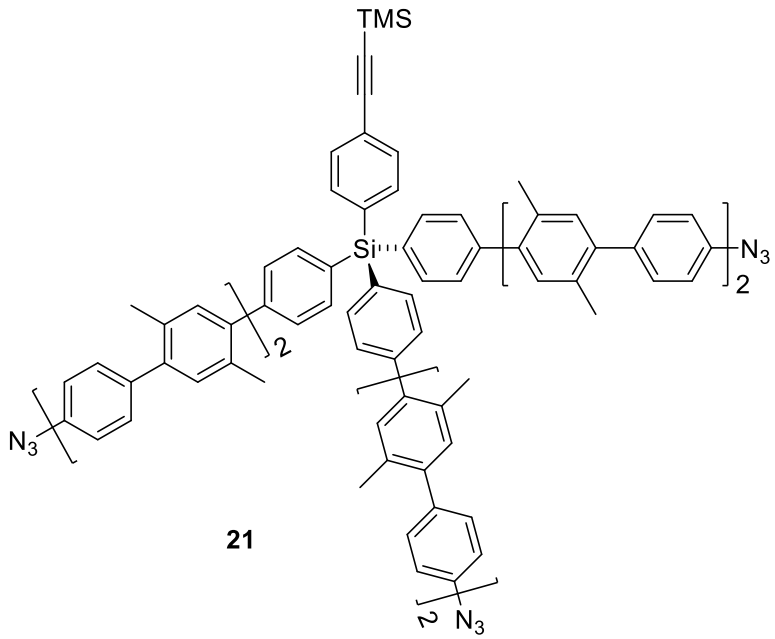

21

Figure II.11 Tripod **21** with azide groups as anchors and five phenylene units.

[23] Hierrezuelo, J.; Guillén, E.; López-Romero, J. M.; Rico, R.; López-Ramírez, M. R., Otero, J. C.; Cai, C. *Eur. J. Org. Chem.* **2010**, 5672.
[24] Li, Y.; Wang, J.; Cai, C. *Langmuir* **2011**, *27*, 2437.

Grafting tripod-shaped molecules on modified silicon surfaces has proven to be very dependent on experimental conditions and only around 30% yield is usually obtained concerning the surface coverage. This circumstance can be explained by a partial reaction of alkyne and azide groups resulting in unbound legs, which has been observed mainly when alkynyl groups are attached to the surface.[25]

Despite this fact, and since we have previously obtained good results for the attachment of the small tripod **12** (three phenylene units) on alkynyl modified silicon surfaces, we initially prepared the penta(*p*-phenylene) modified surfaces with **21** by following the same procedure. The clickable silicon surfaces were prepared by photo-activated hydrosilylation reaction of the alkyne derivative **49** onto H-Si(111) substrates (Surface A in scheme II.1). Then, tripod **21**-modified silicon surfaces were built by click reaction onto the previously prepared surfaces in the presence of **21**, a copper source and a base (Surface B in scheme II.1).

For the preparation of surface B in this case, the optimum base/copper and source/solvent combination in click reaction was analyzed. Initially, $Cu(MeCN)_4PF_6$ was used as copper source together with the copper ligand (shown in scheme II.1), in a methanol/THF mixture at room temperature, thus resulting in surface B(**4**) (entry 1, Table II.1).

At the same time, due to the poor solubility of the tripod **21** in methanol, we analyzed the effect of changing the solvent using only THF along with a new copper salt (CuI) and a base (*N,N*-diisopropyletilamine, DIPEA), since previous Cu-complex is not soluble in THF, obtaining surface B(**5**) (entry 2, Table II.1). In both cases the concentration of tripod **21** used during the click reaction was 5 mM.

[25] Yam, C. M.; Cai, C. *Colloid Interface Sci.* **2006**, *301*, 441.

Table II.1 Concentration of tripod **21**, copper source, base, solvent and conditions used in the different click reactions performed onto alkynyl-terminated surfaces.

Entry	Tripod **21** [mM]	Copper Source	Base [mM]	Reaction Solvent	Shaking	Temp.	Surface
1	5	$Cu(MeCN)_4PF_6$	**Copper ligand** 37.5	THF/MeOH	No	RT	B(**4**)
2	5	CuI	**DIPEA** 500	THF	No	RT	B(**5**)
3	0.05	CuI	**DIPEA** 5	THF	Yes	35ºC	B1
4	0.05	CuI	**DIPEA** 5	THF	Yes	RT	B2
5	0.05	CuI	**DIPEA** 5	THF	No	RT	B3
6	0.5	CuI	**DIPEA** 50	THF	No	RT	B4
7	0.25	CuI	**DIPEA** 25	THF	No	RT	B5

As commented above, the presence of tripod **21** on the alkynyl-terminated surfaces was studied first by XPS measurements (figure II.12). The XPS spectrum corresponding to the untreated H-Si(111) substrate only shows a narrow Si2p peak at 99.3 eV, with no presence of SiOx species in the 102-104 eV region (figure II.12 a). Figure II.12 b and II.12 c shows XPS survey scan for surface B(**4**) prepared with $Cu(MeCN)_4PF_6$/copper ligand/MeOH/THF and surface B(**5**) under CuI/DIPEA/THF conditions (entries 1 and 2, respectively, Table II.1).

By XPS analysis, surface B(**4**) is composed by C 1s (60.91%), N 1s (1.74%), O 1s (18.98%) and Si 2p (17.45%), and surface B(**5**) by C 1s (80.5%), N1s (2.84%), O1s (10.6%) and Si 2p (3.57%). As it is observed, in surface B(**5**) the amounts of C 1s and N 1s are higher when compared with that for surface B(**4**). Moreover, the percentage of Si 2p after click reaction is remarkably lower for surface B(**5**) in comparison with surface B(**4**). It means a more homogeneous tripod grafting and a better covering density in surface B(**5**).

We have also calculated the yields for both click reactions by using the same equation as for tripod **12**. This parameter is derived from $(C/N)_{XPS} = (22 + 113x\%) / 9x\%$, where here again C/N is the intensity ratio measured by XPS, 22 is the number of C atoms before the click reaction, 9 is the number of N atoms in the azide, and 113 is the number

of C atoms in the tripod deposited after click reaction. On the base of the C/N ratio, the click reaction yield was estimated to be 25.9% for surface B(**4**). This value is lower than the one obtained in our previous work concerning tripodal-shaped oligo(*p*-phenylene)s with three phenylene units (31.2%), using the same cooper salt.

On contrary, by performing the click reaction with CuI and DIPEA the reaction yield remarkably increases up to 52.0% (surface B(**5**)). This increment is probably produced due to the higher solubility of the tripod **21** in THF, instead of using a MeOH/THF mixture.

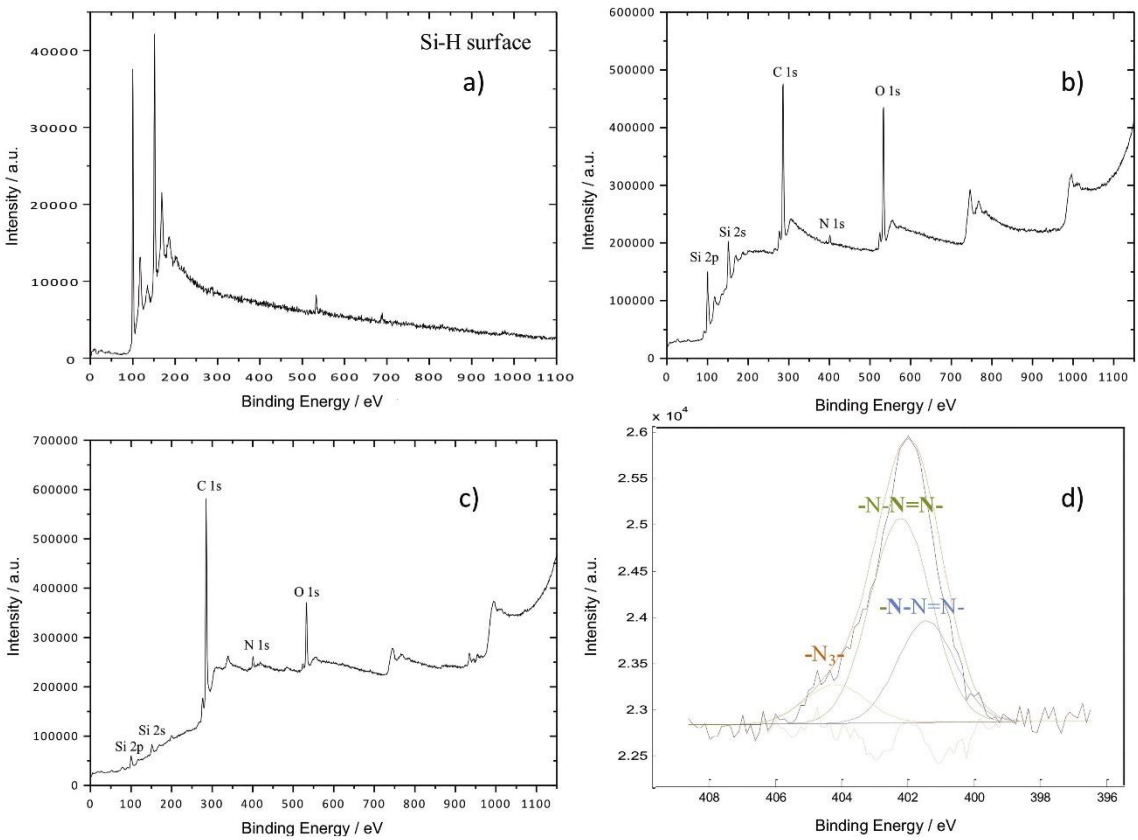

Figure II.12 XPS survey scan for a) a pristine H-Si(111) surface; b) surface B(**4**) prepared under conditions shown in entry 1, Table II.1 ($Cu(MeCN)_4PF_6$/copper ligand); c) surface B(**5**) prepared under conditions shown in entry 2, Table II.1 (CuI/DIPEA). d) XPS narrow scan of the N 1s region for surface B(**5**).

It is important to note that the XPS analysis also demonstrates the presence of the triazole group after click reaction. Figure II.12 d represents the deconvolution of the N 1s narrow scan for tripod **21** grafted on surface B(**5**) (entry 2, Table II.1, surface B(**5**)), where the three different bands are obtained.

First two, at 400.5 eV (**N-**N=N-) and 401.7 eV (N**-N=N-**), are assigned to the triazole group, being 1:2 the calculated ratio for these areas, respectively, as extracted from the

N 1s narrow scan, which is consistent with the stoichiometric ratio. Moreover, the band at 403.0 eV corresponds to free azide groups not grafted to the terminal triple bond. The calculated ratio for this area with respect to that of the triazole group is 1:7, meaning that only 12% of free azide groups are presented on the modified resulting surface.

From these results, we can conclude that the use of CuI/DIPEA/THF combination provides better results for the modification of silicon surfaces with tripod **21**. Then, morphology of the prepared surface B(**5**) was analyzed by tapping mode in AFM technique (figure II.13 a,b). Even when good yields for the click reaction were obtained, poor results are found regarding parameters such as monolayer thickness and nanostructuration extent. In fact, when this surface was analyzed by AFM (figure II.13), it was found a thickness corresponding to multilayer deposition: an almost complete silicon surface coverage with heights reaching a maximum peak height of 25 nm, and an average of 10 nm.

Figures II.13 c and d are also included, for comparison purposes, showing AFM images of one just-etched and clean Si(111) wafer having a roughness or 0.57 nm over an area of 25 μm^2 (figure II.13 c) and of one alkynyl modified silicon surface (surface A in figure II.13 d) showing a roughness or 0.25 nm along 500 nm^2.

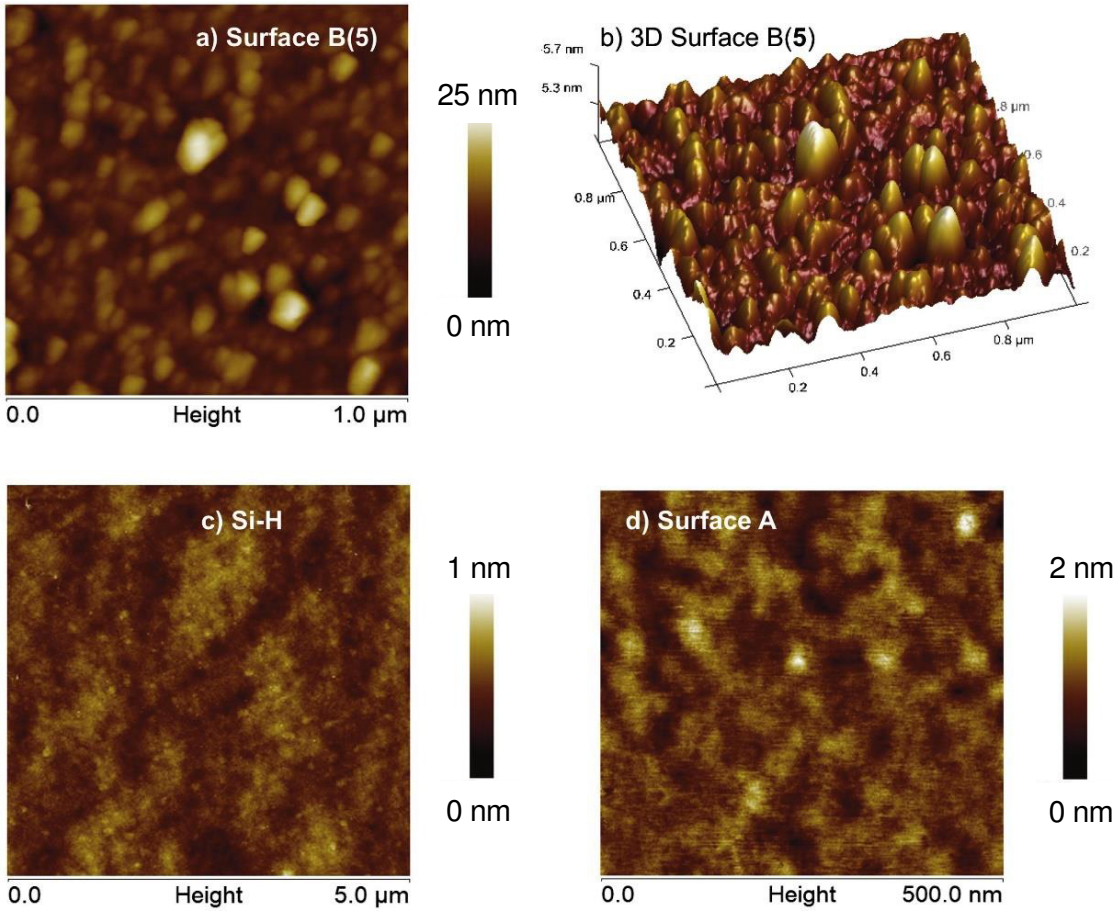

Figure II.13 Tapping mode 2D and 3D AFM images of surfaces Si(111), A and B(**5**).

This result prompted us to optimize not only the concentration of **21** used for the click reaction, but also the reaction temperature. Moreover, we also analyze the effect of shaking while the reaction is carried out. With this purpose, we first tested the click reaction by using CuI, DIPEA and a 0.05 mM tripod **21** solution in THF, at different experimental conditions (entries 3, 4 and 5 in Table II.1, surfaces B1, B2 and B3).

In figure II.14, we include representative tapping mode 2D and 3D AFM images, corresponding to surfaces B1, B2 and B3.

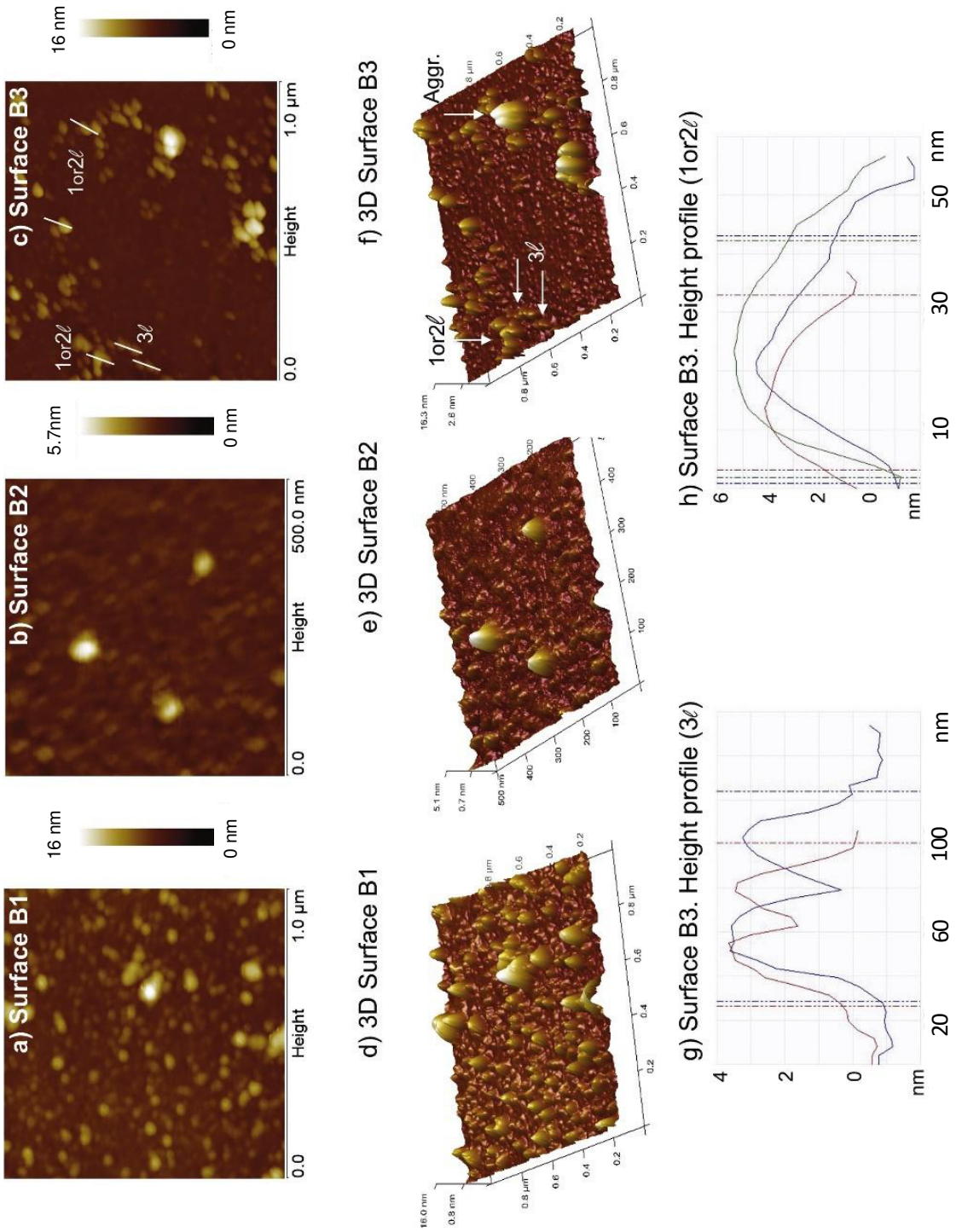

Figure II.14. Tapping mode 2D and 3D AFM images (1 x 1 µm and 500 x 500 nm) of the alkynyl-terminated silicon wafer after incorporation of a solution 0.05 mM tripod **21** by click reaction, and height profile of several tripods extracted from AFM images: tripods attached by the three legs (3l) and by one or two legs (1 or 2l).

As can be observed, in all cases the alkynyl-terminated silicon surfaces presented structures grafted on it. 3D AFM images display, in a better detail, the morphology of the molecule attached on the silicon surface, and the height of the incorporated tripods. Images from figure II.14 a,d correspond to the surface B1 prepared by heating at 35 ºC and shaking; images from figure II.14 b,e correspond to the surface B2, obtained under shaking and at room temperature; and images from II.14 c,f correspond to surface B3 with tripods grafted at room temperature and no-shaking conditions (entries 3, 4 and 5, respectively, in Table II.1), all of them prepared from a 0.05 mM solution of **21**.

As can be seen in figure II.14 a,d, surface B1 presented an improved tripods distribution with a lower aggregation that those prepared with higher concentrations of **21** (5 mM, surface B(**5**)). Moreover, surfaces with low tripods aggregation are a common result obtained with 0.05 mM concentration (surfaces B2 and B3). Surface B2, which represents an alkynyl-terminated silicon surface after click reaction, carried out under shaking and at room temperature, presented a lower amount of tripods but in a well-defined distance between them, with no aggregation. Separation of tripods for this surface was estimated by analyzing AFM images in an average of around 360 nm. Surface B3, which represents 0.05 mM concentration of **21** without shaking and at room temperature, shows low amount of tripods and few irregular aggregates after grafting.

It is important to note that, as was previously mentioned, these azide-terminated penta(*p*-phenylene) tripods can be attached on a alkynyl-terminated surface by one, two or the three azide groups. In this Thesis, we are interested in finding the conditions that provide tripods linked by the three legs (three azide groups), since this configuration would allow the incorporation of the theophylline derivative perpendicular to the silicon surface (see scheme II.1).

We have established the height of the tripods deposited on the silicon surfaces by analyzing the height profile from AFM images (figure II.14 g,h), which have been later compared with the height obtained by DFT calculations (see figure II.16). We estimate in 3.4 nm the height for a tripod attached to the surface with the three legs, and 4.0 nm and 5.5 nm when it is attached with only two and one, respectively. In surface B3 (figure II.14 c,f) we have also indicated that some tripods have been attached forming bilayers or aggregates, but the resulting height profiles confirmed a higher number of tripods attached by the three legs, compared with the other conformations.
On the other hand, in surface B1 we can observe several tripods deposited as bilayer or aggregates, and the number of tripods deposited with one or two legs is higher when

compared to that for tripods attached by the three legs. Therefore, at same concentration values, shaking difficults the adsorption of adsorbates to the surface by the three legs, while heating speed up the process but also leads to obtain aggregates. No heating and no shaking seems to be the better experimental condition for the preparation of ordered tripod surfaces with our desired configuration (surface B3). However, by carrying out the surface preparation with solutions of low tripod **21** concentrations (0.05 mM), poor surface coverages are obtained.

We studied the click reaction with concentrations of **21** in the range of more concentrated solutions, between 0.5-0.05 mM (figure II.15). Surface B4 (figure II.15 a, b and c) represents substrates with 0.5 mM of **21**, without shaking and at room temperature (entry 6, Table II.1). In this case the amount of tripods is higher when compared to the previous cases, the grafting density is higher, and now tripods are in contact between them. However, if we observe the image at the lower magnification (figure II.15 a) tripods form aggregates which are randomly distributed on the silicon surface.

Surface B5 (figure II.15 d, e and f) corresponds to a sample with a tripod concentration of 0.25 mM prepared without shaken and at room temperature (entry 7, Table II.1). The image at low magnification shows a well-distributed tripod configuration and a higher amount of tripods grafted on the silicon surface was obtained if compared with the previous one at 0.05 mM. Indeed, the image (figure II.15 e) shows a large number of tripods attached by the three legs in comparison with the other possible configurations. We can conclude that, even when the grafting density is higher (surface B4), the homogeneity of the surface is better in surface B5, with almost absence of random aggregates, and with a higher amount of tripods attached by the three legs.

Surface B5 was also analyzed by ellipsometry. A thickness of 1.87 ± 0.0348 nm of native Si-alkyne was measured by means of this technique, while measurements determined a thickness of 2.94 ± 0.1173 nm for the tripod **21** monolayer in surface B5.

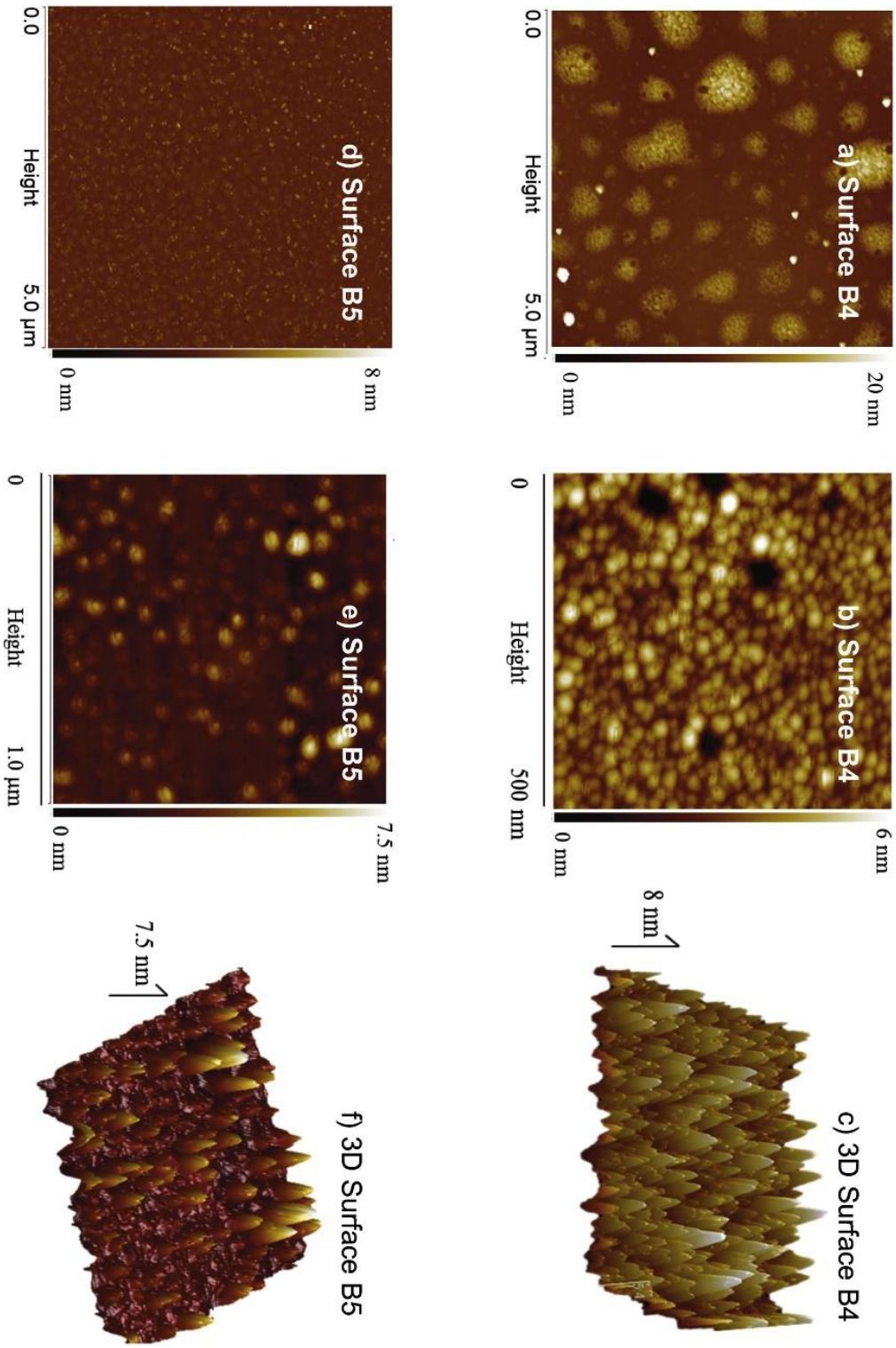

Figure II.15. Tapping mode 2D and 3D AFM images of the alkynyl-terminated silicon wafer after incorporation of tripod **21** at 0.5 (surface B4) and 0.25 mM (surface B5) concentrations by click reaction.

Surface B in scheme II.1, represents the three possible different final conformations of the grafted tripod on the alkynyl-terminated silicon surface after click reaction. The structure and possible orientations of the tripod **21** attached to the surface have been analyzed by DFT calculations.

Figure II.16 includes DFT optimized geometries for **21** in gas phase and grafted on the silicon surface at the three possible configurations. We have denoted (*a*) the distance between azide group and the Si core, (*b*) the distance between two azides groups, (*c*) the distance between an azide and the TMS group, and (*d*) the distance from the alkynyl group and the base of the tripod, being the calculated distances 25.0, 39.5, 30.4 and 31.1 Å, respectively (gas phase).

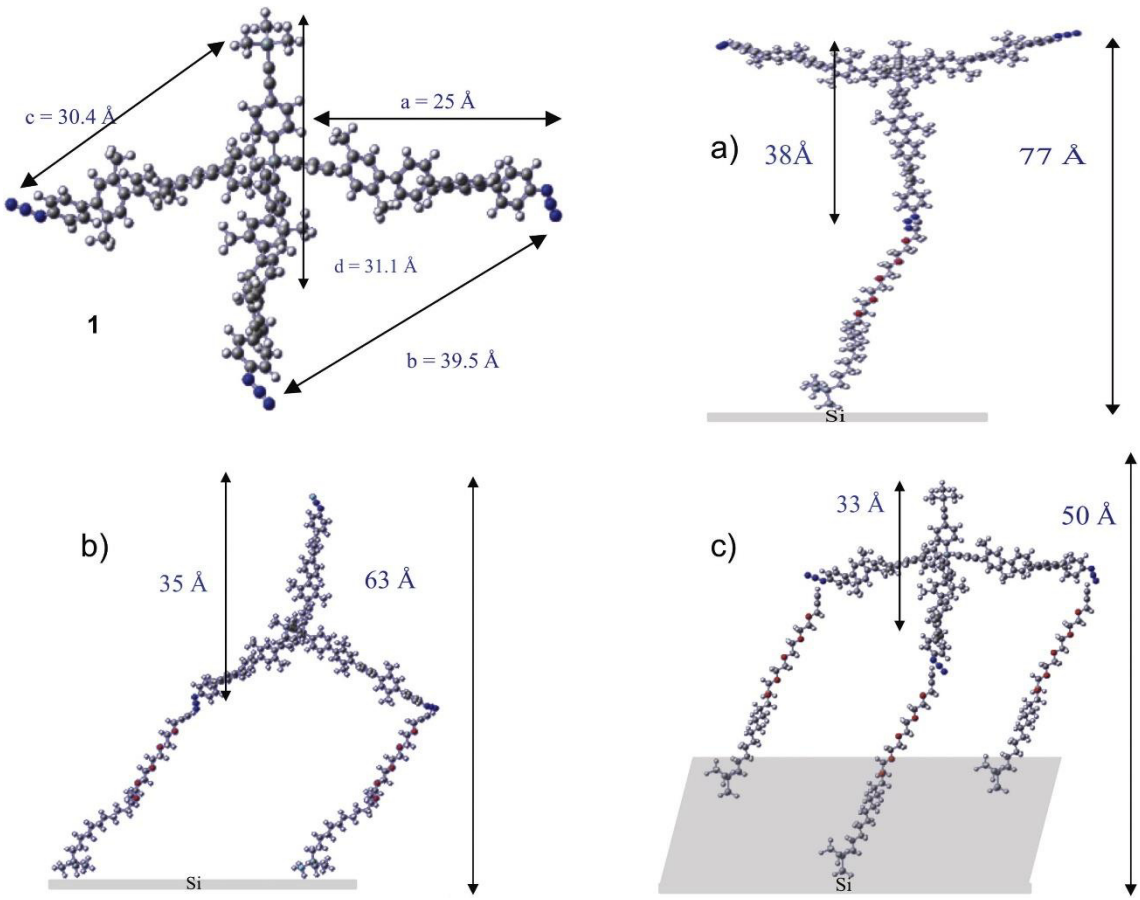

Figure II.16 1) Draw of tripod **21** denoting main DFT calculated dimensions, and optimized geometries representation of possible orientations of tripod **21** on alkynyl-terminated Si(111) surface: a) only one bound, b) two and c) three.

Figure II.16 a-c represents the optimized geometries for tripod **21** grafted on the surface by one, two or three azide groups, respectively. As we deduced from AFM images the final tripod height is different for each conformation. The **21**-calculated heights from the silicon surface (comprises spacer compound **49** and tripod **21**) are 77, 63 and 50 Å, respectively. Is important to mention that for DFT calculations, the total height is not the same from that extracted in the 3D AFM images. DFT calculations include one, two or three molecules of compound **49**, so the angle in which it is attached on the silicon wafer is different, resulting in different thickness.

On contrary, for our experimental conditions, the thickness of the silicon surface after compound **49** incorporation (Surface A in scheme II.1) measured by ellipsometry was 24 Å. As it can be observed, the calculated height of **21** (distance from the base of the tripod to the TMS group) is higher when is attached to the surface (33.0 Å) than when it is calculated in solution (31.1 Å, 3.1 nm). This fact can be attributed to a more rigid configuration when the position of the three legs is fixed to the surface. In any case, the calculated height is in concordance with the measured tripod **21** height of 3.4 nm in surface B3. It also means a possible uncompleted attachment of the three legs of tripod **21** to the Si in surface B2 since the height observed in tripod is closed to 6 nm, and a high percentage of this situation is found on surface B1, which can be also explained by the shaking conditions.

Moreover, based on height measurements, in surface B3 only 10% of tripod molecules are attached to the surface only by one or two legs, concluding that most of the tripods (90%) are attached through the three azide points to the silicon surface B3. Similar result is obtained for surface B5, so we can conclude that grafting at room temperature without shaking and using a 0.25 mM concentration of **21** lead us to achieve good homogeneity on the surface, with almost the absence of random aggregates, and with most of the tripods attached by the three legs to the surface. Consequently, and as we have mentioned above, surface B5 is the appropriated one for theophylline incorporation.

II.2.3 Theophylline attachment and protein adhesion study.

Theophylline is a molecule with many known activities, including formation of complexes with DNA, serving as a strong antioxidant that prevents DNA damage,[26] or the high affinity with a family of adenosine receptors known as A_1, A_{2A}, A_{2B}, and A_3.[27] Their

[26] Nafisi, S.; Manouchehri, F.; Tajmir-Riahi, H.-A.; Varavipour, M. J. *J. Mol. Struct.* **2008**, *875*, 392.
[27] Legraverend, M.; Grierson, D. S. *Bioorg. Med. Chem.* **2006**, *14*,3987.

derivatives are also well known to influence neuronal activities by binding with the above adenosine receptors.[28] A theophylline-oligo(ethyleneglycol)-alkene derivative presenting activity against adenosine receptors[29] has been incorporated onto poly(vinylidene fluoride) and regenerated cellulose membranes. It can be also used to monitorize streptavidin interactions when adsorbed on polymeric support.[30] However, by using these polymeric systems, random interaction between theophylline derivative and surfaces were observed.

Our approach was to prepare silicon substrates modified with tripod-shaped molecule **21**, and attached then azido-terminated theophyllines based on click chemistry. For this purpose, the terminal alkynyl group on the functional arm of tripod **21** was in situ deprotected by removing TMS groups under basic conditions, such as K_2CO_3 in methanol. Removing trialkyl silyl groups on monolayer has previously been carried out with F^- in various solvents, in a sluggish method that requires high concentration of F^-, long reaction time and high temperature.[12] However, by using K_2CO_3 in methanol, TMS groups can be removed under very mild conditions. In our work, the subsequent attachment of the azido-terminated theophylline **52** was carried out over the deprotected surface B5, employing the optimized click conditions for tripod **21**, thus resulting in surface C (scheme II.2).

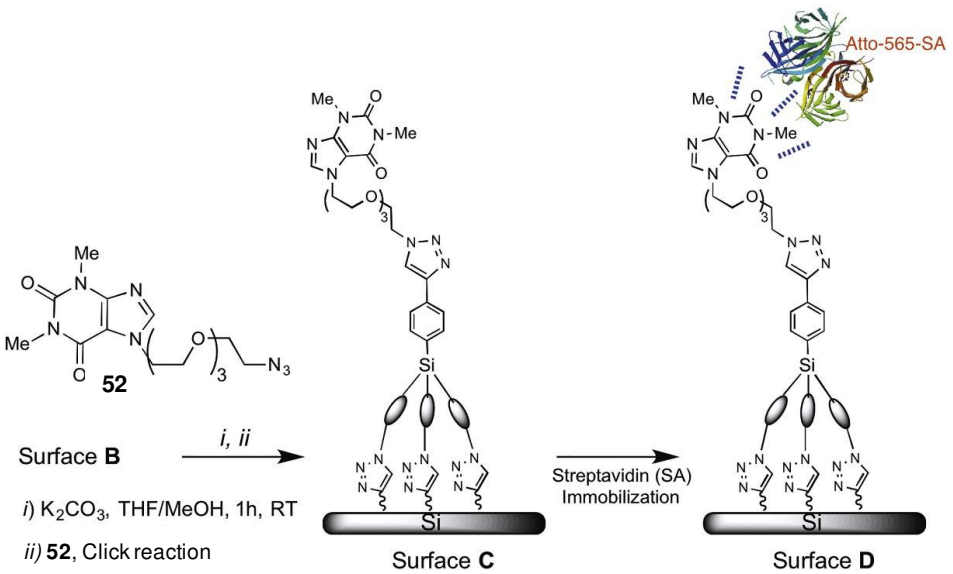

Scheme II.2. Covalent attachment of the theophylline **52** on an optimized silicon surface with tripod **21** and subsequent streptavidin adhesion.

[28] Ribeiro, J. A.; Sebastião, A. M.; Mendonça, A. *Prog. Neurobiol.* **2003**, *68*, 377.
[29] Hierrezuelo, J.; López-Romero, J. M.; Rico, R.; Brea, J.; Loza, M. I.; Cai, C.; Algarra, M. *Bioorg. Med. Chem.* **2010**, *18*, 2081.
[30] a) Vázquez, M. I.; Romero, V.; Benavente, J.; Romero, R.; Hierrezuelo, J.; López-Romero, J. M.; Contreras-Cáceres, R. *Microporous Mesoporous Mater.* **2016**, *226*, 88. b) Hierrezuelo, J.; Romero, V.; Benavente, J.; Rico, R.; López-Romero, J.M. *Colloids Surf. B: Biointerf.* **2014**, *113*, 176.

Upon grafting the theophylline **52** onto the **21** terminated surfaces, bioactivation of these surfaces was demonstrated performing protein adhesion test. The samples were incubated in solutions of conjugated ATTO-565 streptavidin (SA) in phosphate aqueous buffer (PBS).

XPS investigation confirmed the presence of the theophylline derivative **52** and the incorporation of SA on the tripod-modified surface. Figure II.17 shows the N 1s scan for tripod-modified silicon surface (surface B5, black line), after theophylline incorporation (surface C, red line) and after SA treatment (surface D, blue line), respectively.

As can be observed, the N 1s signal intensity increased from surface B5 to surface C due to the presence of both the triazole groups provided after the click reaction and the nitrogen atoms included in the theophylline derivative **52**. After SA treatment, the remarkably increase of the N 1s intensity is attributed to the adsorbed protein.

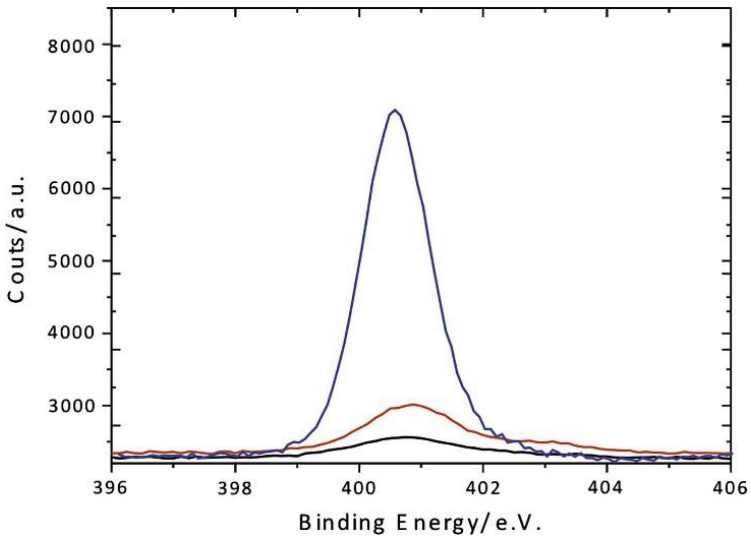

Figure II.17 N 1s scans for surface B5 (black line), surface C (red line) and surface D (blue line).

Selective binding of the protein to the surface has been analyzed by bright field confocal images (figure II.18). This figure shows a comparison of bright field micrographs, obtained with surface B5 treated with SA (figure II.18 a) and surface C once is treated with the same protein (figure II.18 b). As it can be seen, the characteristic red color of the Atto streptavidin chromophore is only observed in the latter, which confirms the protein immobilization on the surface in turn associated with the bioactivation by compound **52**.

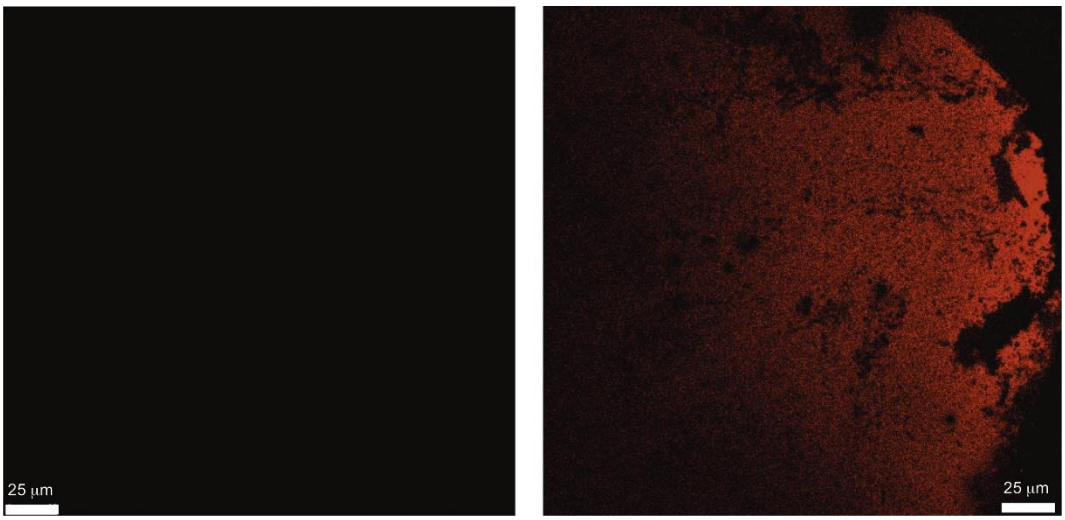

Figure II.18. Fluorescent images of modified surfaces incubated with streptavidin. a) Tripod **21** terminated surface B5, without **52** and treated with streptavidin. No protein adhesion was observed. b) Surface C treated with streptavidin, its presence is revealed by the characteristic red spots.

Versatility of modified surfaces offers the possibility of using theophylline derivatives as an alternative to the surface activation, by chemical grafting, to study receptor-ligand interactions without false positives (according to Hunt *et al.*)[31] and improving biochemical sensor devices for the protein immobilization.[32]

[31] Dahmen, J. L.; Yang, Y.; Greenlief, C. M.; Stacey, G.; Hunt, H. K. *Colloids Surf. B* **2014**, *122*, 241.
[32] Vitola, G.; Mazzei, R.; Fontananova, E. Giorno, L. *J. Membr. Sci*. **2015**, *476*, 483.

II.3 Modification of gold substrates with tripods 26 and 31

II.3.1 XPS

We have designed novel thioacetate/alkyne-substituted tripod-shaped (*p*-phenylene)s molecules (**26** and **31**, figure II.19), which are potentially capable of monomolecular assembly on gold substrates, maintaining, due to their rigidity and specific geometry, the orientation of the functional arm in a perpendicular fashion with respect to the substrate.[33]

Along these lines, we describe the experimental procedures and present the results regarding their assembly on Au(111) substrates over the thiolate-gold bonds. The molecules **26** and **31** differ by the length of the anchoring "legs" which we consider as a parameter affecting their self-assembling ability.

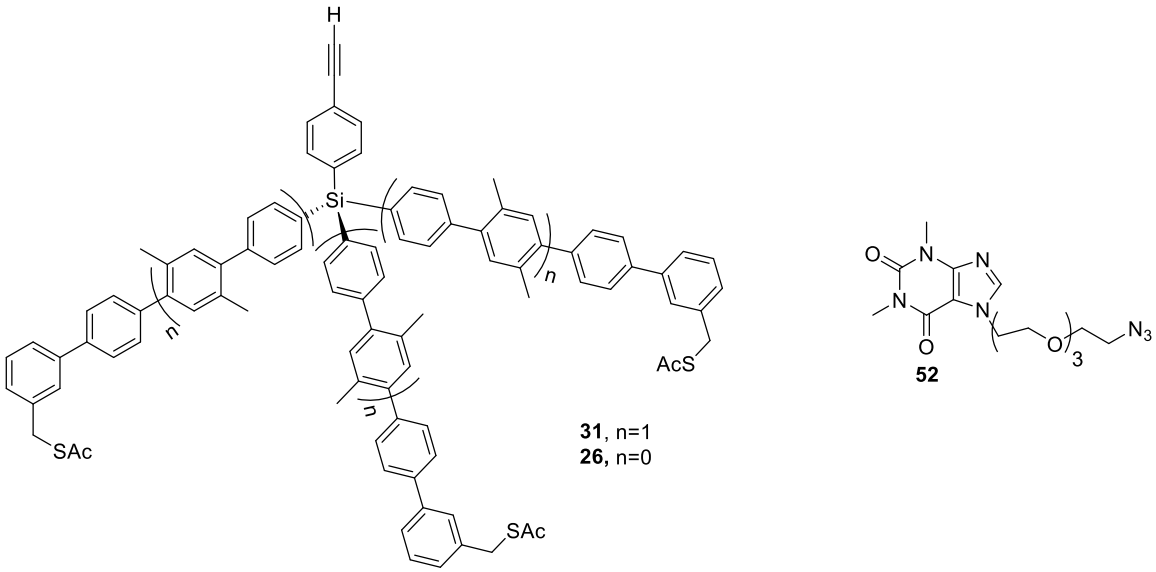

Figure II.19 Tripod-shaped molecules **26** and **31** end-capped with SAc groups. Theophylline **52**.

The self-assembly process of **26** and **31** on Au(111) substrates was carried out with the *in situ* deprotection of the terminal thioacetate groups. Three different deprotection agents (bases) were tested, viz. triethylamine (TEA), ammonia and *N*,*N*,*N'*,*N''*,*N''*-pentamethyldiethylenetriamine (PMDTA).

The C 1s XPS spectra of the resulting films are presented in figure II.20. These spectra exhibit a main peak at a binding energy (BE) of 284.0-284.15 eV for **31** (figure II.20 a) and 284.25-284.45 eV for **26** (figure II.20 b), which is predominantly associated with the

[33] López-Tocón, I.; Peláez, D.; Soto, J.; Rico, R.; Cai, C.; López-Romero, J. M.; Otero, J. C. *J. Phys. Chem. B,* **2008**, *112*, 5363.

phenyl rings in the three "legs" and terminal phenylacetylene group of these molecules, and a weak shoulder (or shoulders, in the case **26**/PDMTA) at 286.0-288.0 eV, which can be tentatively assigned to contaminants or non-deprotected thioacetate groups (C=O).

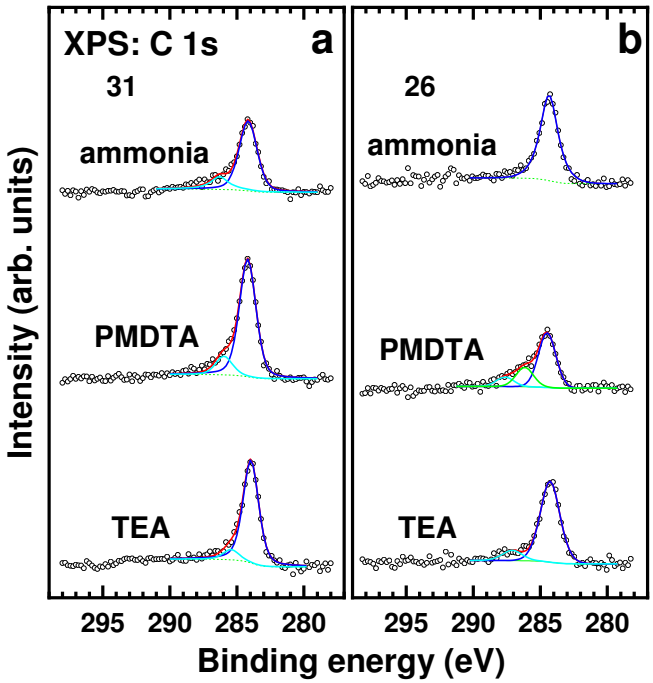

Figure II.20 C 1s XPS spectra of the **31** (a) and **26** (b) films on Au(111) prepared using ammonia, PMDTA or TEA as the deprotection agent. The spectra are decomposed in individual component peaks shown in different colors (main peak - blue lines, high energy shoulder/shoulders - cyan and green lines; the sum of the component peaks - red lines).

The full width at half maximum (fwhm) of the main component peak, characteristic of the film heterogeneity, is noticeably larger for the cases of **31**/ammonia, **26**/ammonia, **26**/PDMTA and **26**/TEA as compared to **31**/TEA and **31**/PDMTA, which suggests a larger structural inhomogeneity and a poorer quality of the former films. The thicknesses of the **31** films were estimated at 1.84 nm, 1.95 nm, and 1.12 nm for the PMDTA, TEA, and ammonia deprotection, respectively.

Consequently, the films prepared by using PMDTA or TEA have the similar thicknesses, close to the "height" of **31** upon adsorption in the desired monomolecular fashion, while that for the film prepared with ammonia is noticeably smaller, implying a lower grafting density. In the case of **26**, the thicknesses values for the TEA and ammonia deprotection were estimated at 1.41 nm and 1.50 nm, respectively, while we refrained from any

evaluation for **26**/PMDTA in view of the poor character of the spectrum. Note that the somewhat lower thickness values than the ones obtained for the films derived from tripod **31** are in accordance with the smaller size of the molecule (see figure II.19). Note also that, according to the above considerations, the best films were formed from the tripod **31** upon the TEA or PMDTA deprotection.

The S 2p XPS spectra of the **31** and **26** films are presented in figure II.21. With the exception of **26**/PMDTA, for which the situation is not clear, the spectra of all films are dominated by a doublet at ~162.0 eV (S $2p_{3/2}$) assigned to the thiolate species bound to the gold substrate[34] and accompanied by a weaker doublet at ~163.4 eV (S $2p_{3/2}$), that can correspond to weakly bound sulfur, unbound sulfur, disulfide or non-deprotected thioacetate.[13a] The relative weights of both doublets are given in figure II.21, no traces of oxidized sulfur species (higher binding energies) are observed.

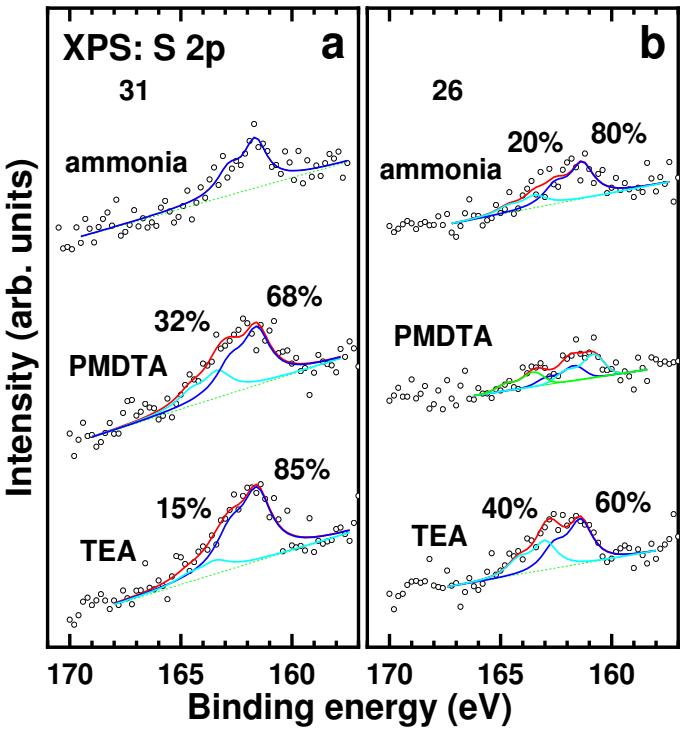

Figure II.21 S 2p XPS spectra of the **31** (a) and **26** (b) films on Au(111). The spectra are decomposed in individual component doublets shown in different colors (thiolate - blue lines; unbound sulfur - cyan lines; their sum - red lines). The spectral weights of these doublets are given.

[34] Zharnikov, M. *J. Electron Spectr. Relat. Phenom.* **2010**, *178-179*, 380.

As seen in figure II.21 a, where the data for the **31** films are presented, the higher absolute intensity of the sulfur signal is observed in the cases of the PMDTA and TEA deprotection. At the same time, the latter film exhibits comparably higher percentage of the thiolate signal with only 15% of unbound sulfur. This suggests that this film represents a well-defined SAM, with most of the potential anchor groups deprotected and bound as thiolates to the gold substrate. This is also true for the **31** film prepared with ammonia, for which, according to the S 2p spectrum, all anchor groups were deprotected and bound as thiolates to the gold substrate. However, in view of the C 1s data, the packing density of this film is much smaller than for the case of TEA, so that its entire quality can be considered as inferior. Note that the effective packing density of the **31** SAM prepared with the TEA deprotection was estimated at ~1.6 x 10^{14} molecules/cm^2; this value is quite reasonable and similar to that reported recently for another type of tripods assembled on Au(111).[21]

As to the tripod **26** (figure II.21 b), the quality of the films is quite poor in the case of the PMDTA deprotection (a low intense and heterogeneous S 2p signal) and somewhat better for the ammonia and TEA deprotection. For ammonia, the highest spectral weight of thiolate among the **26** films is observed (80%), but the absolute intensity of the thiolate signal is lower than in the case of TEA, for which, however, the spectral weight of thiolate is much lower (60%). So, it is difficult to decide which **26** film, representing, in view of the XPS data, SAMs as well, is of a better quality, but the overall quality of the **26** monolayers is certainly lower than that of the **31** SAMs. This can be tentatively attributed to a higher stability of the tripod **31** under basic conditions due to the sterical hindrances that are associated with its size. Since the legs in **31** are longer compared to **26**, they might induce a higher steric effect around the silicon atom, which is located at the core, thus resulting in a lower probability of tripod breakage by the attack of the base and, therefore, a more reliable and better SAM formation.

Note that in some cases multiple Si 2p features and a peak at ~103.0 eV, corresponding to oxidized silicon species, were observed in the respective XPS spectra of the **26** films (not shown). The Si 2p spectrum of SAMs derived from tripod **31** (not shown), exhibited a well-defined Si 2p signal at 100.4 eV, which can be associated with the intact Si core atom. This is an additional evidence that the use of a strong base such as ammonia can destroy the tripod structure, providing poorly-defined SAMs.

II.3.2 X-Ray absorption fine structure spectroscopy (NEXAFS)

The representative, best-quality **31** and **26** SAMs (deprotection by TEA) were characterized by near edge X-ray absorption fine structure (NEXAFS) spectroscopy and the respective data are shown in figure II.22.

Two kinds of spectra are presented, viz. the spectra acquired at the so-called "magic angle" of X-ray incidence (55°) and the difference between the spectra acquired at the normal and grazing incidence angles of X-rays (90°-20°). Whereas the 55° spectra are exclusively representative of the electron structure of the samples, the difference curves are characteristic of the molecular orientation and orientational order in the samples, relying on linear dichroism in X-ray absorption.[35]

The 55° spectra of the **31** and **26** SAMs are very similar, which is understandable in view of the similar chemical compositions. The spectra are dominated by the characteristic absorption resonances of the phenyl rings which are the major building blocks of **31** and **26**. These resonances include the intense π_1* resonance at ~285.0 eV (1), R*/C-S* resonance at ~287.3 eV (2), π_2* resonance at ~288.9 eV (3), and several σ* resonances (4-5) at higher excitation energies.[36] The most prominent π* resonance of the terminal alkyne group, expected at ~285.9 eV, is not perciptable since there is only one such group per molecule and the spectra are normilized to the entire amount of the carbon atoms. The characteristic absorption structure is more pronounced in the case of **31**, which is in particular emphasized by the higher intensity of the π_1* resonance. This is understandable since **31** contains more phenyl rings than **26**.

[35] Stöhr, J. *NEXAFS Spectroscopy*; Springer series in surface sciences; 25; 1. ed., corr. 2. print.; Springer: Berlin [u.a.], 2003

[36] a) Stöhr, J.; Hitchcock, A. P.; Newbury, D. C.; Johnson, A. L.; Sette, F. *J. Chem. Phys.* **1985**, *83*, 6099. b) Yokoyama, T.; Seki, K.; Morisada, I.; Edamatsu, K.; Ohta, T. *Phys. Scr.* **1990**, *41*, 189. c) Frey, S.; Stadler, V.; Heister, K.; Eck, W.; Zharnikov, M.; Grunze, M.; Zeysing, B.; Terfort, A. *Langmuir* **2001**, *17*, 2408.

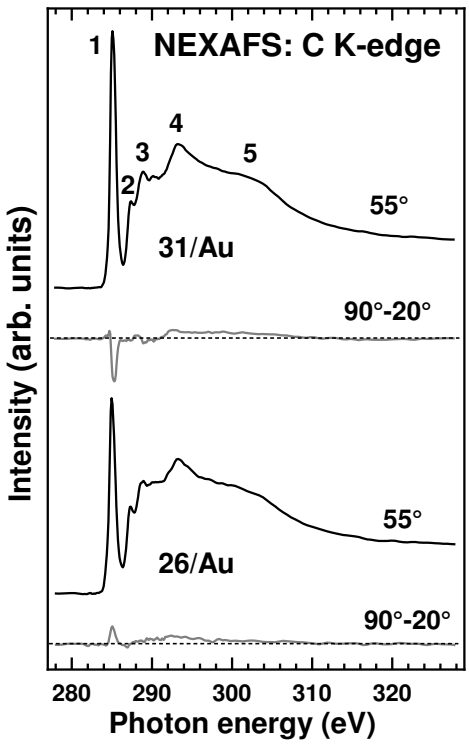

Figure II.22. C K-edge NEXAFS data for the **31** and **26** SAMs prepared with the TEA deprotection, including the spectra acquired at an X-ray incidence angle of 55° (black lines) and the difference between the spectra acquired at X-ray incidence angles of 90° and 20° (gray lines). Characteristic absorption resonances are marked by numbers (see text for details). Horizontal dashed lines correspond to zero.

The difference spectra of the **31** and **26** SAMs in figure II.22 exhibit only small linear dichroism, reflected in the peaks at the positions of the absorption resonances. Even though these peaks are oppositely directed for the **31** and **26** SAMs, their amplitude is quite small as compared to the intensity of the respective resonances in the 55° spectra.

This means that the average inclination of the oligophenyl legs of **31** and **26** with respect to the surface normal is close to 35° (90°-"magic angle") or that this inclination is not really defined in view of the different orientation of all three legs with respect to the substrate and possible deviations from the perfect tripodal geometry (all three legs are attached to the substrate) for individual molecules.

II.3.3. Atomic force microscopy

The **31** SAM prepared with the deprotection by TEA was characterized by atomic force microscopy (AFM); representative images are presented in figure II.23. These images exhibit well-pronounced peaks which can be associated with the individual **31** molecules.

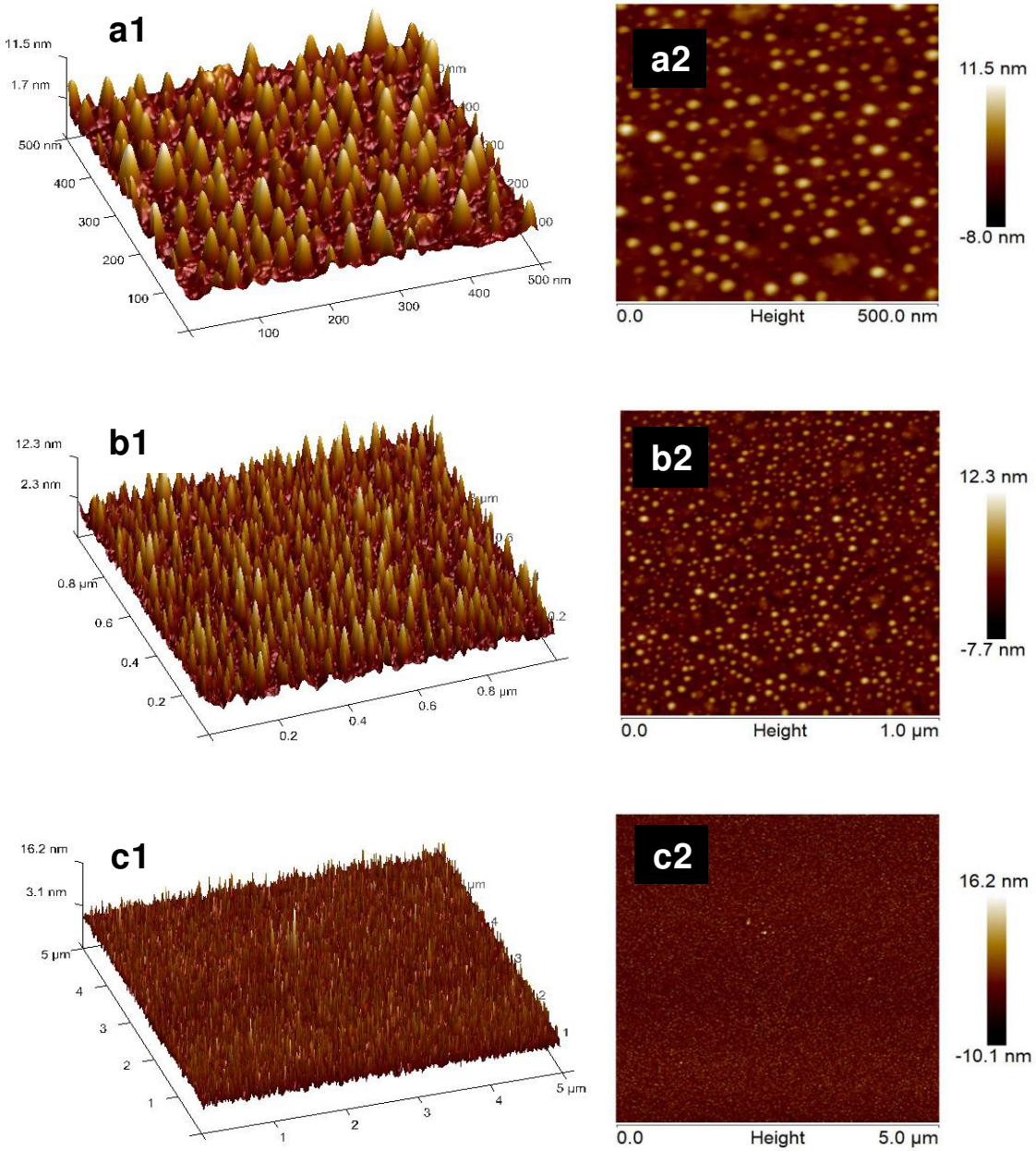

Figure II.23 Tapping mode 3D (a1, b1, c1) and 2D (a2, b2, c2) AFM images of the **31** SAM on Au(111) (with TEA deprotection). The scan area was set at 500 nm x 500 nm (a1, a2), 1 µm x 1 µm (b1, b2), and 5 µm x 5 µm (c1, c2). Roughness values for these scans were estimated at 1.92, 1.85 and 1.55 nm, respectively.

From the morphology analysis of the images, an almost complete Au(111) surface coverage is observed. Most of these peaks (~95%) have similar height, with a calculated height-average of 2.1 nm, which we associate with the uprightly oriented tripods, bound to the substrate by all three anchoring groups. Accordingly, the portion of the tripod-shaped molecules that are attached to the surface by one or two legs only is quite low (~5%), in agreement with the XPS data.

II.3.4 Click reaction with theophylline 52

In view of the good quality of the **31** SAMs prepared with TEA deprotection and the tripodal adsorption geometry for most of the molecules in these films, we selected them as a test template for the click reaction between the terminal alkyne group of **31** and the theophylline decorated with the azide moiety (**52**, figure II.19). The goals were (i) to test the functionality of the tripod SAMs in terms of the click reaction ability and (ii) to prepare functional films for protein immobilization.

The conditions of the click reaction (scheme II.3) were set in accordance with literature data[37] (see experimental section for details) while the concentrations of **52** was varied, set at either 0.05 mM or 0.5 mM, which we will denote as "click 1" and "click 2", respectively.

[37] Sánchez-Molina, M.; Díaz, M.; Valpuesta, M.; Contreras-Cáceres, R.; López-Romero, J. M.; López-Ramírez, M. R. *Appl. Surf. Sci.* **2018**, *445*, 175.

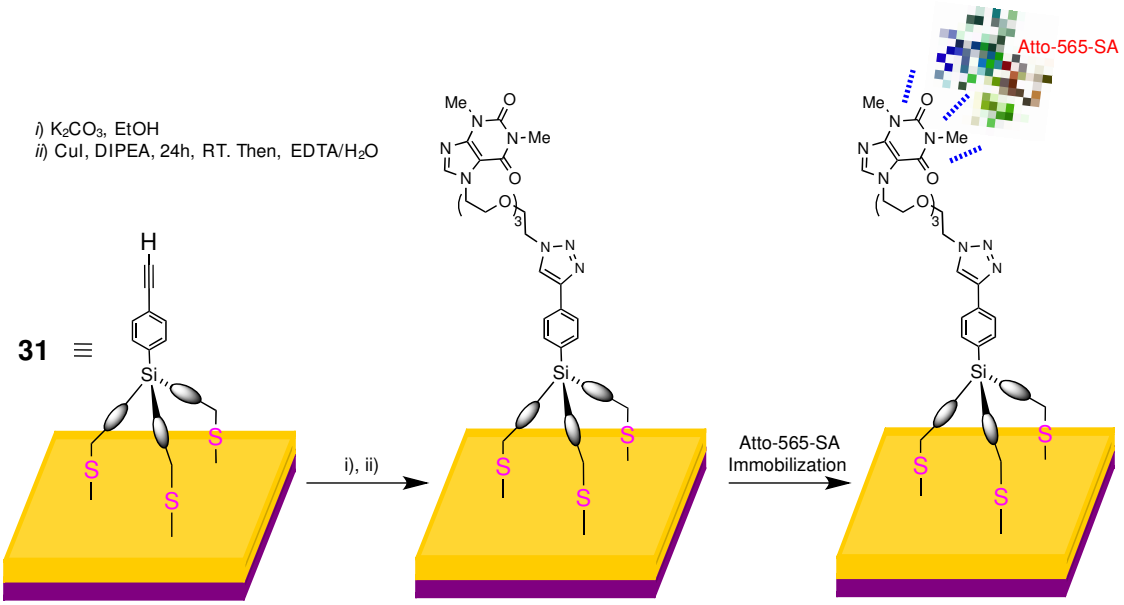

Scheme II.3 Schematic representation of the click reaction between the terminal alkyne group of the **31** SAM and the azide group of the azide-decorated theophylline **52**, followed by immobilization of streptavidin labeled with a fluorescence marker (Atto-565-SA).

The outcome of the click reaction was monitored by synchrotron-based XPS. The data are presented in figure II.24. The C 1s spectrum of the pristine SAM in figure II.24 b is similar to that obtained by the laboratory XPS (figure II.20 a), with the main component peak appearing more sharp and narrow because of the higher energy resolution. The N 1s spectrum of this SAM in figure II.24 c exhibits, as expected, no signal. After the click reaction, we observe considerable changes in all these spectra, which indicate the attachment of theophylline **52** to the **31** SAM. These changes include the decrease of the Au 4f intensity (figure II.24 a), broadening of the main peak and appearance of new peaks in the C 1s spectra (figure II.24 b), and appearance of the N 1s signal (figure II.24 c). The latter represents the most important fingerprint of the click reaction, since, in contrast to the features in the C 1s spectra, which are not entirely specific, the N 1s signal is characteristic of theophylline and the triazole ring formed after the reaction of alkyne with azide. The intensity of this signal is higher for the "click 2" reaction, accompanied by the stronger changes of the Au $4f_{7/2}$ and C 1s spectra as compared to the "click 1" case. This is understandable in view of the higher concentration of theophylline used in the case of "click 2". Such a higher concentration results obviously in a larger amount of the attached theophylline.

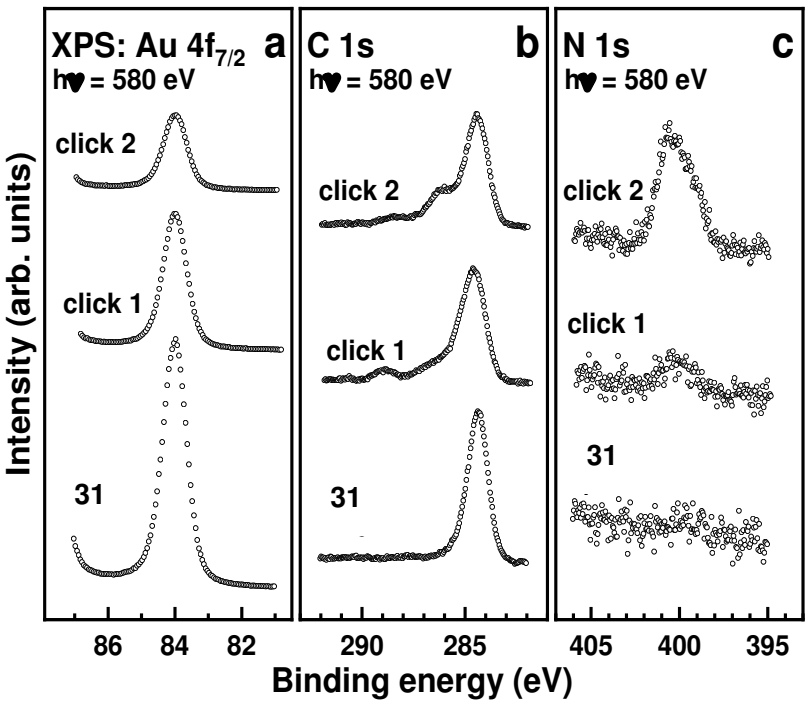

Figure II.24 Au $4f_{7/2}$ (a), C 1s (b), and N 1s (c) XPS spectra of the **31** SAMs before and after the click reaction (click 1 or click 2). The spectra were acquired at the synchrotron at the primary photon energy of 580 eV.

II.3.5 Protein adhesion study

The fabricated **31-**SAMs functionalized with theophylline (**52**-**31**/Au in figure II.25) were tested as templates for specific protein immobilization taking labeled streptavidin (Atto-565-SA) as a test protein. The immobilization was monitored by XPS, relying on the N 1s signal, which is a standard approach for such studies. Representative spectra are shown in figure II.25, which also presents the reference data obtained by treating the theophylline-functionalized SAM surface with a non-specific protein, the bovine serum albumine (BSA), under the same conditions as in the **52**-**31**/Au case. Thus, we were able to compare the amount of specifically and non-specifically adsorbed protein onto the **52**-**31**/Au templates.

Whereas the N 1s XPS spectrum of the pristine **31** SAMs does not exhibit any signal, and the intensity of this signal in the spectrum of **52**-**31**/Au is comparably low, the intensity of the N 1s signal in the spectrum of SA-**52**-**31**/Au is very high, highlighting the attachment of streptavidin to the **52**-**31** template. The latter intensity is also significantly higher than that for BSA-**52**-**31**/Au, suggesting that the specific adsorption of the streptavidin onto the **52**-**31** template, mediated by the terminal theophylline receptors, is much more efficient than a non-specific adsorption onto the same substrate.

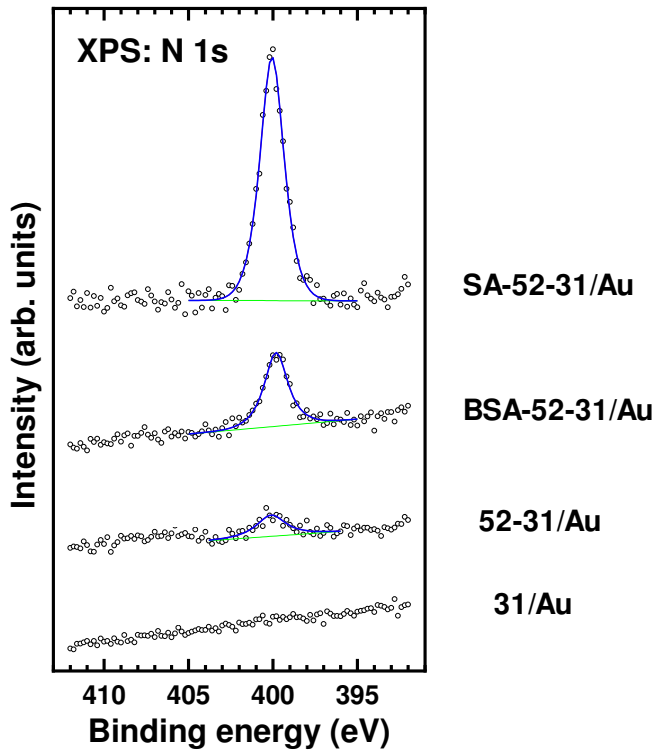

Figure II.25 N 1s XPS spectra of the pristine and theophylline-decorated **31** SAMs (TEA deprotection) before and after the immobilization of streptavidin (SA) and BSA.

4. EXPERIMENTAL SECTION

Experimental Section

In this section, it will be described the experimental procedures carried out for both synthesis of organic adsorbates and modification of metallic substrates (Si and Au) via click reaction or self-assembled monolayers. Experimental Section is divided in four parts covering: general experimental methods (which includes solvents, spectroscopic techniques for the compounds characterization and surface techniques used to study the organic-modified surfaces), the synthetic procedures followed to afford the different compounds used along this work, methodologies employed for the modification of Si/Au substrates and finally sensing experiments with DMABI tripods.

General Experimental Methods

Diethyl ether, dimethoxyethane (DME) and tetrahydrofurane (THF) were distilled from sodium/benzophenone under argon atmosphere while CH_2Cl_2 and pyridine was distilled over CaH_2. All other reagents and solvents were purchased from commercial sources and used without further purification. All solvents were evaporated at reduced pressure by using rotary evaporator.

Mass spectrometry (MS) measurement was carried out using electron impact (EI), electrospray ionization (ESI) or matrix-assisted laser desorption ionization time-of-flight (MALDI-TOF) technique. Samples for MALDI-TOF MS were prepared in a 2,5-dihydroxybenzoic acid (DHB) matrix or Ditranol. ^{1}H and ^{13}C-NMR spectra were recorded with a 400 MHz ARX 400 Bruker spectrometer by using the residual solvent peak in $CDCl_3$ (δ 7.24 ppm, 400 MHz, for ^{1}H and δ = 77.0 ppm, 100 MHz, for ^{13}C). The multiplicity of the signals is indicated as: s (singlet), d (doublet), t (triplet), c (quadruplet), m (multiplet) and for any of them, br (broad). Coupling constants *J* are given in Hertz (Hz). TLC analyses were performed on Merck silica gel 60 F 254 plates and column chromatography was performed on silicagel 60 (0.040–0.063 mm).

XPS for silicon substrates were performed with a PHI 5700 X-ray photoelectron spectrometer equipped with a monochromatic Al Kα X-ray source (1486.7 eV) at a takeoff angle (TOA) of 45º from the film surface. The spectrometer was operated at both high and low resolution with windows pass energies of 23.5 and 187.85 eV, respectively. Electron binding energies were calibrated with respect to the C1s line at 286.4 eV (C-C)

or the Si2p line at 99.0 eV. Signal deconvolution was performed first by Shirley background subtraction, followed by nonlinear fitting to mixed Gaussian-Lorentzian function with 80% Gaussian and 20% Lorentzian character. XPS for gold substrates were performed with a MAX 200 spectrometer (Leybold-Heraeus) equipped with a Mg Kα X-ray source (1253.6 eV; 200 W) and a hemispherical analyzer. The X-ray source was positioned ~1.5 cm away from the sample. The spectra were recorded in normal emission geometry with an energy resolution of ~0.9 eV. The raw spectra were corrected for the spectrometer transmission by division through the respective function; the binding energy scale was referenced to the Au $4f_{7/2}$ peak of clean gold at 84.0 eV. XPS spectra were fitted by symmetric Voigt functions and either linear or Shirley-type background. Hexadecanethiolate (C16) SAM was prepared using standard protocol, this film served as the reference sample for the thickness evaluation XPS data were used to calculate the effective thicknesses and packing density of the films. For the calculation of the effective thickness a standard procedure was used,[1] based on the C 1s/Au 4f intensity ratio and a SAM (C16/Au) of well-defined thickness (~1.84 nm) as the reference. Attenuation length values characteristic of densely packed alkanethiolate SAMs on Au(111) were used. The packing density was calculated based on the S 2p/Au 4f intensity ratio and a C16 SAM on Au(111) as the reference (4.63×10^{14} molecules/cm^2).[2]

Synchrotron-based XPS measurements were performed at few selected samples only. The experiments were carried out at the HE-SGM beamline (bending magnet) of the synchrotron storage ring BESSY II in Berlin, Germany Germany, using a Scienta R3000 electron energy analyzer. The synchrotron light served as the primary X-ray source. The spectra acquisition was carried out in normal emission geometry with an energy resolution of ~0.3 eV at an excitation energy of 350 eV and ~0.5-0.6 eV at an excitation energy of 580 eV. NEXAFS measurements were performed at the same beamline as the synchrotron-based XPS experiments. Spectra acquisition was carried out at the C K-edge in the partial electron yield mode with a retarding voltage of −150 V. Linearly polarized synchrotron light with a polarization factor of ~88% was used as the primary X-ray source; the incidence angle of the light was varied following the standard approach.[3] The energy resolution was ca. 0.30 eV. The photon energy scale was referenced to the pronounced π* resonance of highly oriented pyrolytic graphite at

[1] Sauter, E.; Gilbert, C.-O.; Boismenu-Lavoie, J.; Morin, J.-F.; Zharnikov, M. *J. Phys. Chem. C*, **2017**, *121*, 23017–23024.
[2] Schreiber, F. *Prog. Surf. Sci.* **2000**, *65,* 151–256.
[3] Stöhr, J. *NEXAFS Spectroscopy*; Springer series in surface sciences; 25; 1. ed., corr. 2. print.; Springer: Berlin [u.a.], 2003

285.38 eV.[4] The spectra were corrected for the photon energy dependence of the incident photon flux by division through the spectrum of clean gold and reduced to the standard form, getting zero intensity in the pre-edge region and the unity jump in the far post-edge region.

AFM imaging of the surfaces was performed using a Multi Mode Nanoscope V AFM (Digital Instrument Ins., Santa Barbara, California). Images were acquired in tapping mode using a silicon nitride cantilever (MikroMasch, San Jose, California) with resonant frequency of 132.9 kHz and a nominal force constant of 1.75 N/m.

Fluorescence images were taken on a Leica TCS SP5 Confocal (Leica). We characterized the localized emission fluorescence from 1 cm x 1 cm surfaces between 550-650 nm, excited with a laser at 458 nm using 20x objective.

[4] Batson, P. E. *Phys. Rev. B* **1993**, *48*, 2608–2610.

4.1 Synthesis of tripods with azide groups as headgroups

4.1.1 Tripods with 3 phenylene units

4.1.1.1 Synthesis of triethoxy(4-((trimethylsilyl)ethynyl)phenyl)silane (**1**)

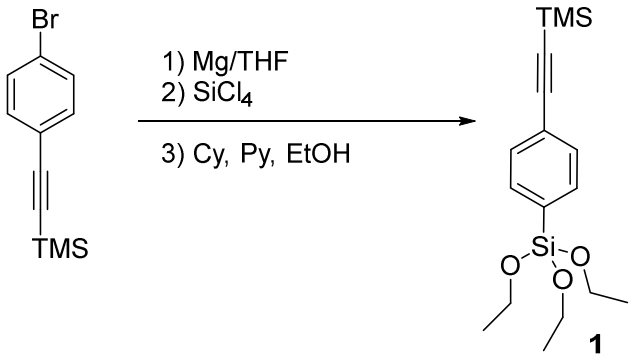

Under an argon atmosphere, a solution of distilled $SiCl_4$ (9.2 mL,79.1 mmol) in anhydrous THF (10 mL) was added at -78 ºC to a suspension of ((4-bromophenyl)ethynyl)trimethylsilane (10.00 g, 39.5 mmol) and magnesium (1.20 g, 51.40 mmol) in anhydrous THF (50 mL). The reaction mixture was stirred overnight at 20 ºC. After this period, the mixture was concentrated to dryness under vacuum. The crude residue was dissolved in anhydrous cyclohexane (200 mL) and absolute ethanol (131 mL, 197.7 mmol) and anhydrous pyridine (10 mL, 123.4 mmol) was slowly added. The reaction mixture was stirred at 20 ºC for 12 h. After this period, the reaction mixture was filtered and the solution was washed with 1M HCl (50 mL), saturated $NaHCO_3$ (50 mL), and water (2x50 mL). The organic phase was dried over anhydrous $MgSO_4$ and the solvent was removed under vacuum. The residue was purified by distillation under reduced pressure and the silane **1** was obtained as a colorless oil (8.76 g, 66%).[5]

^{1}H-RMN ($CDCl_3$) δ (ppm): 7.60 (d, 2H, *J*= 8.0 Hz, ArH), 7.45 (d, 2H, *J*= 8.0 Hz, ArH), 3.85 (c, 6H, *J*= 7.0 Hz, 3 x CH_2), 1.25 (t, 9H, *J*= 7.0 Hz, 3 x CH_3), 0.03 (s, 9H, TMS).

^{13}C-RMN ($CDCl_3$) δ (ppm): 142 (C-Si), 131.9 (2 x CH), 125.6 (2 x CH), 124.0 (C), 106.4 (C≡C), 98.0 (C≡C), 58.0 (3 x CH_2), 18.4 (3 x CH_3), 0.0 (TMS).

[5] Horsham, M. A.; Palmer, C. J.; Cole, L. M; Casida, J.E. *J. Agric. Food Chem*. **1990**, *38*, 1734.

4.1.1.2 Synthesis of tris(4-iodophenyl)(4-((trimethylsilyl)ethynyl)phenyl)silane (**2**)

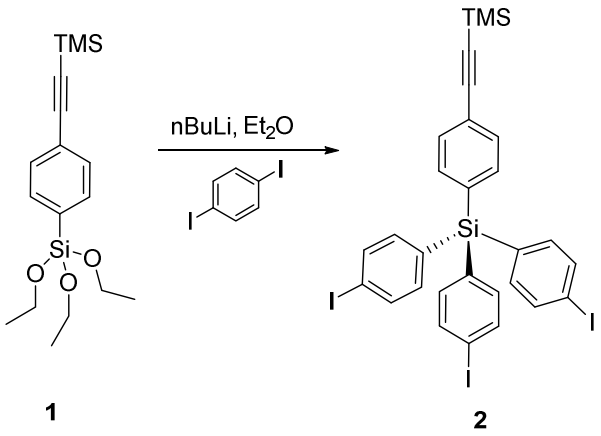

1 **2**

Under an argon atmosphere, n-butyl lithium (1.6 M, 50 mL, 80.8 mmol) was added to a solution of *p*-diiodobenzene (34.31 g, 104.3 mmol) in anhydrous diethyl ether (500 mL) at -78 ºC. The mixture was stirred for 1 h at -78 ºC and, after this period, a solution of **1** (8.76 g, 26.1 mmol) in anhydrous diethyl ether (50 mL) was added at -78 ºC. The reaction mixture was stirred for 30 min at this temperature, and then for 12 h at 20 ºC. After this period, 1M HCl (70 mL) was added. The organic phase was extracted and washed with water and brine (2 x 30 mL), dried over anhydrous $MgSO_4$, and concentrated to dryness. Compound **2** was isolated by column chromatography (cyclohexane) as a white solid (2.30 g, 16%).[6]

^{1}H-RMN ($CDCl_3$) δ (ppm): 7.75 (d, 6H, *J*= 8.0 Hz, ArH), 7.45 (d, 2H, *J*= 8.0 Hz, ArH), 7.41 (d, 2H, *J*= 8.0 Hz, ArH), 7.19 (d, 6H, *J*= 8.0 Hz), 0.25 ppm (s, 9H, TMS).
^{13}C-RMN ($CDCl_3$) δ (ppm): 137.2 (6 x CH), 135.5 (C-Si), 134.2 (6 x CH), 133.2 (3 x C-Si), 131.9 (4 x CH), 124.0 (C), 105.4 (C≡C), 98.0 (C≡C), 95.7 (3 x C-I), 0.0 (TMS).

[6] Yao, Y.; Tour, J. M. *J. Org. Chem*. **1999**, *64*, 1968.

4.1.1.3 Synthesis of (4-bromophenyl)triethoxysilane (**3**)

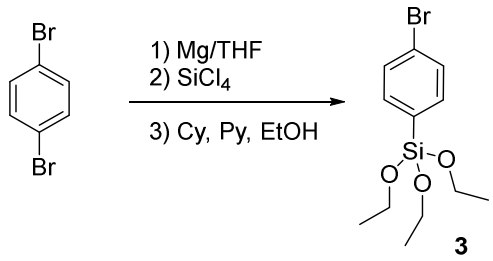

3

Following the procedure outlined for **1**, from *p*-dibromobenzene (14.02 g, 59.4 mmol), $SiCl_4$ (15 mL, 130.7 mmol), magnesium (1.88 g, 77.2 mmol), anhydrous THF (65 mL), cyclohexane (250 mL), pyridine (15 mL), and ethanol (17 mL), compound **3** was prepared and purified by distillation under reduced pressure to obtain it as a colorless oil (5.95 g, 31%).[7]

^{1}H-RMN ($CDCl_3$) δ (ppm): 7.55 (s, 4H), 3.85 (c, 6H, *J*= 7.0 Hz, 3 x CH_2), 1.22 (t, 9H, *J*= 7.0 Hz, 3 x CH_3).
^{13}C-RMN ($CDCl_3$) δ (ppm): 136.3 (2 x CH), 131.0 (C-Si), 130.3 (2 x CH), 125.3 (C-Br), 58.8 (3 x CH_2), 18.1 (3 x CH_3).

[7] Erben, Christoph Georg; US 20050214479 A1 2005

4.1.1.4 Synthesis of (4-bromophenyl)tris(4-iodophenyl)silane (**4**)

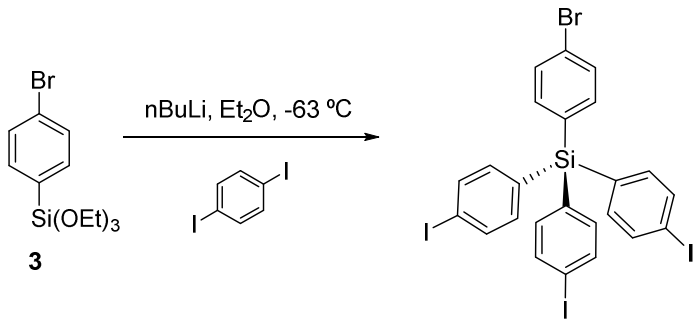

Following the procedure outlined for **2**, from compound **3** (5.95 g,18.6 mmol), *p*-diiodobenzene (20.30 g, 61.5 mmol), n-BuLi (1.6 M, 38.47 mL, 61.5 mmol), anhydrous Et_2O (350 mL), and further column chromatography (cyclohexane), compound **4** was obtained as a white solid (3.00 g, 20%).

M.p. 280 ºC dec.[8]

^{1}H-RMN ($CDCl_3$) δ (ppm): 7.72 (d, 6H, *J*= 8.0 Hz, ArH), 7.51 (d, 2H, *J*= 8.0 Hz, ArH), 7.31 (d, 2H, *J*= 8.0 Hz, ArH), 7.17 (d, 6H, *J*= 8.0 Hz, ArH).
^{13}C-RMN ($CDCl_3$) δ (ppm): 137.6 (6 x CH), 137.4 (4 x C-Si), 131.9 (6 x CH), 131.5 (2 x CH), 131.3 (2 x CH), 125.4 (C-Br), 97.8 (3 x C-I).

[8] Hierrezuelo-Leon, J.; Rico, R.; Valpuesta, M.; Díaz, A.; López-Romero, J. M.; Rutkis, M.; Kreigberga, J.; Kampars, V.; Algarra, M. *Tetrahedron* **2013**, *69*, 3465.

4.1.1.5 Synthesis of (4´-bromo-2´,5´-dimethyl)biphenyl-4-yl)trimethylsilane (**5**)

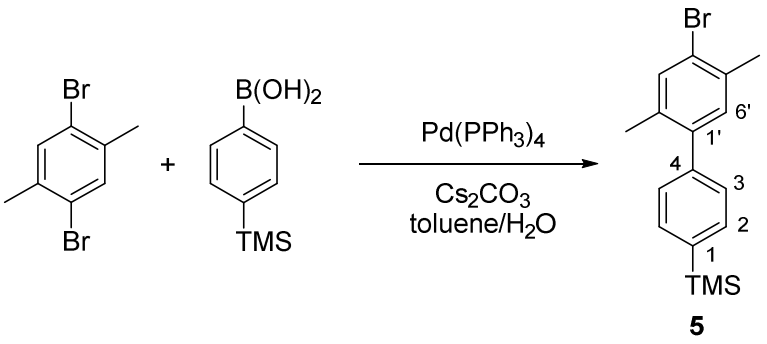

5

An oven-dried round-bottomed flask was placed under an argon atmosphere and filled with *p*-trimethylsilylphenylboronic acid (5.00 g, 25.76 mmol), *p*-dibromoxylene (34.00 g, 128.79 mmol), Cs_2CO_3 (16.80 g, 51.52 mmol), and $Pd(PPh_3)_4$ (2.98 g, 2.58 mmol). The flask was purgued and refilled with argon (3x) and then toluene/water (1:1, 200 mL) was added. The reaction mixture was heated to reflux for 18 h. When the reaction was completed, the inorganic solids were removed by filtration through celite and washing with several portions of dichloromethane; then the solvent was evaporated. The residue was purified by column chromatography using cyclohexane as eluent to give **5** as a white solid (8.41 g, 98%).

M.p. 67-69 °C. [9]

^{1}H-RMN ($CDCl_3$) δ (ppm): 7.55 (d, 2H, *J*= 8.0 Hz, H-3, H-5), 7.43 (s, 1H, H-6´), 7.26 (d, 2H, *J*= 8.0 Hz, H-2, H-6), 7.08 (s, 1H, H-3´), 2.37 (s, 3H, CH_3), 2.21 (s, 3H, CH_3), 0.29 (s, 9H, TMS).

^{13}C-RMN ($CDCl_3$) δ (ppm): 141.2 (C-Si), 141.0, 139.0 (C_{Ar}), 135.0 (C_{Ar}-CH_3), 134.6 (C_{Ar}-CH_3), 133.7 (C-3´), 133.1 (C-2,6), 132.0 (C-6´), 128.3 (C-3,5), 123.4 (C-Br), 22.3 (CH_3), 19.7 (CH_3), -1.1 (TMS).

[9] Andreitchenko, E. V.; Clark, C. G.; Bauer, R. E.; Lieser, G.; Mìllen, K. *Angew. Chem. Int. Ed.* **2005**, *44*, 6348.

4.1.1.6 Synthesis of 4-bromo-4'-iodo-2,5-dimethyl-1,1'-biphenyl (**6**)

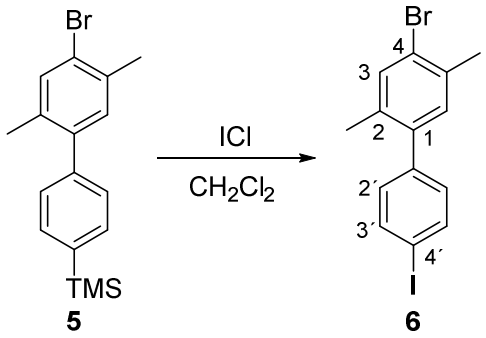

5 **6**

Under an argon atmosphere, a solution of ICl 1M in CH_2Cl_2 (3 mL, 3 mmol) was added to a solution of **5** (500 mg, 1.54 mmol) in dichloromethane (10 mL) at 0 ºC. The reaction mixture was stirred at 20 ºC for 1 h. After this period, an aqueous solution of Na_2SO_3 was added to remove the excess of iodine. The organic phase was then extracted with CH_2Cl_2, washed with water, dried over anhydrous $MgSO_4$, filtered and the solvent was removed under vacuum. The obtained residue was purified by column cromatography (cyclohexane) obtaining compound **6** as a pale oil (524 mg, 90%).[9]

^{1}H-RMN ($CDCl_3$) δ (ppm): 7.72 (d, 2H, *J*= 8.0 Hz, H-3´,5´), 7.42 (s, 1H, H-6), 7.02 (s, 1H, H-3), 7.01 (d, 2H, *J*= 8.0 Hz, H-2´,6´), 2.36 (s, 3H, CH_3), 2.17 (s, 3H, CH_3).
^{13}C-RMN ($CDCl_3$) δ (ppm): 140.4, 139.9 (C_{Ar}), 137.3 (C-3´,5´), 135.2 (C_{Ar}-CH_3), 134.5 (C_{Ar}-CH_3), 133.9 (C-3), 131.7 (C-6), 130.9 (C-2´,6´), 123.9 (C-Br), 92.8 (C-I), 22.3, 19.6 (2 x CH_3).

4.1.1.7 Synthesis of 4´-azide-4-bromo-2,5-dimethyl-1,1'-biphenyl (**7**)

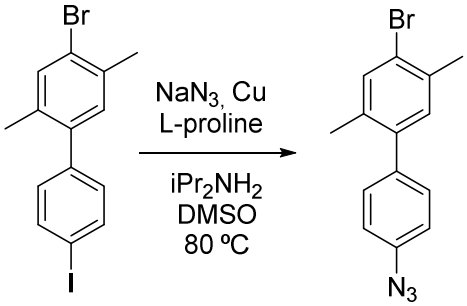

A dried round-bottom flask was fitted with **6** (1.4 g, 3.6 mmol), NaN_3 (4.0 g, 7 mmol), *L*-proline (83 mg, 0.7 mmol), *i*-Pr_2NH (73 mg, 0.7 mmol), DMSO (30 mL), porous Cu (11.4 mg, 0.2 mmol) and ascorbic acid (32 mg, 0.2 mmol). Then, the flask was degassed and the mixture of reaction was stirred at 80 ºC until no starting product was observed. After that, water was poured into the mixture and filtered. The filtrate was extracted with ethyl acetate and the organic layer was washed with brine, dried over anhydrous Mg_2SO_4 and concentrated in vacuum. The residue was purified by column chromatography (cyclohexane/EtOAc, 1:1) to give compound **7** as a yellow oil (467 mg, 43%).

^{1}H-RMN ($CDCl_3$) δ (ppm): 7.42 (s, 1H, ArH, H-6), 7.25 (d, 2H, *J*= 8.5 Hz, H-3´,5´), 7.05 (d, 2H, *J*= 8.5 Hz, H-2´,6´), 7.04 (s, 1H, H-3), 2.36 (s, 3H, CH_3), 2.18 (s, 3H, CH_3).
^{13}C-RMN ($CDCl_3$) δ (ppm): 143.0 (C-N_3) 140.1, 139.0 (C_{Ar}), 135.1 (C_{Ar}-CH_3), 134.6 (C_{Ar}-CH_3), 133.8 (C-3), 131.9 (C-6), 130.9 (C-2´,6´), 123.7 (C-Br), 118.8 (C-3´,5´), 22.3, 19.6 (2 x CH_3).

EI-MS *m/z* (%): 303 (M^+, 20), 275 (100), 194 (82), 167 (85), 152 (57), 82 (25).

4.1.1.8 Synthesis of *tert*-butyl (4'-bromo-2',5'-dimethyl-[1,1'-biphenyl]-4-yl) carbamate (**9**)

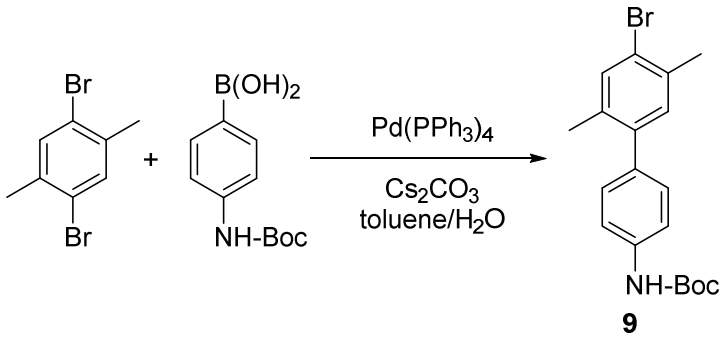

9

Following the procedure outlined for compound **5**, 4-(*N*H-Boc-amino)phenylboronic acid (2.5 g, 10.5 mmol), *p*-dibromoxylene (13.28 g, 50.3 mmol), Cs_2CO_3 (6.45 g, 19.8 mmol) and $Pd(PPh_3)_4$ (1.22 g, 1.0 mmol), in toluene/H_2O (1:1, 100 mL) was heated to reflux for 18 h. Then, the crude was purified by column chromatography (cyclohexane/EtOAc, 9:1) gave compound **9** as a white solid (2.50 g, 50%).

M.p. 130-133 ºC.

^{1}H-RMN ($CDCl_3$) δ (ppm): 7.41 (s, 1H, H-6´), 7.39 (d, 2H, *J*= 8.6 Hz, H-3,5), 7.19 (d, 2H, *J*= 8.6 Hz, H-2,6), 7.05 (s, 1H, H-3´), 6.60 (brs, 1H, NH), 2.36 (s, 3H, CH_3), 2.18 (s, 3H, CH_3), 1.53 (s, 9H, 3 x CH_3, *t*-Bu).
^{13}C-RMN ($CDCl_3$) δ (ppm): 152.8 (C=O), 140.6 (C-N), 135.6, 134.9 (C_{Ar}), 134.7 (2 x C_{Ar}-CH_3), 133.7 (C-3´), 132.1 (C-6´), 129.6 (C-2,6) , 123.3 (C-Br), 118.3 (C-3,5), 80.7 (C, *t*-Bu), 28.4 (3 x CH_3, *t*-Bu), 22.3, 19.7 (2 x CH_3).

HRMS: calcd for $C_{19}H_{22}NO_2Br$ [M+Na$^+$] 398.07261; found 398.07281.

4.1.1.9 Synthesis of *tert*-butyl (2',5'-dimethyl-4'-(4,4,5,5-tetramethyl-1,3,2-dioxaborolan-2-yl)-[1,1'-biphenyl]-4-yl)carbamate (**10**)

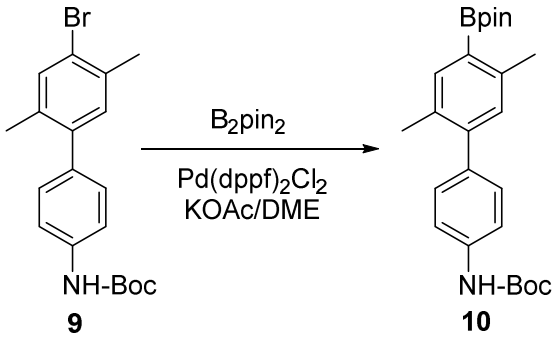

Under an argon atmosphere, a degassed solution of **9** (1.60 g, 4.30 mmol), bis(pinacolato)diboron (1.37 g, 5.4 mmol), $Pd(dppf)_2Cl_2$ (0.70 g, 0.8 mmol) and potassium acetate (1.26 g, 12.9 mmol) in dry DME (63 mL) was refluxed for 12 h. After this period, the reaction was cooled to room temperature, filtered, and diluted with CH_2Cl_2 (15 mL). The organic solution was washed with H_2O (2 x 10 mL) and brine, then dried with $MgSO_4$, and concentrated to dryness. The residue was separated by column chromatography (cyclohexane/EtOAc, 9:1) to give compound **10** as a white solid (1.40 g, 77%).

M.p. 75-77 ºC.

^{1}H-RMN ($CDCl_3$) δ (ppm): 7.64 (s, 1H, H-3´), 7.35 (d, *J*= 8.5 Hz, 2H, H-3,5), 7.22 (d, *J*= 8.5 Hz, 2H, H-2,6), 7.01 (s, 1H, H-6´), 6.47 (brs, 1H, NH), 2.50 (s, 3H, CH_3), 2.21 (s, 3H, CH_3), 1.51 (s, 9H, 3 x CH_3, *t*-Bu), 1.33 (s, 12H, 4 x CH_3, Bpin).

^{13}C-RMN ($CDCl_3$) δ (ppm): 152.9 (C=O), 143.8 (C_{Ar}-CH_3), 142.3 (C-N), 138.1 (C-B), 137.2 (C_{Ar}-CH_3), 136.7 (C-3´), 131.5 (2 x C_{Ar}), 131.4 (C-6´), 129.6 (C-2,6), 118.3 (C-3,5), 83.4 (2 x C, Bpin), 80.6 (C, *t*-Bu), 28.4 (3 x CH_3, *t*-Bu), 24.9 (4 x CH_3, Bpin), 21.7, 19.7 (2 x CH_3).

HRMS: calcd for $C_{25}H_{34}BNO_4$ [M+Na$^+$] 446.24731; found 446.24722.

4.1.1.10 Synthesis of tripod **11**

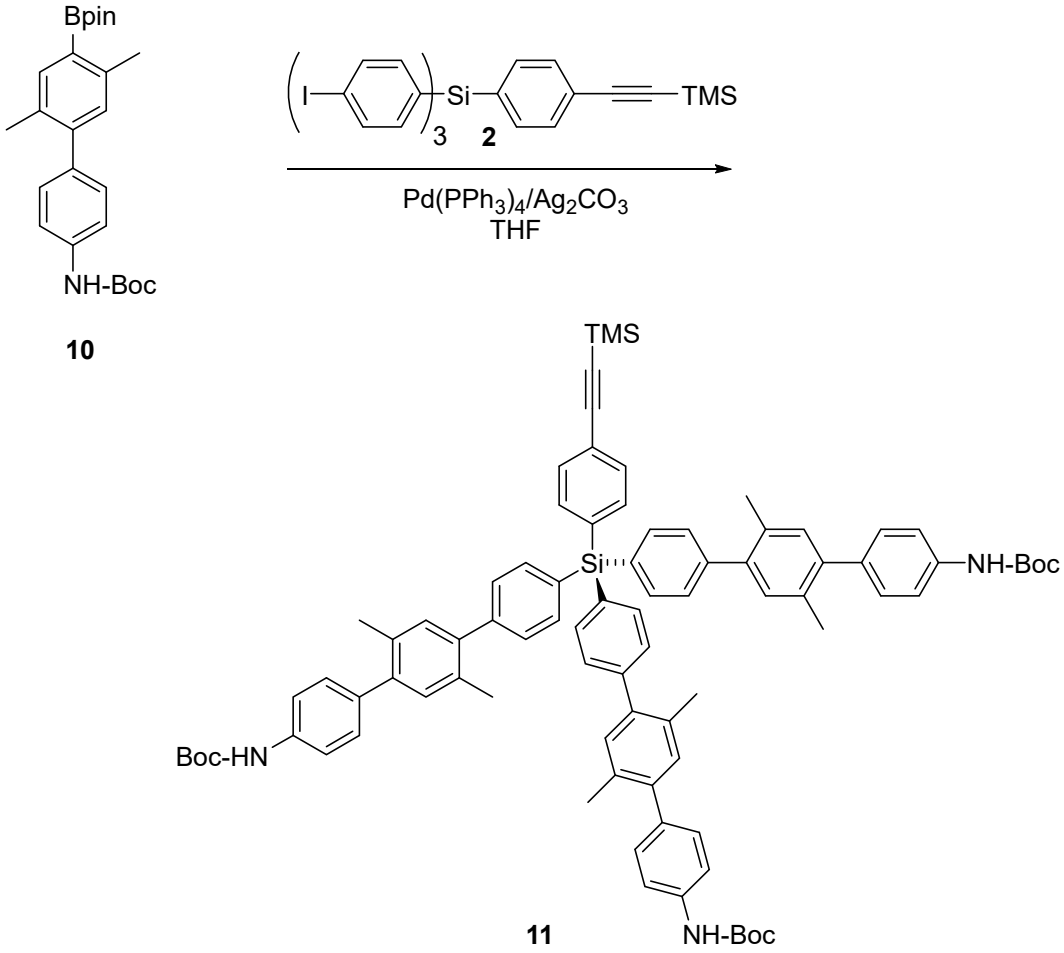

Under argon atmosphere, compound **10** (166 mg, 0.4 mmol), compound **2** (98 mg, 0.13 mmol), $Pd(PPh_3)_4$ (31 mg, 0.027 mmol), $AgCO_3$ (330 mg, 1.20 mmol) were dissolved in dry THF (10 mL). The mixture was stirred under argon atmosphere at 20 ºC for 12 h. After this period, the reaction mixture was filtered through celite, washed with several portions of CH_2Cl_2 and the solvent was removed under vacuum. The product was purified by column chromatography (cyclohexane/EtOAc, 8:2) to yield tripod **11** as a pale yellow oil (210 mg, 40%).

^{1}H-RMN ($CDCl_3$) δ (ppm): 7.68 (d, 6H, *J*= 8.2 Hz, ArH), 7.63 (d, 2H, *J*= 8.3 Hz, 2 x ArH), 7.52 (d, 2H, *J*= 8.3 Hz, 2 x ArH), 7.42 (d, 6H, *J*= 8.2 Hz, ArH), 7.40 (d, 6H, *J*= 8.0 Hz, ArH), 7.30 (d, 6H, *J*= 8.0 Hz, ArH), 7.18 (s, 3H, ArH), 7.13 (s, 3H, ArH), 6.51 (s, 3H, 3 x NH), 2.31 (s, 9H, 3 x CH_3), 2.27 (s, 9H, 3 x CH_3), 1.53 (s, 27H, 9 x CH_3, *t*-Bu), 0.25 (s, 9H, TMS).

^{13}C-RMN ($CDCl_3$) δ (ppm): 152.8 (C=O), 143.2 (C-N), 140.5, 140.4, 137.1 (C_{Ar}), 136.2 (CH_{Ar}), 132.7, 132.6, 132.0 (C_{Ar}), 131.9, 131.8 (CH_{Ar}), 131.2 (C_{Ar}), 129.8, 128.8, 118.3 (CH_{Ar}), 80.6 (3 x C, *t*-Bu), 26.9 (3 x CH_3, *t*-Bu), 20.0, 19.9 (2 x CH_3), -0.03 (TMS).

MALDI-TOF MS (DHB as matrix) (*m/z*): calcd for $C_{86}H_{91}N_3O_6Si_2$ [M^+] 1317.645; found 1317.174.

4.1.1.11 Synthesis of tripod **12**

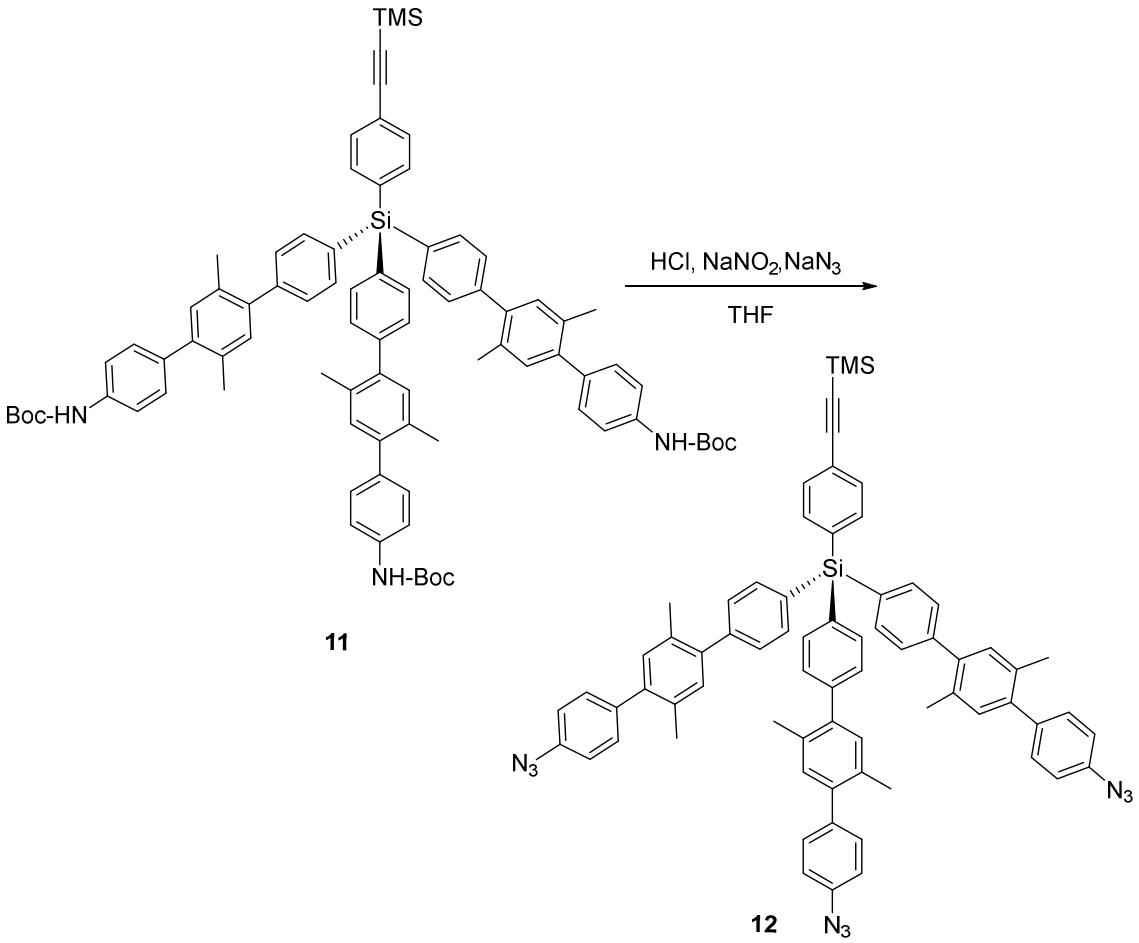

11 **12**

Under argon atmosphere, a solution of concentrated HCl (0.09 mL, 0.72 mmol) was added drop-wise to a round-bottom flask containing a solution of compound **11** (210 mg, 0.16 mmol) in THF (2 mL) at 0 ºC. Then, a solution of $NaNO_2$ (50 mg, 0.72) in THF (2 mL) was slowly added along 30 min. After this period, a solution of NaN_3 (48 mg, 0.7 mmol) in THF (2 mL) was added drop-wise during 30 min. The reaction mixture was then heated to reflux for 24 h and then the solvent was concentrated in vacuum. The mixture was washed with water and extracted with EtOAc. The organic layer was dried over

$MgSO_4$, filtered, and the solvent was removed under vacuum. The crude was purified by column chromatography (cyclohexane/EtOAc, 8:2) giving compound **12** as a yellow oil (115 mg, 65%).

^{1}H-RMN ($CDCl_3$) δ (ppm): 7.68 (d, 6H, *J*= 8.1 Hz, ArH), 7.63 (d, 2H, *J*= 8.2 Hz, ArH), 7.50 (d, 2H, *J*= 8.2 Hz, ArH), 7.41 (d, 6H, *J*= 8.1 Hz, ArH), 7.36 (d, 6H, *J*= 8.5 Hz, ArH), 7.19 (s, 3H, ArH), 7.13 (s, 3H, ArH), 7.08 (d, 6H, *J*= 8.5 Hz, ArH), 2.31 (s, 9H, CH_3), 2.26 (s, 9H, CH_3), 0.25 (s, 9H, TMS).
^{13}C-RMN ($CDCl_3$) δ (ppm): 143.0 (C-N_3), 140.8, 138.7, 138.5, 136.3 (C_{Ar}), 136.2 (CH_{Ar}), 134.9, 134.8, 132.8, 132.7, 132.6, 132.5 (C_{Ar}), 131.9, 131.8 (CH_{Ar}), 131.3, 131.2 (C_{Ar}), 130.6, 130.3, 128.9, 128.8, 128.4, 128.1, 118.7 (CH_{Ar}), 20.0, 19.9 (2 x CH_3), -0.03 (TMS).

MALDI-TOF MS (DHB as matrix) (*m/z*): calcd for $C_{71}H_{61}N_9Si_2$ [M^{+2}+2K^+] 586.729; found 587.012.

4.1.1.12 Synthesis of tripod **13**

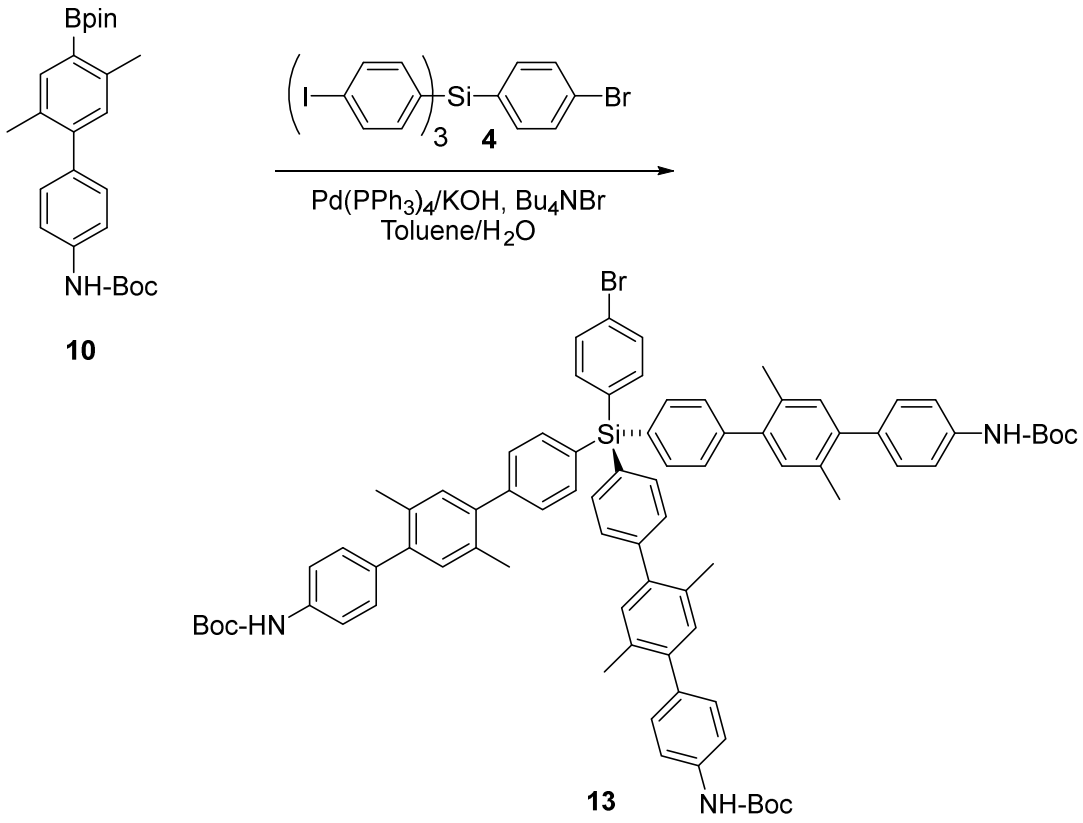

Under an argon atmosphere, compound **10** (254 mg, 0.60 mmol) was coupled with compound **4** (141.60 mg, 0.20 mmol) in the presence of $Pd(PPh)_3$ (32 mg, 0.028 mmol), KOH (168 mg, 3 mmol), *n*-BuNBr (16 mg, 0.025 mmol) and a degassed mixture of toluene/H_2O (8:2, 10 mL). The reaction mixture was heated to reflux for 24 h. After this period, the reaction was filtered through celite and washed with several portions of CH_2Cl_2. The solution was decanted, the aqueous layer was extracted with toluene and the combined organic layers were dried over anhydrous $MgSO_4$. Then the solvent was evaporated and the residue was purified by column chromatography (cyclohexane) to give the tripod **13** as a yellow oil (220 mg, 84%).

^{1}H-RMN ($CDCl_3$) δ (ppm): 7.79 (d, 6H, *J*= 8.1 Hz, ArH), 7.71 (d, 6H, *J*= 8.1 Hz, ArH), 7.67 (d, 2H, *J*= 8.4 Hz, ArH), 7.58 (d, 2H, *J*= 8.4 Hz, ArH), 7.49-7.40 (m, 12H, ArH), 7.22 (s, 3H, ArH), 7.20 (s, 3H, ArH), 6.62 (s, 3H, 3 x NH), 2.36-2.28 (m, 18H, 6 x CH_3), 1.55 (s, 27H, 9 x CH_3, *t*-Bu).

^{13}C NMR ($CDCl_3$) δ (ppm): 152.9 (C=O), 143.3 (C-N), 140.5, 138.1, 137.9, 137.2, 136.3, 136.2, 132.8-132.2 (C_{Ar}), 131.9 (CH_{Ar}), 131.2 (C_{Ar}), 129.8, 129.1, 128.9, 128.8, 128.3

(CH_{Ar}), 125.3 (C-Br), 118.3 (CH_{Ar}), 80.6 (3 x C, *t*-Bu), 28.4 (3 x CH_3, *t*-Bu), 20.1, 20.0 (2 x CH_3).

MALDI-TOF MS (DHB as matrix) (*m/z*): calcd for $C_{81}H_{82}BrN_3O_6Si$ [M+Na^+] 1322.505; found 1322.240.

4.1.1.13 Synthesis of tripod **14**

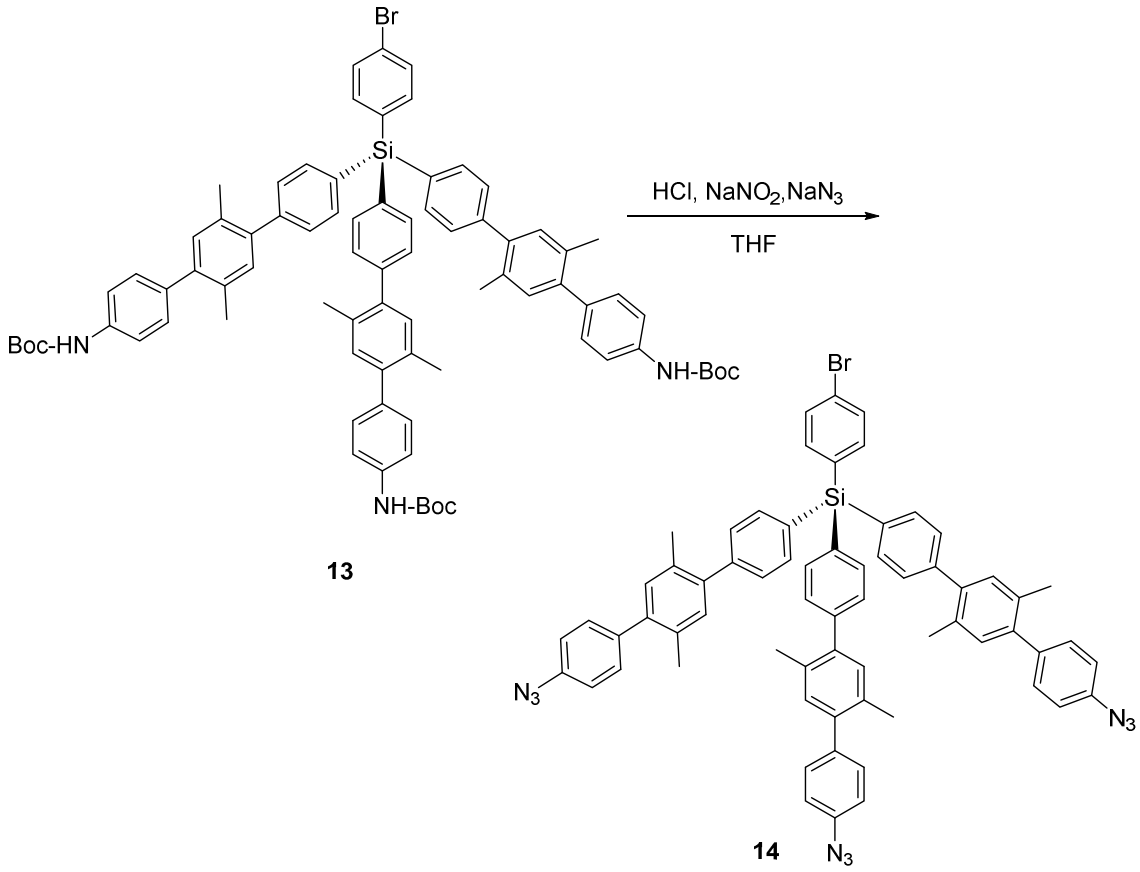

Following the procedure outlined for **12**, tripod **14** was obtained from compound **13** (186 mg, 0.14 mmol), concentrated HCl (0.1 mL, 0.70 mmol), $NaNO_2$ (44 mg, 0.70 mmol), and NaN_3 (41 mg, 0.70 mmol) in THF (5 mL). The crude was purified by column chromatography (cyclohexane/CH_2Cl_2, 9:1) obtaining tripod **14** as a yellow oil (70 mg, 46%).

^{1}H-NMR ($CDCl_3$) δ (ppm): 7.76 (d, 2H, *J*= 8.0 Hz, ArH), 7.71 (d, 2H, *J*= 8.0 Hz, ArH), 7.68 (d, 6H, *J*= 8.2 Hz, ArH), 7.58 (d, 3H, *J*= 8.3 Hz, ArH), 7.45-7.35 (m, 12H, ArH), 7.19 (s,

3H, ArH), 7.13 (s, 3H, ArH), 7.08 (d, 3H, *J*= 8.2 Hz, ArH), 2.34 (s, 3H, CH_3), 2.31 (s, 6H, CH_3), 2.27 (s, 6H, CH_3), 2.26 (s, 3H, CH_3).

^{13}C-NMR ($CDCl_3$) δ (ppm): 143.0 (C-N), 139.9, 139.0, 138.7, 138.1, 136.3 (C_{Ar}), 136.1 (CH_{Ar}), 132.7(C_{Ar}), 131.9, 131.8 (CH_{Ar}), 131.3 (C_{Ar}), 130.6 (CH_{Ar}), 130.5 (C_{Ar}), 129.2 (CH_{Ar}), 128.9 (C_{Ar}), 128.8, 128.1 (CH_{Ar}), 126.0 (C-Br), 118.8 (CH_{Ar}), 20.0, 19.9 (2 x CH_3).

MALDI-TOF MS (DHB as matrix) (*m/z*): calcd for $C_{66}H_{52}BrN_9Si$ [M^+] 1077.329; found 1077.611.

4.1.2 Tripods with 5 phenylene units

4.1.2.1 Synthesis of *tert*-butyl (4'''-bromo-2',2''',5',5'''-tetramethyl-[1,1',4',1',4'',1'''-quaterphenyl]-4-yl)carbamate (**15**)

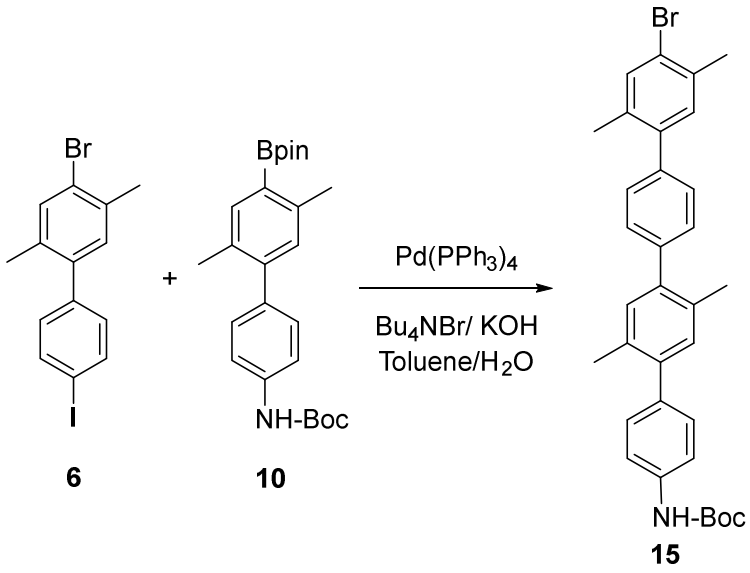

6 **10** **15**

Following the procedure outlined for compound **13**, compound **15** was synthesized from **6** (0.90 g, 2.32 mmol), **10** (1.00 g, 2.32 mmol), $Pd(PPh_3)_4$ (0.14 g, 0.12 mmol), KOH (1.96 g, 35.00 mmol), *n*Bu_4NBr (0.20 g, 0.61 mmol) in toluene/H_2O (1:1, 100 mL). The reaction mixture was stirred for 12 h at 100 ºC. Then, the solvent was evaporated and the residue was purified by column chromatography (cyclohexane/EtOAc, 9:1) to give **15** as a white solid (520 mg, 41%).

M.p. 186-188 ºC.

^{1}H-NMR ($CDCl_3$) δ (ppm): 7.45 (s, 1H, ArH), 7.41 (d, 2H, *J*= 8.2 Hz, ArH), 7.39 (d, 2H, *J*= 8.0 Hz, ArH), 7.32 (d, 2H, *J*= 8.0 Hz, ArH), 7.30 (d, 2H, *J*= 8.2 Hz, ArH), 7.18 (s, 1H, ArH), 7.15 (s, 1H, ArH), 7.14 (s, 1H, ArH), 6.52 (brs, 1H, NH), 2.39 (s, 3H, CH_3), 2.31 (s, 3H, CH_3), 2.27 (s, 3H, CH_3), 2.26 (s, 3H, CH_3), 1.53 (s, 9H, CH_3, *t*-Bu).

^{13}C-NMR ($CDCl_3$) δ (ppm): 152.8 (C=O), 141.0 (C-N), 140.5, 140.4, 140.3, 139.3, 137.1, 136.4, 135.0, 134.7 (C_{Ar}), 133.8 (CH_{Ar}), 132.7, 132.6 (C_{Ar}), 132.1, 131.9, 129.8, 129.0, 128.7 (CH_{Ar}), 123.5 (C-Br), 118.3 (CH_{Ar}), 80.6 (C, *t*-Bu), 28.4 (CH_3, *t*-Bu), 22.3, 20.0, 19.9, 19.8 (4 x CH_3).

HRMS: calcd for $C_{33}H_{34}NO_2Br$ [M+Na^+] 578.16651; found 578.16718.

4.1.2.2 Synthesis of *tert*-butyl (2',2''',5',5'''-tetramethyl-4'''-(4,4,5,5-tetramethyl-1,3,2-dioxaborolan-2-yl)-[1,1',4',1',4'',1'''-quaterphenyl]-4-yl)carbamate (**16**)

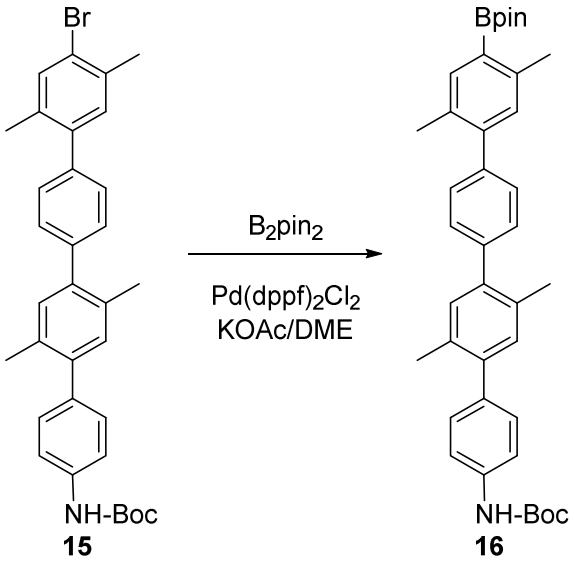

Following the procedure outlined for **10**, compound **16** was prepared by using **15** (520 mg, 1.00 mmol), bis(pinacolato)diboron (338 mg, 1.30 mmol), $Pd(dppf)_2Cl_2$ (163 mg, 0.2 mmol) and KOAc (294 mg, 3 mmol) in dry DME (17 mL). The mixture was refluxed for 12 h. Compound **16** was isolated by column chromatography (cyclohexane/EtOAc, 9:1) as a white solid (300 mg, 50%).

M.p. 130-132 ºC.

^{1}H-NMR ($CDCl_3$) δ (ppm): 7.76 (s, 1H, ArH), 7.46 (d, 2H, *J*= 8.4 Hz, ArH), 7.42 (d, 2H, *J*= 8.4 Hz, ArH), 7.41 (d, 2H, *J*= 8.4 Hz, ArH), 7.35 (d, 2H, *J*= 8.4 Hz, ArH), 7.25 (s, 1H, ArH), 7.19 (s, 1H, ArH), 7.18 (s, 1H, ArH), 6.66 (brs, 1H, NH), 2.60 (s, 3H, CH_3), 2.37 (s, 3H, CH_3), 2.36 (s, 3H, CH_3), 2.33 (s, 3H, CH_3), 1.58 (s, 9H, 3 x CH_3, *t*-Bu), 1.40 (s, 12H, 4 x CH_3, Bpin).

^{13}C-NMR ($CDCl_3$) δ (ppm): 152.8 (C=O), 144.1 (C-N), 142.2, 140.5 (C_{Ar}), 140.3 (CH_{Ar}), 140.2 (C_{Ar}), 138.1 (C-B), 137.1, 136.5, 132.8, 132.7 (C_{Ar}), 132.0 (CH_{Ar}), 131.9 (C_{Ar}), 131.5 (CH_{Ar}), 131.4 (C_{Ar}), 129.9, 128.9, 128.8, 118.3 (CH_{Ar}), 83.4 (2 x C, Bpin), 80.6 (C, *t*-Bu), 28.4 (3 x CH_3, *t*-Bu), 24.9 (2 x CH_3, Bpin), 21.7, 20.0, 19.9, 19.8 (4 x CH_3).

HRMS: calcd for $C_{39}H_{46}BNO_4$ [M+Na^+] 626.34121; found 626.34149.

4.1.2.3 Synthesis of tripod **17**

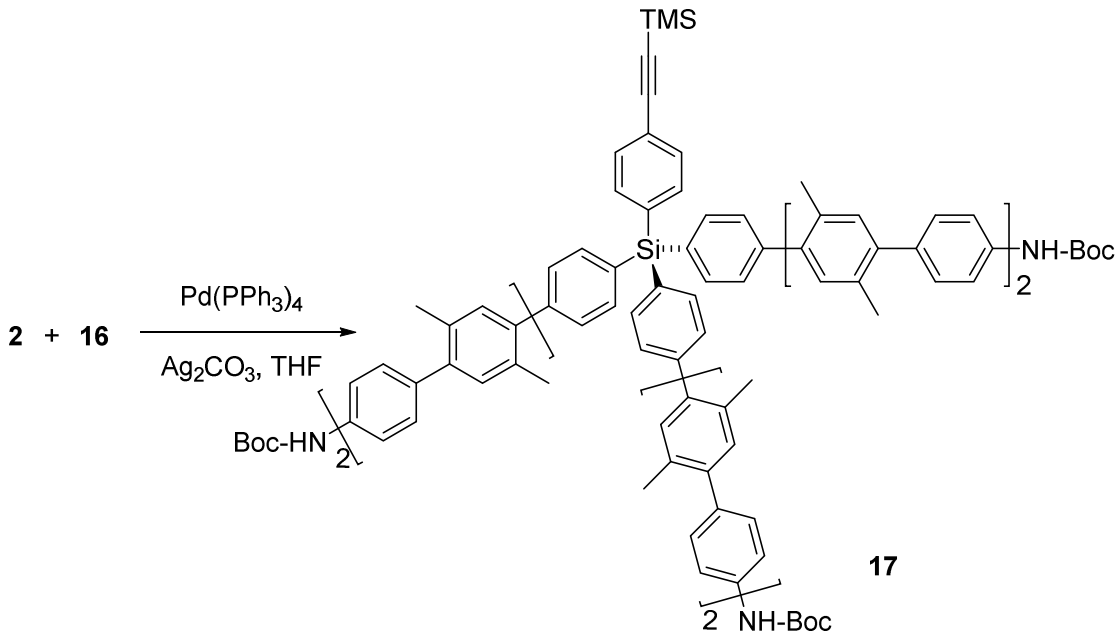

Following the procedure outlined for tripod **11**, compound **17** was obtained by using **16** (217 mg, 0.4 mmol), **2** (100 mg, 0.13 mmol), $Pd(PPh_3)_4$ (25 mg, 0.022 mmol), $AgCO_3$ (270 mg, 1 mmol) and dry THF (10 mL) as the solvent. The mixture was stirred at room temperature for 12 h and, after that, purification by column chromatography (cyclohexane/EtOAc, 8:2) gave compound **17** as a yellow oil (150 mg, 61%).

^{1}H-NMR ($CDCl_3$) δ (ppm): 7.72 (d, 4H, *J*= 8.2 Hz, ArH), 7.66 (d, 2H, *J*= 8.3 Hz, ArH), 7.54 (d, 2H, *J*= 8.3 Hz, ArH), 7.47 (d, 6H, *J*= 8.2 Hz, ArH), 7.43 (s, 12H, ArH), 7.42 (d, 6H, *J*= 8.5 Hz, ArH), 7.32 (m, 11H, ArH), 7.25 (s, 3H, ArH), 7.21 (s, 3H, ArH), 7.16 (s, 3H, ArH), 6.53 (brs, 3H, 3 x NH), 2.36 (s, 9H, 3 x CH_3), 2.35 (s, 9H, 3 x CH_3), 2.34 (s, 9H, 3 x CH_3), 2.29 (s, 9H, 3 x CH_3), 1.54 (s, 27H, 9 x CH_3, *t*-Bu), 0.26 (s, 9H, TMS).
^{13}C-NMR ($CDCl_3$) δ (ppm): 152.8 (C=O),143.2 (C-N), 140.8-140.0, 137.1, 136.5, 136.1 (C_{Ar}), 136.3 (CH_{Ar}), 132.8-132.6, 132.1 (C_{Ar}), 131.9, 131.8 (CH_{Ar}), 131.3 (C_{Ar}), 129.8, 128.9-128.8, 118.3 (CH_{Ar}), 80.6 (C, *t*-Bu), 28.4 (3 x CH_3, *t*-Bu), 20.1, 20.0 (2 x CH_3), 0.0 (TMS).

MALDI-TOF MS (DHB as matrix) (*m/z*): calcd for $C_{128}H_{127}N_3O_6Si_2$ [M^{+3}] 619.306; found 619.130.

4.1.2.4 Synthesis of 4'''-bromo-2',2''',5',5'''-tetramethyl-[1,1':4',1'':4'',1'''-quaterphenyl]-4-amine (**18**)

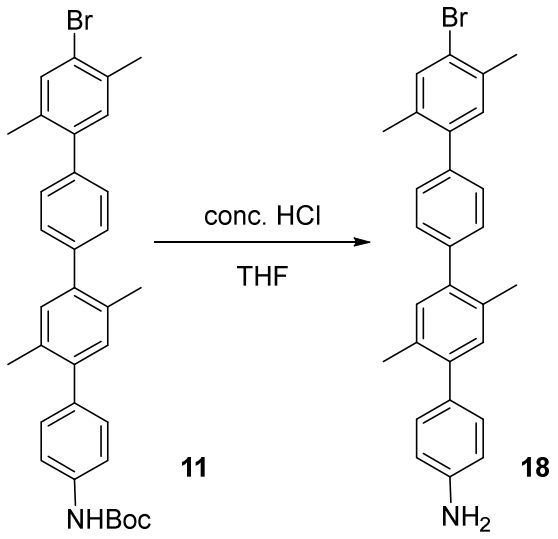

To a solution of **11** (1.0 g, 2.0 mmol) in THF (44 mL) an excess of concentrated HCl (5.72 mL, 57.2 mmol) was added drop-wise at 0 ºC. Then the reaction mixture was warmed to room temperature and stirred for 24 h. After this period, the solvent was concentrated in vacuum and the reaction crude was basified with ammonia to pH= 8, then extracted with ethyl acetate and the organic layer was dried over $MgSO_4$ anhydrous. The solvent was concentrated under vacuum and the crude was purified by column chromatography (cyclohexane/EtOAc, 8:2) giving compound **18** as a colorless oil (805 mg, 88%).

^{1}H-NMR ($CDCl_3$) δ (ppm) 7.45 (s, 1H, ArH), 7.39 (d, 2H, *J*= 8.4 Hz, ArH), 7.31 (d, 2H, *J*= 8.4 Hz, ArH), 7.18 (d, 2H, *J*= 8.5 Hz, ArH)**,** 7.17 (s, 1H, ArH), 7.15 (s, 1H, ArH), 7.14 (s, 1H, ArH), 6.74 (d, 2H, *J*= 8.5 Hz, ArH), 3.71 (brs, 2H, NH_2), 2.39 (s, 3H, CH_3), 2.30 (s, 3H, CH_3), 2.29 (s, 3H, CH_3), 2.27 (s, 3H, CH_3).
^{13}C-NMR ($CDCl_3$) δ (ppm): 145.1 (C-N), 140.9, 140.5, 139.9, 139.2, 135.0, 134.7 (C_{Ar}), 133.8 (CH_{Ar}), 132.8, 132.5 (C_{Ar}), 132.1, 131.9, 131.8, 130.2, 129.1, 128.7 (CH_{Ar}), 123.5 (C-Br), 114.8 (CH_{Ar}), 22.3, 20.1, 19.9, 19.8 (4 x CH_3).

HRMS: calcd for $C_{28}H_{26}NBr$ [M+H$^+$] 456.13214; found 456.13275.

4.1.2.5 Synthesis of 2',2''',5',5'''-tetramethyl-4'''-(4,4,5,5-tetramethyl-1,3,2-dioxaborolan-2-yl)-[1,1':4',1'':4'',1'''-quaterphenyl]-4-amine (**19**)

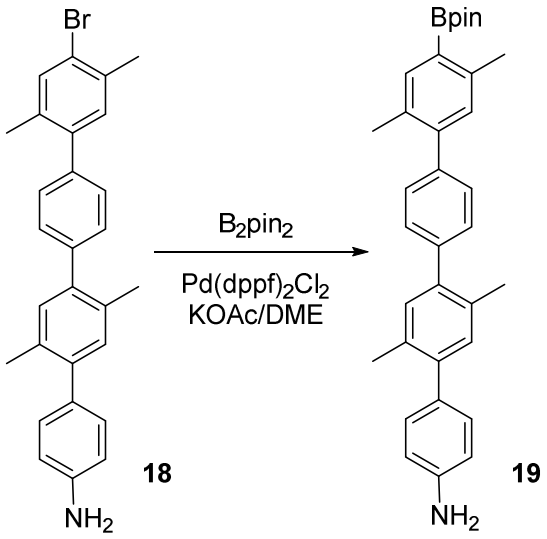

Following the procedure outlined for **10**, compound **18** (805 mg, 1.76 mmol), bis(pinacolato)diboron (508 mg, 2.0 mmol), $Pd(dppf)_2Cl_2$ (219 mg, 0.36 mmol) and KOAc (530 mg, 5.41 mmol) in dry DME (26 mL) were heated to reflux for 12 h. Compound **16** was isolated by column chromatography (cyclohexane/EtOAc, 8:2) as a yellow oil (700 mg, 80%).

^{1}H-NMR ($CDCl_3$) δ (ppm): 7.71 (s, 1H, ArH), 7.41 (d, 2H, *J*= 8.3 Hz, ArH), 7.37 (d, 2H, *J*= 8.3 Hz, ArH), 7.20 (d, 2H, *J*= 8.4 Hz, ArH), 7.18 (s, 1H, ArH), 7.16 (s, 1H, ArH), 7.14 (s, 1H, ArH), 6.75 (d, 2H, *J*= 8.4 Hz, ArH), 2.56 (s, 3H, CH_3), 2.33 (s, 3H, CH_3), 2.32 (s, 3H, CH_3), 2.31 (s, 3H, CH_3), 1.37 (s, 12H, 4 x CH_3, Bpin).
^{13}C-NMR ($CDCl_3$) δ (ppm): 145.2 (C-N), 144.1, 142.3, 140.8, 140.3, 140.2, 140.0 (C_{Ar}), 138.1 (C-B), 132.7, 132.0, 131.9 (CH_{Ar}), 131.6 (C_{Ar}), 131.5, 130.2, 128.9, 128.7, 114.8 (CH_{Ar}), 83.5 (2 x C, Bpin), 24.9 (4 x CH_3, Bpin), 21.7, 20.1, 20.0, 19.8 (4 x CH_3).

HRMS: calcd for $C_{34}H_{38}BNO_2$ [M+H$^+$] 504.30684; found 504.30731.

4.1.2.6 Synthesis of tripod **20**

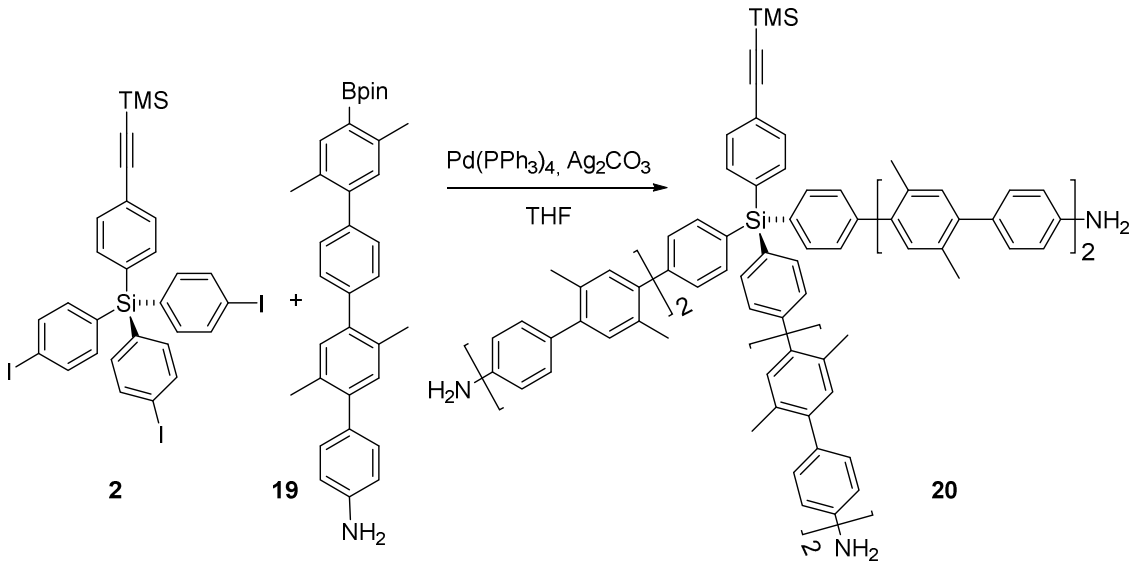

Following the procedure outlined for tripod **11**, from compound **19** (536 mg, 1.1 mmol), **2** (734 mg, 0.4 mmoles), $Pd(PPh_3)_4$ (77 mg, 0.07 mmol), $AgCO_3$ (827 mg, 3.0 mmoles) and dry THF (40 mL) as the solvent, compound **20** was obtained after purification by column cromatography (cyclohexane/EtOAc, 1:1) as a yellow oil (200 mg, 37%).

^{1}H-NMR ($CDCl_3$) δ (ppm): 7.76 (d, 6H, *J*= 8.0 Hz, ArH), 7.70 (d, 2H, *J*= 8.1 Hz, ArH), 7.58 (d, 2H, *J*= 8.1 Hz, ArH), 7.50 (d, 6H, *J*= 8.0 Hz, ArH), 7.46 (s, 12H, ArH), 7.28 (s, 3H, ArH), 7.27 (s, 3H, ArH), 7.24 (s, 3H, ArH), 7.22 (d, 6H, *J*= 8.4 Hz, ArH), 7.20 (s, 3H, ArH), 6.77 (d, 6H, *J*= 8.4 Hz, ArH), 3.40 (brs, 6H, 3 x NH_2), 2.40 (s, 9H, 3 x CH_3), 2.39 (s, 9H, 3 x CH_3), 2.37 (s, 9H, 3 x CH_3), 2.34 (s, 9H, 3 x CH_3), 0.30 (s, 9H, TMS).
^{13}C-NMR ($CDCl_3$) δ (ppm): 145.3 (C-N), 143.2, 140.9, 140.8, 140.6, 140.4, 140.1, 140.0, 136.4 (C_{Ar}), 136.3 (CH_{Ar}), 132.8, 132.7, 132.6 (C_{Ar}) 132.2, 132.1, 132.0 (CH_{Ar}), 131.3 (C_{Ar}), 130.2, 129.1, 128.9, 114.9 (CH_{Ar}), 107.7 (C≡C), 20.1 (CH_3), 20.0 (CH_3), 0.1 (TMS).

MALDI-TOF MS (DHB as matrix) (*m/z*): calcd for $C_{113}H_{103}N_3Si_2$ [M^+] 1557.769; found 1557.694.

4.1.2.7 Synthesis of tripod **21**

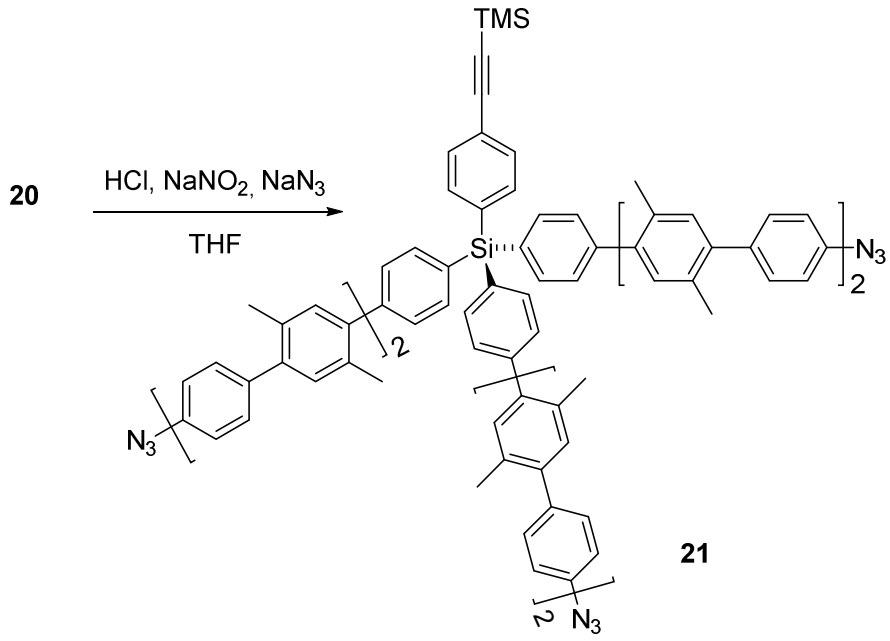

Following the procedure outlined for tripods **12** and **14** and by using conc. HCl (0.02 mL, 0.27 mmol), **20** (95 mg, 0.06 mmol), $NaNO_2$ (18 mg, 0.27 mmol), NaN_3 (17 mg, 0.27 mmol) in THF (10 mL), compound **21** was isolated by column cromatography (cyclohexane/EtOAc, 9:1) as a yellow oil (53 mg, 54%).

^{1}H-NMR ($CDCl_3$) δ (ppm) 7.71 (d, 6H, *J*=8.1 Hz, ArH), 7.65 (d, 2H, *J*= 8.3 Hz, ArH), 7.54 (d, 2H, *J*= 8.3 Hz, ArH), 7.46 (d, 6H, *J*= 8.1 Hz, ArH), 7.43-7.42 (m, 12H, ArH), 7.38 (d, 6H, *J*= 8.5 Hz, ArH), 7.24 (s, 6H, ArH), 7.22 (s, 3H, ArH), 7.14 (s, 3H, ArH), 7.09 (d, 6H, *J*= 8.5 Hz, ArH), 2.36 (s, 9H, CH_3), 2.35 (s, 9H, CH_3), 2.34, (s, 9H, CH_3), 2.28 (s, 9H, CH_3), 0.26 (s, 9H, TMS).

^{13}C-NMR ($CDCl_3$) δ (ppm): 143.2 (C-N), 140.8, 140.7, 140.6, 140.2, 140.0, 139.8, 138.7, 138.5 (C_{Ar}), 136.3, 136.2, 134.0, 132.9, 132.8, 132.6, 132.1, 131.9, 131.8, 131.3, 130.7, 129.8, 129.0, 128.9, 118.8 (CH_{Ar}), 20.0 (CH_3), 19.9 (CH_3), 0.0 (TMS).

MALDI-TOF MS (DHB as matrix) (*m/z*): calcd for $C_{113}H_{97}N_9Si_2$ [M^+] 1635.740; found 1635.197.

4.2 Synthesis of tripods with thioacetate groups as headgroups

4.2.1 Tripods with 2 phenylene units

4.2.1.1 Synthesis of *tert*-butyldimethyl((3-(4,4,5,5-tetramethyl-1,3,2-dioxaborolan-2-yl)benzyl)oxy)silane **(23)**

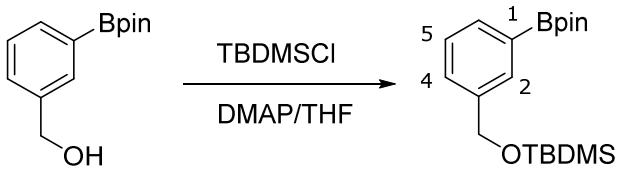

23

Under an argon atmosphere, DMAP (772 mg, 6.32 mmol) was slowly added over a solution of 3-(hydroxymethyl) phenylboronic acid pinacol ester (1.0 g, 4.27 mmol) and TBDMSCl (900 mg, 5.98 mmol) in dry THF (20 mL) cooled at 0 ºC. The mixture was stirred for 24 h at 20 ºC. The white solid was filtered off, washed with cold THF and the organic filtrates were concentrated to dryness under vacuum. The residue was purified by column chromatography using as eluent CH_2Cl_2, giving compound **23** as a white solid (1.06 g, 71%).[8]

^{1}H-NMR ($CDCl_3$) δ (ppm): 7.73 (s, 1H, H-2), 7.72 (d, 1H, *J*= 7.7 Hz, H-6), 7.52 (d, 1H, *J*= 7.7 Hz, H-4), 7.37 (t, 1H, *J*= 7.7 Hz, H-5), 4.77 (s, 2H, -CH_2O-), 1.35 (s, 12H, 4 x CH_3, Bpin), 0.96 (s, 9H, 3 x CH_3, *t*-Bu), 0.11 (s, 6H, 2 x CH_3, DMS).
^{13}C-NMR ($CDCl_3$) δ (ppm): 140.4 (C-3), 133.1 (C-2), 132.2 (C-6), 129.0 (C-5), 127.6 (C-4), 83.6 (2 x C, Bpin), 64.9 (-CH_2O-), 26.0 (C, *t*-Bu), 24.9 (4 x CH_3, Bpin), 18.5 (3 x CH_3, *t*-Bu), 5.2 (2 x CH_3, DMS).

HRMS: *m*/*z* Calcd for $C_{19}H_{33}BO_3Si$ [M+Na^+]: 371.2190; found 371.2191.

4.2.1.2 Synthesis of tripod **24**

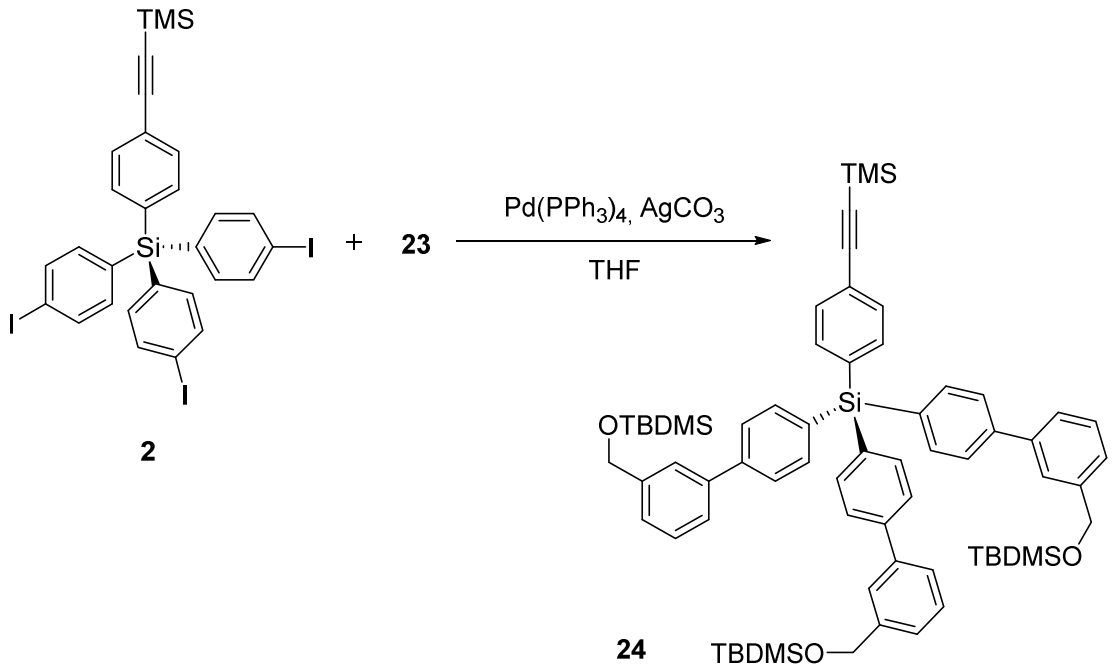

Following the procedure outlined for tripod **11**, compound **23** (1g, 2.87 mmol), the silicon core **2** (734.3 mg, 1 mmol), $Pd(PPh_3)_4$ (159.4 mg, 0.14 mmol), and Ag_2CO_3 (1.6 g, 6 mmol) were dissolved in anhydrous THF (40 mL) and stirred under an argon atmosphere at 20 ºC for 24 h. Then, the product was purified by column chromatography (cyclohexane/CH_2Cl_2, 1:1) to yield tripod **24** as a colorless oil (500 mg, 50%).

^{1}H-NMR ($CDCl_3$) δ (ppm): 7.66 (d, 6H, *J*= 8.3 Hz, ArH), 7.62 (d, 6H, *J*= 8.3 Hz, ArH), 7.60-7.57 (m, 5H, ArH), 7.51-7.48 (m, 5H, ArH), 7.40 (t, 3H, *J*= 7.7 Hz, ArH), 7.31 (d, 3H, *J*= 7.7 Hz, ArH), 4.69 (s, 6H, -CH_2O-), 0.95 (s, 27H, 9 x CH_3, *t*-Bu), 0.24 (s, 9H, TMS), 0.10 (s, 18H, 6 x CH_3, DMS).

^{13}C-RMN ($CDCl_3$) δ (ppm): 142.6, 142.1, 140.8 (C_{Ar}), 136.9 (CH_{Ar}), 136.3, 135.2 (C_{Ar}), 132.5, 131.3, 128.8, 126.7, 125.8, 125.4, 124.9 (CH_{Ar}), 124.4 (C_{Ar}), 105.1 (C≡C), 95.5 (C≡C), 65.1 (-CH_2O-), 26.1 (CH_3, *t*-Bu), 18.5 (C, *t*-Bu), 0.0 (TMS), -5.1 (CH_3, DMS).

MALDI-TOF MS (DHB as matrix): m/z: calcd for $C_{68}H_{88}O_3Si_5$ [M+]: 1092.558; found 1092.504.

4.2.1.3 Synthesis of tripod **25**

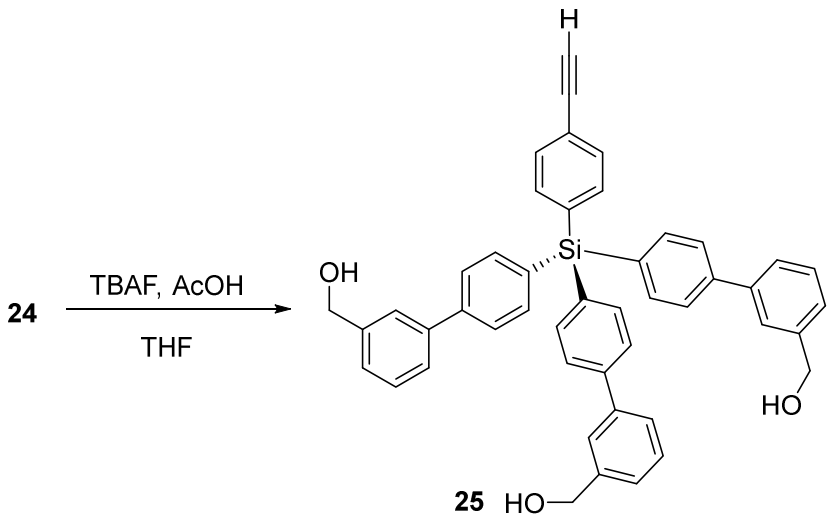

Over a solution of **24** (352 mg, 0.32 mmol) in dry THF (50 mL), TBAF (2.5 mL, 1 mmol) and AcOH (60 μL, 1 mmol) were added. The reaction mixture was stirred at 20 ºC for 6 h. After this period, the mixture was poured into water (10 mL) and extracted with EtOAc (3 x 10 mL). The organic phase was washed with water (15 mL), brine (15 mL), dried over anhydrous $MgSO_4$, filtered and concentrated to dryness under vacuum. The residue was separated by column chromatography (cyclohexane/AcOEt, 3:7) to give **25** as a colorless oil (170 mg, 80%).

^{1}H-NMR ($CDCl_3$) δ (ppm): 7.67 (d, 6H, *J*= 8.3 Hz, ArH), 7.63 (d, 6H, *J*= 8.3 Hz, ArH), 7.62 (s, 3H, ArH), 7.60 (d, 2H, *J*= 8.3 Hz, ArH), 7.55 (d, 3H, *J*= 7.6 Hz, ArH), 7.52 (d, 2H, *J*= 8.3 Hz, ArH), 7.44 (t, 3H, *J*= 7.6 Hz, ArH), 7.36 (d, 3H, *J*= 7.6 Hz, ArH), 4.76 (s, 6H, 3 x $-CH_2OH$), 3.12 (s, 1H, -C≡C<u>H</u>).

^{13}C-RMN ($CDCl_3$) δ (ppm): 142.3, 141.5, 141.2 (C_{Ar}), 136.9 (CH_{Ar}), 136.3 (C_{Ar}), 132.5, 131.5, 129.1, 126.8, 126.5 (CH_{Ar}), 126.2 (C_{Ar}), 126.8 (CH_{Ar}), 65.4 ($-CH_2OH$).

MALDI-TOF MS (DHB as matrix): m/z: calcd for $C_{47}H_{38}O_3Si$ [M+]: 678.259; found 678.260.

4.2.1.4 Synthesis of tripod **26**

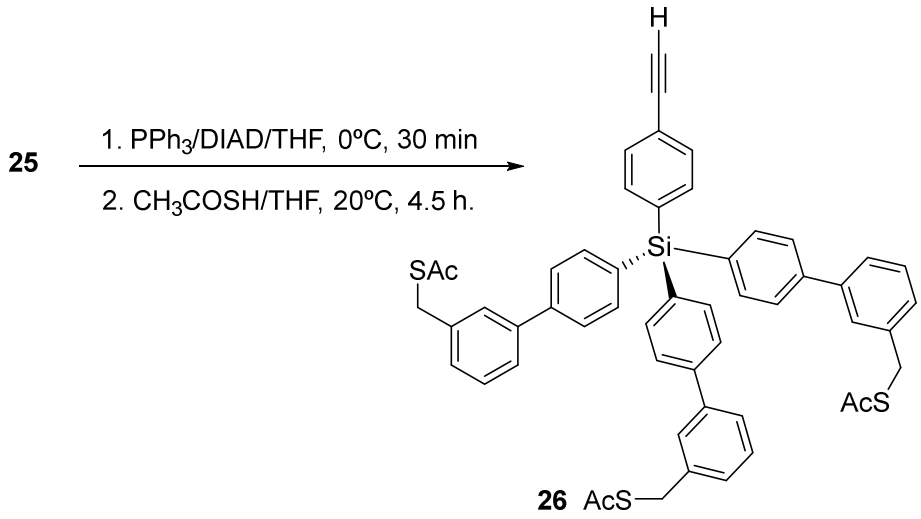

Over a solution of PPh_3 (1 g, 4 mmol) in dry THF (40 mL), DIAD (0.8 mL, 4 mmol) was added at 0 ºC. The mixture was stirred at 0 ºC for 30 min. Then a solution of **25** (150 mg, 0.2 mmol) and thioacetic acid (0.3 mL, 4 mmol) in dry THF (10 mL) was slowly added, and, when the reaction mixture reached 20 ºC, it was stirred for 4.5 h at this temperature. After this period, the mixture was poured into water (40 mL) and extracted with EtOAc (2 x 30 mL). The organic phase was washed with water (1 x 20 mL), brine (1 x 20 mL), dried over anhydrous $MgSO_4$, filtered, and concentrated to dryness under vacuum. Compound **26** was obtained after purification by column chromatography (cyclohexane/EtOAc 9:1) as yellow oil (100 mg, 60%).

^{1}H-NMR ($CDCl_3$) δ (ppm): 7.65 (d, 6H, *J*= 8.3 Hz, ArH), 7.61 (d, 6H, *J*= 8.3 Hz, ArH), 7.60 (d, 2H, *J*= 8.3 Hz, ArH), 7.52 (d, 2H, *J*= 8.3 Hz, ArH), 7.51 (s, 3H, ArH), 7.49 (d, 3H, *J*= 7.7 Hz, ArH), 7.37 (t, 3H, *J*= 7.7 Hz, ArH), 7.27 (d, 3H, *J*= 7.7 Hz, ArH), 4.17 (s, 6H, 3 x -CH_2SAc), 3.12 (s, 1H, -C≡C<u>H</u>), 2.34 (s, 9H, 3 x SAc).

^{13}C-RMN ($CDCl_3$) δ (ppm): 195.1 (3 x C=O), 142.2, 141.3 (C_{Ar}), 138.3, 136.9, 136.2 (CH_{Ar}), 135.5, 132.5 (C_{Ar}), 131.5, 129.2 (CH_{Ar}), 128.0 (C_{Ar}), 127.7, 126.8, 126.2 (CH_{Ar}), 123.5 (C_{Ar}), 33.5 (-CH_2SAc), 30.4 (SAc).

MALDI-TOF MS (DHB as matrix): m/z: calcd for $C_{53}H_{44}O_3S_3Si$ [M+]: 852.222; found: 852.221.

4.2.2 Tripods with 4 phenylene units

4.2.2.1 Synthesis of ((4''-Bromo-2'',5''-dimethyl-[1,1':4',1''-terphenyl]-3-yl)methoxy)(*tert*-butyl)dimethylsilane (**27**)

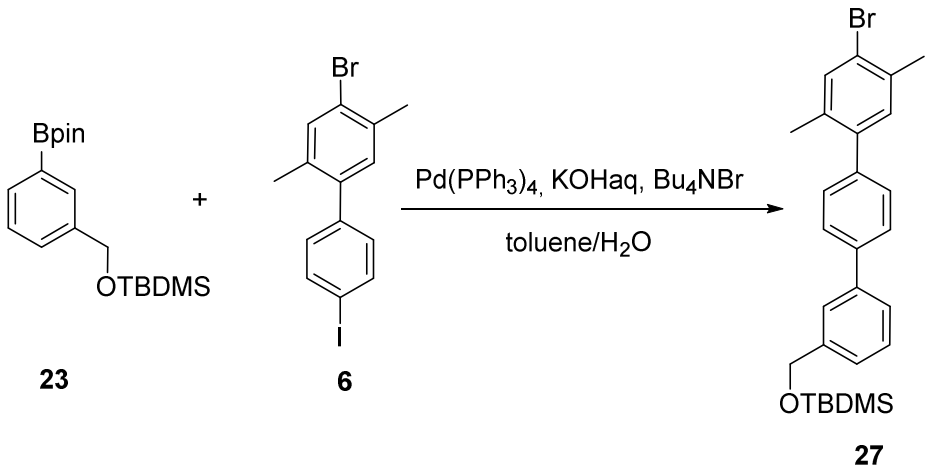

Following the procedure outlined for compound **13**, a mixture of **6** (1.23 g, 3.2 mmol), **23** (1.00 g, 3.2 mmol), $Pd(PPh_3)_4$ (0.23 g, 0.2 mmol), KOH (3.2 g, 58.00 mmol), and nBu_4NBr (0.31 g, 0.95 mmol) in a degassed mixture of toluene/H_2O (8:2, 100 mL) was stirred for 12 h at 100 ºC. The residue was purified by column chromatography (cyclohexane/CH_2Cl_2, 7:3) to give **27** as a colorless oil (1.35 g, 90%).

^{1}H-RMN ($CDCl_3$) δ (ppm): 7.65 (d, 2H, *J*= 8.5 Hz, ArH), 7.64 (s, 1H, ArH), 7.51 (d, 1H, *J*= 7.7 Hz, ArH), 7.48 (s, 1H, ArH), 7.43 (t, 1H, *J*= 7.7 Hz, ArH), 7.37 (d, 2H, *J*= 8.5 Hz, ArH), 7.34 (d, 1H, *J*= 7.7 Hz, ArH), 7.15 (s, 1H, ArH), 4.84 (s, 2H, -CH_2O-), 2.41 (s, 3H, CH_3), 2.27 (s, 3H, CH_3), 0.99 (s, 9H, 3 x CH_3, *t*-Bu), 0.16 (s, 6H, 2 x CH_3, DMS).
^{13}C-RMN ($CDCl_3$) δ (ppm): 142.1, 141.0, 140.5, 140.0, 139.8, 135.1, 134.7(C_{Ar}), 133.8, 132.1, 129.5, 128.8, 126.9, 125.7, 125.2, 124.8 (CH_{Ar}), 123.6 (C-Br), 65.1 (-CH_2O-), 26.1 (3 x CH_3, *t*-Bu), 22.3, 19.8 (2 x CH_3), 18.5 (C, *t*-Bu), -5.1 (CH_3, DMS).

HRMS: m/z: calcd for $C_{21}H_{18}Br$ [*M* – OTBDMS]: 350.06701; found: 350.06183.

4.2.2.2 Synthesis of *tert*-Butyl((2'',5''-dimethyl-4''-(4,4,5,5-tetramethyl-1,3,2-dioxaborolan-2-yl)-[1,1':4',1''-terphenyl]-3-yl)methoxy)dimethylsilane (**28**)

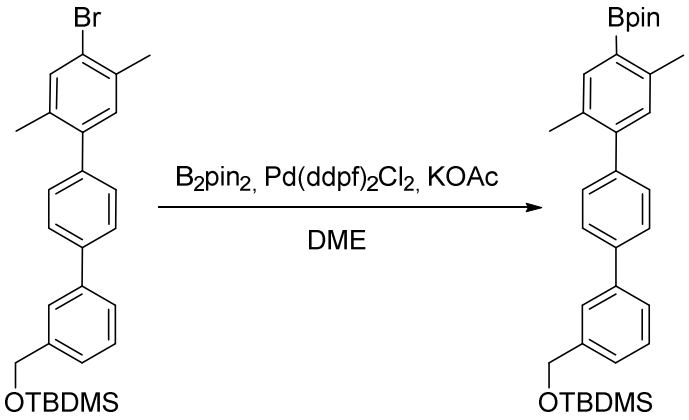

27 **28**

Following the procedure outlined for compound **10**, compound **28** was synthesized by using **27** (1 g, 2.1 mmol), bis(pinacolato)diboron (470 mg, 1.80 mmol), $Pd(dppf)_2Cl_2$ (248 mg, 0.3 mmol) and KOAc (450 mg, 4.5 mmol) in anhydrous DME (15 mL). Compound **28** was isolated by column chromatography (cyclohexane/CH_2Cl_2, 6:4) obtaining a colorless oil (900 mg, 90%).

^{1}H-RMN ($CDCl_3$) δ (ppm): 7.69 (s, 1H, ArH), 7.63 (d, 2H, *J*= 8.1 Hz, ArH), 7.60 (s, 1H, ArH), 7.52 (d, 1H, *J*= 7.7 Hz, ArH), 7.41 (t, 1H, *J*= 7.7 Hz, ArH), 7.38 (d, 2H, *J*= 8.1 Hz, ArH), 7.31 (d, 1H, *J*= 7.7 Hz, ArH), 7.10 (s, 1H, ArH), 4.81 (s, 2H, -CH_2O-), 2.54 (s, 3H, CH_3), 2.29 (s, 3H, CH_3), 1.35 (s, 12H, 4 x CH_3, Bpin), 0.96 (s, 9H, 3 x CH_3, *t*-Bu), 0.12 (s, 6H, 2 x CH_3, DMS).

^{13}C-RMN ($CDCl_3$) δ (ppm): 143.8, 142.3, 142.0, 140.9, 140.8, 139.8 (C_{Ar}), 138.0 (C-B), 131.5 (C_{Ar}), 131.4, 129.5, 128.7, 126.8, 125.7, 125.0, 124.8 (CH_{Ar}), 83.4 (2 x C, Bpin)), 65.1 (-CH_2O-), 26.0 (4 x CH_3, Bpin), 24.9 (3 x CH_3, *t*-Bu), 21.6, 19.7 (2 x CH_3), 18.5 (C, *t*-Bu), -5.2 (2 x CH_3, DMS).

HRMS: m/z: calcd for $C_{27}H_{30}BO_2$ [*M* – OTBDMS]: 397.23389; found: 397.23285.

4.2.2.3 Synthesis of tripod **29**

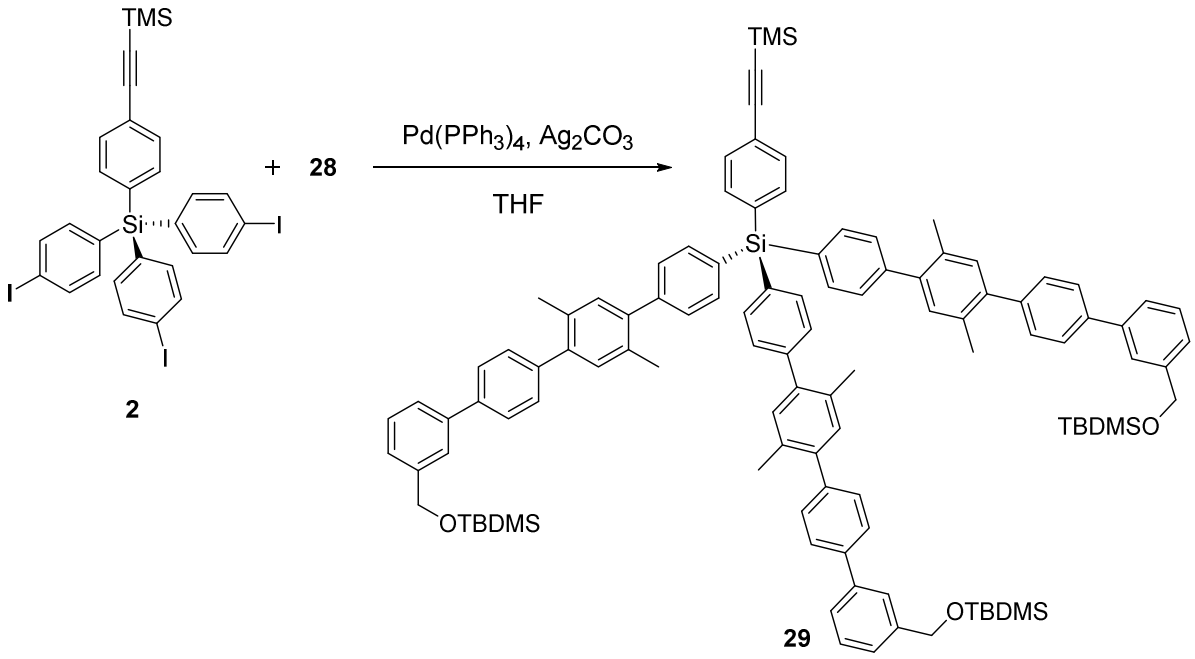

Following the procedure outlined for tripod **11**, compound **29** was prepared by using compound **28** (500 mg, 1 mmol), the corresponding silicon core **2** (253 mg, 0.33 mmol), $Pd(PPh_3)_4$ (250 mg, 0.2 mmol), and Ag_2CO_3 (700 mg, 2.5 mmol) in anhydrous THF (15 mL). The product was purified by column chromatography (cyclohexane/CH_2Cl_2, 6:4) to yield tripod **29** as a colorless oil (232 mg, 43%).

^{1}H-NMR ($CDCl_3$) δ (ppm): 7.71 (d, 6H, *J*= 8.3 Hz, 3 x ArH), 7.66 (d, 6H, *J*= 8.3 Hz, 3 x ArH), 7.65 (d, 2H, *J*= 8.6 Hz, ArH), 7.62 (s, 3H, 3 x ArH), 7.54 (d, 3H, *J*= 7.7 Hz, 3 x ArH), 7.53 (d, 2H, *J*= 8.6 Hz, ArH), 7.46 (d, 12H, *J*=, 8.0 Hz, ArH), 7.42 (t, 3H, *J*= 7.7 Hz, 3 x ArH), 7.33 (d, 3H, *J*= 7.7 Hz, 3 x ArH), 7.23 (s, 3H, ArH), 7.22 (s, 3H, ArH), 4.82 (s, 6H, -CH_2O-), 2.35 (s, 18H, 6 x CH_3), 0.97 (s, 27H, 3 x *t*-Bu), 0.26 (s, 9H, TMS), 0.13 (s, 18H, 6 x CH_3, DMS).

^{13}C-RMN ($CDCl_3$) δ (ppm): 142.0, 140.8, 140.6, 139.7, 136.3 (C_{Ar}), 136.2 (CH_{Ar}), 132.7, 132.6, 132.1 (C_{Ar}), 131.9 (CH_{Ar}), 131.3 (C_{Ar}), 129.7, 128.9, 128.7 (C_{Ar}), 126.8, 125.7 (CH_{Ar}), 125.1 (C_{Ar}), 124.8 (CH_{Ar}), 65.1 (-CH_2O-), 26.0 (CH_3, *t*-Bu), 20.1 (CH_3), 18.5 (C, *t*-Bu), -0.1 (TMS), -5.2 (CH_3, DMS).

MALDI-TOF MS (DHB as matrix): m/z: calcd for $C_{110}H_{124}O_3Si_5$ [M+]: 1632.839; found: 1632.612.

4.2.2.4 Synthesis of tripod **30**

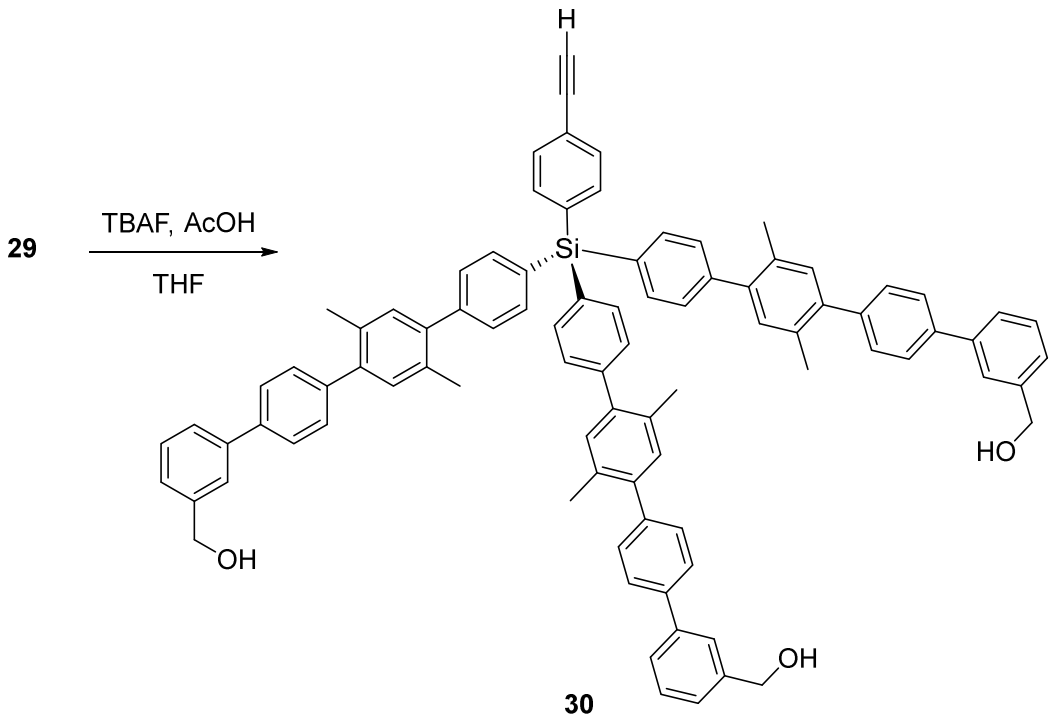

Tripod **30** was prepared by following the procedure outlined for tripod **25**, by using a solution of **29** (230 mg, 0.14 mmol) in dry THF (40 mL), TBAF (1 mL, 0.40 mmol) and AcOH (23 μL, 0.40 mmol) were added. Compound **30** was isolated by column chromatography (cyclohexane/EtOAc, 6:4) as a colorless oil (120 mg, 70%).

^{1}H-NMR ($CDCl_3$) δ (ppm): 7.71 (d, 6H, *J*= 8.3 Hz, ArH), 7.68 (d, 2H, *J*= 8.1 Hz, ArH), 7.67-7.65 (m, 8H, ArH) 7.58 (d, 3H, *J*= 7.5 Hz, ArH), 7.57 (d, 2H, *J*= 8.1 Hz, ArH), 7.48-7.44 (m, 16H, ArH) 7.36 (d, 3H, *J*= 7.5 Hz, ArH), 7.23 (s, 3H, ArH), 7.22 (s, 3H, ArH), 4.78 (s, 6H, 3 x -CH_2OH), 3.14 (s, 1H, -C≡C<u>H</u>), 2.35 (s, 18H, 6 x CH_3).
^{13}C-RMN ($CDCl_3$) δ (ppm): 143.2, 141.5, 141.2, 140.8, 140.7, 140.6, 139.5, 136.5 (C_{Ar}), 136.3 (CH_{Ar}), 132.8, 132.7 (C_{Ar}), 132.0 (CH_{Ar}), 131.6 (C_{Ar}), 129.8, 129.2, 129.0, 126.9, 126.5, 126.0 (CH_{Ar}), 125.8 (C_{Ar}), 65.4 (-CH_2OH), 20.2 (CH_3), 20.1 (CH_3).

MALDI-TOF MS (DHB as matrix): m/z: calcd for $C_{89}H_{74}O_3Si$ [M+]:1218.540; found 1218.544.

4.2.2.5 Synthesis of tripod **31**

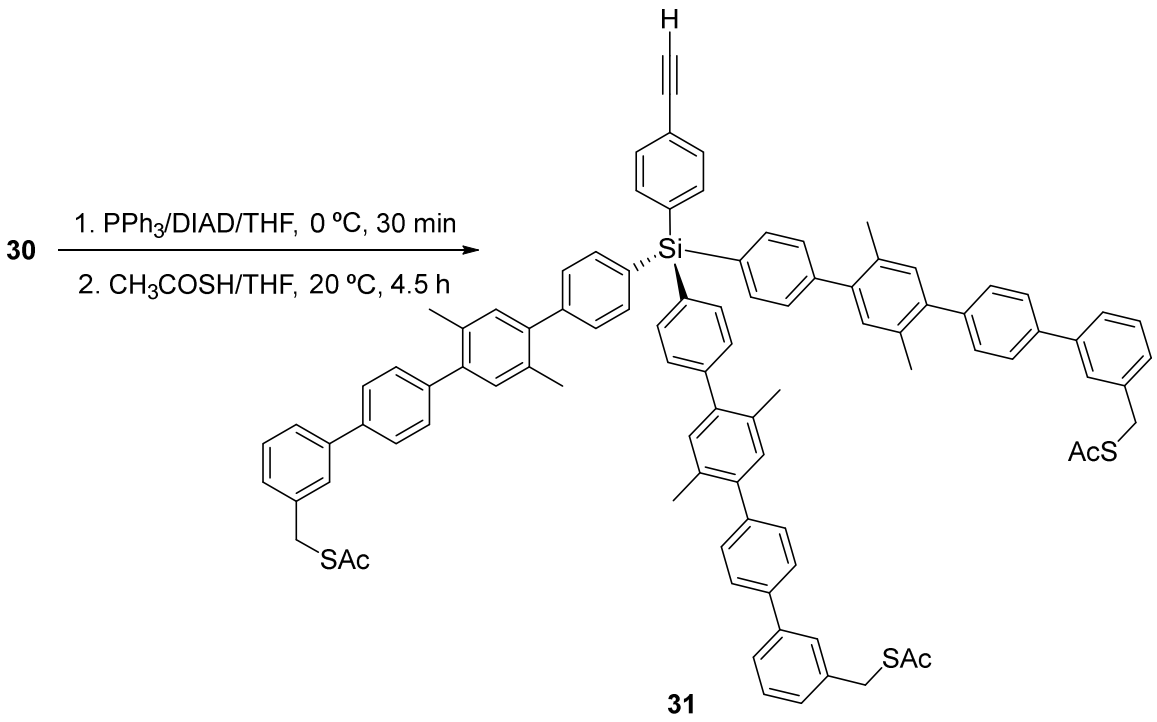

Following the procedure outlined for **26**, compound **31** was prepared from **30** (100 mg, 0.08 mmol), DIAD (0.32 mL, 1.6 mmol), PPh_3 (415 mg, 1.6 mmol) and thioacetic acid (0113 mL, 1.6 mmol) in dry THF (25 mL). Tripod **31** was obtained after purification by column chromatography (CH_2Cl_2/cyclohexane, 6:4) as a pale yellow oil (90 mg, 81%).

^{1}H-NMR ($CDCl_3$) δ (ppm): 7.72 (d, 6H, *J*= 8.2 Hz, ArH), 7.68 (d, 2H, *J*= 8.3 Hz, ArH), 7.64 (d, 6H, *J*= 8.5 Hz, ArH), 7.57 (d, 2H, *J*=8.3 Hz, ArH), 7.56 (s, 3H, ArH), 7.53 (d, 3H, *J*= 7.6 Hz, ArH), 7.46 (d, 6H, *J*= 8.2 Hz, ArH), 7.45 (d, 6H, *J*= 8.5 Hz, ArH), 7.39 (t, 3H, *J*= 7.6 Hz, ArH), 7.28 (d, 3H, *J*= 7.6 Hz, ArH), 7.23 (s, 3H, ArH), 7.21 (s, 3H, ArH), 4.20 (s, 6H, -CH_2SAc), 3.14 (s, 1H, -C≡C<u>H</u>), 2.36 (s, 9H, 3 x SAc), 2.35 (s, 9H, 3 x CH_3), 2.33 (s, 9H, 3 x CH_3).

^{13}C-RMN ($CDCl_3$) δ (ppm): 195.1 (C=O), 143.1, 141.3, 140.8, 140.6, 140.5, 139.2 (C_{Ar}), 138.2 (CH_{Ar}), 136.4 (C_{Ar}), 136.2 (CH_{Ar}), 132.7, 132.6, 132.0 (C_{Ar}), 131.9, 131.8 (CH_{Ar}), 131.5 (C_{Ar}), 129.7, 129.1, 128.9, 127.6, 126.9, 126.1 (CH_{Ar}), 33.5 (-CH_2SAc), 30.3 (SAc), 20.0 (CH_3), 19.9 (CH_3).

MALDI-TOF MS (DHB as matrix) m/z: calcd for $C_{95}H_{80}O_3S_3Si$ [M+] 1392.504; found 1392.367.

4.3 Synthesis of tripods laterally substituted with ethylene glycols

4.3.1 With molecule 4 as silicon core

4.3.1.1 Synthesis of (2',5'-dimethyl-4'-(4,4,5,5-tetramethyl-1,3,2-dioxaborolan-2-yl)-[1,1'-biphenyl]-4-yl)trimethylsilane (**32**)

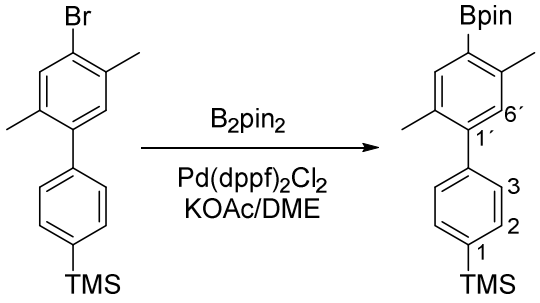

Following the procedure outlined for compound **10**, compound **32** was prepared by using **5** (1.10 g, 3.30 mmol), bis(pinacolato)diboron (0.72 g, 2.9 mmol), $Pd(dppf)_2Cl_2$ (0.389 g, 0.4 mmol) and KOAc (0.70 g, 7.16 mmol) in dry DME (25 mL). The crude was separated by column chromatography (cyclohexane/EtOAc, 9:1) to give compound **10** as a white foam (1 g, 80%).

^{1}H-NMR ($CDCl_3$) δ (ppm): 7.70 (s, 1H, H-6´), 7.57 (d, 2H, *J*= 8.3 Hz, H-3,5), 7.33 (d, 2H, *J*= 8.3 Hz, H-2,6), 7.08 (s, 1H, H-3´), 2.55 (s, 3H, CH_3), 2.28 (s, 3H, CH_3), 1.37 (s, 12H, 4 x CH_3, Bpin), 0.32 (s, 9H, TMS).
^{13}C-RMN ($CDCl_3$) δ (ppm): 144.3, 142.4, 142.3 (C_{Ar}), 138.7 (C-Si), 138.0 (C-B), 133.1 (C-2,6), 131.5, 131.4 (C-3´,6´), 128.4 (C-3,5), 83.4 (2 x C, Bpin), 24.9 (4 x CH_3, Bpin), 21.7, 19.8 (2 x CH_3), -1.0 (TMS).

4.3.1.2 Synthesis of tripod **33**

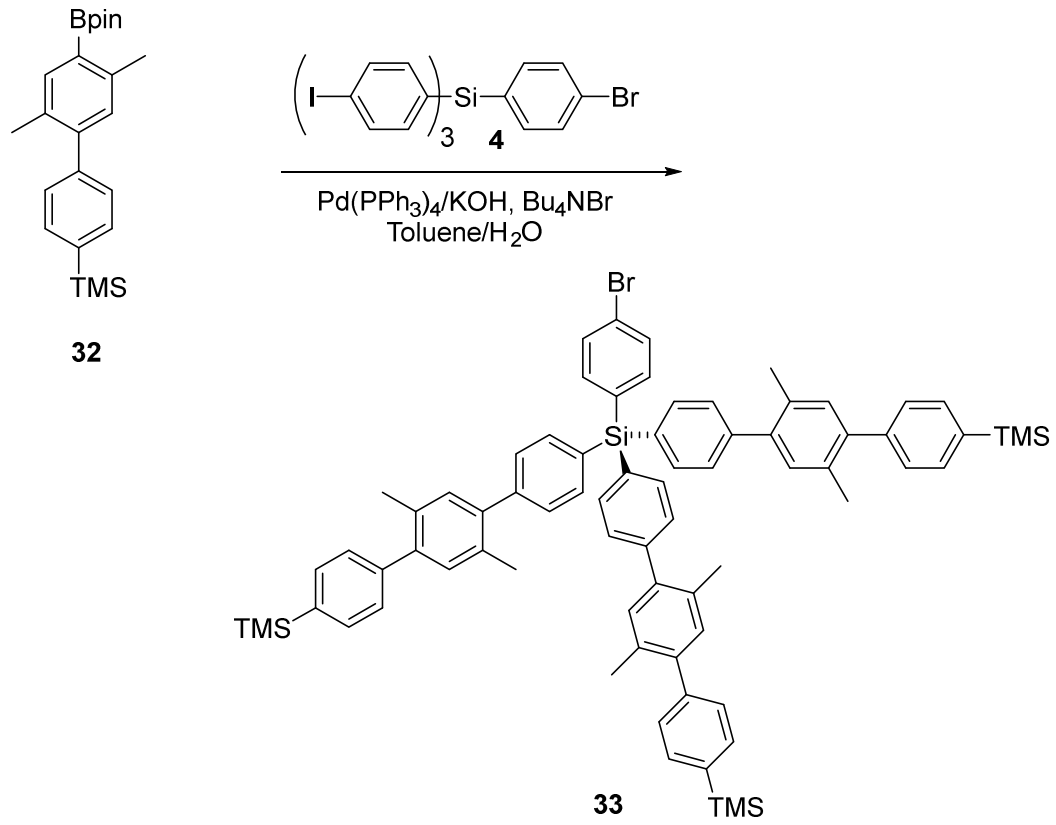

Following the procedure outlined for tripod **13,** tripod **33** was obtained by using **32** (752 mg, 2.27 mmol), the corresponding silicon core **4** (523 mg, 0.76 mmol), $Pd(PPh_3)_4$ (40 mg, 0.038 mmol), KOH (556 mg, 11.4 mmol), and *n*-BuNBr (53 mg, 0.19 mmol) in toluene/H_2O (8:2, 24 mL). The product was purified by column chromatography (cyclohexane/CH_2Cl_2, 9.5:0.5) to give tripod **33** as a pale oil (300 mg, 40%).

^{1}H-NMR ($CDCl_3$) δ (ppm): 7.79 (d, 2H, *J*= 8.2 Hz, ArH), 7.71 (d, 4H, *J*= 8.2 Hz, ArH), 7.59 (m, 10H, ArH), 7.48 (d, 2H, *J*= 8.2 Hz, ArH), 7.46 (d, 4H, *J*= 8.2 Hz, ArH), 7.39 (d, 2H, *J*= 8.1 Hz, ArH), 7.38 (d, 4H, *J*= 8.1 Hz, ArH), 7.21 (s, 3H, ArH), 7.18 (s, 3H, ArH), 2.35 (s, 3H, CH_3), 2.33 (s, 6H, 2 x CH_3), 2.32 (s, 3H, CH_3), 2.31 (s, 6H, 2 x CH_3), 0.30 (s, 27H, 3 x TMS).

^{13}C-NMR ($CDCl_3$) δ (ppm): 143.2, 142.9, 142.1, 142.0, 141.0, 140.9, 140.6, 140.5, 138.7 (C_{Ar}), 138.6 (CH_{Ar}), 138.1 (C_{Ar}), 136.3, 136.1, 133.1, 132.6, 132.1, 131.9, 131.8 (CH_{Ar}), 131.2 (C_{Ar}), 128.9, 128.8, 128.6 (CH_{Ar}), 20.0 (CH_3), 19.9 (CH_3), -1.0 (TMS).

4.3.1.3 Synthesis of tripod **34**

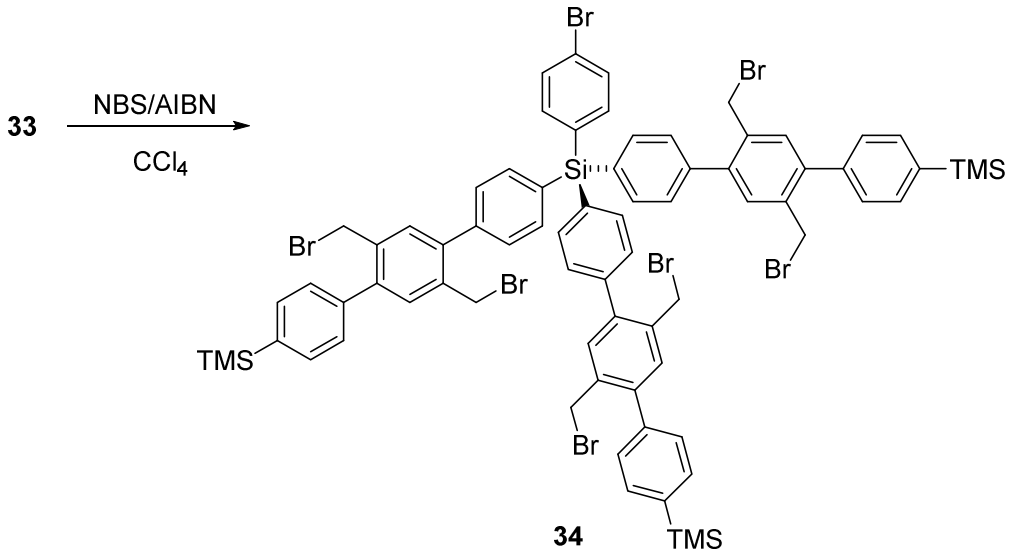

To a solution of tripod **33** (282 mg, 0.25 mmol) and AIBN (23.5 mg, catalytic amount) in CCl_4 (15 mL), NBS (256.62 mg, 6 mmol) was added. Then, the mixture was heated at 90 ºC overnight. After that, the crude was hot filtered and concentrate to dryness. Tripod **34** was obtained after purification by column cromatography (cyclohexane/CH_2Cl_2, 9:1) as a yellow oil (150 mg, 40%).

^{1}H-NMR ($CDCl_3$) δ (ppm): 7.77 (d, 4H, *J*= 8.2 Hz, ArH), 7.65-7.57 (m, 15H, ArH), 7.51-7.46 (m, 15H, ArH), 4.52 (s, 6H, CH_2Br), 4.48 (s, 6H, CH_2Br), 0.33 (s, 27H, 3 x TMS).
^{13}C-NMR ($CDCl_3$) δ (ppm): 141.86, 141.21, 140.99, 140.11, 139.56 (C_{Ar}), 138.03 (CH_{Ar}), 136.62 (C_{Ar}), 136.50, 135.66, 135.48 (CH_{Ar}), 133.83, 133.58 (C_{Ar}), 133.50, 133.19, 133.12 (CH_{Ar}), 131.44 (C_{Ar}), 128.76, 128.26 (CH_{Ar}), 31.49 (CH_2Br), -1.07 (TMS).

4.3.1.4 Synthesis of tripod **35**

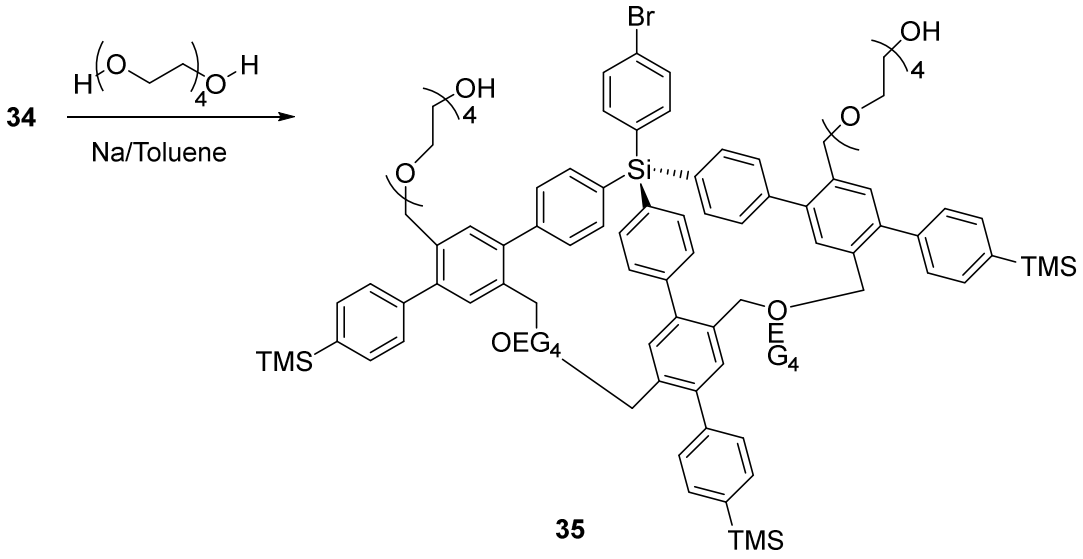

Under an argon atmosphere, tetra(ethylene) glycol (OEG_4) (39 mg, 0.2 mmol) and sodium (10 mg, 0.4 mmol) was added to a round-bottom flask in small portions at 0 ºC and, after 30 min, the mixture was warm up to room temperature. When all sodium was dissolved, a solution of **34** (100 mg, 0.06 mmol) in toluene (5 mL) was added via canula and the mixture was heated at 70 ºC during overnight. After this period, the mixture was cooled down to room temperature, dissolved in ether, washed with water (3x 5mL), and the combined organic layers were dried over anhydrous $MgSO_4$. Then the solvent was evaporated and the residue was purified by column cromatography (CH_2Cl_2/MeOH, 9.5:0.5) giving tripod **35** as a pale oil (30 mg, 30%).

^{1}H-NMR ($CDCl_3$) δ (ppm): 7.77-7.35 (m, 34H, ArH), 4.57-4.43 (m, 12H, -CH_2O-), 3.69-3.44 (m, 64H, OEG), 0.30 (s, 27H, 3 x TMS).

^{13}C-NMR ($CDCl_3$) δ (ppm): 142.1 (C_{Ar}), 140.9 (C_{Ar}), 140.6 (C_{Ar}), 139.1 (C_{Ar}), 137.9 (CH_{Ar}), 136.1 (CH_{Ar}), 134.7 (C_{Ar}), 133.2 (CH_{Ar}), 131.2 (CH_{Ar}), 130.9 (CH_{Ar}), 128.9 (CH_{Ar}), 128.6 (CH_{Ar}), 72.5 (-CH_2O-), 70.7 (PhCH_2), 70.5 (PhCH_2), 69.6 (-CH_2O-), 61.6 (-CH_2O-), -1.1 (TMS).

4.3.2 *With molecule 2 as silicon core*

4.3.2.1 Synthesis of tripod **36**

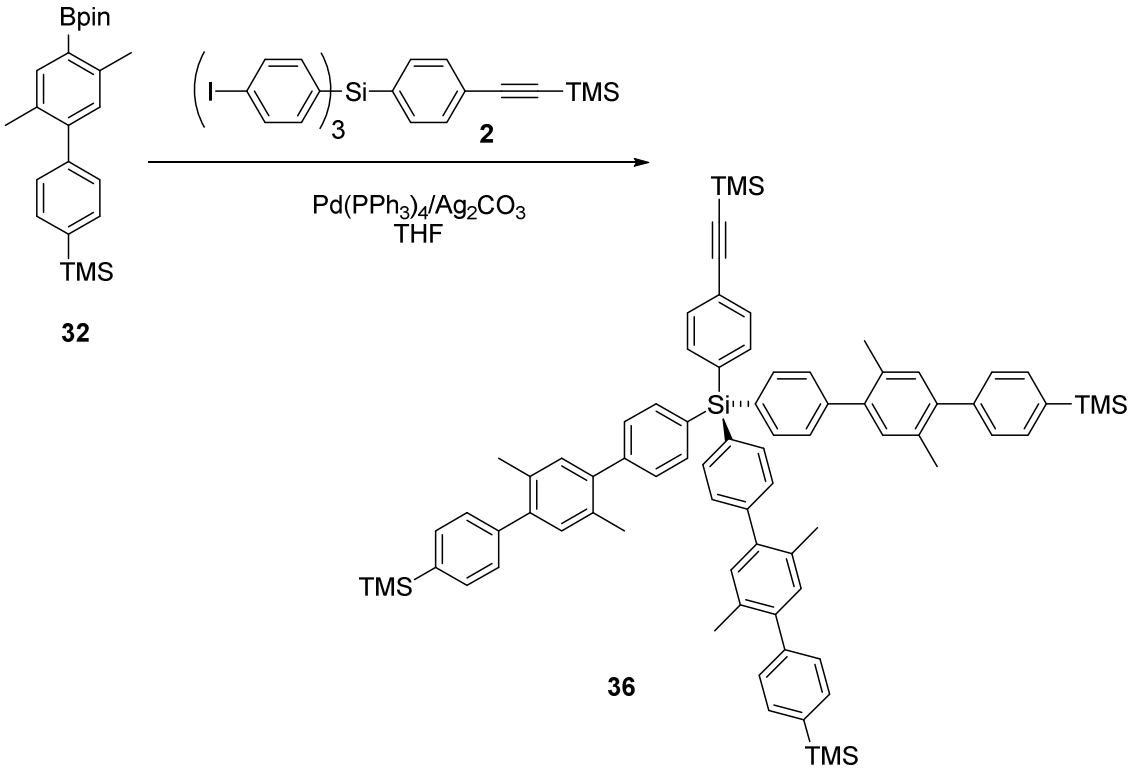

Following the procedure outlined for tripod **11**, compound **32** (517 mg, 1.36 mmol), silicon core **2** (333 mg, 0.45 mmol), $Pd(PPh_3)_4$ (72 mg, 0.062 mmol), $AgCO_3$ (717 mg, 2.6 mmol) were stirred in dry THF (20 mL), at room temperature for 12 h. The crude was purified by column chromatography (cyclohexane/CH_2Cl_2, 8:2) giving compound **36** as a colorless oil (398 mg, 74%).

^{1}H-NMR ($CDCl_3$) δ (ppm): 7.68 (d, 6H, *J*= 8.1 Hz, ArH), 7.63 (d, 2H, *J*= 8.2 Hz, ArH), 7.57 (d, 6H, *J*= 8.1 Hz, ArH), 7.52 (d, 2H, *J*= 8.2 Hz, ArH), 7.43 (d, 6H, *J*= 8.1 Hz, ArH), 7.36 (d, 6H, *J*= 8.1 Hz, ArH), 7.20 (s, 3H, ArH), 7.16 (s, 3H, ArH), 2.31 (s, 9H, 3 x CH_3), 2.29 (s, 9H, 3 x CH_3), 0.30 (s, 27H, 3 x TMS), 0.25 (s, 9H, TMS).

^{13}C-NMR ($CDCl_3$) δ (ppm): 143.1, 141.9, 140.9, 140.5, 138.6, 136.3 (C_{Ar}), 136.2, 133.1, 132.7, 132.6 (CH_{Ar}), 132.0 (C_{Ar}), 131.9, 131.8 (CH_{Ar}), 131.2 (C_{Ar}), 128.8, 128.5 (CH_{Ar}), 20.0 (CH_3), 19.9 (CH_3), -0.1 (TMS), -1.0 (3 x TMS).

4.3.2.2 Synthesis of tripod **37**

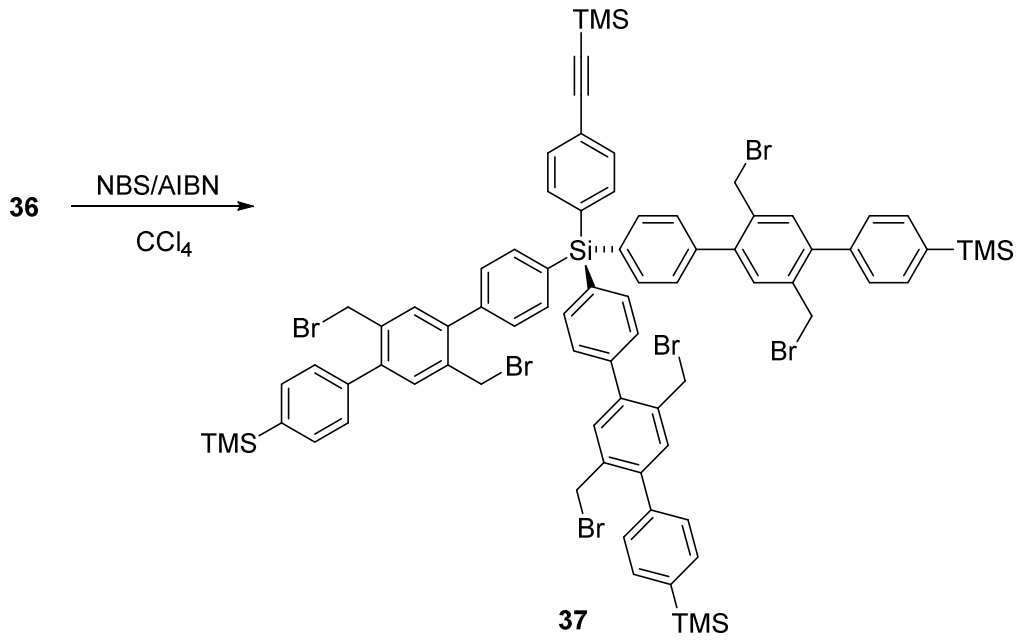

Following the procedure outlined for tripod **34**, tripod **36** (283 mg, 0.24 mmol), NBS (267 mg, 1.5 mmol) and AIBN (23 mg, 0.14 mmol) in CCl_4 (20 mL) were stirred at 90 ºC overnight. Purification by column cromatography (cyclohexane/CH_2Cl_2, 9:1) gave tripod **37** as a colorless oil (235 mg, 65%).

^{1}H-NMR ($CDCl_3$) δ (ppm): 7.75 (d, 6H, *J*= 8.2 Hz, ArH), 7.60 (m, 16H, ArH), 7.50 (s, 3H, ArH), 7.49 (d, 6H, *J*= 8.2 Hz, ArH), 7.45 (s, 3H, ArH), 4.51 (s, 6H, 3 x CH_2Br), 4.48 (s, 6H, 3 x CH_2Br), 0.31 (s, 27H, 3 x TMS), 0.25 (s, 9H, TMS).
^{13}C-NMR ($CDCl_3$) δ (ppm): 141.8, 141.3, 140.1, 139.6 (C_{Ar}), 136.6, 136.3, 135.7, 135.6 (CH_{Ar}), 133.9 (C_{Ar}), 133.6, 133.3, 133.2 (CH_{Ar}), 131.5 (C_{Ar}), 128.8, 128.3 (CH_{Ar}), 128.1 (C_{Ar}), 31.5 (CH_2Br), 0.1 (TMS), -0.9 (TMS).

4.3.2.3 Synthesis of tripod **38**

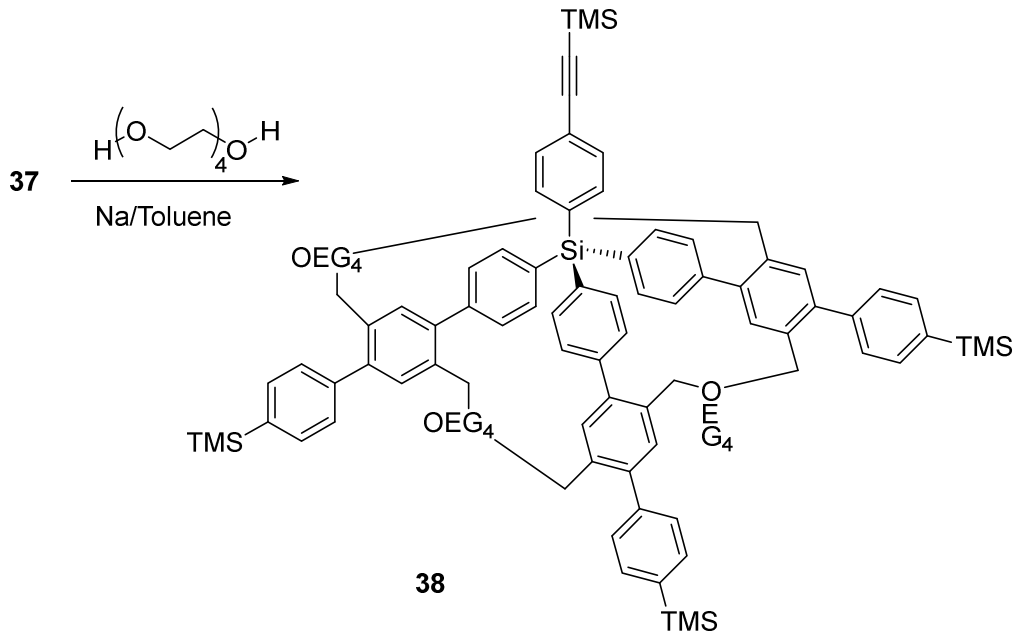

Following the procedure outlined for tripod **35**, compound **38** was synthesized by using **37** (235 mg, 0.14 mmol), OEG_4 (81.5 mg, 0.42 mmol), and sodium (19.3 mg, 0.84 mmol) in toluene (5 mL). The crude was purified by column cromatography (CH_2Cl_2/MeOH, 9.5:0.5) giving tripod as a colorless oil **38** (70 mg, 30%).

^{1}H-NMR ($CDCl_3$) δ (ppm): 7.77-7.40 (m, 34H, ArH), 4.50 (s, 12H, 6 x CH_2O), 3.65-3.52 (m, 48H, OEG_4), 0.31 (s, 27H, 3 x TMS), 0.26 (s, 9H, TMS).
^{13}C-NMR ($CDCl_3$) δ (ppm): 136.4, 136.2, 133.6, 133.4, 133.3, 133.2, 128.9, 128.7, 128.5, 128.4, 127.9 (C_{Ar}, CH_{Ar}), 72.5 (-CH_2O-), 70.6 (PhCH_2), 70.3 (PhCH_2), 61.7 (-CH_2O-), 0.0 (3 x TMS), -1.0 (TMS).

MALDI-TOF MS (Ditranol as matrix): m/z: calcd for $C_{104}H_{130}O_{15}Si_5$ [M+Na]: 1781.825; found: 1781.339.

4.4 Synthesis of tripods with cromophore groups

4.4.1 Synthesis of 3-bromo-4-(*N*, *N*-dimethylamino)benzaldehyde (**40**)

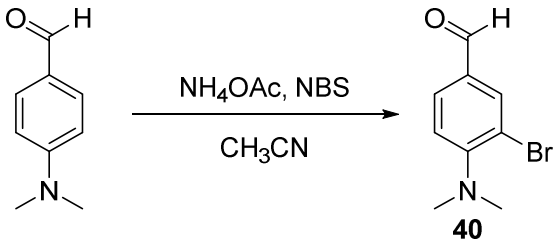

Under an argon atmosphere, NBS (16 mmol, 2.90 g) was added to a mixture of 4-(*N*,*N*-dimethyl)aminobenzaldehyde (13.5 mmol, 2.01 g) and NH_4OAc (10%) in CH_3CN (75 mL). The reaction mixture was stirred at room temperature for 15 min. After completion of the reaction, indicated by TLC, the mixture was concentrated under vacuum and extracted with EtOAc/H_2O (1:1) (3x 50 mL). The organic phase was then concentrated to dryness and purified by column chromatography (cyclohexane/EtOAc, 10:1) to obtain compound **40** as a pale yellow oil (2.69 g, 88%).[10]

^{1}H-NMR ($CDCl_3$) δ (ppm): 9.79 (s, 1H, CHO), 8.01 (s, 1H, H-2), 7.72 (d, 1H, *J*= 8.4 and 2 Hz, H-6), 7.06 (d, 1H, *J*= 8.4 Hz, H-5), 2.93 (s, 6H, -NMe_2).
^{13}C-NMR ($CDCl_3$) δ (ppm): 189.5 (C=O), 156.9 (C–N), 135.9 (C-1), 130.9 (C-2), 129.8 (C-6), 119.3 (C-5), 116.4 (C–Br), 43.3 (-NMe_2).

[10] Das, B.; Venkateswarlu, K.; Majhi, A.; Siddaiah, V.; Ravinder, K. *Journal of Molecular Catalysis A: Chemical* **2007**, *267*, 30.

4.4.2 Synthesis of 2-(3-bromo-4-(dimethylamino)benzylidene)-1H-indene-1,3(2H)-dione (**41**)

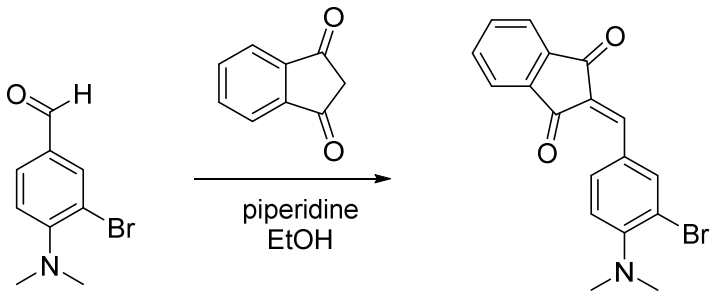

40 **41**

At room temperature, aromatic aldehyde **40** (13.4 mmol, 3.05 g) was added to a solution of 1,3-indandione (13.5 mmol, 1.97 g) in ethanol (100 mL), over a period of 3 min with constant stirring. Then, 2–3 drops of piperidine were added to maintain alkaline medium. The mixture was refluxed for 3 h. After this period, the volume was reduced to half under vacuum and then poured into crushed ice. The separated solid was filtered off and recrystallized from ethanol to give the desired 2-benzylideneindandione derivative **41** as an orange solid (4.14 g, 87%).

^{1}H-NMR ($CDCl_3$) δ (ppm): 8.84 (s, 1H, H_{vin}), 8.36 (dd, *J*= 8.8 Hz and 2 Hz, 1H, H-6), 7.94 (m, 2H, ArH), 7.77 (m, 2H, ArH), 7.70 (s, 1H, H-2), 7.04 (d, *J*= 8.8 Hz, 1H, H-5), 2.99 (s, 6H, $–NMe_2$).

^{13}C-NMR ($CDCl_3$) δ (ppm): 190.6 (C=O), 189.5 (C=O), 155.9 (C–N), 145.3 (CH_{vin}), 142.4 (C_{vin}), 140.9 (CH_{Ar}), 140.1 (C_{Ar}), 135.1 (C-2), 135.0 (C-1), 134.8 (C-6), 127.6 (CH_{Ar}), 127.0 (C_{Ar}), 123.1, 123.0 (CH_{Ar}), 118.9 (C-5), 115.2 (C–Br), 43.5 ($–NMe_2$).

MS (70 eV) m/z (%): 358 (17), 357 (92), 355 (100), 354 (61).

4.4.3 Synthesis of 2-bromo-4-(1,3-dioxolan-2-yl)-*N*,*N*-dimethylaniline (**44**)

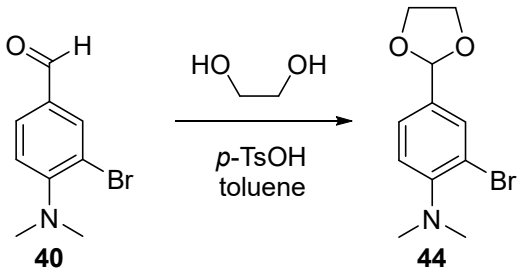

40 **44**

To a solution of **40** (10.03 g, 44.2 mmol) in toluene (80 mL), ethylene glycol (48.9 mL, 877 mmol) and *p*-toluenesulfonic acid monohydrate (0.51 g, 2.6 mmol) were added. The reaction was heated under reflux for 12 h while removing water using a Dean–Stark apparatus. After this period, the solution was cooled to room temperature, aqueous potassium carbonate 10% was added and then extracted with EtOAc (3x 20 mL). The organic phase was washed with brine and water, dried over $MgSO_4$ and concentrated under vacuum. Compound **44** was obtained without further purification as an oil (11.68 g, 98%).

^{1}H-NMR ($CDCl_3$) δ (ppm): 7.66 (d, 1H, *J*= 2.0 Hz, H-3), 7.32 (dd, 1H, *J* = 8.4 Hz, 2.0 Hz, H-5), 7.05 (d, 1H, *J*= 8.4 Hz, H-6), 5.70 (s, 1H, OCHO), 4.07 (m, 2H, OCH_2), 3.97 (m, 2H, OCH_2), 2.77 (s, 6H, -NMe_2).
^{13}C-NMR ($CDCl_3$) δ (ppm): 152.1 (C–N), 133.4 (C-1), 131.8, 126.2 (C-2, C-6), 120.0 (C-5), 109.2 (C–Br), 102.7 (OCO), 65.3 (2 x CH_2), 43.3 (-NMe_2).

4.4.4 Synthesis of (6-(dimethylamino)-3-formylphenyl)boronic acid (**45**)

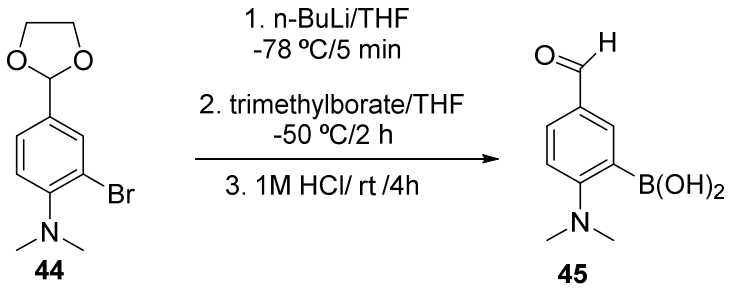

Under an argon atmosphere, over a solution of **44** (4.00 g, 14.7 mmol) in THF (40 mL) cooled to -78 ºC, n-BuLi (13.8 mL, 1.6 M, 22.05 mmol) was added dropwise. The mixture was stirred for 5 min and trimethylborate (4.92 mL, 44.1 mmol) was added dropwise. Then, the reaction mixture was stirred at -50 ºC for 2 h, after that warmed up to room temperature and stirred overnight. After this period, 1 M HCl solution (25 mL) was slowly added to the reaction mixture and stirred for 4 h. Then 10% K_2CO_3 solution (5 mL) was added to the reaction mixture, adjusting the pH to 6–7. The solution was extracted with EtOAc and the organic phase was washed with water, brine and dried over $MgSO_4$. The solution was filtered and concentrated under vacuum. The residue was purified by column chromatography (cyclohexane/EtOAc, 1:1) to obtain product **45** as a brown oil (2.21 g, 78%).

^{1}H-NMR ($CDCl_3$) δ (ppm): 9.64 (s, 1H, CHO), 7.86 (s, 1H, H-2), 7.61 (d, 1H, *J*= 8.8 Hz, H-6), 7.46 (d, 1H, *J*= 8.8 Hz, H-5), 6.70 (brs, $B(OH)_2$), 2.87 (s, 6H, -NMe_2).
^{13}C-NMR ($CDCl_3$) δ (ppm): 192.1 (CHO), 153.1 (C–N), 142.1 (C-6), 132.1 (C-4), 128.7, 124.0 (C-1, C-5), 116.0 (C-3), 42.1 (–NMe_2).

HRMS: calcd for $C_{19}H_{12}BNO_3$ [M+H$^+$] 193.0910; found 193.0917.

4.4.5 Synthesis of tripod **46**

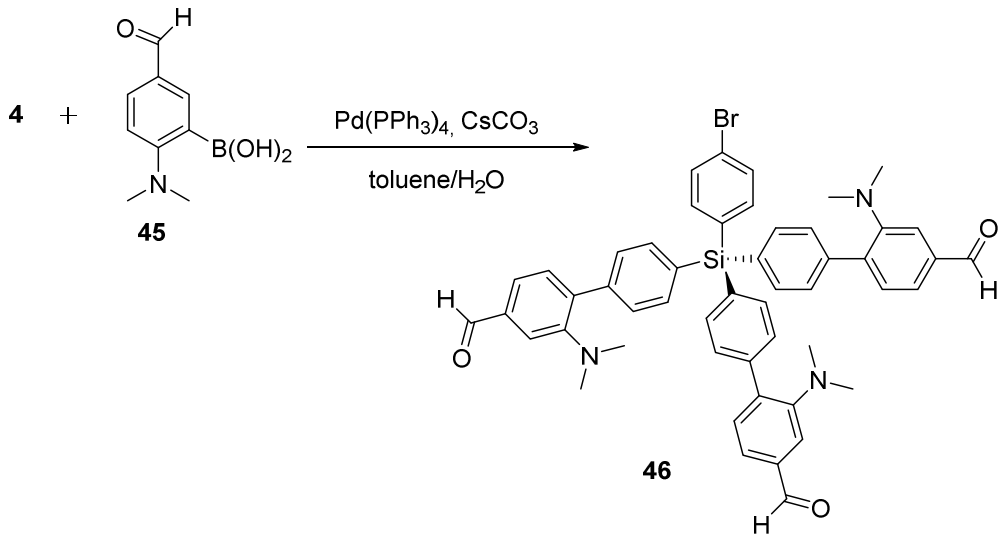

Under an argon atmosphere, Cs_2CO_3 (206 mg, 0.6 mmol), **4** (250 mg, 0.3 mmol) and $Pd(PPh_3)_4$ (36.4 mg, 0.03 mmol) were placed in an oven-dried round-bottom flask. Then a degassed solution of **45** (202 mg, 1 mmol) in a solution of toluene/H_2O (1:1, 25 mL) was added. The reaction mixture was refluxed for 18 h and, after this period, the inorganic solids were removed by filtration through celite and washed with CH_2Cl_2. Finally, the solvent was evaporated under vacuum and the residue was purified by column chromatography (cyclohexane/EtOAc, 8:2) to give **46** as a yellow solid (219 mg, 87%).

^{1}H-NMR ($CDCl_3$) δ (ppm): 9.84 (s, 3H, CHO), 7.75 (d, 6H, *J*= 8.4 Hz, ArH), 7.72 (d, 3H, *J*= 2.1 Hz, ArH) 7.65 (d, 6H, *J*= 8.4 Hz, ArH), 7.7–7.4 (m, 7H, ArH), 7.03 (d, 3H, *J*= 8.4 Hz, ArH), 2.72 (s, 18H, 3 x -NMe_2).

^{13}C-NMR ($CDCl_3$) δ (ppm): 190.6 (CHO), 156.0 (C-N), 143.2, 137.9 (C_{Ar}), 136.6 (CH_{Ar}), 134.2, 133.2, 132.1 (C_{Ar}), 131.0 (CH_{Ar}), 130.7, 128.6 (C_{Ar}), 127.9 (CH_{Ar}), 124.9 (C-Br), 116.3 (CH_{Ar}), 111.0 (C_{Ar}), 42.9 (-NMe_2).

HRMS: calcd for $C_{51}H_{46}N_3O_3SiBr$ 855.2492; found 855.2500.

4.4.6 Synthesis of tripod **47**

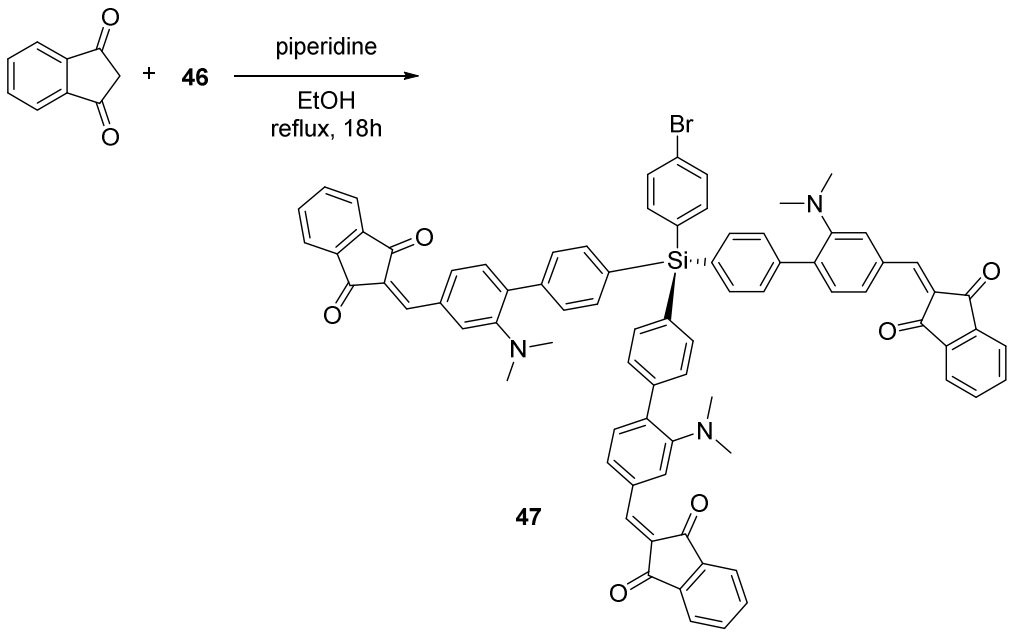

A solution of **46** (119 mg, 0.14 mmol) in toluene (25 mL) was added over a stirred solution of 1,3-indandione (180 mg, 1.23 mmol, 8.8 equiv.) in EtOH (10 mL), under an argon atmosphere. Then, 2–3 drops of piperidine were then added. The reaction mixture was refluxed for 18 h, the solvent was removed under vacuum and the residue was purified by column cromatography (cyclohexane/EtOAc, 2:1) to give **47** as an orange solid (50 mg, 29%).

Mp: 287-288 ºC.

^{1}H-NMR ($CDCl_3$) δ (ppm): 8.53 (s, 3H, H_{vin}), 8.45 (d, *J*= 8.8 Hz, 3H, ArH), 7.94-7.91 (m, 6H, ArH), 7.83 (s, 3H, ArH), 7.73-7.51 (m, 22H, ArH), 7.02 (d, *J*= 8.8 Hz, 3H, ArH), 2.79 (s, 18H, 3 x -NMe_2).

^{13}C-NMR ($CDCl_3$) δ (ppm) (100 MHz): 190.1 (C=O), 190 (C=O), 155.5 (C-N), 147.0, 143.2, 142.3, 140.0, 138.0 (C_{Ar}), 136.8 (CH_{Ar}), 136.4, 134.7, 134.4 (C_{Ar}), 132.1, 131.3, 130.4, 127.9 (CH_{Ar}), 124.9 (C-Br), 122.7, 116.2 (CH_{Ar}), 42.7 (NMe_2).

HRMS: calcd. for $C_{78}H_{59}N_3O_6SiBr$ 1239.3378; found 1239.3348.

4.5 Alkynyl terminated molecules for the functionalization of silicon substrates

4.5.1 Synthesis of 3,6,9,12-tetraoxatricos-22-en-1-ol (**48**)

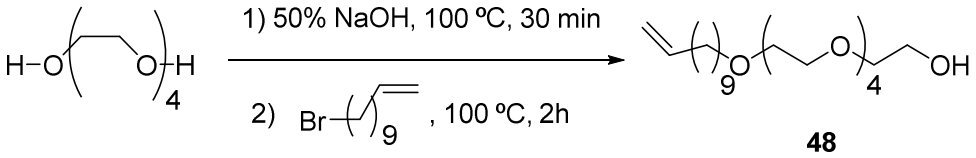

48

Under an argon atmosphere, a mixture of 50% sodium hydroxide (1 mL) and tetra(ethylene glycol) (20.8 mL, 120 mmol) was stirred at 100 ºC for 30 min. After this period, 11-bromoundec-1-yl (2.62 mL, 12.0 mmol) was added. The reaction was followed by tlc (EtOAc/cyclohexane 1:1) to completion. The reaction mixture was cooled to 20 ºC and extracted with cyclohexane (3 x 20 mL), the organic phase was washed with brine, dried over $MgSO_4$ and concentrated to dryness. The residue was purified by column chromatography (cyclohexane/EtOAc, 1:1) to obtain compound **48** as a yellow oil (3.45 g, 83%).[11]

^{1}H-NMR ($CDCl_3$) δ (ppm): 5.83–5.73 (m, 1H, CH_{vin}), 4.95 (d, 1H, *J*= 16.0 Hz, CH_{2vin}), 4.89 (d, 1H, *J*= 9.6 Hz, $=CH_2$), 3.69 (d, *J*= 4.4 Hz, 2H, CH_2OH), 3.64-3.54 (m, 18H, 9 x CH_2O), 3.41 (t, 2H, *J*= 7.0 Hz, $-CH_2O-$), 2.01-1.99 (m, 2H, $=CH-C\underline{H}_2$), 1.56-1.53 (m, 2H, CH_2), 1.33-1.21 (m, 12H, 6 x CH_2).

^{13}C-NMR ($CDCl_3$) δ (ppm): 139.1 (CH_{vin}), 114.0 (CH_{2vin}), 72.5 ($-CH_2O-$), 71.4 ($-CH_2O-$), 70.5 ($-CH_2O-$), 70.4 ($-CH_2O-$), 70.3 ($-CH_2O-$), 70.1 ($-CH_2O-$), 69.9 ($-CH_2O-$), 61.57 ($-CH_2O-$), 33.7, 29.4, 29.4, 29.3, 29.3, 29.0, 28.8, 25.9 (CH_2).

[11] Hierrezuelo,J.; López-Romero, J.M.; Rico, R.; Brea, J.; Loza, I.; Cai, C.; Algarra, M. *Bioorganic and Medicinal Chemistry* **2010**, *18*, 2081.

4.5.2 Synthesis of 4,7,10,13,16-pentaoxaheptacos-26-en-1-yne (**49**)

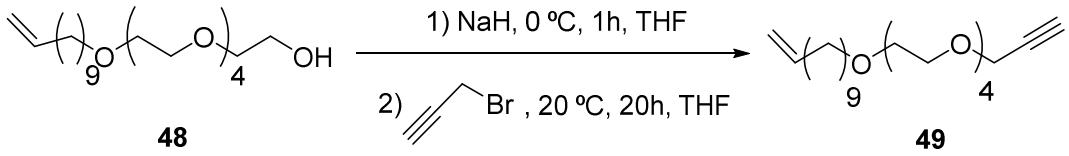

48 **49**

Compound **48** (0.54 g, 1.55 mmol) was dissolved in THF (5 mL) at 0 ºC under an argon atmosphere. Then, NaH (62 mg, 5.1 mmol) was portion wise added to the magnetically stirred mixture of reaction, and then stirred for 1 h at 0 ºC. After that, propargyl bromide (80%, 146 μL, 1.55 mmol) was slowly added and the reaction mixture was stirred at 20 ºC for 20 h. After this period, it was quenched with water and extracted with EtOAc (3 x 20 mL). The organic phase was washed with brine (3 x 20 mL), dried over anhydrous $MgSO_4$ and concentrated to dryness. The crude was then purificated by column chromatography (EtOAc) giving compound **49** as a colorless oil (280 mg, 46%).[12]

^{1}H-NMR ($CDCl_3$) δ (ppm): 5.87–5.74 (m, 1H, CH_{vin}), 4.80–4.60 (m, 2H, CH_{2vin}), 3.70–3.53 (m, 16H, -CH_2O-), 3.44 (t, *J*= 6.9 Hz, 2H, -CH_2O-), 2.38 (s, 1H, ≡CH), 1.80 (m, 2H, CH_2), 1.31 (t, 2H, *J*= 6.6 Hz, CH_2), 1.18–1.28 (m, 14H).

^{13}C-NMR ($CDCl_3$) δ (ppm): 139.2 (CH_{vin}), 114.9 (CH_{2vin}), 79.8, 78.2 (-C≡CH), 72.3 (-CH_2O-), 71.5 (-CH_2O-), 71.3 (-CH_2O-), 71.0 (-CH_2O-), 69.3 (-CH_2O-), 35.6, 29.4, 29.1, 28.7, 28.3, 28.1, 25.9 (CH_2).

[12] Lucena-Serrano A.; Lucena-Serrano, C.; Contreras-Cáceres, R.; Díaz, A.; Valpuesta, M.; Cai, C.; López-Romero, J.M. *Applied Surface Science* **2016**, *360*, 419.

4.6 Synthesis of theophylline derivatives

4.6.1 Synthesis of ((oxybis(ethane-2,1-diyl))bis(oxy))bis(ethane-2,1-diyl) bis(4-methylbenzenesulfonate) (**50**)

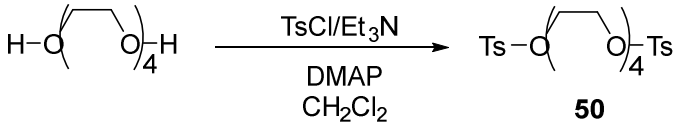

50

To a solution of TsCl (14.72 g, 77.21 mmol) in CH_2Cl_2 (70 mL) at 0 ºC, a solution of Et_3N (11.41 mL), OEG_4 (5.0 g, 25.77 mmol) and DMAP (3.10 mg) in CH_2Cl_2 (140 mL) was slowly added (within 2 h.). The mixture was stirred at 20 ºC for 12 h and, after this period, it was washed with water (2 x 200 mL) and 10% citric acid in water (2 x 100 mL). The combined organic phases were dried over anhydrous $MgSO_4$ and concentrated to dryness without further purification, obtaining compound **50** as a colorless oil (12.92 g, 99%).[13]

^{1}H-NMR ($CDCl_3$) δ (ppm): 7.78 (d, 4H, *J*= 8.2 Hz, ArH), 7.33 (d, 4H, *J*= 8.6 Hz, ArH), 3.53-4.15 (m, 16H, 8 x -CH_2O-), 2.42 (s, 6H, 2 x CH_3).

[13] Bonger, K.M.; van den Berg, R.; Heitman, L.; Ijzerman, P. *Bioorg. Med. Chem*. **2007**, *15*, 4841.

4.6.2 Synthesis of 2-(2-(2-(2-(1,3-dimethyl-2,6-dioxo-1,2,3,6-tetrahydro-7H-purin-7-yl)ethoxy)ethoxy)ethoxy)ethyl 4-methylbenzenesulfonate (**51**)

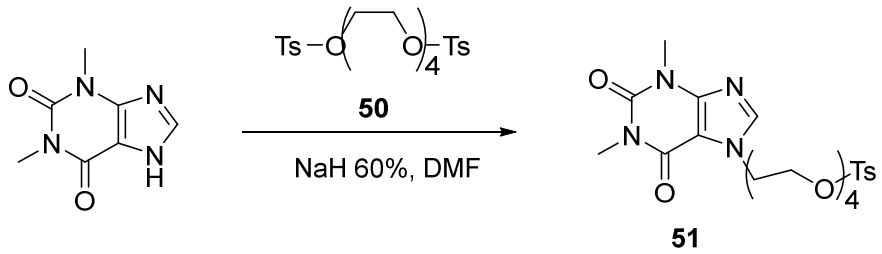

Over a solution of theophylline (1 g, 5.6 mmol) in DMF (55 mL), NaH (60%) (0.244g, 6.1 mmol) was added. After H_2 evolution ceased, a solution of **50** (5 g, 27.8 mmol) in DMF (70 mL) was added, and the mixture of the reaction was stirred at 20 ºC for 12 h. After this period, the reaction was diluted with CH_2Cl_2 (100 mL), washed with water (3 x 50 mL) and brine (2 x 50 mL). The organic phase was dried over $MgSO_4$ and concentrated to dryness under vacuum. Compound **51** was isolated by column cromatography (EtOAc/cyclohexane, 2:1) as a brown oil (1.41 g, 50%).[11]

^{1}H-NMR ($CDCl_3$) δ (ppm): 7.77 (d, 2H, *J*= 8.0 Hz, ArH), 7.69 (s, 1H, H-8), 7.31 (d, 2H, *J*= 8.0 Hz, ArH), 4.47–3.54 (m, 16H, 7 x OCH_2, 1 x NCH_2), 3.53 (s, 3H, -NMe), 3.37 (s, 3H, -NMe), 2.41 (s, 3H, CH_3).

^{13}C-NMR ($CDCl_3$) δ (ppm): 155.7 (C=O), 151.5 (C=O), 149.1 (C-4), 145.1 (C-1´), 142.9 (C-8), 142.0 (2 x CH_{Ar}), 130.1 (C_{Ar}), 128.3 (2 x CH_{Ar}), 106.8 (C-5), 71.0, 70.8, 70.7, 69.71, 69.69, 69.0.4 (-CH_2O-), 47.1 (NCH_2), 30.1 (-NMe), 28.2 (-NMe), 21.9 (CH_3).

HRMS m/z: calcd for $C_{22}H_{30}N_4O_8S$ [M+Na] 533.1682; found 533.1700.

4.6.3 7-(2-(2-(2-(2-azidoethoxy)ethoxy)ethoxy)ethyl)-1,3-dimethyl-3,7-dihydro-1H-purin-2,6-dione (**52**)

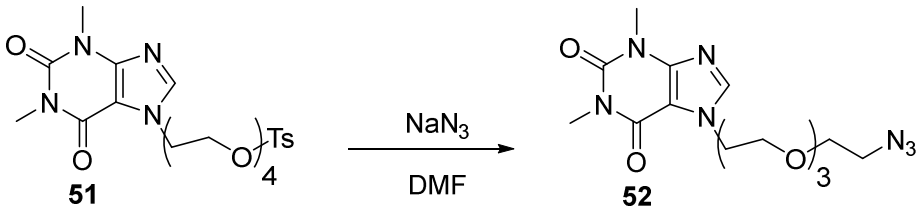

A solution of **51** (1.4 g, 2.75 mmol), NaN_3 (0.218 g, 3.4 mmol) in DMF (30 mL) was stirred at 60 ºC for 12 h. After this period, the reaction mixture was concentrated to dryness under vacuum, and then CH_2Cl_2 (100 mL) was added. The solution was washed with water (3 x 100 mL) and brine (100 mL), dried over $MgSO_4$, filtered and the solvent removed in vacuum. The residue was purified by column cromatography (EtOAc), to obtain **52** as a pale yellow oil (0.34 g, 33%).[11]

^{1}H-NMR ($CDCl_3$) δ (ppm): 7.69 (s, 1H, H-8), 4.49– 3.58 (m, 16H, 8 x CH_2), 3.62 (s, 3H, NMe), 3.39 (s, 3H, NMe).
^{13}C-NMR ($CDCl_3$) δ (ppm): 155.4 (C=O), 151.7 (C=O), 148.8, 142.5 (C-8), 106.4 (C-5), 70.7, 70.6, 70.53, 70.49, 70.0, 69.4 (6 x -CH_2O-), 50.6 (NCH_2), 46.8 (CH_2N_3), 29.8 (NMe), 27.9 (NMe).

HRMS m/z: calcd for $C_{15}H_{23}N_7O_5$ [M+Na] 404.1658; found 404.1667.

4.7 Surface modification

4.7.1 Modification of silicon substrates

4.7.1.1 Preparation of H-Si (111) substrates and fabrication of alkynyl-terminated Si surfaces with **49**

Single-side polished, p-type (boron-doped, 1-10 Ω/cm resistivity) Si(111) wafers (Silicon Quest International, Inc.) were cut into pieces of 1 cm x 1 cm and cleaned with Piranha solution (concentrated H_2SO_4/30% H_2O_2 3:1 v/v) for 30 min at 80 ºC to remove impurities. *Caution: Piranha solutions react violently with organic materials and should be handled with extreme care*. In order to reduce the SiO_2 substrate to H-Si, the freshly cleaned sample was immersed in an argon-saturated, 2.5% HF solution for 10 min, followed by rapid rinse with argon-saturated water and dried with a stream of argon.

The freshly prepared 1 cm x 1 cm H-Si(111) substrate was placed in a simple vacuum chamber setup combining a Schlenk tube with a quartz cell for photo-induced surface hydrosilylation. The H-Si(111) sample was put in contact with a droplet of **49** on a quartz disk, forming an uniform layer of the molecule sandwiched by the quartz disk and the silicon slide. Hydrosilylation process was carried out at 254 nm UV light illumination during 2 h at atmospheric under high vacuum condition (0.05 mbar). The substrates were finally washed sequentially with ethanol and CH_2Cl_2, and finally dried with a stream of argon to obtain surface A.

4.7.1.2 Click reaction of tripods **12**, **14** and **21** onto alkynyl modified H-Si(111) (surface B)

The grafting of these molecules was performed by click reaction onto freshly prepared Si-alkynyl surfaces (surface A) obtaining surfaces B. We have performed the reaction by using two different copper salts and two different bases (procedures a and b). *Procedure a)* this method was carried out with tripods **12, 14** and **21**. Briefly, a 0.5 mm x 0.5 mm piece of surface A was immersed into a degassed THF/MeOH (1:1 v/v) solution containing $Cu(MeCN)_4PF_6$ (3.75 mM), corresponding tripod (5 mM) and the copper ligand (37.5 mM, see scheme IV.1 in chapter IV) during 24 h at room temperature. *Procedure b)* a 0.5 mm x 0.5 mm piece of surface A was immersed into a degassed THF (2 mL) solution containing CuI (catalytic amount), DIPEA as base and **21**. After incubation during 24 h, the sample was taken out and immersed into aqueous EDTA

solution (5 mL, 25 mM), sonicated for 10 s, and thoroughly washed with water, then ethanol and finally dried with a stream of argon, obtaining surfaces B.

4.7.1.3 Click reaction with theophylline **52** onto deprotected **21**-Si-surfaces (surfaces C)

A 0.5 mm x 0.5 mm sample of surface B5 was immersed into a degassed methanol (5 mL) solution containing K_2CO_3 (1 mM), then shaked for 1 h at room temperature. After this period, the sample was taken out and thoroughly washed with water, then ethanol and finally dried with a stream of argon. After drying, sample was immersed into methanol (5 mL) solution containing CuI (catalytic amount), DIPEA (500 mM) and **51** (5 mM). After 24 h reaction at room temperature, the sample was taken out and immersed into aqueous EDTA solution (5 mL, 25 mM), sonicated for 10 s, and thoroughly washed with water, then ethanol and finally dried with a stream of argon, obtaining surfaces C.

4.7.1.4 Protein Adhesion

Pieces of pristine and processed SAMs (surface C) were immersed in a solution of streptavidin (0.5 mL, 1 ng/μL) in PBS-buffer (pH= 7.4) and slowly stirred (protected from light) at 25 ºC for 1 h. After immersion, the samples were washed with wáter, dried in a stream of argon and then they were kept in cold (surfaces D).

4.7.2 Modification of gold substrates

4.7.2.1 SAM preparation

The gold substrates for SAM preparation were purchased from Georg Albert PVD-Beschichtungen (Silz, Germany). They were prepared by thermal evaporation of 30 nm of gold (99.99% purity) onto polished sing le-crystal silicon (100) wafers (Silicon Sense) primed with a 9 nm titanium layer for adhesion promotion. The resulting films were polycrystalline with a grain size of 20-50 nm and predominantly possessed (111) orientation.

SAMs from tripods **26** and **31** were prepared by immersion of freshly prepared gold substrates in a 80 μM solution of the target molecules in THF containing 30% of a base (triethylamine, ammonia or *N*,*N*,*N*′,*N*″,*N*″-pentamethyldiethylenetriamine, 1M).

The immersion time was set to 48 h; the samples were kept at room temperature during the immersion. Afterwards, the samples were thoroughly rinsed with THF and ethanol, blown dry with argon, and kept in argon-filled containers until the characterization or subsequent experiments. Note that in addition to THF, DMF was tested as the solvent as well. However, according to the characterization, the quality of the films prepared from DMF was inferior to those fabricated from THF.

4.7.2.2 Click Reaction on **31** films with theophylline **52**

The click reaction experiments were only performed on the **31** films. These films were immersed into two different solutions of azide-decorated theophylline (**52**) (0.05 mM and 0.5 mM) in ethanol (3 mL) with addition of CuI (catalytic amounts) and DIPEA (12.5 mM, 37.5 μL) at room temperature for 24 h.

Afterwards, the samples were taken out and immersed into aqueous EDTA solution (25 mM), sonicated for 10 s, and washed with water, ethanol and, finally, dried under an argon stream. The results of the click reaction were monitored by XPS.

4.7.2.3 Protein adsorption

The theophylline-modified SAMs were immersed into a slowly stirred solution of a labeled streptavidin (Atto-565-SA; *c* = 1 ng/μL) in PBS-buffer (pH= 7.4, 2 mL) at 25 ºC for 1 h. After immersion, the samples were washed with water, dried under an argon stream, and kept protected from light and humidity. The protein adsorption was monitored by XPS, based on the characteristic N 1s peak, which is commonly used for this purpose.[14] For comparison, the adsorption of a non-specific protein, viz. bovine serum albumine (BSA) was tested as well. The adsorption of BSA was performed under the same conditions as in the streptavidin case.

[14] a) Jeyachandran, Y. L.; Weber, T.; Terfort, A.; Zharnikov, M. *J. Phys. Chem. C* **2013**, *117*, 5824–5830. b) Ballav, N.; Thomas, H.; Winkler, T.; Terfort, A.; Zharnikov, M. *Angew. Chem. Int. Ed.* **2009**, *48*, 5833–5836.

4.8 Sensing experiments and Quantum Yield determination of tripods 46 and 47.

4.8.1 Sensing Experiments

For the sensing experiments between 4CDNA and compound **47** different solutions of 4CDNA in EtOAc were prepared: 0.001; 0.01; 0.05; 0.1; 0.75; 2; 5; 10 and 20 mg/L. To these solutions an aliquot of 200 mL containing DMABI tripod **47** 0.1 M was added under mild magnetic stirring.

Emission spectra excitation (295.3 to 671.7 nm) and emission (249.7 to 719.7 nm) spectra were obtained using a Spex 3D luminescence spectrophotometer equipped with a Xenon pulse discharge lamp (75 W) and a CCD detector and 0.25 mm slits and 1s integration times were used in scan mode at room temperature.

Lifetime measurements were recorded using a Horiba Jovin Yvon Fluoromax 4 TCSPC using the following instrumental settings: 470 nm NanoLED; time range, 1.6 ms; peak preset; 10 000 counts; repetition rate, 500 kHz; synchronous delay, 25 μs; emission detection: 535 nm. Lifetime deconvolution analysis was performed using Decay Analysis Software, version 6.4.1 (Horiba JovinYvon).

Fluorescence decays were interpreted in terms of a multi-exponential:

$$I(t) = A + \sum B_i \exp^{-t/\tau i}$$

where A and B_i are the pre-exponential factors and τi the decay times.

4.8.2 Quantum yield determination

The quantum yield (QY) was determined using quinine sulphate as standard, which according to the literature has a QY of 0.54 in sulphuric acid 0.1 M (*n* = 1.38), DMABI-tripod **47** was dissolved in ethyl acetate.

The calibration curve for quinine was obtained. The integrated area under the fluorescence curves (excitation at 470 nm) was plotted versus the absorbance at 370 nm (after subtraction of the solvent absorbance) for different concentrations. The same procedure was repeated for both the compounds (**47** and **46**) dissolved in ethyl acetate (*n* = 1.3720).

The excitation intensity and slit width were held constant for all measurements. The QY of DMABI-tripods **47** and **46** was obtained from equation (1):

$$QYcds = QYst\left[\frac{\left(dI/dA\right)cds}{\left(dI/dA\right)st}\right]\left(\frac{ncds^2}{nst^2}\right)$$

where *I* is the area under the fluorescence curves and *A* is the corresponding absorbance.[15]

[15] Weber G.; Teale, F. W. J. *Trans. Faraday Soc*., **1957**, *53*, 646.

5. CONCLUSIONS

Conclusions from Chapter I

1. We have designed and synthesized novel tripod-shaped molecules with three (**12** and **14**) and five (**21**) *p*-phenylene units bearing azide groups in each leg. The key step of the synthesis was the palladium-catalyzed Suzuki cross-coupling reaction between the corresponding silicon core and the bi- or tetra-phenylene derivative. Tripod **14**, which presents a bromine atom at the functional arm, was obtained in 46% yield, while tripods **12** and **21**, both with a TMS group located at the funcional arm, were obtained in 65% and 54%, respectively. Contrary to the reported procedures, the construction of the tripods legs prior to the Suzuki coupling reaction gave better results than iterative homologation of substituted biphenyl building blocks.

2. We have designed and synthesized novel tripod-shaped molecules with two (**26**) and four (**31**) *p*-phenylene units as tripod legs in good yields (60% and 81% respectively). The legs of these molecules are terminated by thioacetate groups, while the fourth leg bears the alkyne moiety.

3. We have synthesized novel tripod-shaped molecules substituted laterally with tetraethylene glycol (OEG_4) groups (**35** and **38**). In both cases the terminal group in each leg is a TMS group. The synthesis was carried out again by coupling the corresponding *p*-phenylene derivative with the appropiate silicon core. affording **35** and **38** both in low yield, 30%.

4. We have developed the synthesis of tripod-shaped chromophores **46** and **47** in 87% and 29% yield, respectively. The key reactions were the Suzuki crosscoupling between the silicon core and a phenyl substituted boronic acid derivative, followed by aldol condensation with 1,3-indandione. Tripod **47** showed a high thermal stability and a strong and sensitive fluorescence when combine with the explosive 4-chloro-2,6-dinitroaniline. This fact demonstrated that chromophore tripod **47** is a promising optical sensor material for detecting nitro-containing explosives.

Conclusions from Chapter II

1. We have performed the covalent immobilization of tripods **12** and **21** onto alkynyl-modified H-Si(111) silicon wafers by click reaction in good yield and degree of nanostructuration. The better results, in terms of surface density, aggregation and tripod configuration, were found with a 0.25 mM tripod concentration in THF as solvent, without shaking and at room temperature.

2. We have carried out the attachment of the azide-substituted theophylline (**52**) onto the tripod-modified surfaces by click reaction. The covalent incorporation of the theophylline derivative was confirmed by fluorescence microscopy and XPS after binding with SA protein.

3. We have performed the attachment of tripods **26** and **31** on gold substrates by self-assembled monolayer (SAM) process. Well-defined and densely packed monomolecular films with ~85% of all potential anchoring groups bound to the substrate in the thiolate fashion were fabricated with tripod **31** and demonstrated by XPS analysis. The parameters of the preparation procedure, such as the solvent and the thioacetate deprotection agent, were varied, obtaining the better results when TEA (as base) and THF (as solvent) were used.

4. These films were successfully tested as templates for click reaction, taking complementary azide-substituted theophylline (**52**) as a test compound. The resulting theophylline-terminated monolayers were also tested as templates for specific protein adsorption, using SA (specific) and BSA (non-specific) proteins for this end. The XPS analysis showed a higher efficient adsorption, mediated by the terminal theophylline receptors, for the specific protein (SA) when compared to the non-specific one (BSA).

APPENDIX A: RESUMEN DE LA TESIS

RESUMEN DE LA TESIS

1. INTRODUCCIÓN Y ANTEDECENTES

Conceptos como biocompatibilidad, nanoestructuración, transporte de activos y monitorización adecuada, son fundamentales para conseguir la máxima efectividad en cualquier tipo de dispositivo de análisis. Por ello, con este trabajo de tesis se pretende abordar el desarrollo de estructuras híbridas potenciando su biocompatibilidad y así posibilitar el análisis y uso en entornos biológicos, realizar una adecuada nanoestructuración para alcanzar la máxima efectividad y, por último, una funcionalización que permita el análisis de interacciones biológicas concretas. Como modelos base para el diseño de dispositivos de análisis se usarán superficies metálicas (en concreto silicio y oro) y como moléculas cuya función sea la de adsorbatos se emplearán oligo(*p*-fenileno)s con forma de trípode.

La preparacion y caracterización de nuevos materiales y, en particular, la construcción de estructuras a escala nanométrica empleando derivados orgánicos en la modificación de superficies constituye una de las áreas prioritarias en la investigación actual. En el caso particular de modificación de superficies por formación de monocapas de moléculas orgánicas, son fundamentales tanto el control de la orientación y espaciado entre los grupos funcionales de los derivados orgánicos ya adsorbidos en las superficies, como la disponibilidad de métodos fiables para su derivatización, como por ejemplo la reacción de click o el acoplamiento de Suzuki-Miyaura, entre otros.

En la actualidad, el método más común para la preparación de capas orgánicas funcionales se basa en el autoensamblaje de adsorbatos monodentados que presentan cadenas alquílicas largas, como son alquilsiloxanos en superficies polares, derivados de alquenos o alquinos mediante hidrosililación en superficies de silicio o los tan bien conocidos alquiltiolatos en superficies de oro.

La orientación de estas moléculas flexibles se consigue por el elevado grado de empaquetamiento que existe entre ellas generando una monocapa, ya que las moléculas se mantienen cercanas gracias a las fuerzas de Van der Waals entre los restos alquílicos. Sin embargo, y aunque la densidad de grupos funcionales en estas monocapas se puede controlar mediante el co-depósito con adsorbatos análogos pero inertes, no es posible evitar una distribución aleatoria de grupos activos en la monocapa.

Para evitar este problema, se han propuesto cuatro tipos de macromoléculas relativamente rígidas y de tamaño y forma definidos, como puede observarse en la figura 1. Éstas son:

a) Estructuras moleculares con cuatro brazos derivados de fenilacetileno unidos en un centro tetraédrico derivado de silicio (IV).
b) De adamantano (III).
c) Dendrones con forma cónica y con un grupo funcional en el extremo apical (I).
d) Macromoléculas con forma de trípode formadas por tres brazos de oligo-*p*-fenilenos unidos en un vértice derivado de silicio (II).

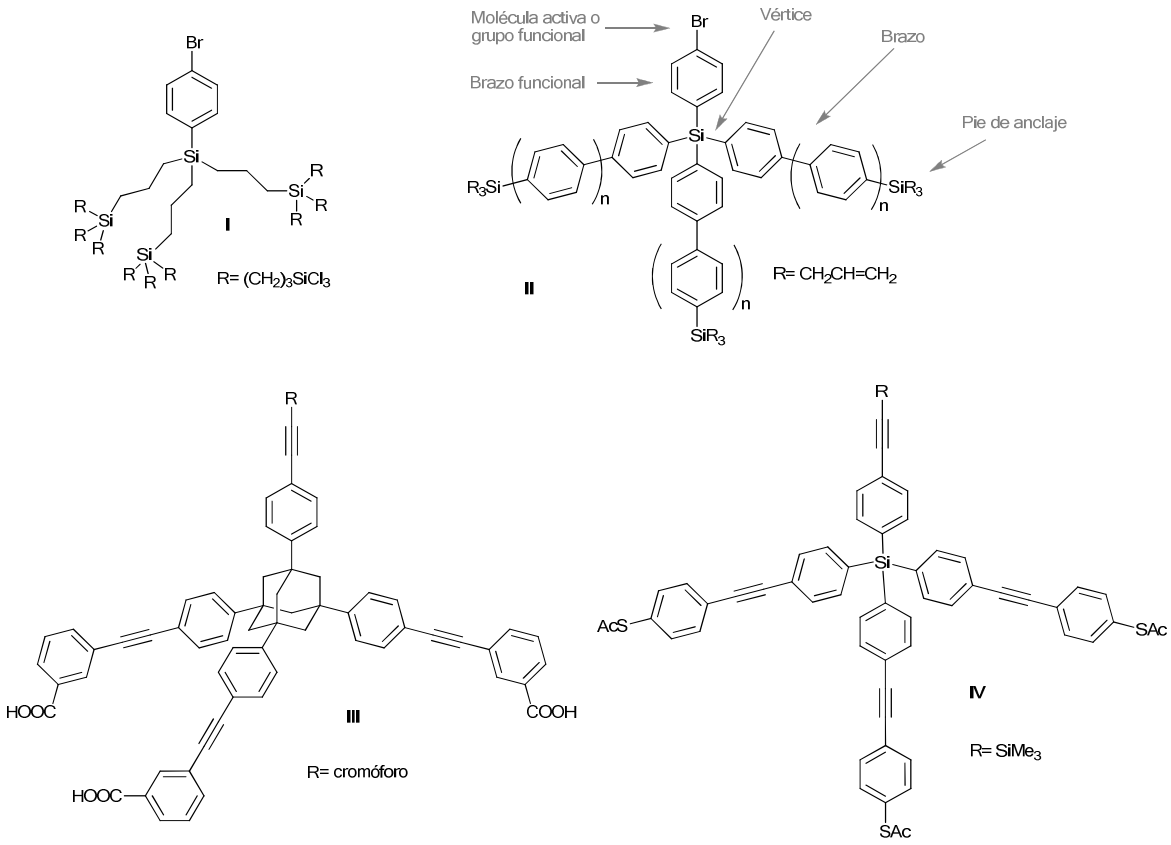

Figura 1. Macromoléculas rígidas para la nanoestructuración de superficies.

El empleo de estas macromoléculas permitirá la nanoestructuración de distintos tipos de superficies, como se indica en la figura siguiente:

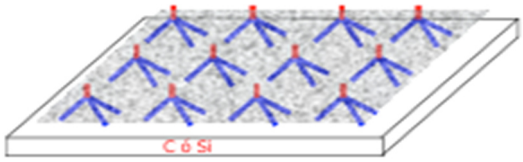

Figura 2. Superficie nanoestructurada con adsorbatos orgánicos

El uso de esta clase macromoléculas orgánicas, como adsorbatos de gran volumen y rigidez, deberá proporcionar una estructuración de la superficie, dejando un espaciado considerable entre los grupos acrtivos que porte dicha molécula, así como una orientación adecuada de los mismos.

Aunque existe una gran cantidad de macromoléculas de estructura definida, construidas a partir de distintos tipos de oligómeros de cadena rígida, muy pocas se han publicado con estructura tripodal. El primer autor que propuso el uso de estas moléculas fue Jim Tour en 1999). Tour describió su síntesis empleando un átomo de silicio como núcleo tetrahédrico central que actúa como unión entre tres cadenas de fenilacetileno, tal y como se observa en la Figura 3.

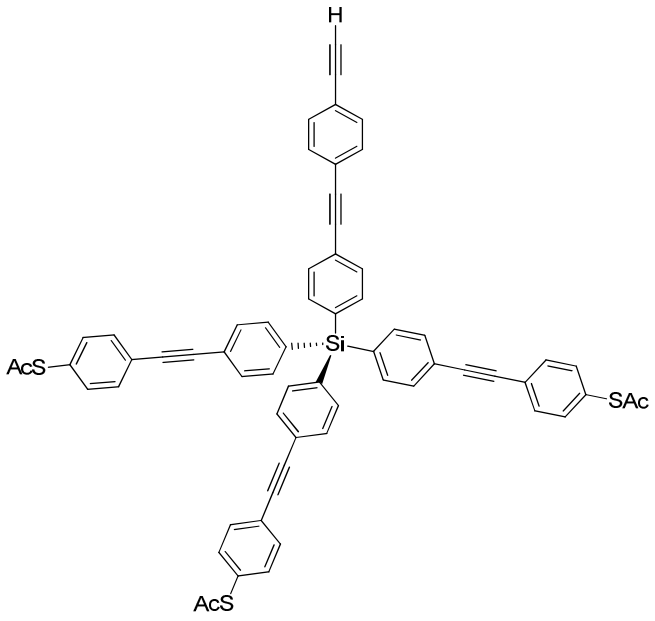

Figura 3. Molécula tripodal derivada de fenilacetileno

Esta misma estrategia fue utilizada por Cheng Zhi Cai en 2002 para la síntesis de una molécula con forma de trípode constituída por tres cadenas de hepta-*p*-fenileno, unidas en un átomo de silicio que actúa como vértice (Figura 4).

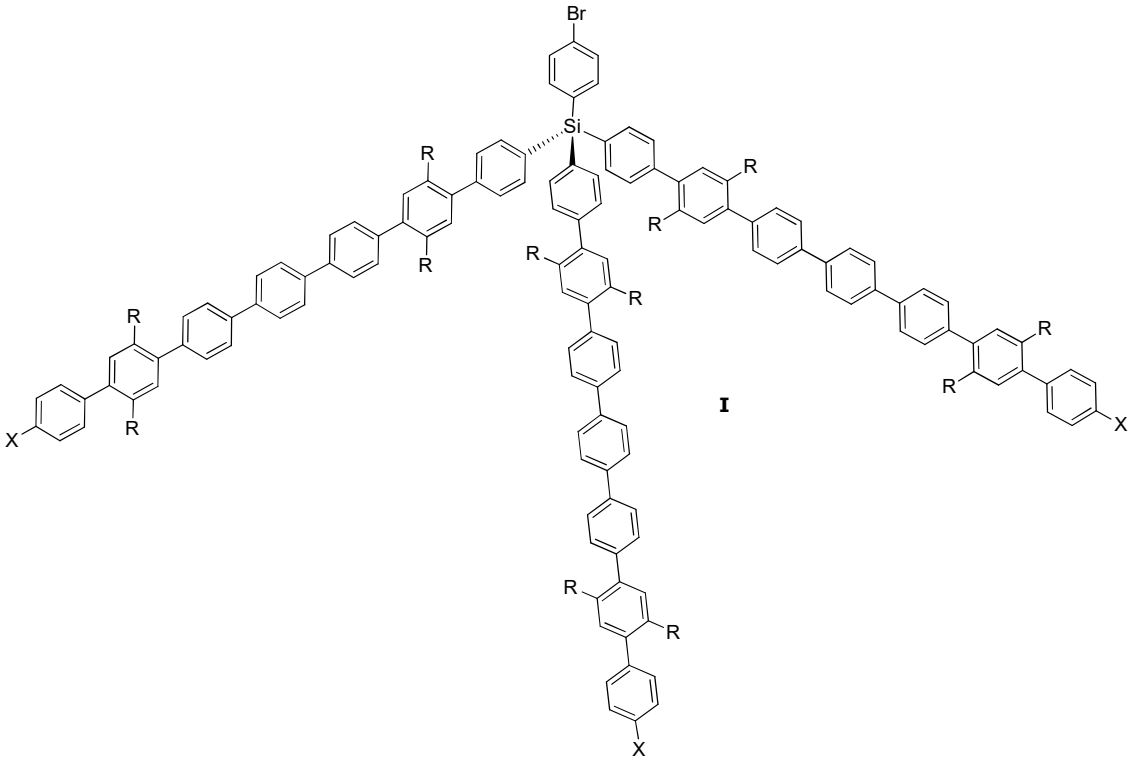

R = Hexilo
X = $Si(CH_2CH{=}CH_2)_3$, $-O-Si(CH_2CH_2CH_2SiCl_3)_3$, $-O-Si(CH_2CH_2CH_2Si(CH_2CH{=}CH_2)_3)_3$

Figura 4. Molécula con forma de trípode derivada de *p*-fenileno y etilenglicoles laterales

Éste es el primer antecedente que describe una molécula tripodal derivada de oligo-*p*-fenileno. Esta molécula se caracteriza por presentar en los extremos de los brazos de oligo-*p*-fenileno dendrones derivados de trialilsilano que se incluyen en la estructura del compuesto para ser usados como puntos de unión a una superficie de silicio Si-H por formación de un enlace covalente Si-C mediante una reacción de hidrosililación.

Además, presenta en el extremo apical un átomo de bromo que puede permitir su derivatización posterior por incorporación de moléculas activas, ya sea una vez que el adsorbato se encuentra unido a la superficie, o previamente. Entre estas moléculas activas se pueden incluir biotina, teofilina, grupos cromóforos, etc.

La síntesis de este compuesto, que está representado como (**I**) en el esquema 1, fue llevada a cabo según el análisis retrosintético A. Aunque en su preparación la etapa clave es el acoplamiento entre el derivado de *p*-fenileno (**II**) y la molécula vértice (**III**), que se realiza mediante una reacción tipo Suzuki, en su síntesis se pueden diferenciar tres partes. La primera consiste en la preparación de la unidad de hexa-*p*-fenileno (**II**) con la longitud deseada y funcionalizada en el extremo R, que constituirá la posición de

anclaje a la superficie, la segunda consiste en la preparación de la molécula derivada de silicio (**III**) que se utiliza como vértcie y, por último, la tercera en la que se lleva a cabo el acoplamiento entre ambas moléculas.

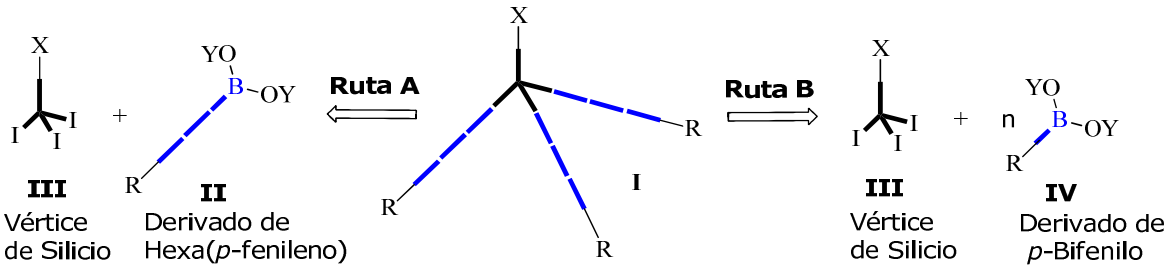

Esquema Retrosintético

Si volvemos a la figura 1, observaremos que los cuatro ejemplos presentan grupos de anclaje en los extremos de los brazos o piernas, para su adecuada inmovilización en las diferentes superficies metálicas, y también una molécula activa o grupo funcional en el cuarto brazo, que quedaría perpendicular a la superficie una vez depositada la molécula. En el caso concreto de la molécula **III**, ésta presenta un grupo cromóforo en el brazo funcional y fue por primera vez descrita por el grupo de Elena Galoppini en 2007.

Esta molécula tripodal, tiene como grupos de anclaje grupos COOH en posición meta, lo que hace que se aumente y mejore la unión de dicha molécula sobre superficies de TiO_2 por los tres grupos de anclaje. Esto, explican los autores, es debido a que al tener los grupos COOH en posición meta, el ángulo para el anclaje en las superficies sea más favorable, dato a tener en cuenta para futuros diseños moleculares.

Este compuesto presenta un cromóforo en el brazo funcional, cuyas propiedades derivan de las típicas de los pirenos sustituidos con fenilacetileno. Además, el espaciado de los colorantes en la superficie de semiconductores mediante el uso de macromoléculas tripodales, cuyos grupos de anclaje se dispongan en posición meta, podría ser de gran utilidad para estudiar los efectos de los excímeros y monómeros que tienen dichos grupos COOH en comparación con la posición para. (Figura 5)

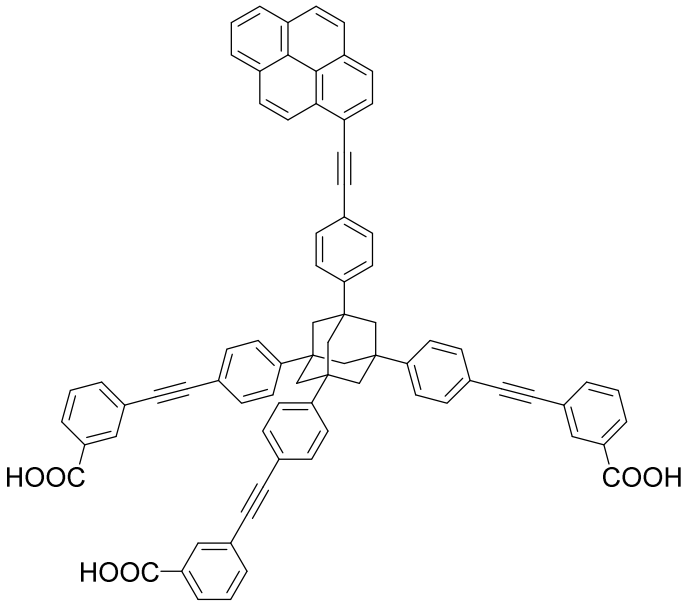

Figura 5. Molécula tripodal con COOH como grupos de anclaje y un cromóforo en el brazo funcional.

En el caso de los derivados de dendrones (molécula **I** en la figura 1), es importante tener en cuenta que estos compuestos están disponibles hoy día comercialmente, como es el caso de los NanoCones, empleándose para el recubrimiento de superficies. Sin embargo, estas estructuras presentan varios inconvenientes; uno de ellos es la facilidad con la que se degradan químicamente, la falta de rigidez en su propia estructura y unas funcionalidades químicas limitadas en el brazo funcional, lo que hace que se diseñen y desarrollen otras macromoléculas más estables para su empleo como adsorbatos.

A partir de la síntesis de todas estas moléculas, y analizando sus ventajas e inconvenientes, el grupo de investigación al que pertenezco ha llevado a cabo la síntesis de varios adsorbatos derivados de oligo-*p*-fenileno. Se han preparado trípodes con derivados de una teofilina activa, de azobenceno, con oligoetilenglicoles laterales para evitar la absorción no específica de proteínas, entre etros. Todos ellos presentan cuatro brazos unidos a un átomo de silicio, que actúa como núcleo tetrahédrico de la molécula en cuestión. Además, se ha estudiado la selectividad en el acoplamiento Suzuki en bifenilos y oligofenilenos, útil en la síntesis de los trípodes moleculares. Algunos ejemplos se representan en la Figura 6.

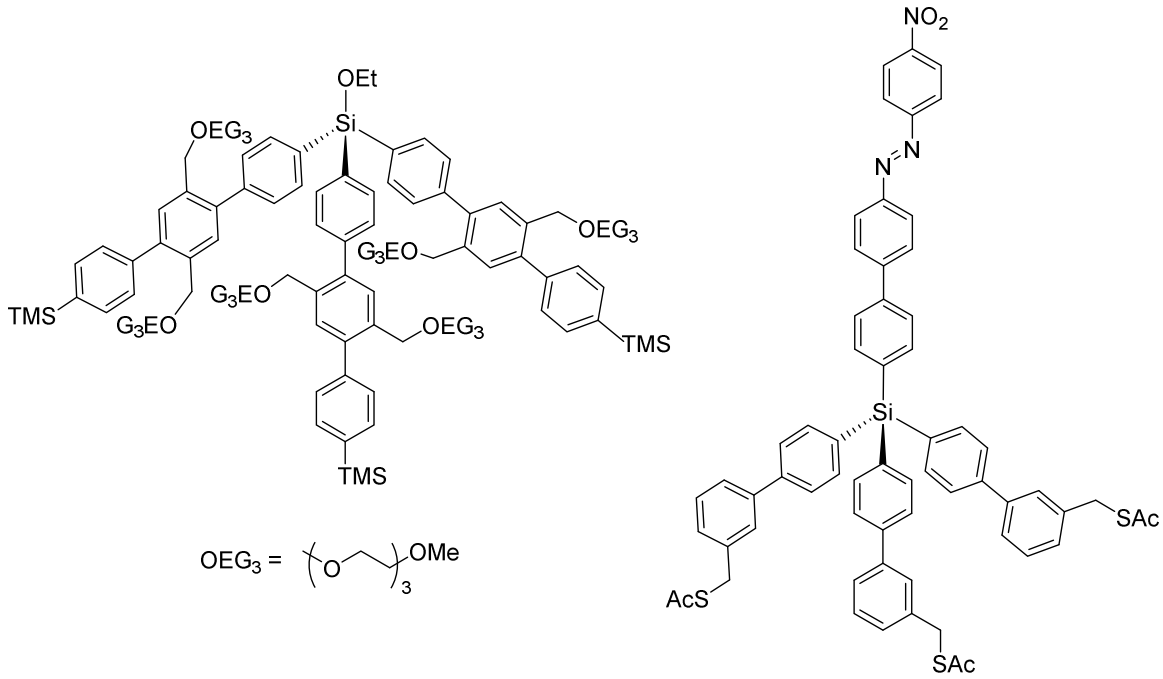

Figura 6. Algunos ejemplos de moléculas tripodales sintetizadas previamente por nuestro grupo de investigación.

Como se ha comentado anteriormente, este trabajo tiene como objetivo abordar el desarrollo de estructuras híbridas que mejoran su biocompatibilidad y, por lo tanto, su uso en entornos biológicos, realizando una nanoestructuración adecuada para lograr la máxima eficacia y, finalmente, una funcionalización que permita el análisis de interacciones biológicas concretas. Para poder estructurar a escala nanométrica las diferentes superficies metálicas, la formación de monocapas por el denominado método de autoensamblaje constituye una de las areas de investigación más importantes actualmente.

Las superficies prístinas de metales y óxidos metálicos tienden a adsorber fácilmente materiales orgánicos contaminantes debido a la menor energía libre que se genera en estos sistemas en la interfase, entre la superficie y el ambiente. Estos adsorbatos también alteran las propiedades de la interfase y tienen una influencia significativa en la estabilidad de las nanoestructuras de metales y óxidos metálicos. Por ejemplo, actúan como una barrera física o electrostática contra la formación de agregados, también actúan como una película eléctricamente aislante o disminuyen la reactividad de los átomos o grupos funcionales de la superficie. En consecuencia, las superficies recubiertas con materiales adventicios no están bien definidas, no presentan funcionalidades químicas específicas y no tienen propiedades físicas reproducibles como la conductividad, humectabilidad o resistencia a la corrosión.

Entre una gran cantidad de procedimientos para la funcionalización de superficies, la generación de monocapas autoensambladas (SAMs) se ha utilizado ampliamente para la fabricación de películas delgadas en una amplia gama de superficies como Au, Ag, Cu, $Al2O_3$, SiO_2, TiO_2 o Si. Estas monocapas (SAMs) tienen como características proporcionar un sistema fácil, flexible y simple con el que se ajustan a las propiedades interfaciales de los metales, los óxidos metálicos y los materiales semiconductores.

Las SAM son conjuntos moleculares formados espontáneamente en la superficie de un sólido por adsorción, puede darse en solución o fase gaseosa. Los adsorbatos que forman las SAM se organizan espontáneamente en dominios ordenados más o menos grandes y los grupos de anclaje, también denominados "headgroups" en inglés, tienen una funcionalidad química con una alta afinidad específica por un sustrato que proporciona el desplazamiento de los materiales orgánicos adventicios adsorbidos de la superficie. Hasta la fecha, el método más común para la preparación de capas orgánicas funcionales, basado en el autoensamblaje, es la incorporación de adsorbatos monodentados con tienen cadenas alquílicas largas (Figura 7).

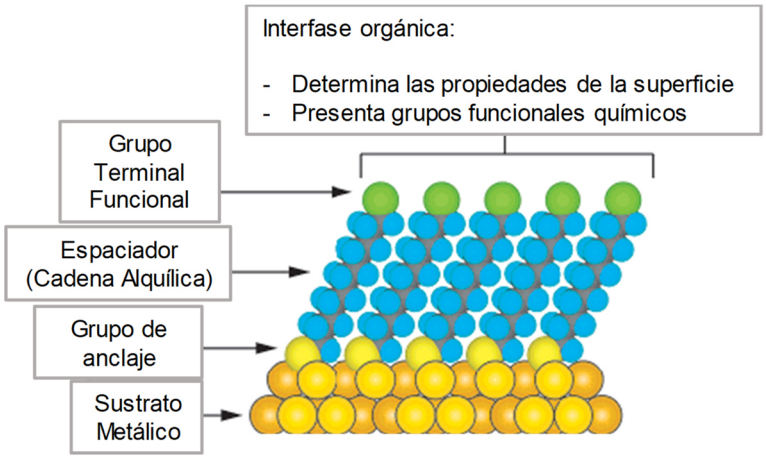

Figura 7. Ejemplo esquemático de una SAM ideal de alcanotiolatos soportados en una superficie de oro (111). Se destacan la anatomía y características de la SAM.

Recientemente, la estrategia ha evolucionado hacia el empleo de adsorbatos con más de una unidad de unión, es decir, moléculas más complejas estructuralmente que cubren un área específica que excede la unidad funcional presente en la molécula. Dependiendo del tamaño de la unidad de unión, estos SAM pueden exhibir una considerable rigidez y separación espacial entre los grupos funcionales insertados en un sustrato particular, ofreciendo, en particular, la posibilidad de fabricar arquitecturas interfaciales en bio-dispositivos con precisión molecular. En este sentido, el uso de estructuras multipodales grandes y rígidas, como las moléculas con forma de trípode,

podrían proporcionar una buena y estable disposición de las mismas en el sustrato seleccionado. Estas moléculas generalmente consisten en una estructura central tetraédrica con un grupo activo posicionado en el brazo funcional, perpendicular a la superficie. Los tres brazos restantes normalmente se componen por un espaciador que o bien puede ser alifático o, como hemos visto en ejemplos anteriores, oligofenilénico y oligofenilacetilénico, con una longitud deseada y los grupos de anclaje terminales dependerán de la naturaleza de los sustratos (Figura 8).

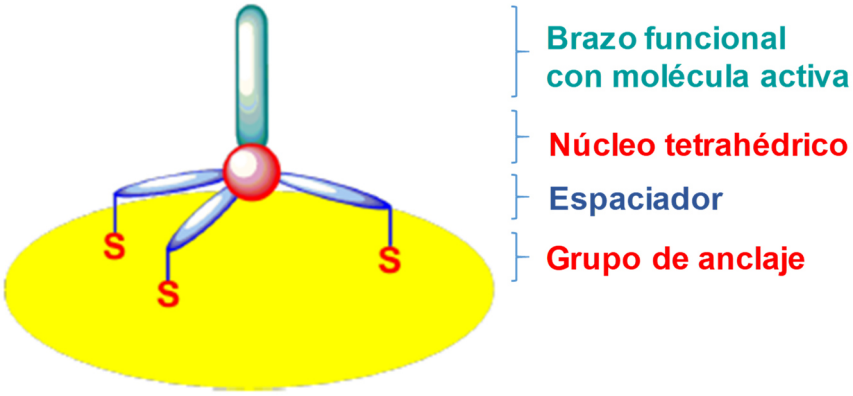

Figura 8. Dibujo esquemático de una molécula con estructura tripodal unida a una superficie metálica por los tres brazos de anclaje.

En nuestro Grupo de Investigación, se ha llevado a cabo la síntesis de algunas moléculas, derivadas de *p*-fenileno, que cumplen parcialmente estos objetivos mediante el acoplamiento de bifenilos con un vértice derivado de silicio (ver primer ejemplo en la figura 6). Aunque la molécula es suficientemente rígida para mantener la orientación del grupo funcional perpendicular a la superficie una vez depositada sobre la superficie, es pequeña (26 Å de distancia entre los grupos TMS, y 286 Å^2 de área) para establecer una distancia mínima entre los activos que posibilite una interacción efectiva proteína-activo en el brazo funcional, una vez adsorbido o unido covalentemente a superficie. Además, no presenta sustitución adecuada en el brazo de anclaje (presenta el grupo TMS) ni en el funcional (OEG), si bien estos grupos pueden ser intercambiados con relativa facilidad por otros. Tampoco la longitud del etilénglicol lateral (3 unidades de etilénglicol) es suficiente como para dar una resistencia efectiva a la adsorción de proteínas, la cual se obtiene con longitudes mayores. Sólo la molécula derivada de azobenceno (ver segundo ejemplo en figura 6) presenta un cromóforo en el brazo funcional y tioacetatos en los de anclaje. Sin embargo, la síntesis desarrollada es versátil

y permite abordar a lo largo esta tesis la preparación de adsorbatos mayores y con funcionalización adecuada para una aplicación práctica directa.

2. HIPÓTESIS Y OBJETIVOS

La principal hipótesis de este trabajo de Tesis consiste en que conceptos como biocompatibilidad, nanoestructuración, transporte de activos y, finalmente, monitorización adecuada, son fundamentales para conseguir la máxima efectividad en cualquier tipo de dispositivo de análisis. Por ello, se pretende conseguir el desarrollo de estructuras híbridas potenciando su biocompatibilidad, para posibilitar así el análisis y su uso en entornos biológicos, una elevada nanoestructuración para alcanzar la máxima efectividad) y una funcionalización adecuada para permitir el análisis de interaciones biológicas concretas. Todo ello sobre superficies metálicas, como modelos de base para el diseño de estos dispositivos de análisis.

La tesis se va a estructurar en dos objetivos fundamentales:

Objetivo 1. “SINTESIS DE ADSORBATOS Y ACTIVOS”.

Parte de la hipótesis de partida de esta tesis consiste en que la máxima efectividad de cualquier dispositivo se logrará con la estructuración a nivel molecular de las superficies. Por ello es necesario disponer de métodos para modificar químicamente estas superficies y dotarlas, de esta forma, de otras propiedades o aplicaciones. Así, el primer objetivo de esta tesis consiste en la preparación de moléculas que permitan alcanzar todas esas caracterísitcas al modificar la superficie. Proponemos derivados de oligo-*p*-fenilenos con forma de trípode y activos derivados de teofilina con potencial actividad biológica; líneas de trabajo en las que nuestro Grupo de Investigación trabaja desde hace años.

Objetivo 2. “MODIFICACIÓN DE SUPERFICIES METÁLICAS”.

En este objetivo proponemos varios tipos de modificación de superficies:

La modificación de superficies de silicio, y su nanoestructuración, por formación de enlace Si-C mediante reacción de hidrosililación sobre los adsorbatos sintetizados previaamente: oligo-*p*-fenilenos, activos de teofilina y sus combinaciones (brazo de anclaje: alqueno).

A su vez, y debido al creciente interés que ha generado en la última década el uso de la reacción tipo Click sobre superficies, se funcionalizarán las superficies de silicio con moléculas orgánicas derivadas de alquinos y se llevará a cabo el anclaje de los adsorbatos con forma tripodal terminados en grupos azida mediante reaccion tipo Click, ya que las condiciones de esta reacción son suaves, de gran eficacia y regioselectiva.

Del mismo modo, se estudiará la inmobilización de adsorbatos sobre superficies de oro (brazo anclaje: tiol o derivado) mediante el conocido proceso de autoensamblaje, en inglés Self-Assembled Monolayers (SAM´s) con grupol tioles (SH).

Además, se llevará a cabo el estudio de la funcionalidad de las superficies fabricadas con los trípodes, como una plataforma para reacciones químicas posteriores y la fabricación de biosensores. Con este propósito, se llevará a cabo la incorporación covalente de las moléculas activas de teofilina, también por reacción de Click, y la posterior prueba de comportamiento de estas superficies para la inmovilización de proteínas, tales como estreptavidina (SA, especifica de teofilina) y la albúmina de suero bovino (BSA, no específica).

Por último, se llevará a cabo la caracterización de las superficies mediante técnicas especializadas como la Espectroscopía de fotoelectrones de rayos X (por sus siglas en inglés, XPS), Microscopía de fuerza atómica (AFM), Espectroscopía de estructura fina cerca del borde de absorción de rayos X (NEXAFS), Microscopía de transmisión óptica de campo brillante y Teoría del funcional de la densidad (DFT).

3. PRINCIPALES RESULTADOS.

De acuerdo a los objetivos indicados en el apartado 2 del Resumen de esta Tesis se comentan los principales resultados:

Con respecto al **Objetivo 1**. “SINTESIS DE ADSORBATOS Y ACTIVOS”.

Esta tesis se centra en la síntesis de oligo-*p*-fenilenos con forma de trípode empleando como núcleo tetrahédrico un átomo de silicio.

En la última década, el éxito de las reacciones Click en solución ha impulsado la extensión de las mismas a ser aplicadas en la funcionalización de una amplia gama de superficies. Estas reacciones tipo Click, definidas primeramente por Sharpless en 2001, presentan una serie de requisitos como: *(i)* ser modulares y amplias en su alcance, *(ii)* requerir materiales de partida y reactivos fácilmente disponibles, *(iii)* utilizar disolventes benignos o ningún disolvente, *(iv)* proporcionar altos rendimientos sin generar subproductos, *(v)* estereoespecificidad, y *(vi)* requerir técnicas de purificación simples. Sin embargo, se han identificado varias reacciones que se ajustan a este concepto mejor que otras, dado que es poco probable que cualquier reacción sea perfecta para cada situación y aplicación. Entre ellas nos encontramos con la cicloadición de azidas y alquinos (1,3-dipolar) de Huisgen, catalizada por Cu(I), y que es a menudo conocida simplemente como "la reacción en un clic".

Por todo lo anteriormente comentado, nos propusimos realizar la síntesis de adsorbatos derivados de *p*-fenilenos con forma tripodal acabados en grupos azida como grupos de anclaje para su posterior inmobilización en superficies de silicio, que previamente habrán sido funcionalizadas con grupos alquino.

Se ha llevado a cabo la síntesis de cuatro trípodes con tres unidades de fenileno (**11**, **12**, **13** y **14**) y tres trípodes con cinco unidades de fenileno (**17**, **20** y **21**). Todos ellos quedan representados en la siguiente figura:

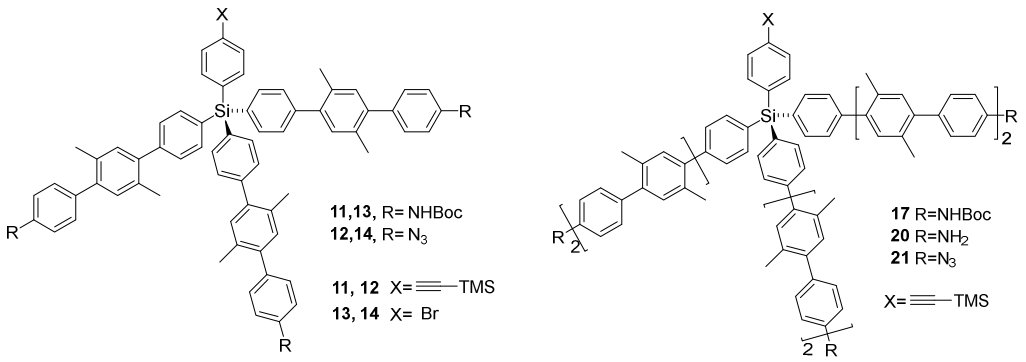

Figura 9. Trípodes precursores **11**,**13** y **17**,**20** y trípodes finales **12**,**14** y **21** con grupos azida terminales.

Como se observa en la figura 9, tres de estos trípodes tienen grupos terminales azida (N_3), diseñados específicamente para su posterior anclaje a las superficies de silicio debidamente funcionalizadas con grupos alquino mediante la reaccion de click catalizada con cobre.

Con respecto a la síntesis de adsorbatos derivados de oligo-*p*-fenilenos con grupos tioacetato para su posterior anclaje en superficies de oro, se han sintetizado diversos trípodes, los precursores **24**, **25**, **29** y **30** y los trípodes objetivo **7** y **8**, con grupos tioacetato (–SAc) en los extremos. Como puede observarse en la figura 10:

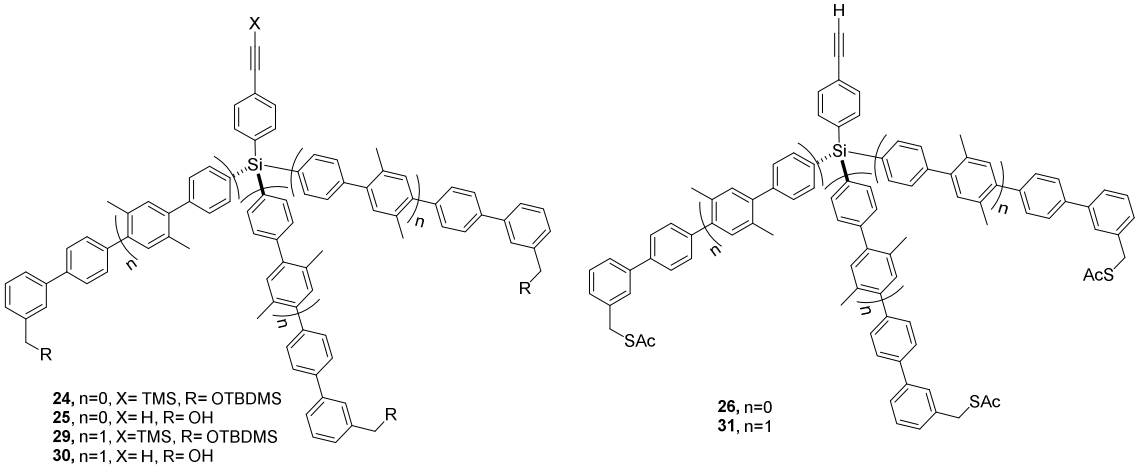

Figura 10. Trípodes precursores **24**, **25**, **29** y **30**, y trípodes objetivo **26** y **31**, con grupos tioacetato terminales.

La estrategia retrosintética llevada a cabo se muestra en la figura 11 y consistió en el ensamblaje de una estructura del tetrafenilsilano en dos pasos. Primero, las tres subunidades oligo-*p*-fenileno idénticas (de longitud adecuada), que portan un sustituyente que permite la introducción posterior del grupo de anclaje, se introdujeron mediante la reacción de acoplamiento cruzado de Suzuki. Para que el acoplamiento fuera efectivo, las moléculas encargadas de reaccionar entre ellas habían de contener un átomo de boro y un haluro, en presencia de un complejo de paladio como catalizador. El segundo paso fue la desprotección del grupo TBDMS mediante la acción de un buen nucleófilo como es el fluoruro de tetrabutil amonio (TBAF), dejando libre el grupo hidroxilo (-OH) en los extremos de los brazos de anclaje. Por último, y mediante la conocida reacción de Mitsunobu se dió paso a la conversión de los grupos –OH en grupos tioacetato (SAc).

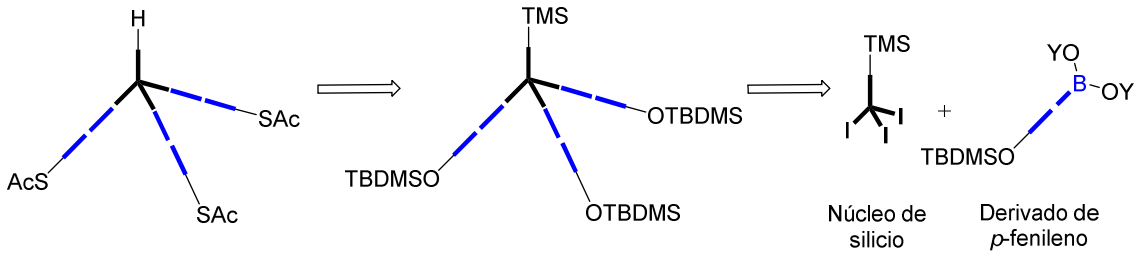

Figura 11. Análisis retrosintético para la obtención de trípodes con grupos tioacetato en las posiciones de anclaje.

Por otro lado, otros de los propósitos que tiene esta tesis es el de poder unir los tres brazos de anclaje de los trípodes con grupos etilenglicoles. Esto tiene principalmente dos objetivos fundamentales:

- El primero de ellos es el hecho de unir las patas, como se muestra en la figura 12, para dar una mayor estabilización a la estructura en el momento de la inmovilización sobre la superficie correspondiente. De esta manera, las patas tendrían menos libertad de movimiento y la efectividad de la fijación del trípode por los tres puntos de anclaje aumentaría.
- El segundo objetivo de llevar a cabo esta síntesis se basa en el empleo de etilenglicoles como moléculas de unión. Debemos desarrollar moléculas tripodales modificadas con cadenas laterales adecuadas para evitar la interacción no específica con moléculas de proteínas, y poder darles una aplicación biológica. Debido a la propia estructura del trípode, cuyas patas están formadas por cadenas de oligo-*p*-fenilenos, estas moléculas son bastante hidrofóbicas, y en consecuencia pueden interactuar de forma no específica con

moléculas proteicas. Para solucionar este problema, hemos diseñado una molécula con forma de trípode (figura 12) con tres unidades de fenileno en cada pata, grupos TMS (pueden ser fácilmente convertibles en iodo y posterior funcionalización) en los extremos y tetraetilenglicoles (OEG_4) como moléculas de unión. Del mismo modo, el radical X puede ser bromo o alquinil-TMS dependiendo de las condiciones de reacción utilizadas.

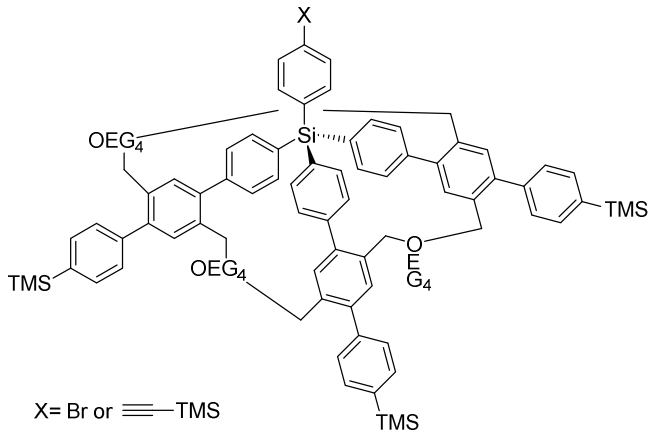

Figura 12. Moléculas tripodales objetivo, con las tres patas unidas con unidades de tetraetilenglicoles.

De las dos moléculas que se observan en la figura sólo pudimos sintetizar y aislar la que tiene en el extremo apical el grupo TMS, trípode **38** en la figura 13. La que contiene bromo en el vértice. no pudo aislarse como tal y su estructura (trípode **35**) puede observarse en la siguiente figura:

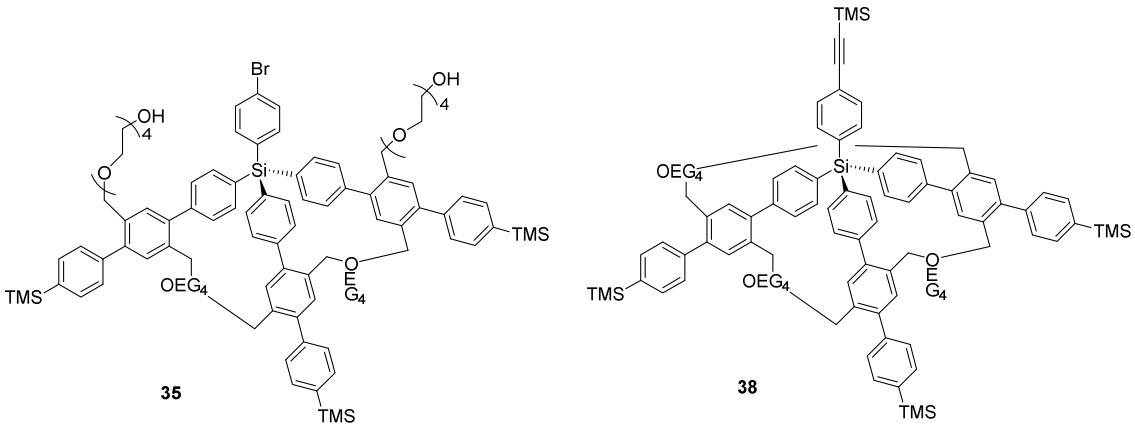

Figura 13. Moléculas sintetizadas con tetraetilenglicoles laterales, trípodes **35** y **38**.

Por último, dentro de los resultados que se incluyen en este primer objetivo se encuentra la síntesis de trípodes con grupos cromóforos, para su aplicación en el desarrollo de dispositivos optoelectrónicos. Un desafío importante a tener en cuenta en este tipo de dispositivos es la mejora de la estabilidad química y fotoquímica de los cromóforos, lo que constuye la principal motivación de los investigadores en la actualidad a la hora de diseñar estos cromóforos.

Como métodos para mejorar las capacidades ópticas de estos materiales se propone optimizar tanto la estructura química como las propiedades espectroscópicas de los cromóforos. En el caso particular de las 2-(*N*,*N*-dimetilamino) benciliden-1,3-indandionas (DMABI), las propiedades ópticas pueden optimizarse incluyendo diferentes sustituyentes en sus estructuras o mediante la modulación de sus estructuras 3D. También se ha encontrado que al aumentar el peso molecular y el número de grupos fenilo en una molécula se puede obtener una mejor sostenibilidad térmica.

Por todo ello, en esta tesis se han sintetizado los trípodes **46** y **47** (ver figura 14), siendo el primero precursor del segundo.

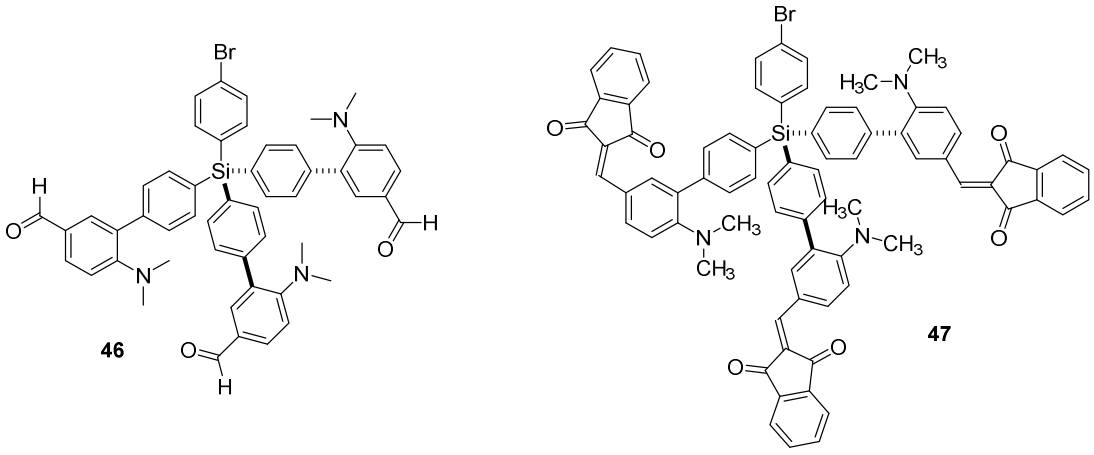

Figura 14. Trípodes con grupos cromóforos, **46** y **47**.

La síntesis de **46** se realizó por acoplamiento de Suzuki entre el ácido fenilborónico de un derivado de *p*-fenileno y el núcleo de silicio, en este caso tri(*p*-yodofenil)-*p*-bromofenilsilano. Tras ello, se llevó a cabo la reacción de **46** con 1,3-indandiona, en condiciones de reacción aldólica y en presencia de piperidina, para finalmente obtener el trípode **47**. Se llevó a cabo la caracterización estructural y espectroscópica de ambos trípodes. Tambíen se evaluó la posibilidad de usar el compuesto **47** como sensor fluorescente mediante el monitoreo del aumento de su fluorescencia, usando como sonda modelo 4-cloro-2,6 dinitroanilina (4CDNA), un conocido explosivo. Se obtuvo una

mejora en la fluorescencia del trípode **47** cuando se combinó con (4CDNA), demostrándose por tanto que este cromóforo en forma de trípode es un sensor óptico prometedor para detectar explosivos que contengan grupos nitro en su estructura.

Con respecto al **Objetivo 2.** MODIFICACIÓN DE SUPERFICIES METÁLICAS.

Distinguimos:

1) Modificación de superficies de silicio.

Se incluye aquí tanto la nanoestructuración de superficies de Si(111) por formación de enlace Si-C mediante hidrosililación, con moléculas funcionalizadas con doble enlace, como la nanoestructuración mediante la reacción tipo Click formando un anillo de triazo con oligo-*p*-fenilenos y activos de teofilina.

Con objeto de estudiar las interacciones con los receptores de adenosina se ha llevado a cabo la funcionalización de superficies de Si con alquenos mediante hidrosililación dejando libres grupos alquino (ver esquema 1). Posteriormente se ha nanoestructurado dicha superficie con los trípodes de la figura 6 (**12** y **21**, R=N_3), mediante reacción tipo Click catalizada por cobre, entre un grupo alquino (presente ya en la superficie de silicio) y los grupos azida de dichos trípodes.

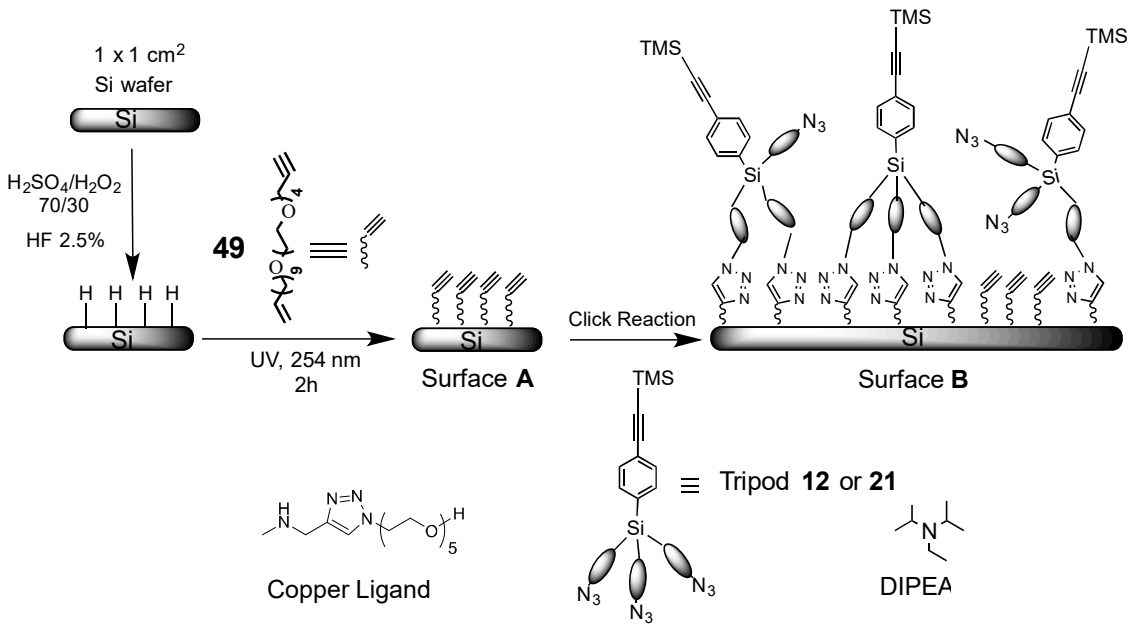

Esquema 1. Anclaje covalente de los trípodes **12** y **21** sobre la superficie de silicio funcionalizadas previamente con triple enlace.

Las condiciones de reacción de Click empleadas para el trípode **12** conllevaron el uso de $Cu(MeCN)_4PF_6$ en MeOH (3.75 mM) como sal de cobre (I), una disolución del ligando (ver esquema 1) en MeOH (37.5 mM) y el trípode correspondiente en THF (5 mM).

Estas condiciones no fueron factibles para el trípode **21**, más voluminoso y por ello más insoluble en MeOH por lo que las condiciones que usamos para llevar a cabo la reacción de Click fueron distintas. Dichas condiciones conllevaron el empleo de CuI como sal de cobre (I) en cantidades catalíticas, diisopropiletilamina (DIPEA) como base y con respecto a las cantidades del trípode **21** éstas fueron modificadas desde 5mM hasta 0.05 mM en THF para optimizar el porcentaje de recubrimiento en la superficie.

El siguiente paso que se llevó a cabo ha sido el anclaje del derivado de teofilina **52** (figura 15), de nuevo por medio de la reacción Click, sobre la superficie ya estructurada. La esctructura de la teofilina sintetizada es la siguiente:

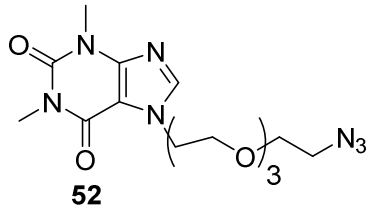

52

Figura 15. Estructura de la teofilina activa, con un grupo azido para su anclaje en las superficies de silicio funcionalizadas con el trípode **21**.

Las condiciones de reacción Click llevadas a cabo para la unión covalente de la teofilina fueron las mismas que se emplearon para el trípode **21**, pero usando como disolvente metanol, ya que la teofilina es más soluble en este medio.

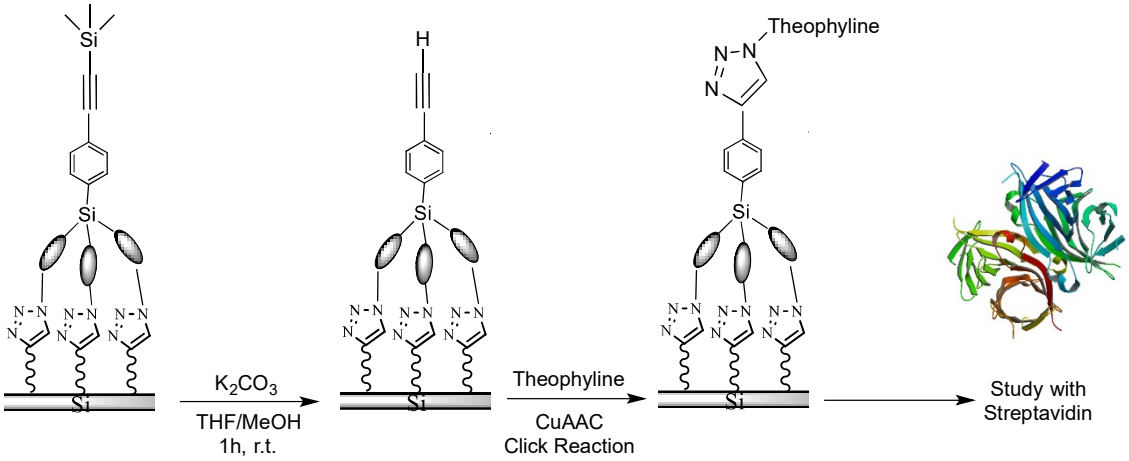

Esquema 2. Anclaje mediante reacción tipo Click catalizada por cobre de la teofilina **52** sobre las superficies funcionalizadas con el trípode **21**.

2) Modificación de superficies de oro.

Una vez fueron sintetizados los trípodes **26** y **31**, se llevó a cabo la nanoestructuración de superficies de oro empleando dichos trípodes cuyos brazos de anclaje están funcionalizados con grupos tioacetato (-SAc). Para ello se empleó el método de inmersión y liberación del grupo tiol simultáneamente por la acción de una base. Esta parte de la tesis se realizó en los laboratorios del Profesor Zharnikov de la Univeridad de Heidelberg, durante mi estancia.

Los trípodes **26** y **31** (figura 10) se diferencian entre ellos por el tamaño y longitud de las patas, el trípode **26** tiene dos unidades de fenileno mientras que el trípode **31** tiene cuatro. Se diseñaron así para comprobar si la diferencia de tamaño entre ellos se traducía en una mayor o menor efectividad en el autoensamblaje y ordenamiento de los trípodes sobre la superficie de oro.

El procedimiento general de autoensamblaje queda reflejado en el siguiente esquema:

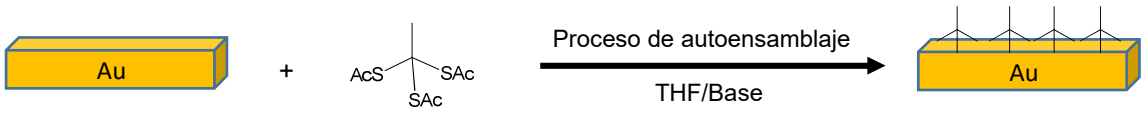

Trípode **26** o **31**

Esquema 3. Procedimiento general por el cual el trípode **26** y **31** se unen covalentemente al oro por la liberación del grupo tiol (SH) in situ mediante la acción de una base.

La optimización de las condiciones de anclaje en las superficies de oro se realizó con ambos trípodes. Lo primero que hicimos fue buscar la base adecuada para la desprotección in situ el grupo SAc y transformarlo en SH (de esta forma puede unirse a los átomos de oro de la superficie de una forma más efectiva). Para ello, se probaron tres bases diferentes; trietilamina (TEA), amoníaco y N, N, N ', N' ', N' '-pentametildietilentriamina (PMDTA). El análisis de las superficies mediante XPS reveló como mejores condiciones para la formación de enlaces S-Au el empleo como base de TEA (trietilamina), en THF (tetrahidrofurano) como disolvente y 48 horas de duración. La comparación de la eficacia en la formación de SAMs entre ambos trípodes, también mediante el análisis por XPS, dio como resultado una mejor homogeneidad y formación de SAM´s con el trípode de mayor tamaño, el **31**.

Una vez optimizadas las condiciones, se procedió a anclar una biomolécula (teofilina **52**) mediante la reacción de Click, en superficies de oro funcionalizadas con el trípode **31**.

Las condiciones de la reacción de Click empleadas fueron soluciones de teofilina a diferentes concentraciones, denominamos Click 1 para una concentración de 0.05 mM y Click 2 para una concentración de 0.5 mM. Los mejores resultados se obtuvieron a la concentración de 0.5 mM de teofilina en etanol, como sal de cobre (I) se usó CuI y como base diisopropiletilamina (DIPEA).

En el análisis por XPS de alta resolución (figura 16) se muestran los espectros correspondientes del oro, carbono, y nitrógeno para el trípode **31**, Click 1 y Click 2. En el espectro normalizado de oro se puede observar claramente cómo la intensidad del pico correspondiente a 84 eV (Au $4f_{7/2}$) va decreciendo conforme nuevas especies (en este caso la teofilina) se incorporan a la monocapa. Con respecto al espectro de carbono, se observan nuevas especies alrededor de 286 y 288 eV, correspondientes a los nuevos carbonos incorporados a la monocapa, pertenecientes a la teofilina. Y lo más importante aquí es el espectro de nitrógeno. Mientras en la monocapa de trípode **31** no encontramos señal alguna de nitrógeno, debido a que no existen átomos del mismo en la molécula, en Click 1 aparece débilmente un pico a 400 eV. Es en Click 2, donde se ha aumentado considerablemente la concentración de teofilina en el medio de reacción, por lo tanto aparece un pico muy intenso a 400 eV, correspondiente a los nitrógenos orgánicos de la molécula de teofilina y al anillo de triazol que se ha formado durante la reacción de Click.

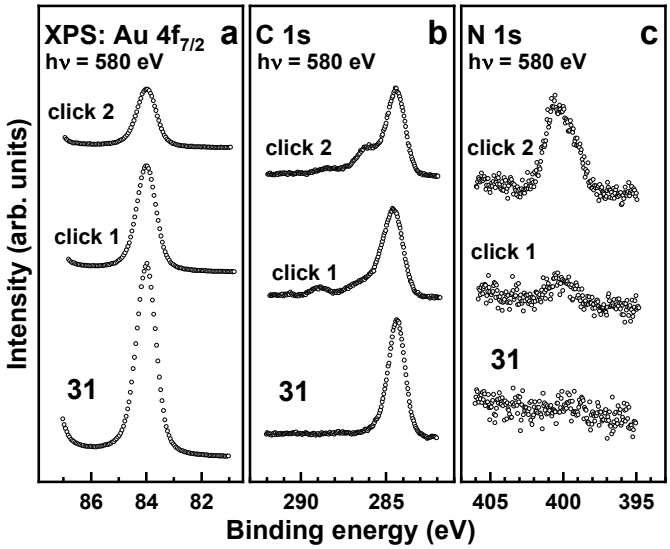

Figura 16. Espectro de XPS de Au $4f_{7/2}$ (a), C 1s (b), y N 1s (c) de las SAMs formadas por el compuesto **31** antes y después de la reacción de Click (Click 1 y Click 2).

Por último, y con la teofilina ya incorporada, estudiamos la adhesión de proteínas; especifica (Estreptavidina, SA) e inespecífica (Albúmina de suero bovino, BSA). Los resultados obtenidos mediante XPS revelan una mayor cantidad de proteína específica adherida en la superficie debido a las interacciones con la teofilina, previamente acoplada a los trípodes. En cuanto a la BSA, podemos concluir que, aunque en una menor proporción, ésta se pega por la propia tendencia de las proteinas a adherirse inespecificamente a las superficies metálicas (biofouling). Además, al tener la teofilina anclada un espaciador de etilenglicol, se impide aún mas el efecto de biofouling.

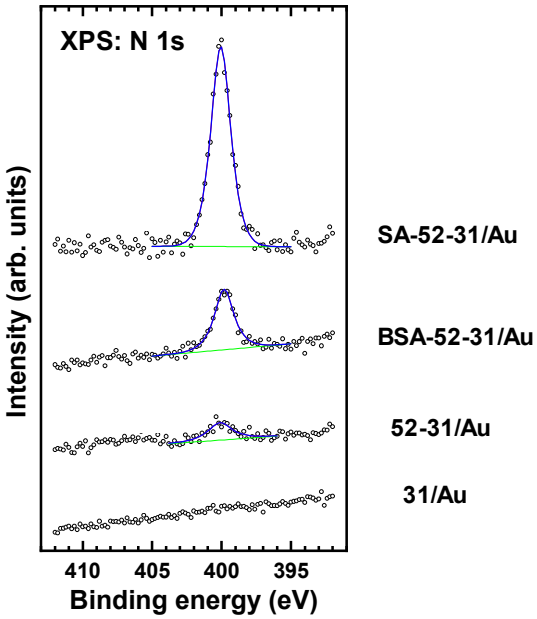

Figura 17. Espectro N1s de: Trípode **31** formando SAM´s en oro (no hay señal de nitrógeno), **52-31**/Au (vemos un pico poco intenso correspondiente al N que proviene de la teofilina), con BSA-**52-31**/Au y con SA-**52-31**/Au. En ambos casos aumenta considerablemente la intensidad de señal de nitrógeno por el tamaño tan grande de las proteínas. En el caso de la Estreptavidina, su adhesión es notablemente superior por la especificidad con la teofilina incorporada.

4. CONCLUSIONES

Derivadas de la síntesis:

1. Se han diseñado y sintetizado nuevos trípodes con tres (**12** y **14**) y cinco (**21**) unidades de *p*-fenileno como patas, portando grupos azida para su posterior anclaje en superficies de silicio previamente funcionalizadas con grupos alquinos, mediante reacción de Click. Al contrario que los anteriores procedimientos publicados, la construcción de las patas de los trípodes antes de llevar a cabo el acoplamiento de Suzuki con el vértice correspondiente proporcionó mejores resultados en todos los casos que si se fueran acoplando poco a poco subunidades de fenileno una vez construido el esqueleto tetrahédrico.
2. Se han diseñado y sintetizado con buenos rendimientos trípodes con dos (**26**) y cuatro (**31**) unidades de *p*-fenileno como patas. Las patas de estas moléculas están funcionalizadas con grupos tioacetato, para su posterior anclaje en superficies de oro por el método de autoensamblaje una vez que se desprotege el grupo tioacetato *in situ* por acción de una base. El brazo funcional de estos trípodes porta un grupo alquino protegido con TMS para poder funcionalizarlo posteriormente y ser susceptible de reaccionar con una azida mediante reacción de Click.
3. Se han diseñado y sintetizado trípodes sustituidos lateralmente con grupos etilenglicoles (**35** y **38**), donde en ambos casos sus patas terminan en grupos TMS, fácilmente intercambiables por átomos de iodo para su anclaje en superficies.
4. Se ha llevado a cabo la síntesis de trípodes que portan grupos cromóforos (**46** y **47**), mostrando este último una alta estabilidad térmica y una fuerte fluorescencia.

Derivadas de la modificación de superficies:

1. Se ha llevado a cabo el anclaje covalente de los trípodes **12** y **21** en superficies de silicio (111) funcionalizadas con alquino mediante la reacción de Click con buenos rendimientos y grado de nanoestructuración. Se han optimizado las condiciones de anclaje en términos de densidad de recubrimiento, agregación y configuración del trípode (esto es, si se ha unido por una pata, dos o por las tres), analizándose todo ello mediante técnicas como XPS y AFM.
2. Se ha realizado la inmovilización de la teofilina **52** (funcionalizada con un grupo azida) en superficies de silicio nanoestructuradas con el trípode **21** también mediante reacción tipo Click. La incorporación covalente de esta molécula fue confirmada por microscopía confocal y XPS, después de probar la unión con una proteína específica como la estreptavidina.
3. Se ha llevado a cabo la construcción de SAMs en superficies de oro con los trípodes **26** y **31**. Mediante análisis de XPS, se comprobó que la fabricación de monocapas con aproximadamente el 85% de los grupos de anclaje unidos al sustrato, formando enlaces tiolatos (Au-S), se consiguió con el trípode de mayor tamaño, trípode **31**. Los parámetros del procedimiento de preparación, como el disolvente y el agente de desprotección del tioacetato, fueron variados, determinando como condiciones óptimas el empleo de trietilamina (TEA) como base y THF como disolvente.
4. Se ha realizado la inmovilización de la teofilina sustituida con azida (**52**) sobre estas superficies funcionalizadas con el trípode **31**, por medio de la reacción de Click. Las superficies resultantes se probaron con éxito como plantillas para la adsorción tanto de proteínas específicas como inespecíficas, tomando estreptavidina (SA) y la albúmina de suero bovino (BSA) como proteínas de prueba. Mediante el análisis por XPS, se encontró una mayor eficacia en la absorción de la proteína específica SA en comparación con la no especifica, BSA.

APPENDIX B: SELECTED NMR SPECTRA

^{1}H NMR spectrum ($CDCl_3$) of compound **7**

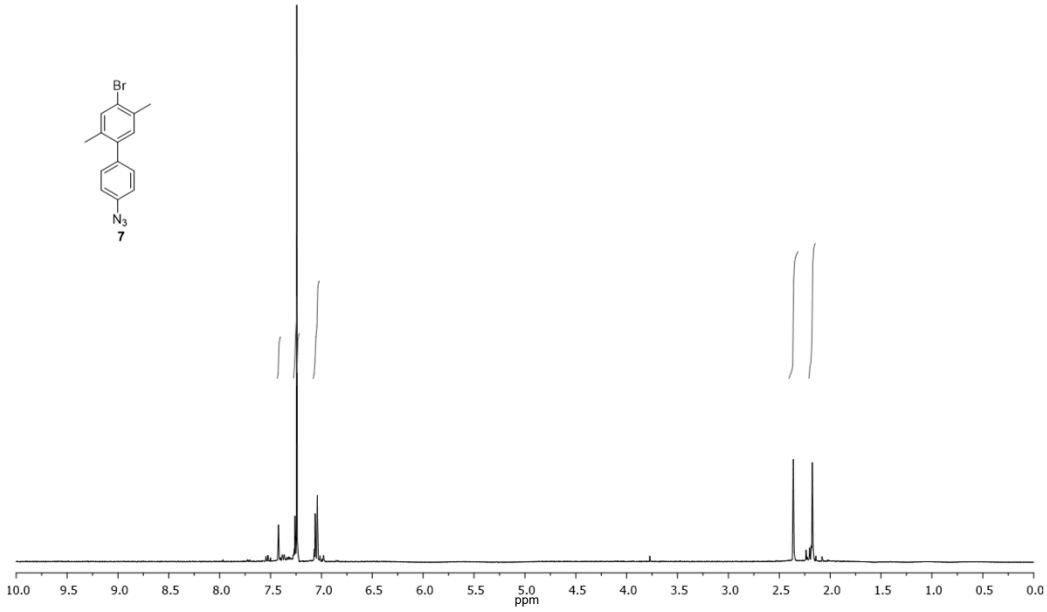

^{13}C NMR spectrum ($CDCl_3$) of compound **7**

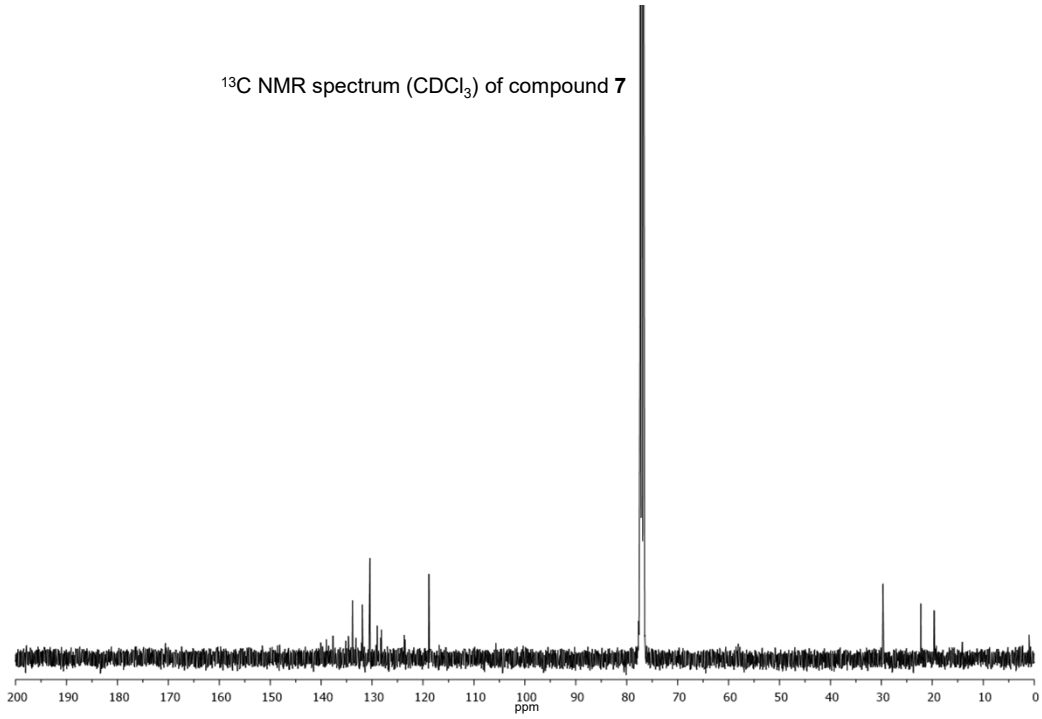

^{1}H NMR spectrum ($CDCl_3$) of compound **9**

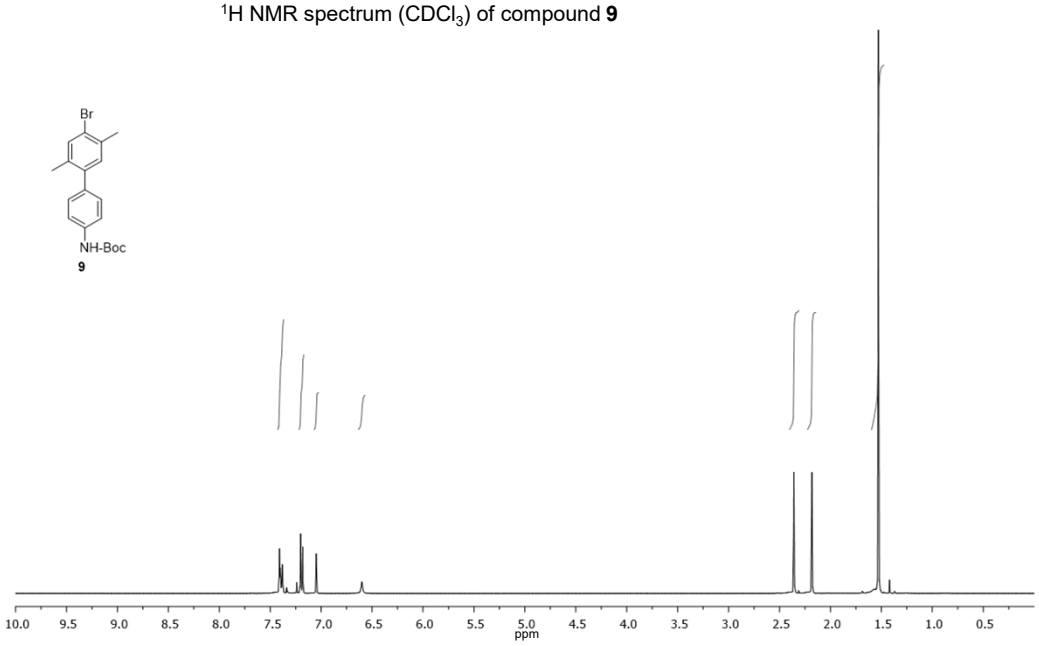

^{13}C NMR spectrum ($CDCl_3$) of compound **9**

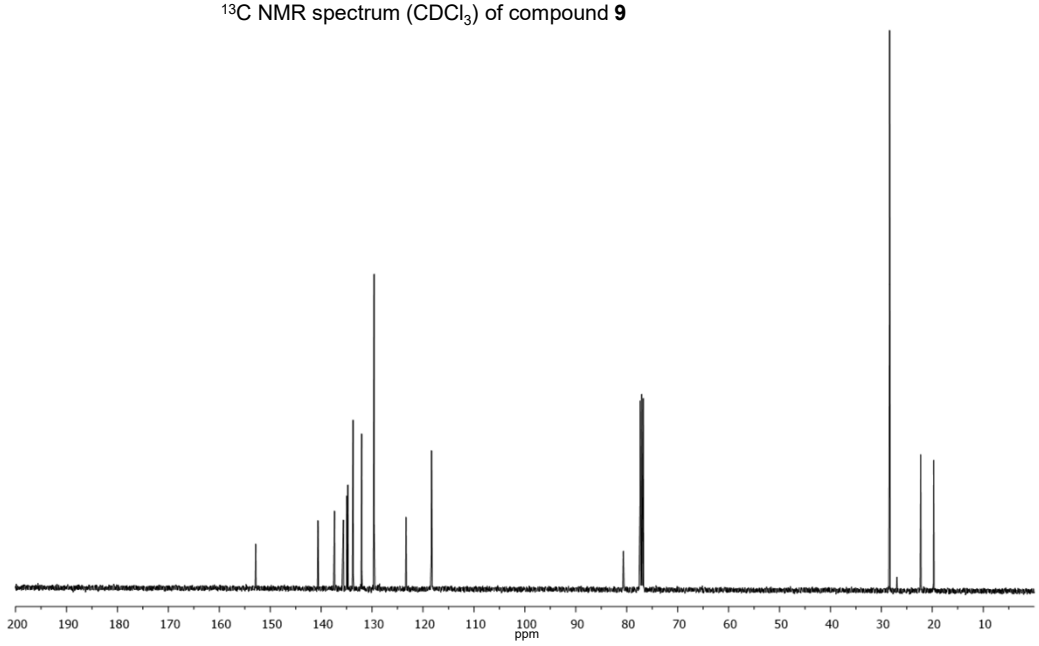

^{1}H NMR spectrum ($CDCl_3$) of compound **10**

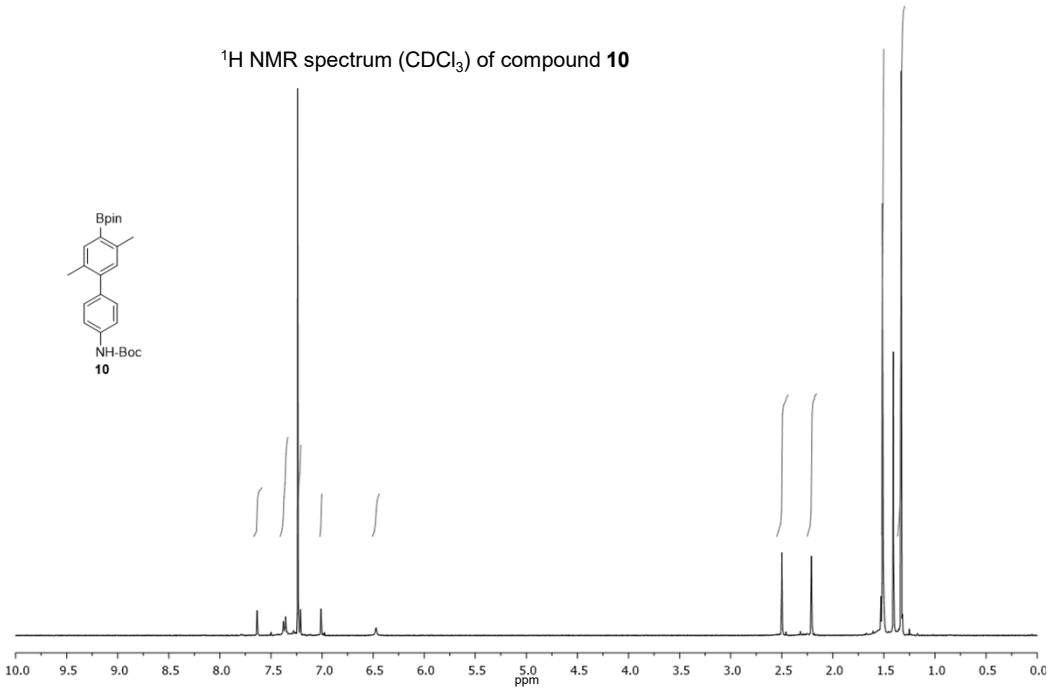

^{13}C NMR spectrum ($CDCl_3$) of compound **10**

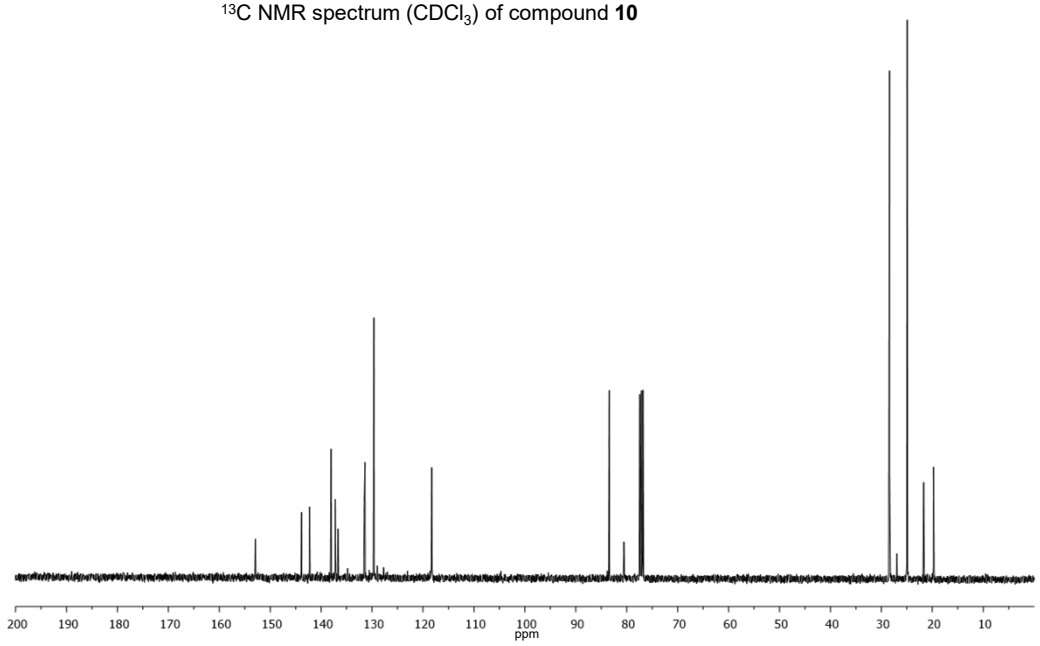

^{1}H NMR spectrum ($CDCl_3$) of compound **11**

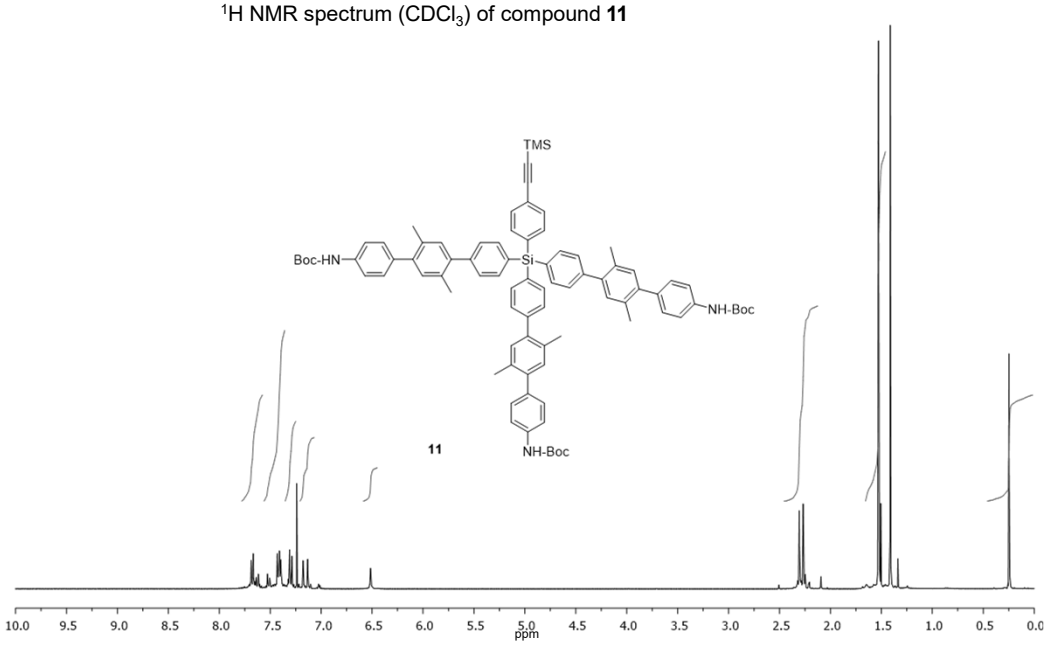

^{13}C NMR spectrum ($CDCl_3$) of compound **11**

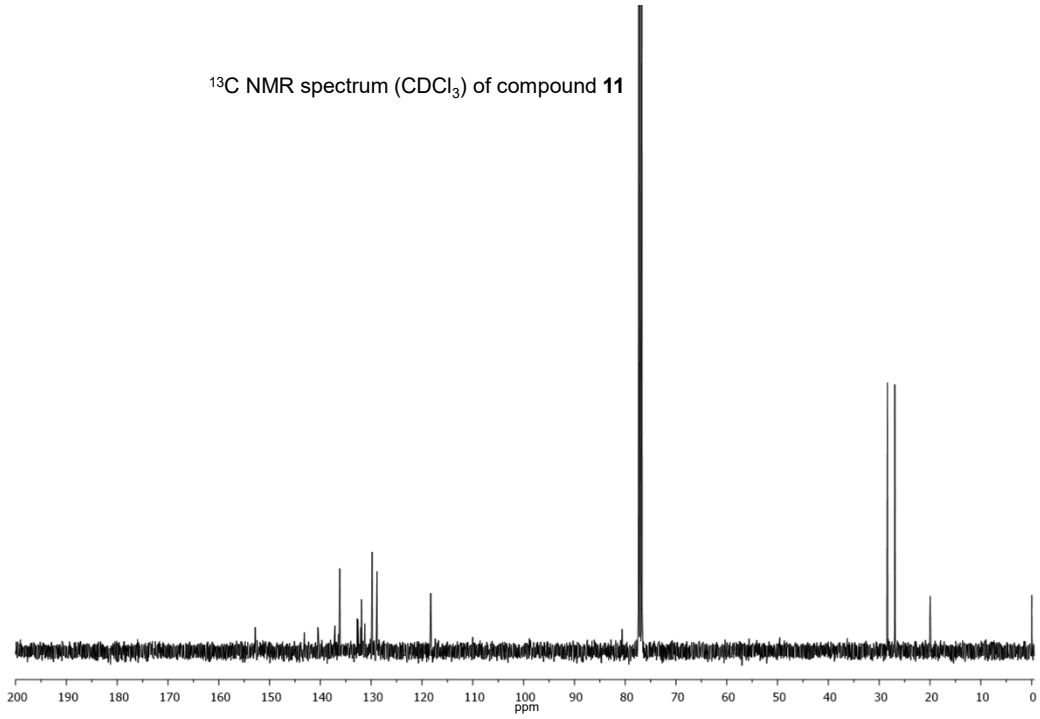

^{1}H NMR spectrum ($CDCl_3$) of compound **12**

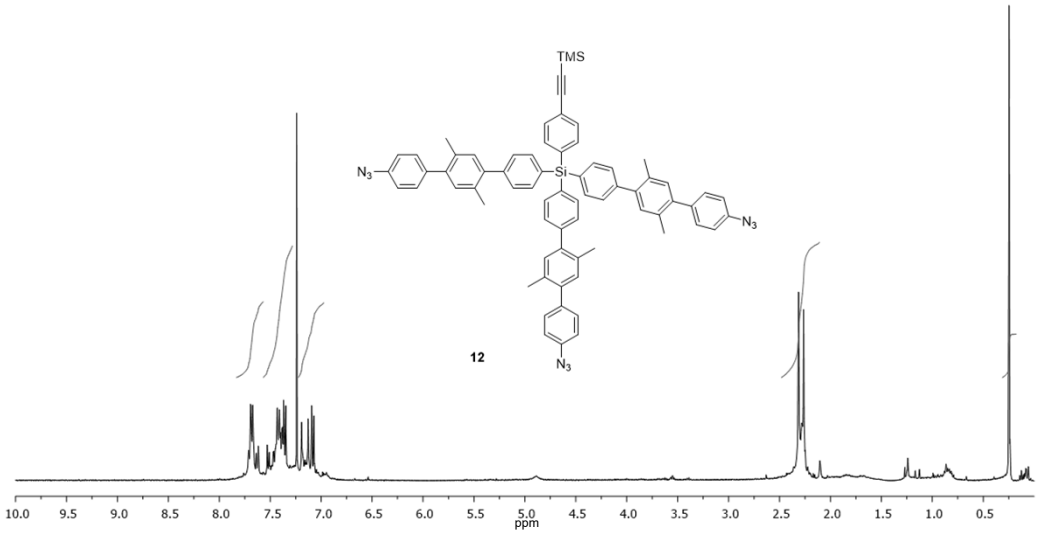

^{13}C NMR spectrum ($CDCl_3$) of compound **12**

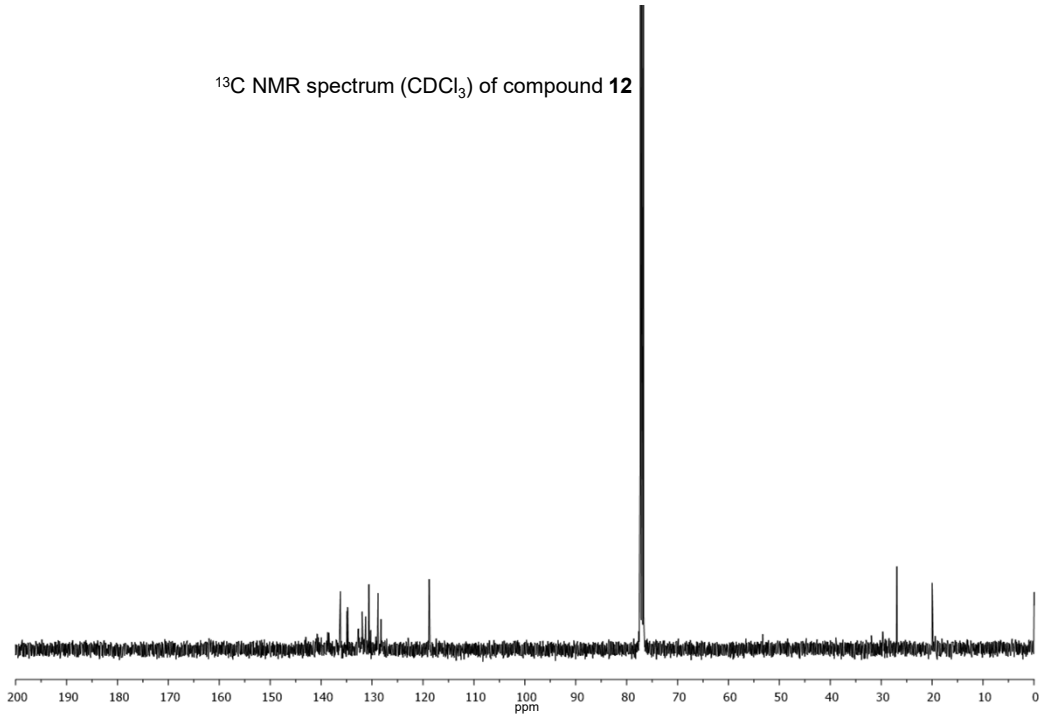

^{1}H NMR spectrum ($CDCl_3$) of compound **13**

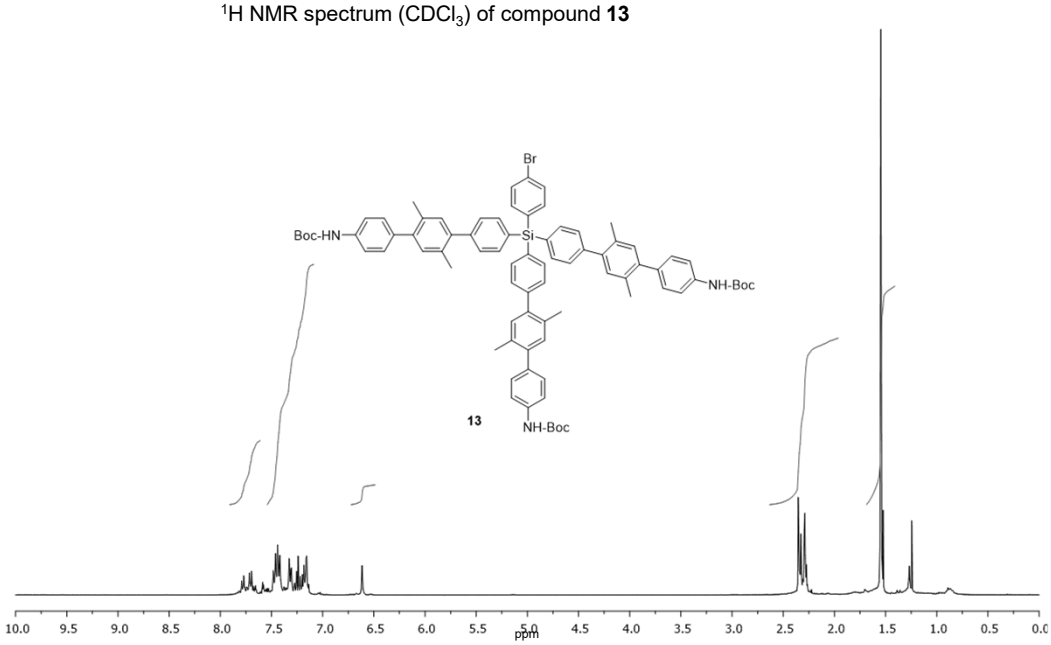

^{13}C NMR spectrum ($CDCl_3$) of compound **13**

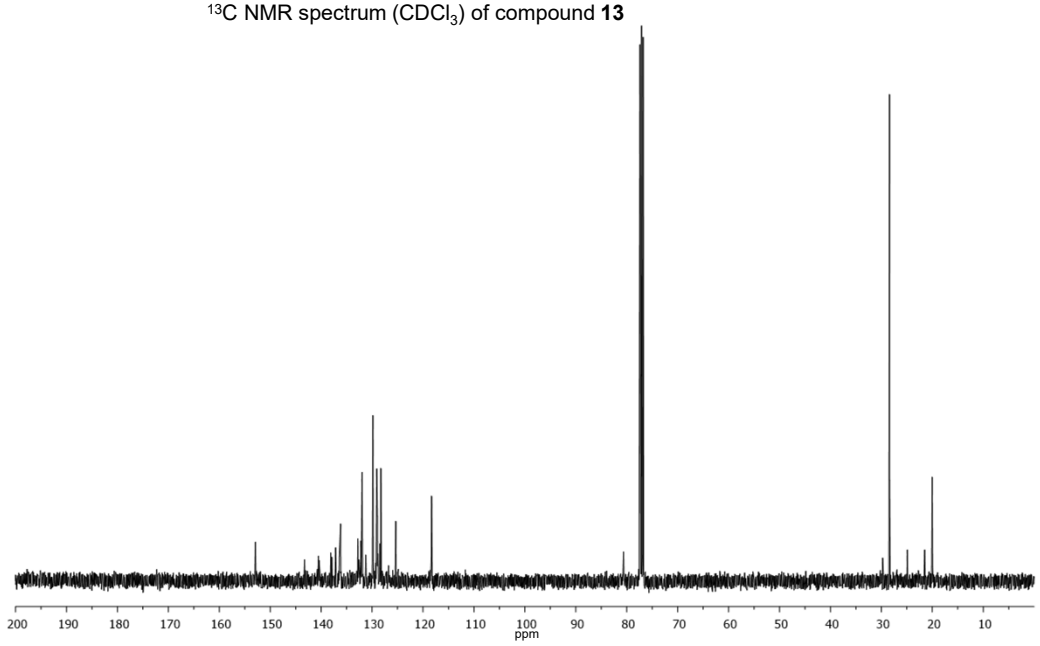

^{1}H NMR spectrum ($CDCl_3$) of compound **14**

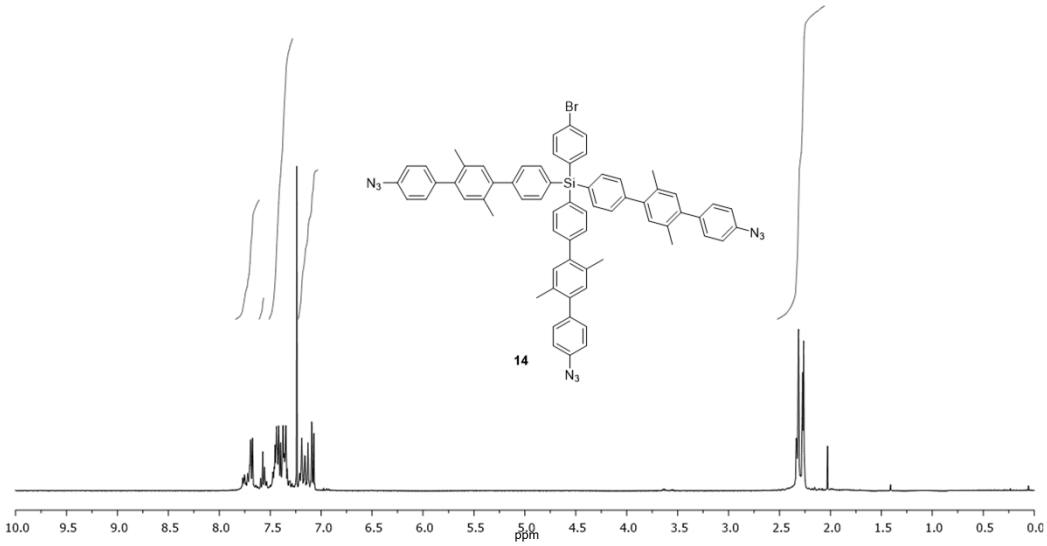

^{13}C NMR spectrum ($CDCl_3$) of compound **14**

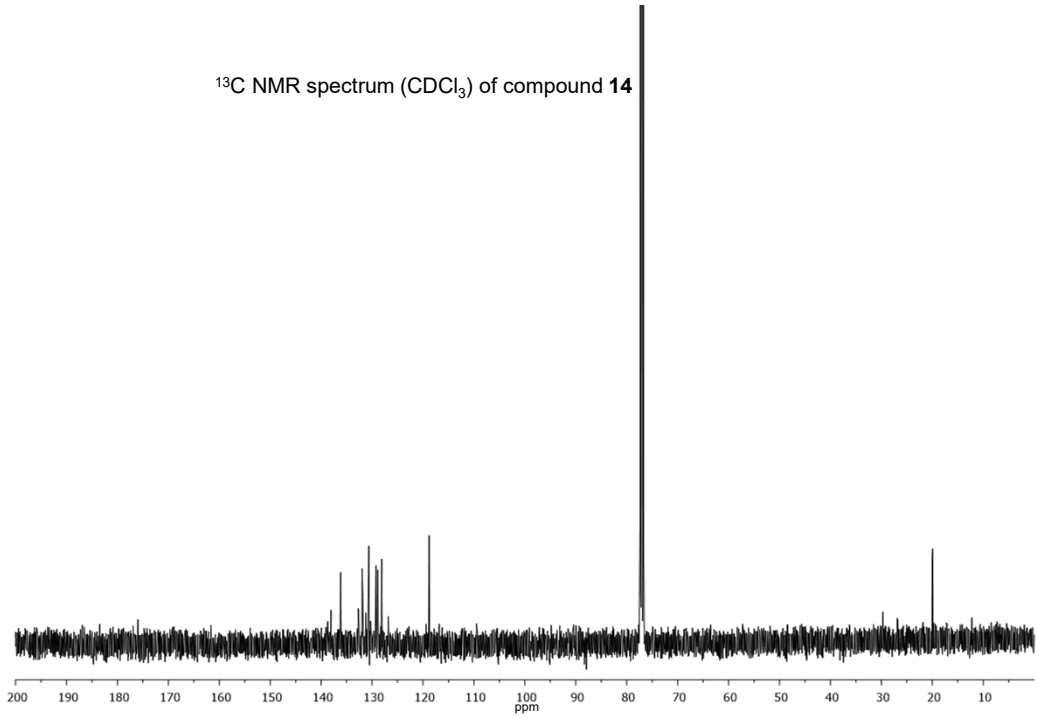

^{1}H NMR spectrum ($CDCl_3$) of compound **15**

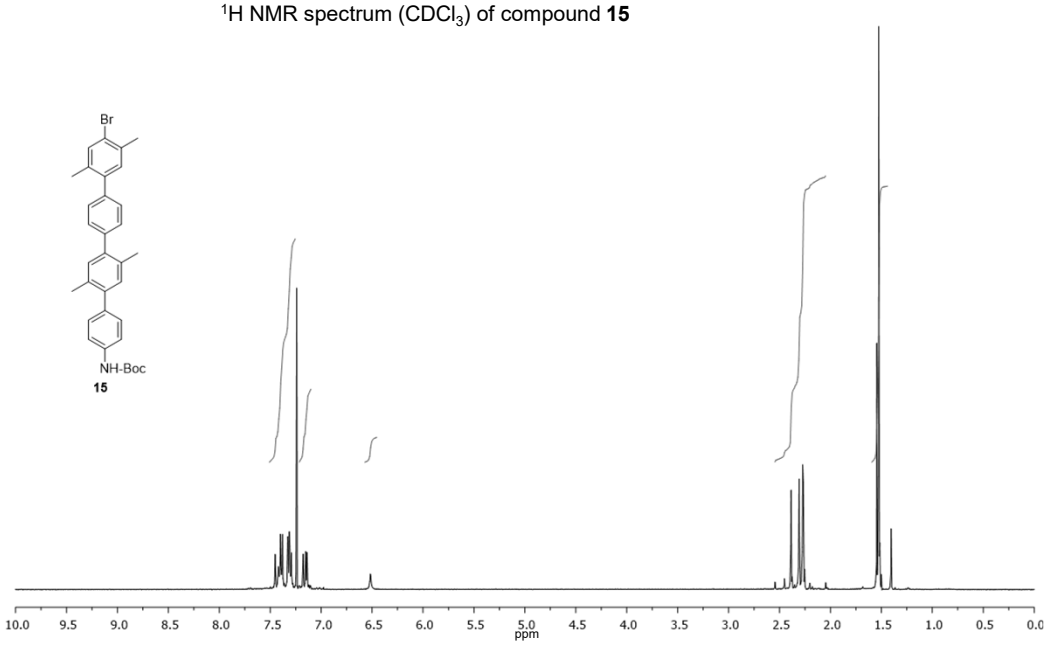

^{13}C NMR spectrum ($CDCl_3$) of compound **15**

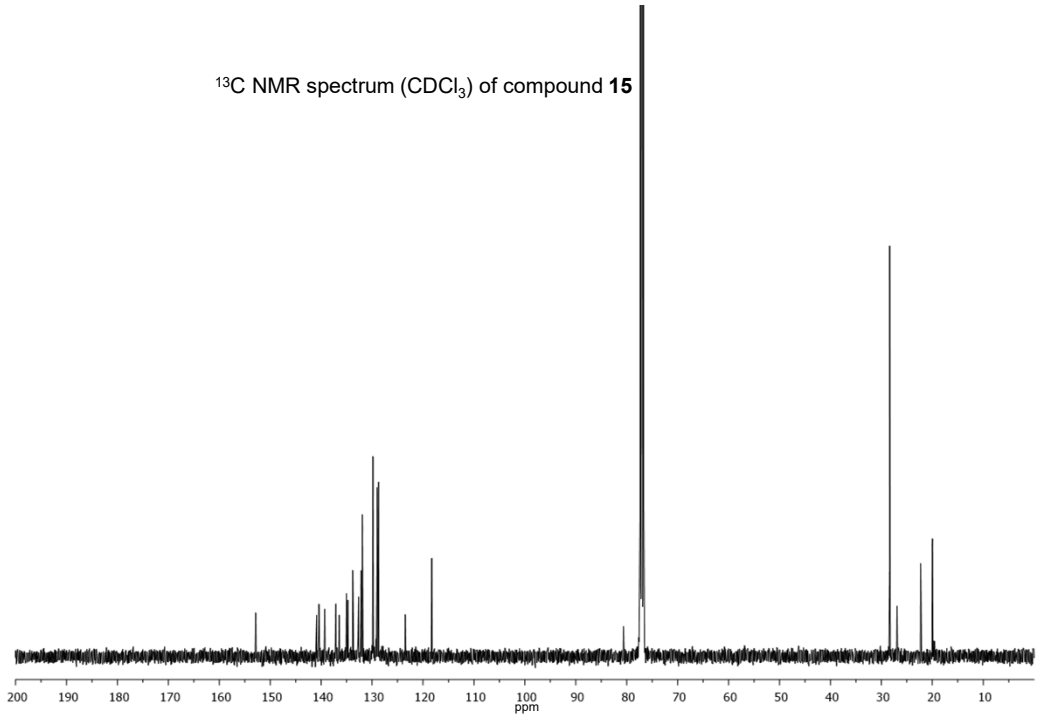

^{1}H NMR spectrum ($CDCl_3$) of compound **16**

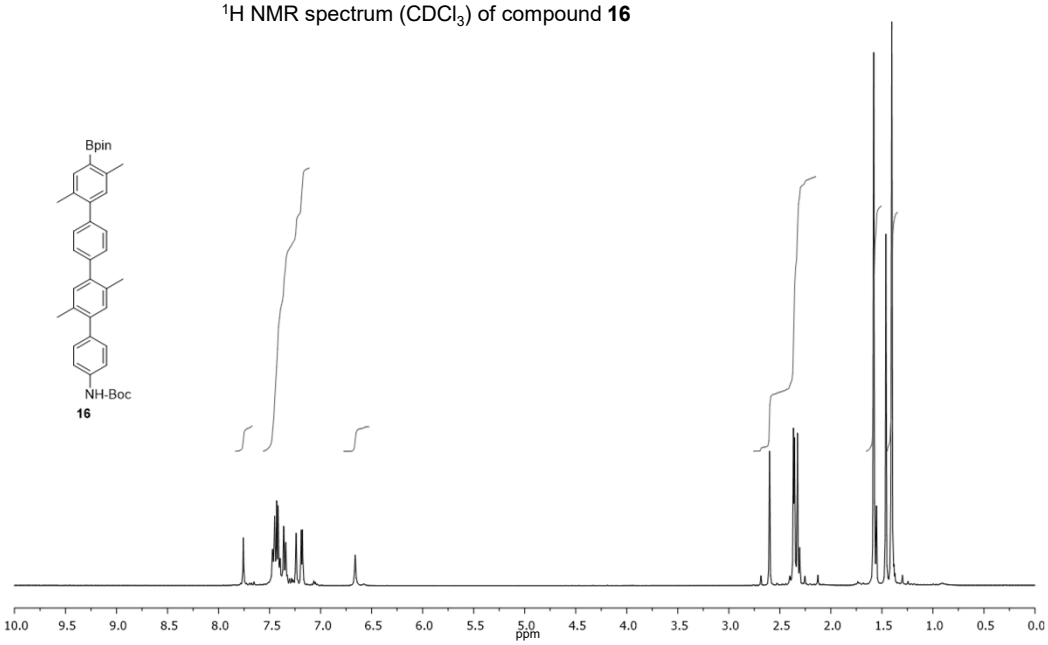

^{13}C NMR spectrum ($CDCl_3$) of compound **16**

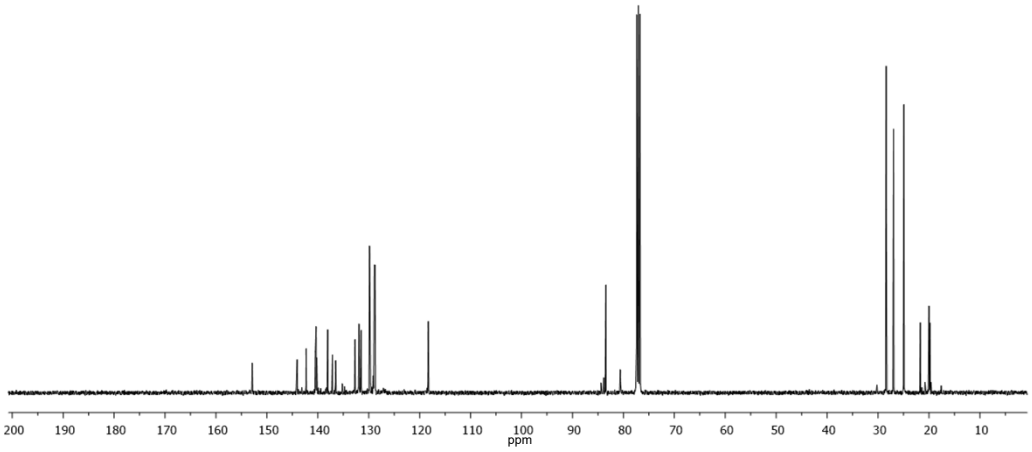

^{1}H NMR spectrum ($CDCl_3$) of compound **17**

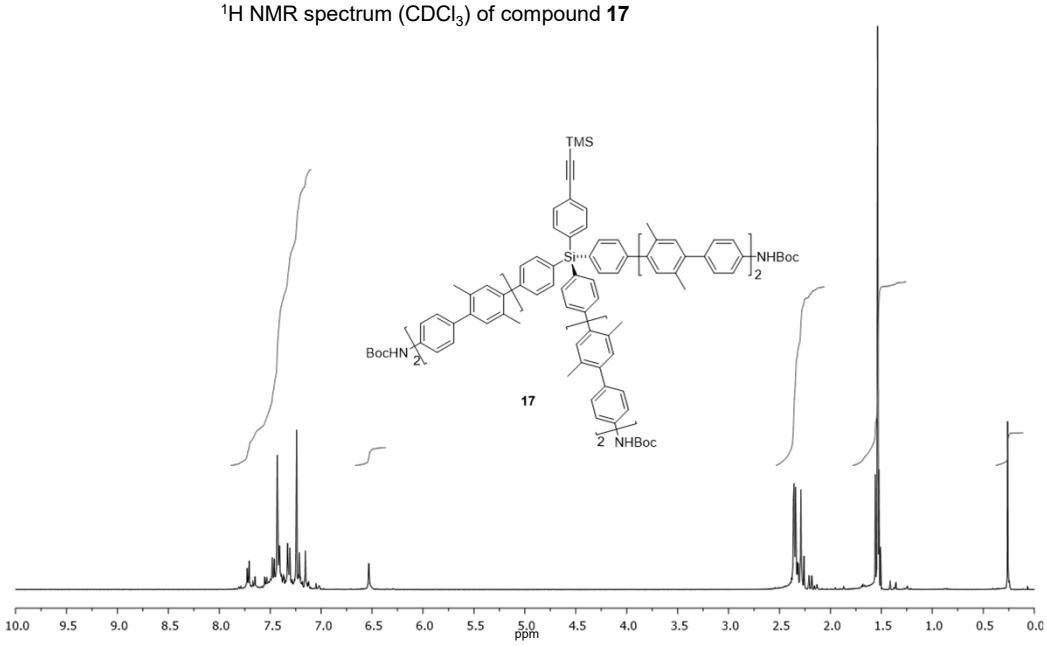

^{13}C NMR spectrum ($CDCl_3$) of compound **17**

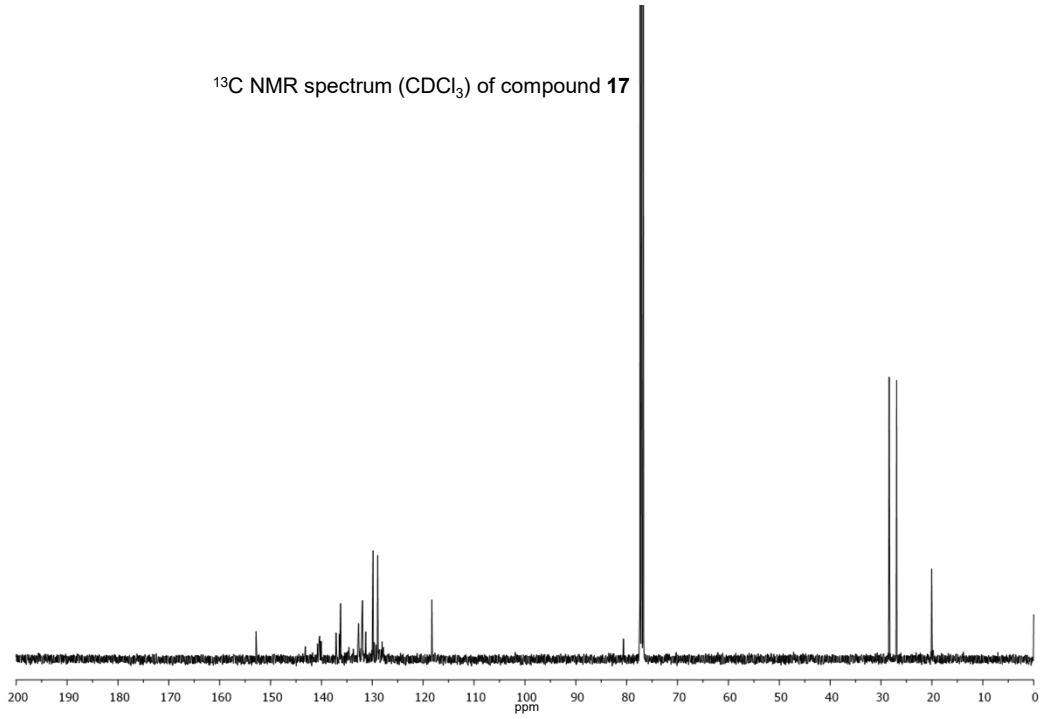

^{1}H NMR spectrum ($CDCl_3$) of compound **18**

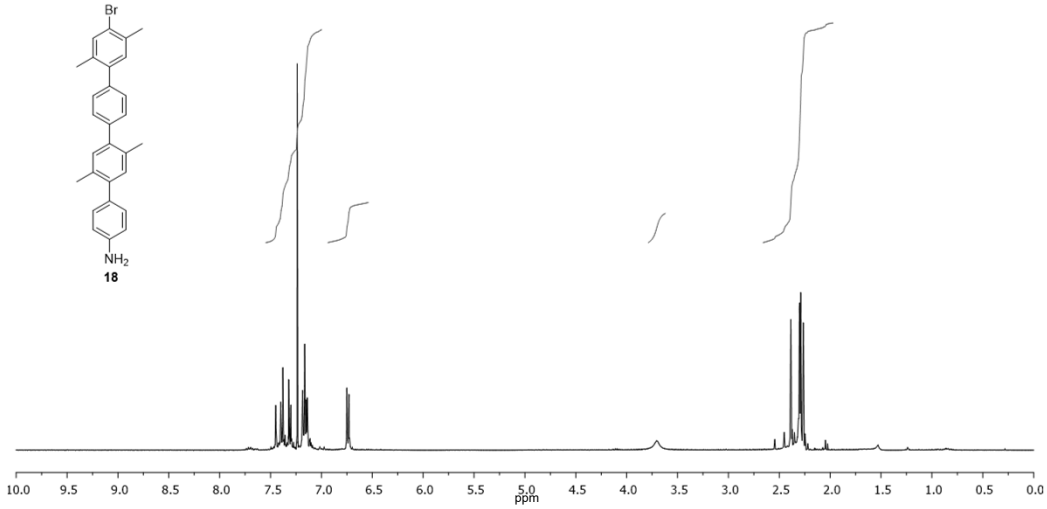

^{13}C NMR spectrum ($CDCl_3$) of compound **18**

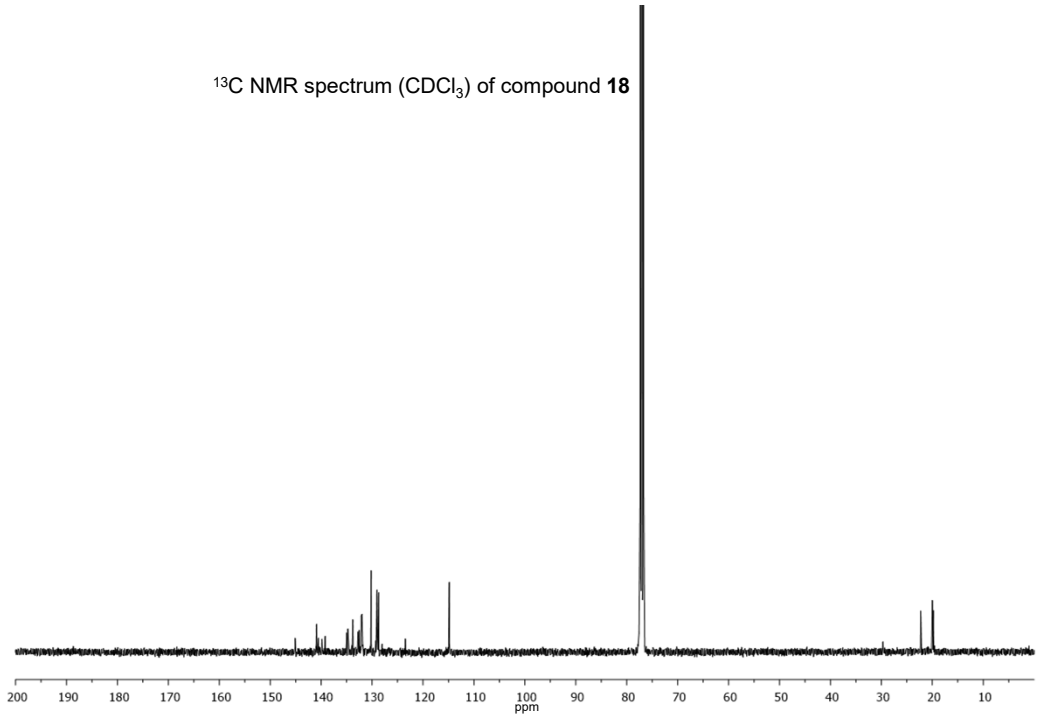

^{1}H NMR spectrum ($CDCl_3$) of compound **19**

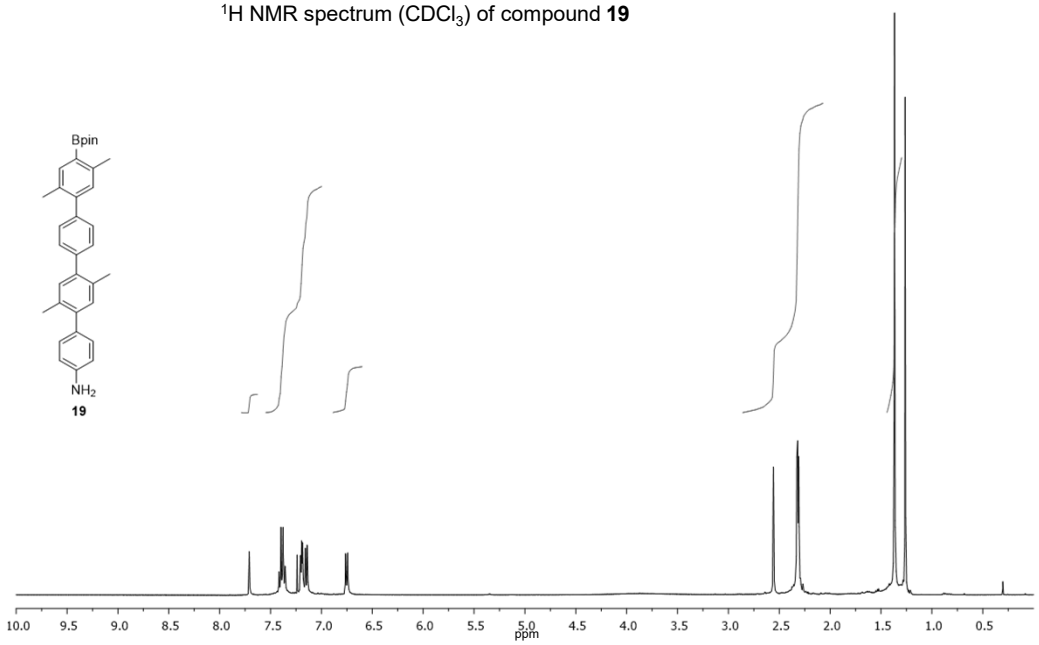

^{13}C NMR spectrum ($CDCl_3$) of compound **19**

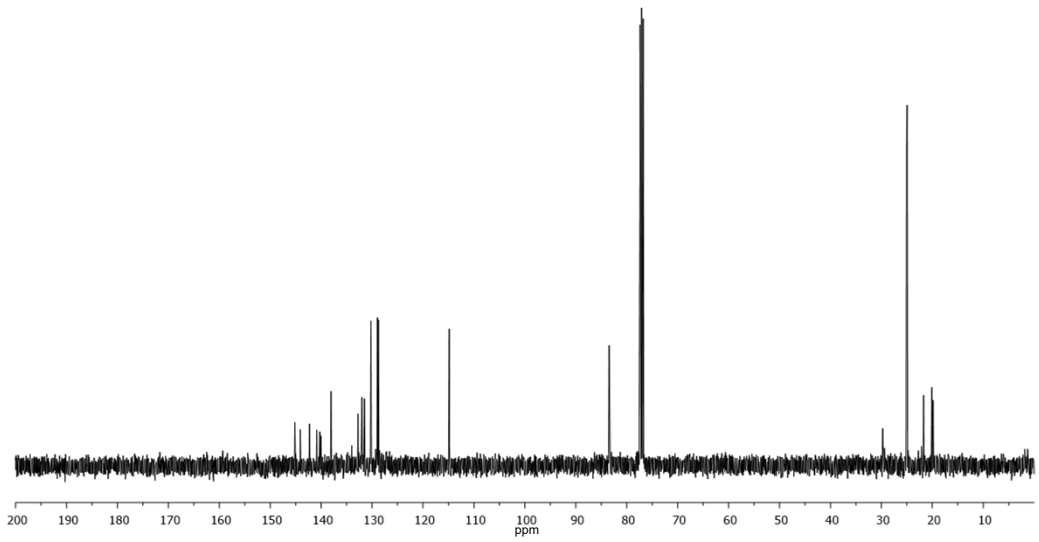

^{1}H NMR spectrum ($CDCl_3$) of compound **20**

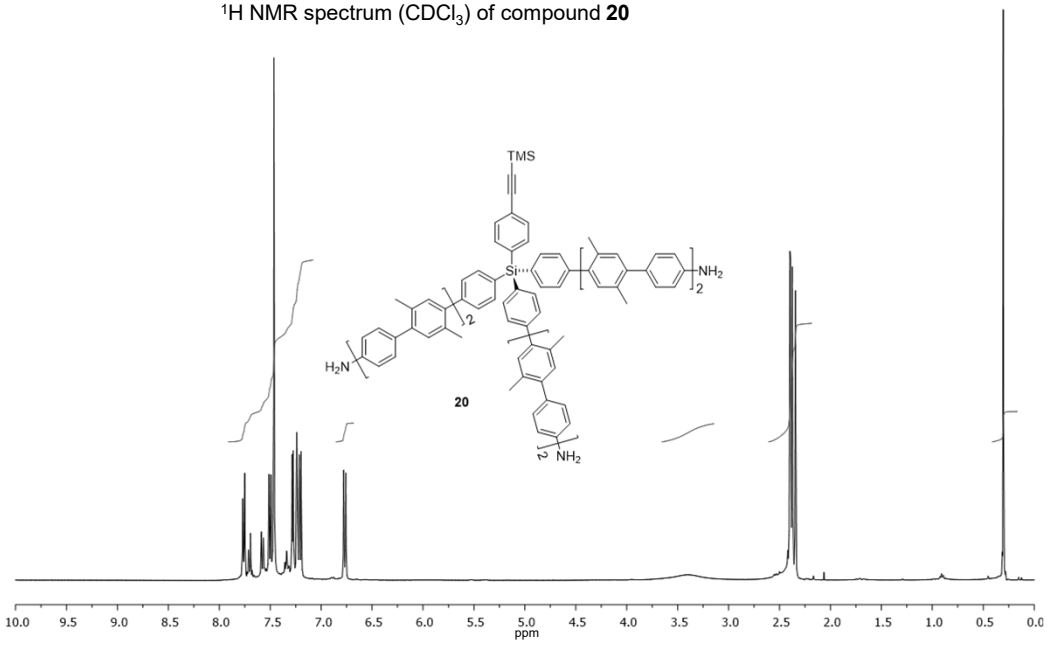

^{13}C NMR spectrum ($CDCl_3$) of compound **20**

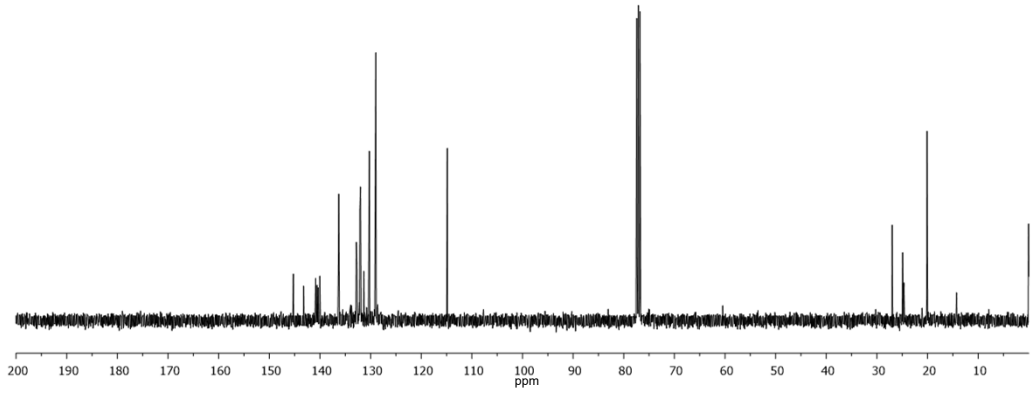

^{1}H NMR spectrum ($CDCl_3$) of compound **21**

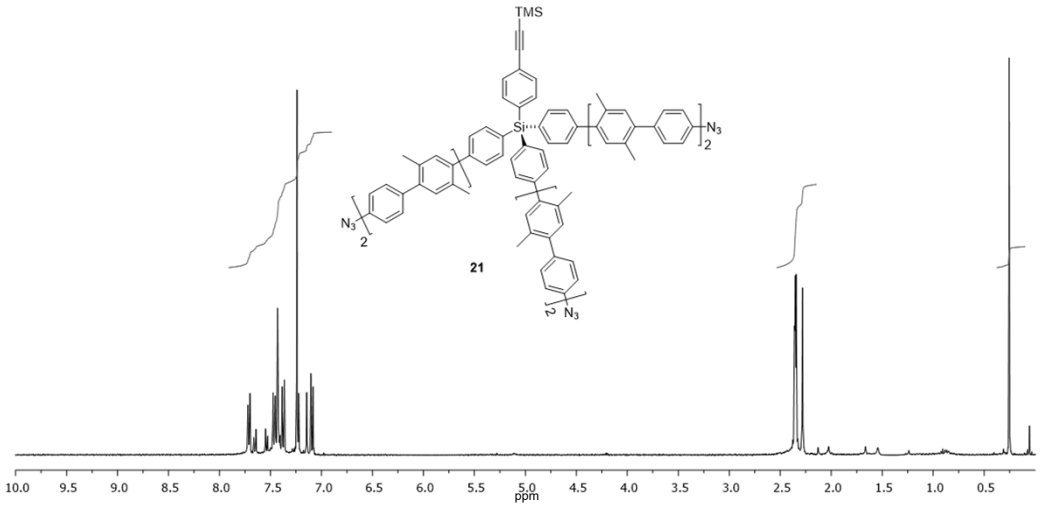

^{13}C NMR spectrum ($CDCl_3$) of compound **21**

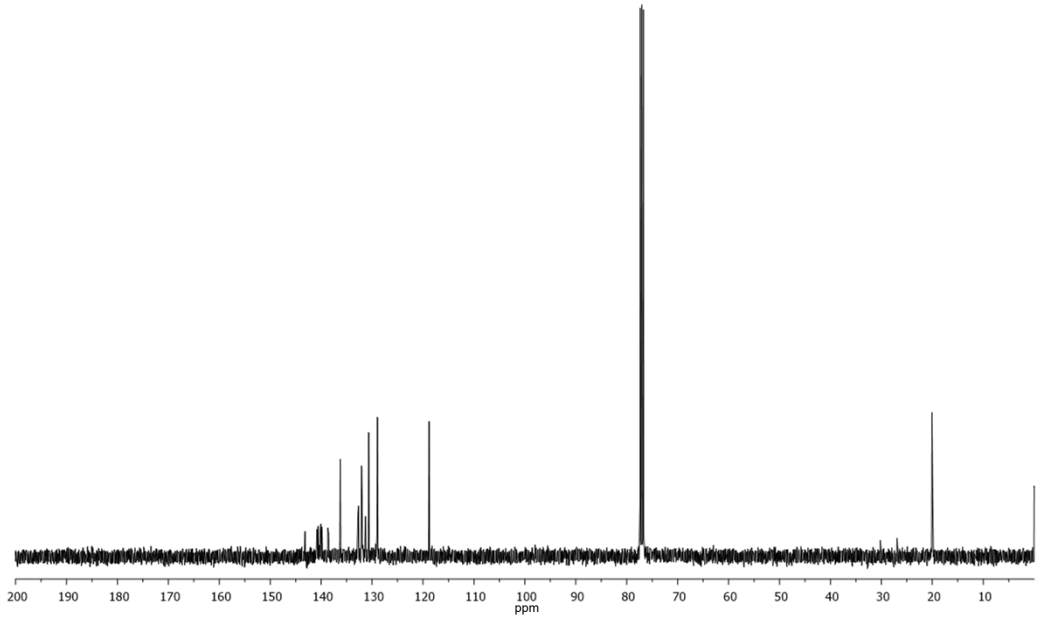

^{1}H NMR spectrum ($CDCl_3$) of compound **24**

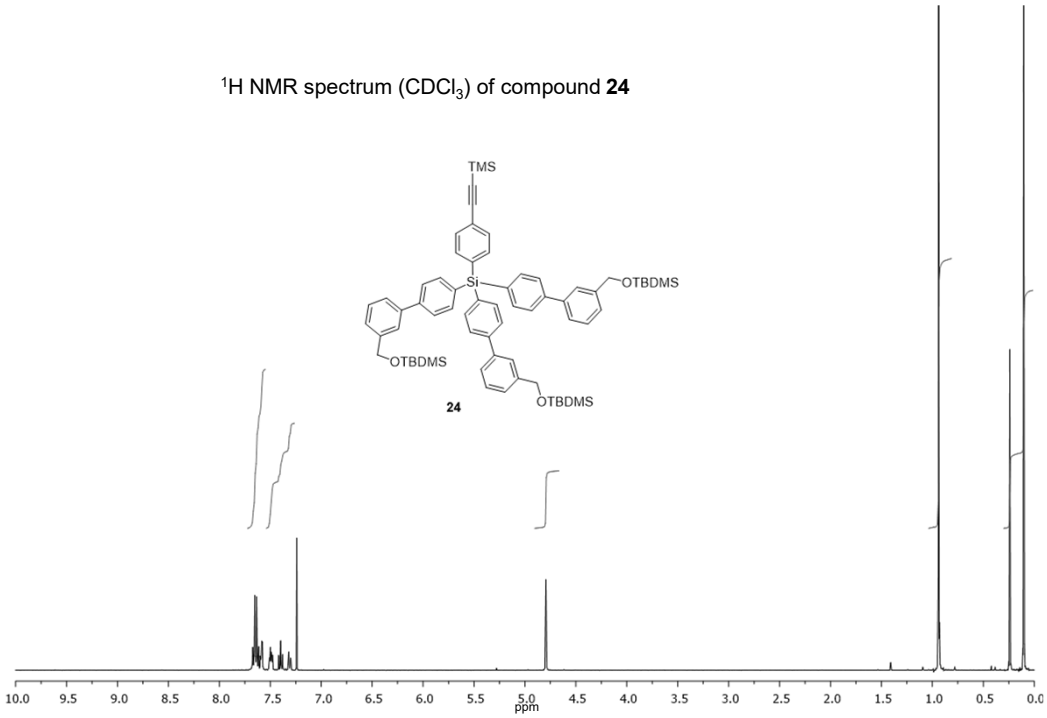

^{13}C NMR spectrum ($CDCl_3$) of compound **24**

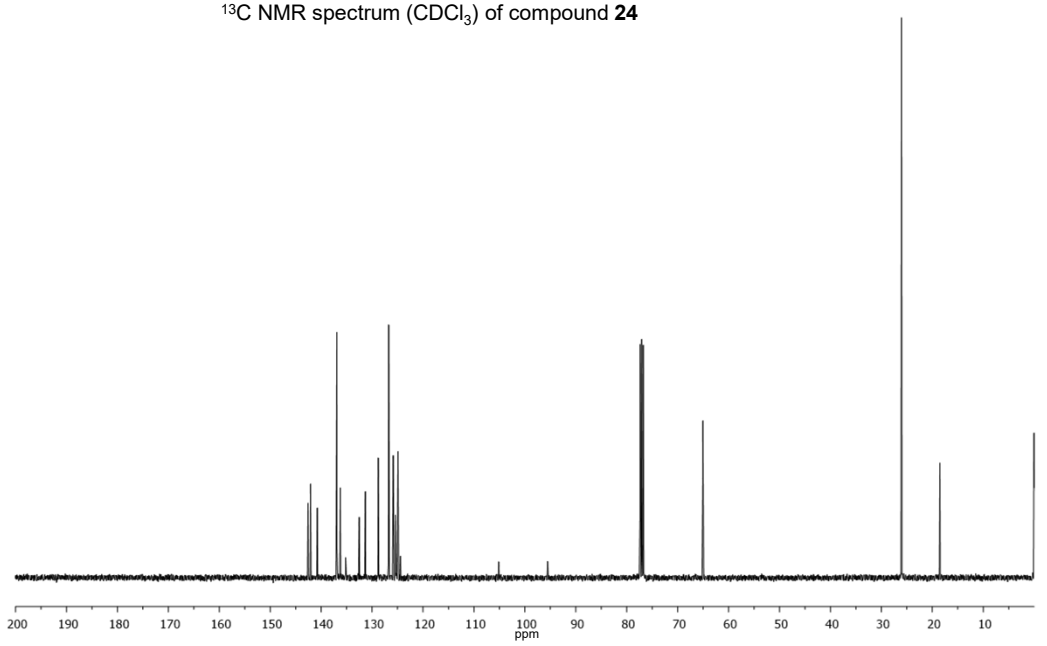

^{1}H NMR spectrum ($CDCl_3$) of compound **25**

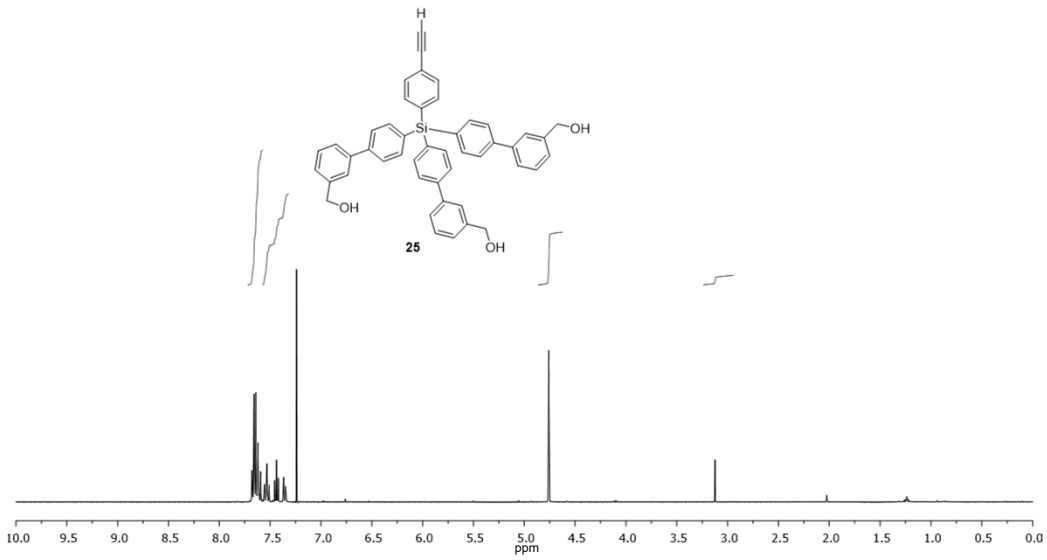

^{13}C NMR spectrum ($CDCl_3$) of compound **25**

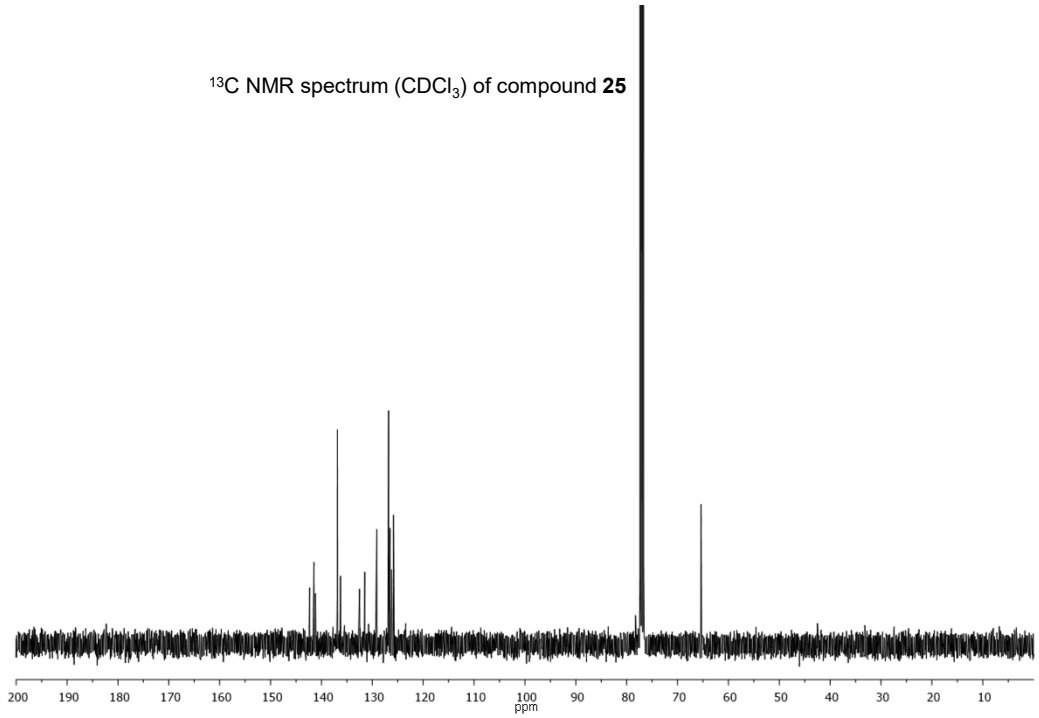

^{1}H NMR spectrum ($CDCl_3$) of compound **26**

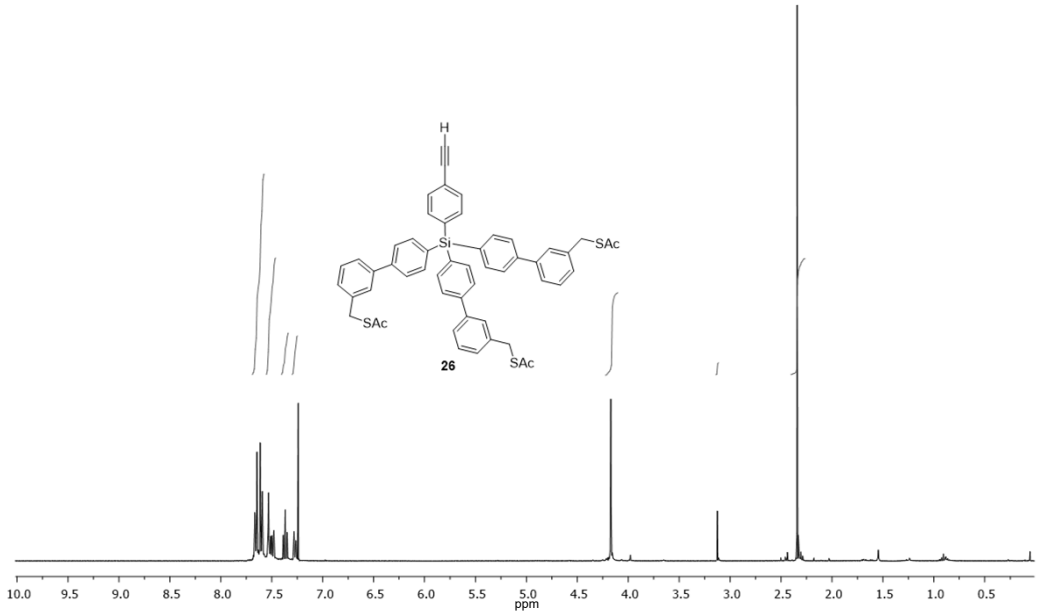

^{13}C NMR spectrum ($CDCl_3$) of compound **26**

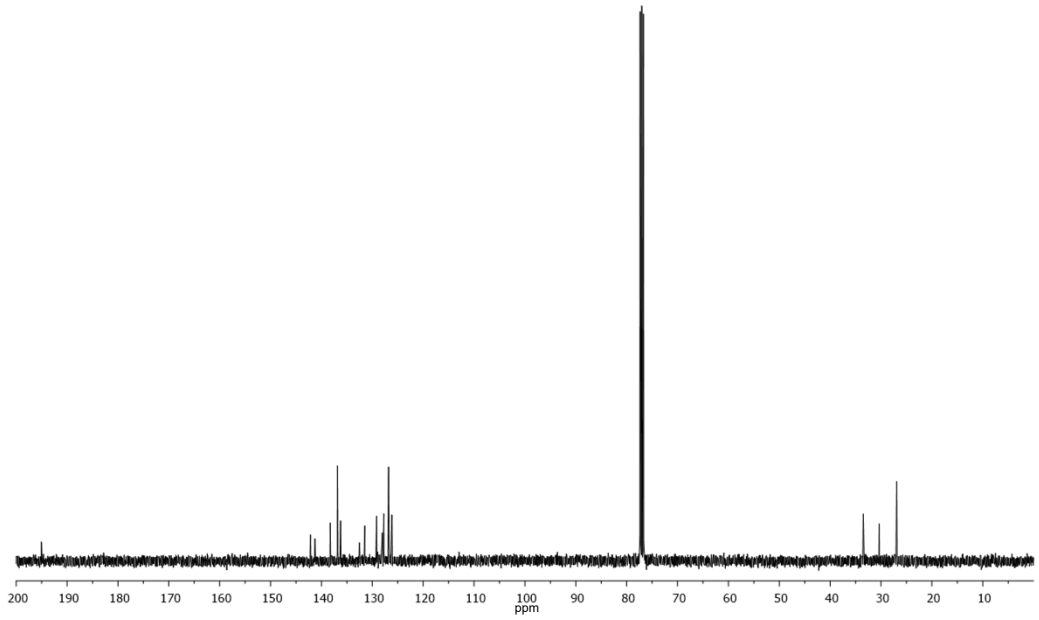

^{1}H NMR spectrum ($CDCl_3$) of compound **27**

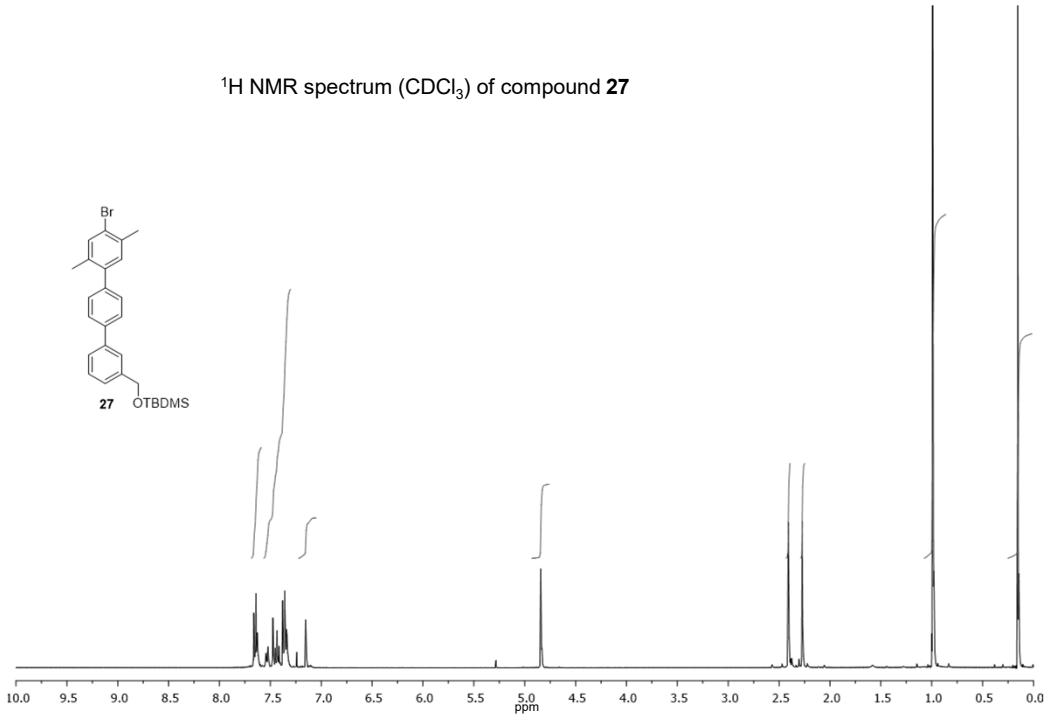

^{13}C NMR spectrum ($CDCl_3$) of compound **27**

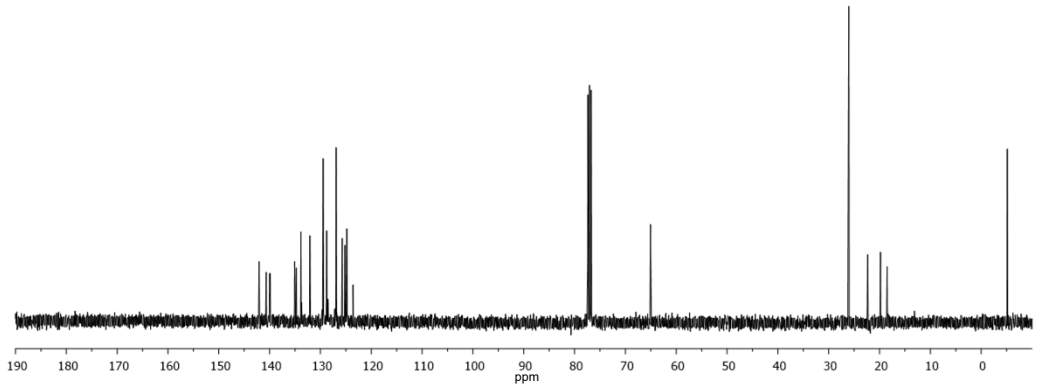

^{1}H NMR spectrum ($CDCl_3$) of compound **28**

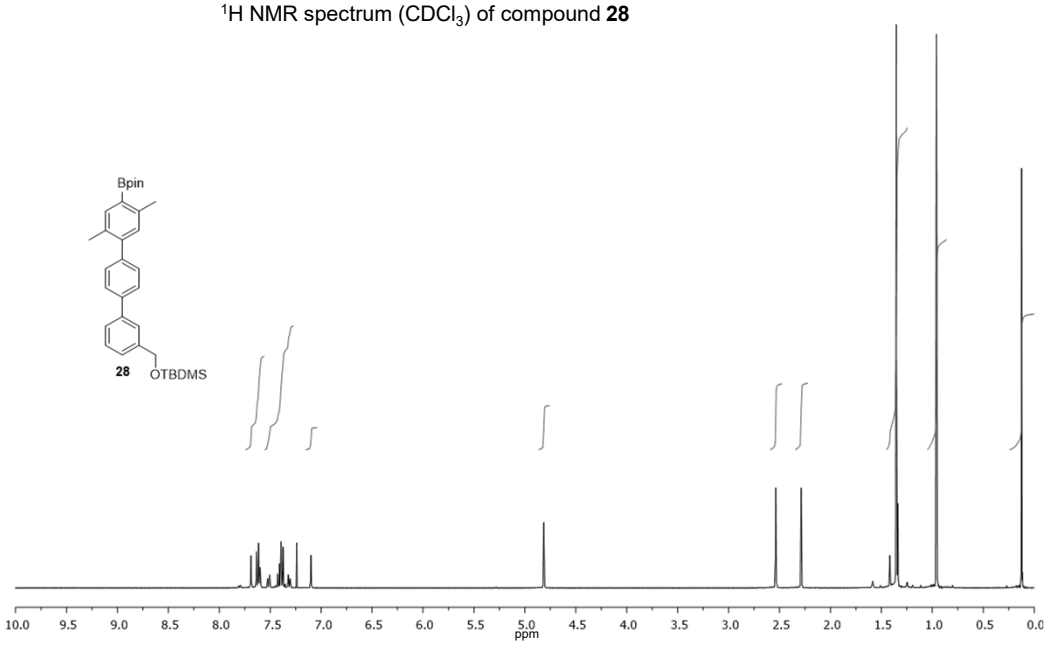

^{13}C NMR spectrum ($CDCl_3$) of compound **28**

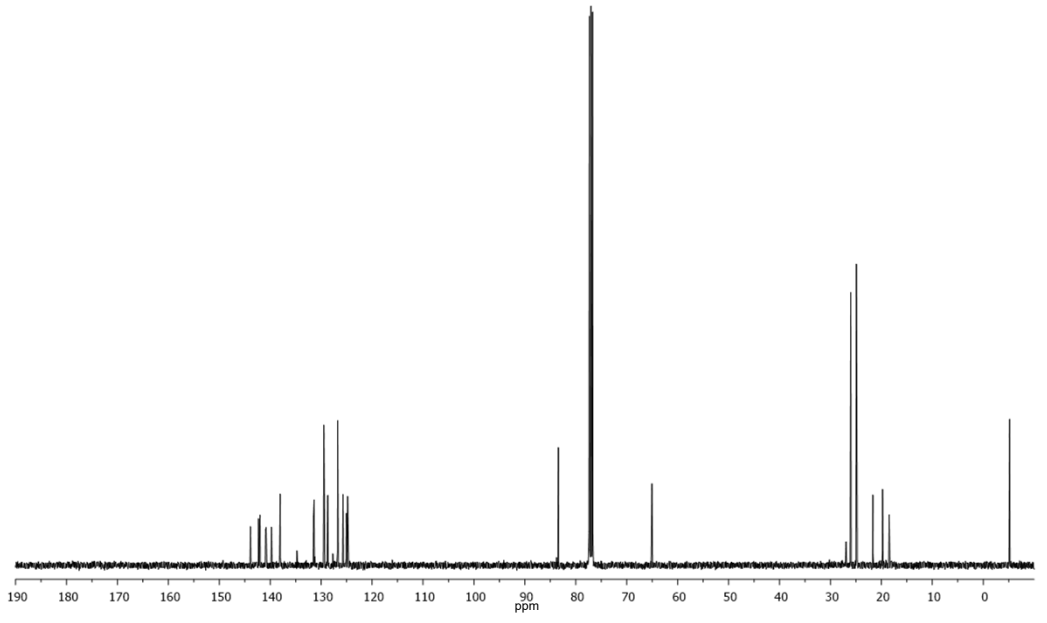

^{1}H NMR spectrum ($CDCl_3$) of compound **29**

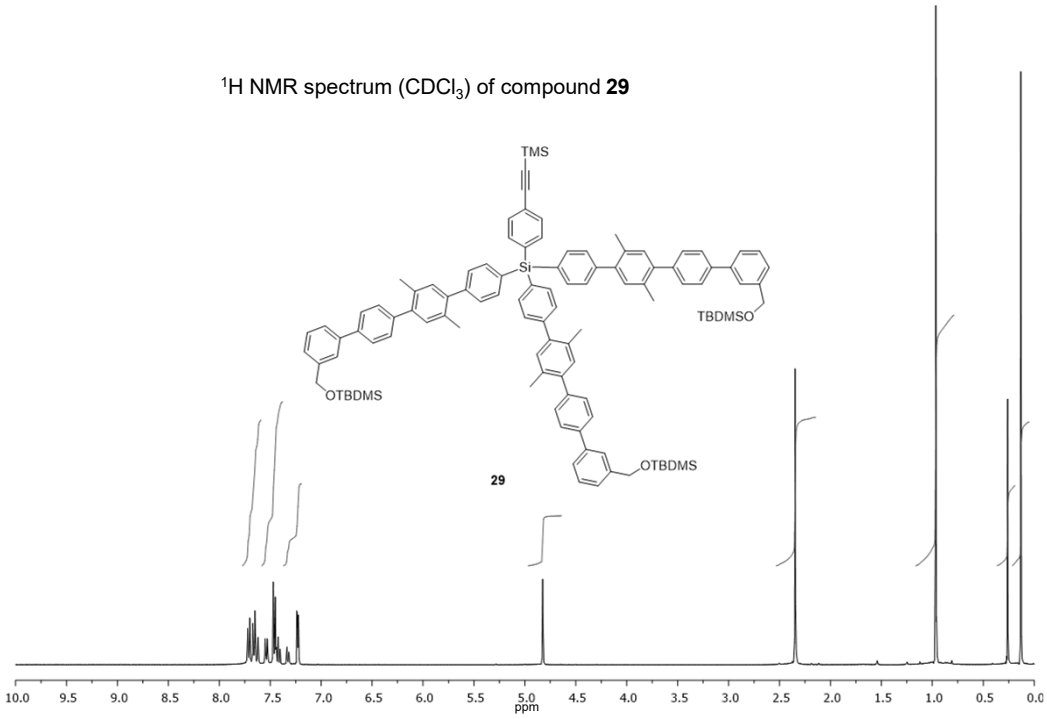

^{13}C NMR spectrum ($CDCl_3$) of compound **29**

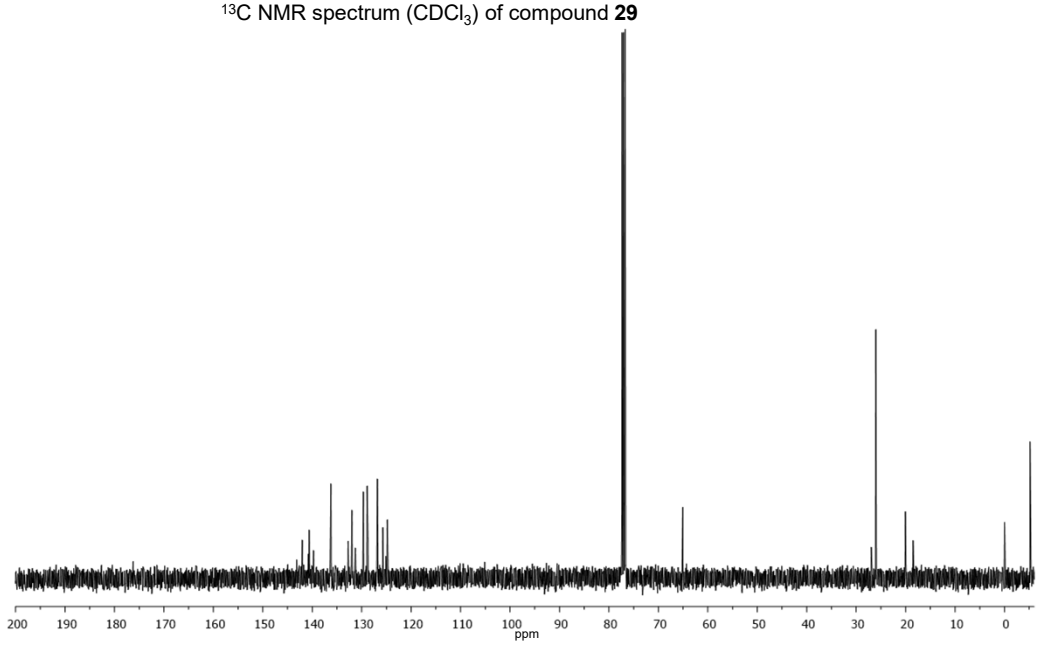

^{1}H NMR spectum ($CDCl_3$) of compound **30**

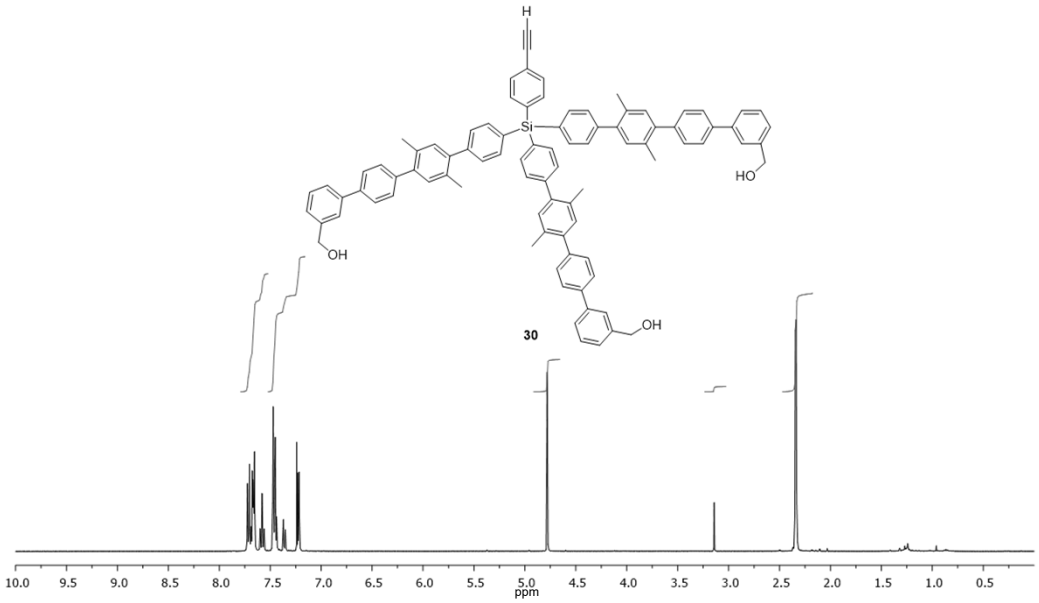

^{13}C NMR spectrum ($CDCl_3$) of compound **30**

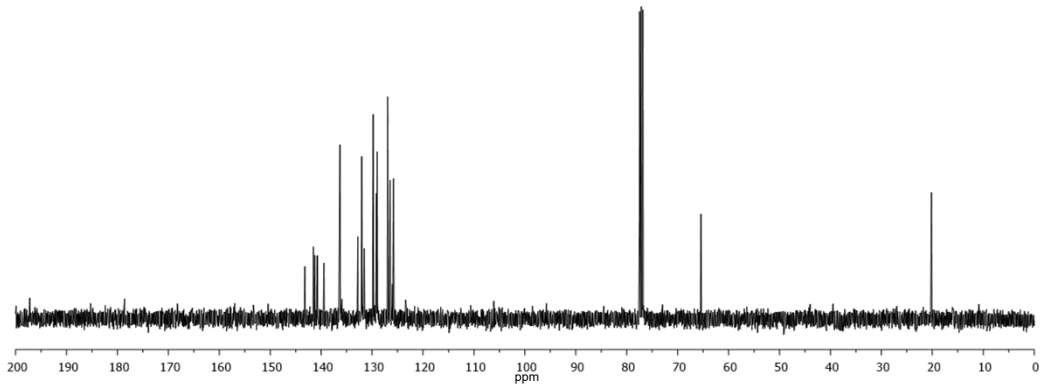

^{1}H NMR spectrum ($CDCl_3$) of compound **31**

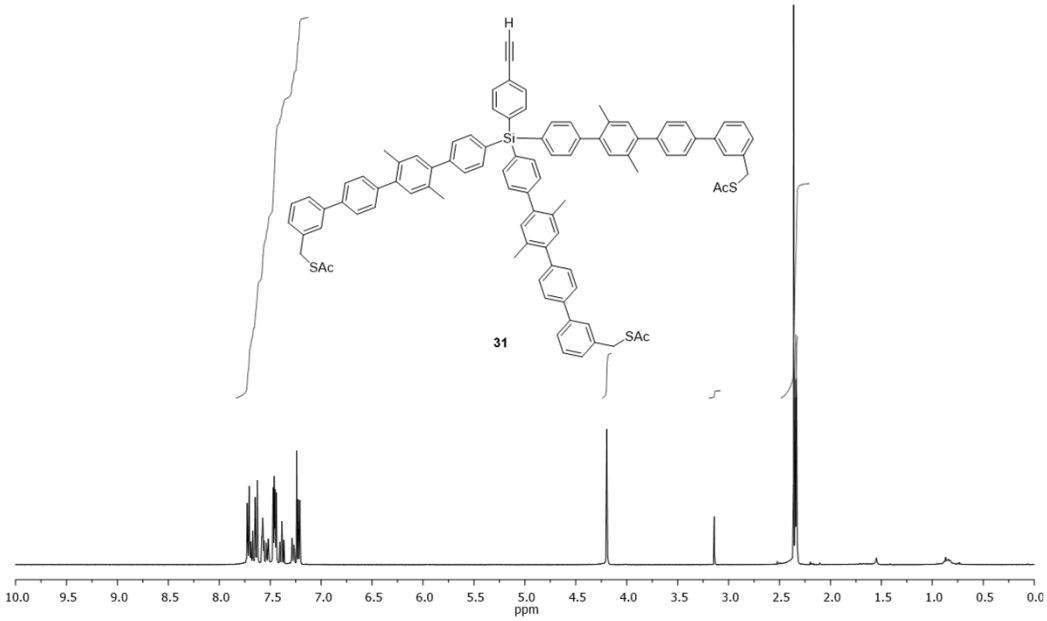

^{13}C NMR spectrum ($CDCl_3$) of compound **31**

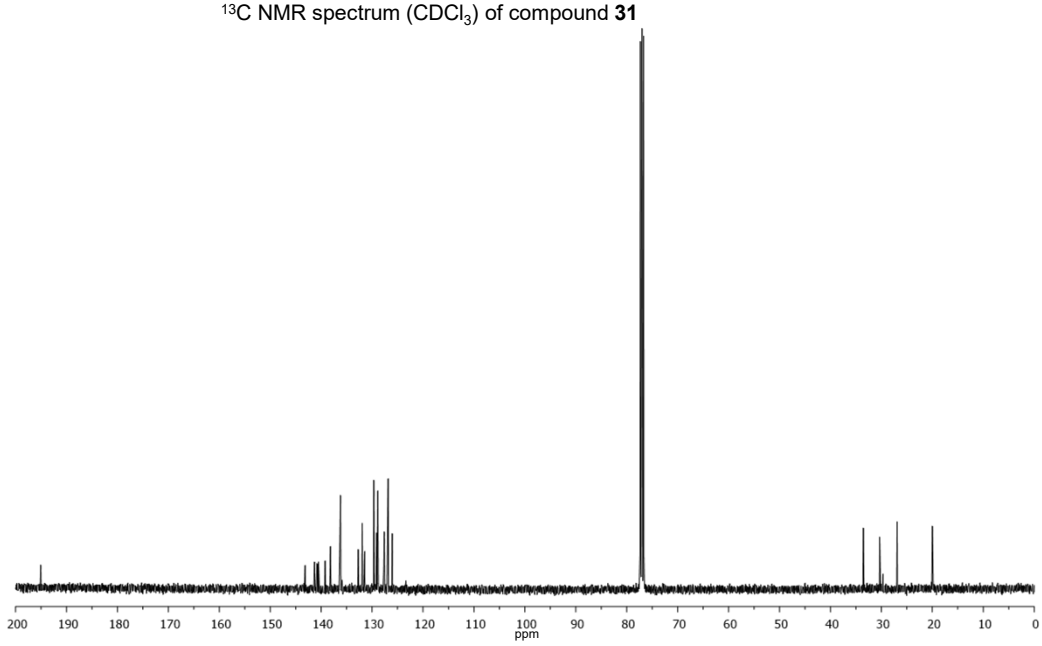

^{1}H NMR spectrum ($CDCl_3$) of compound **32**

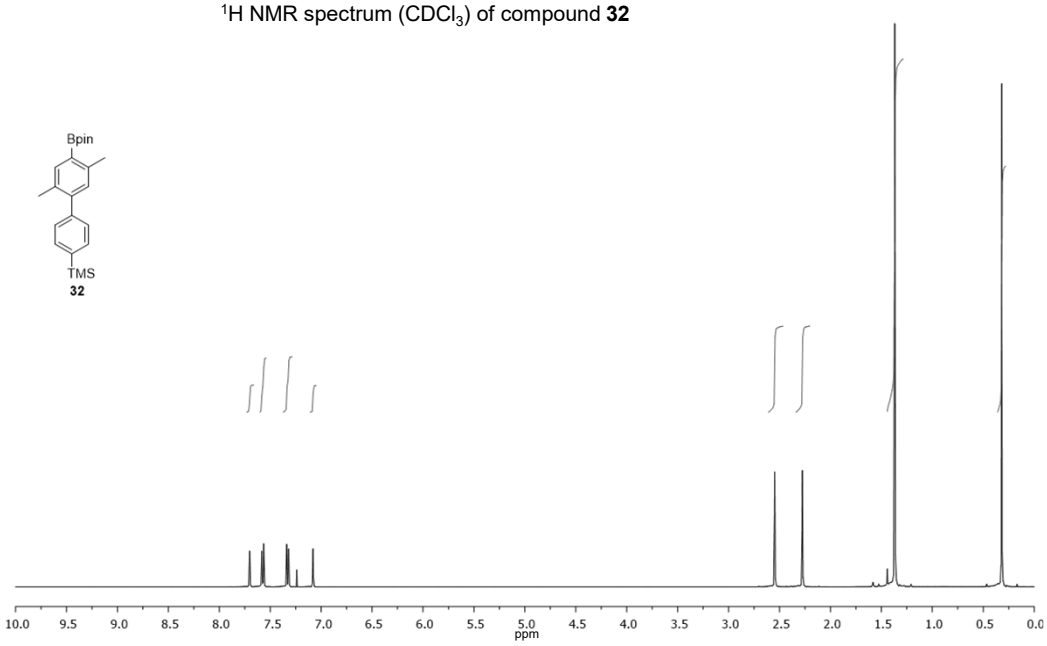

^{13}C NMR spectrum ($CDCl_3$) of compound **32**

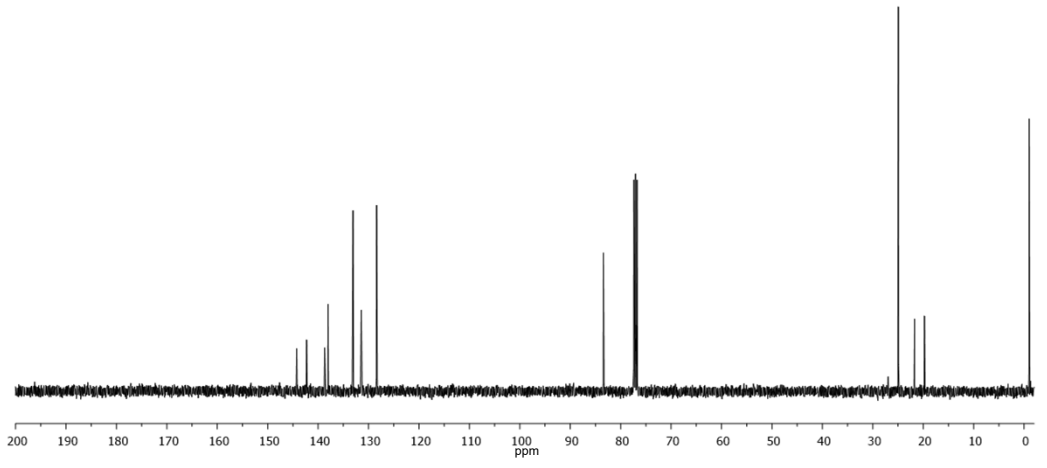

^{1}H NMR spectrum ($CDCl_3$) of compound **33**

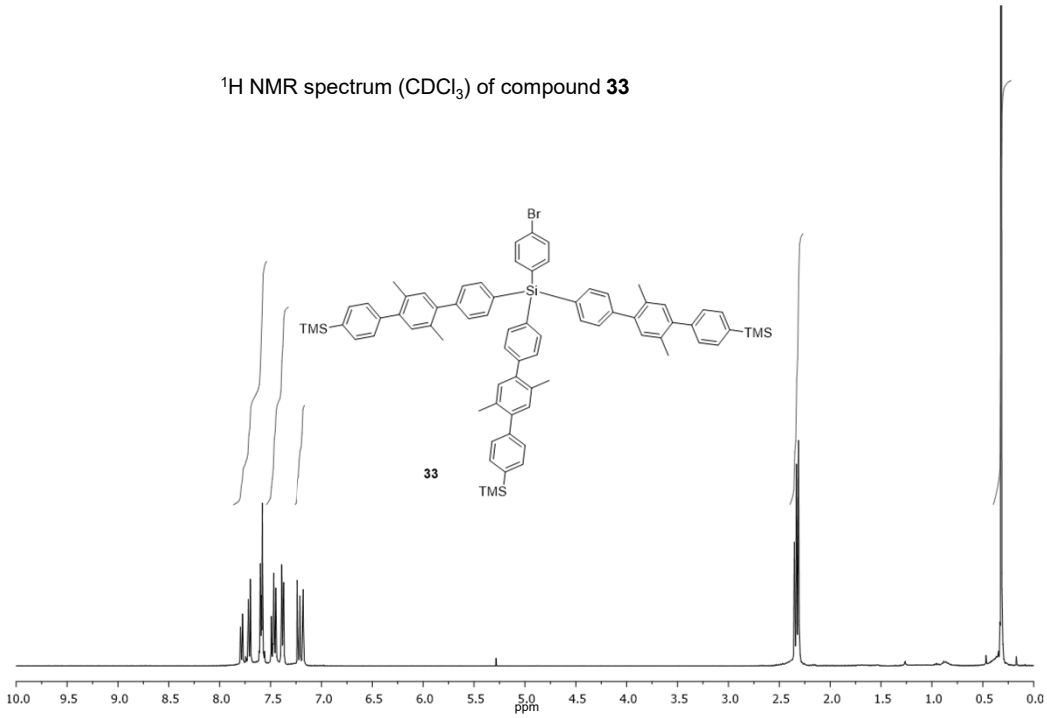

^{13}C NMR spectrum ($CDCl_3$) of compound **33**

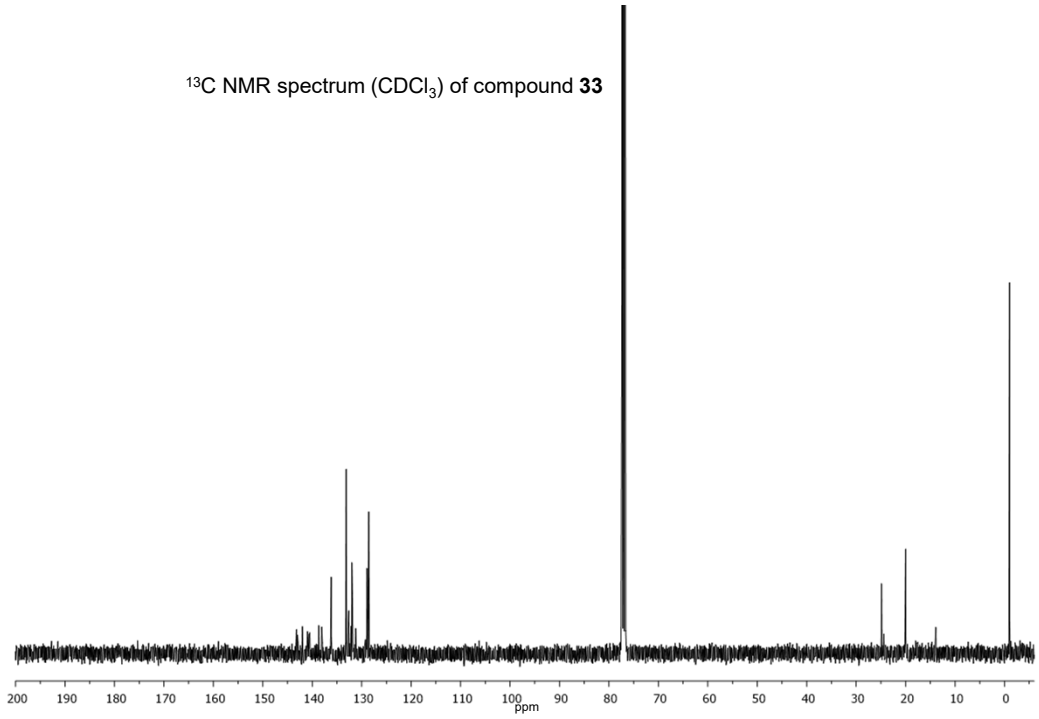

^{1}H NMR spectrum ($CDCl_3$) of compound **34**

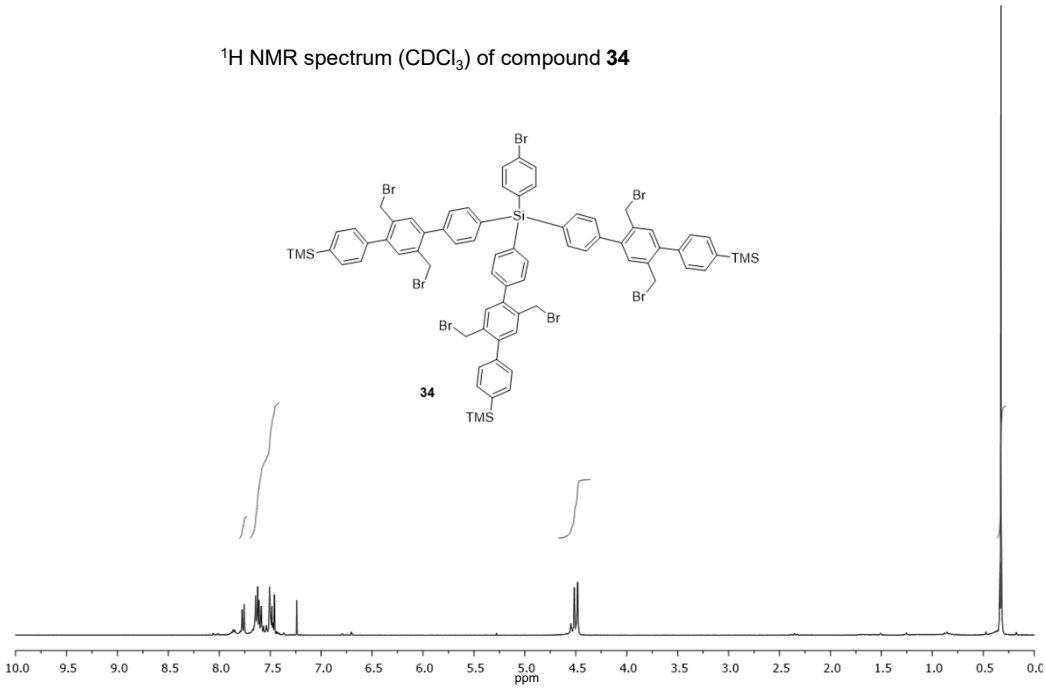

^{13}C NMR spectrum ($CDCl_3$) of compound **34**

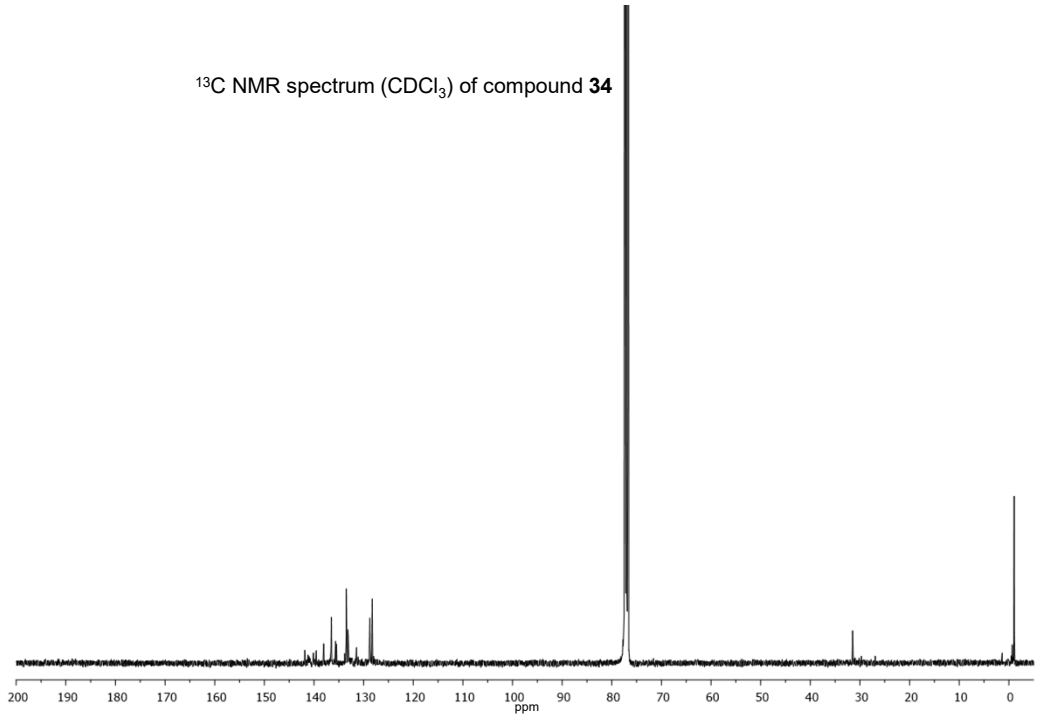

^{1}H NMR spectrum ($CDCl_3$) of compound **35**

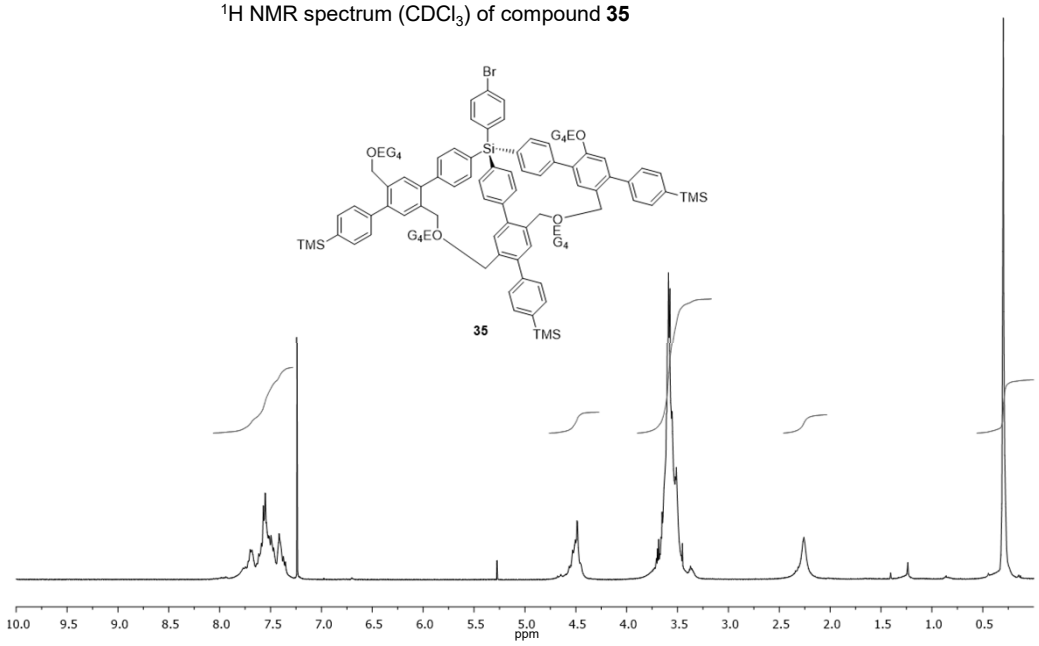

^{13}C NMR spectrum ($CDCl_3$) of compound **35**

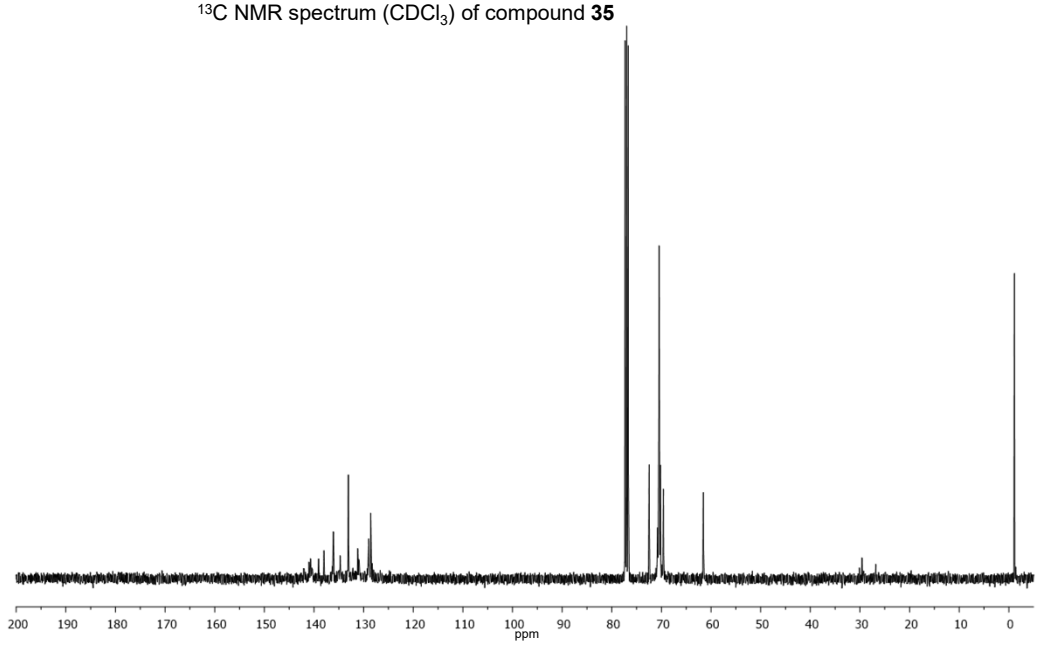

^{1}H NMR spectrum ($CDCl_3$) of compound **36**

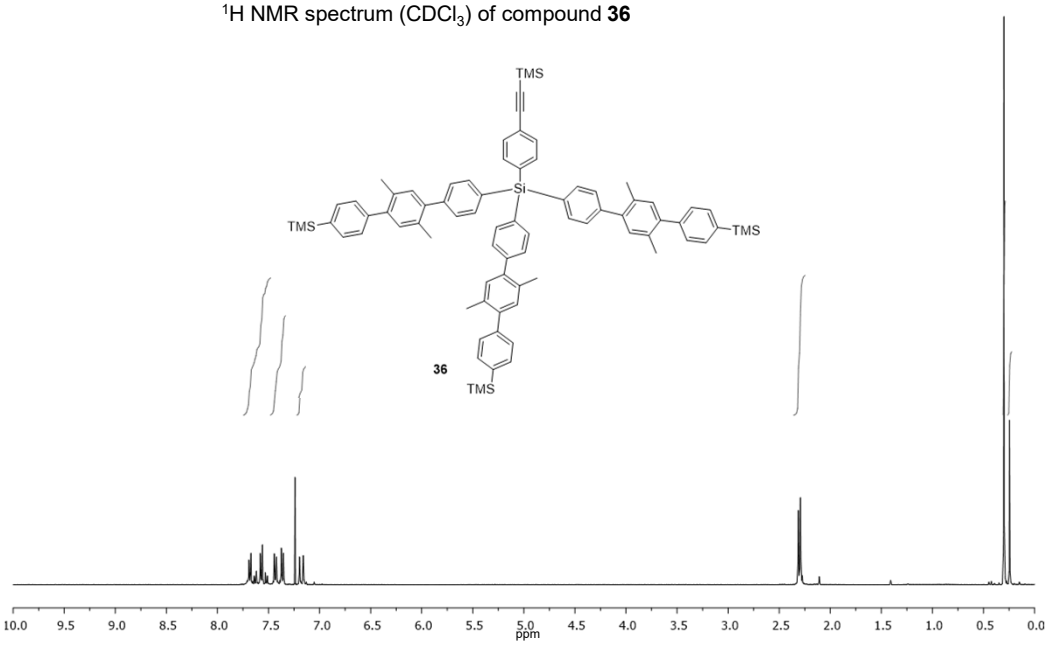

^{13}C NMR spectrum ($CDCl_3$) of compound **36**

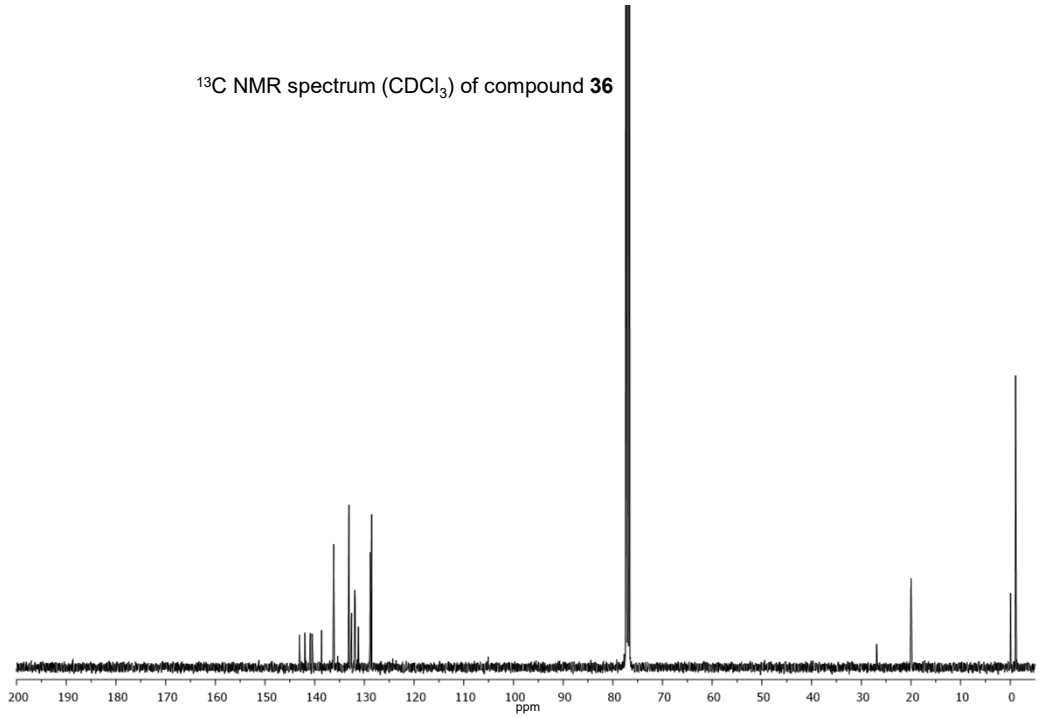

^{1}H NMR spectrum ($CDCl_3$) of compound **37**

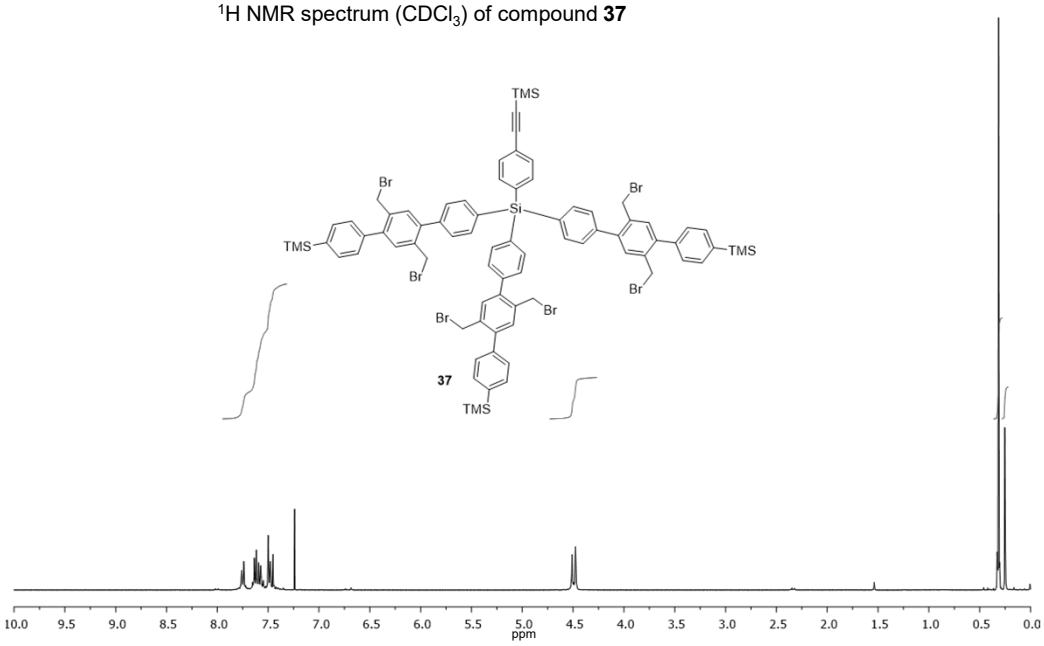

^{13}C NMR spectrum ($CDCl_3$) of compound **37**

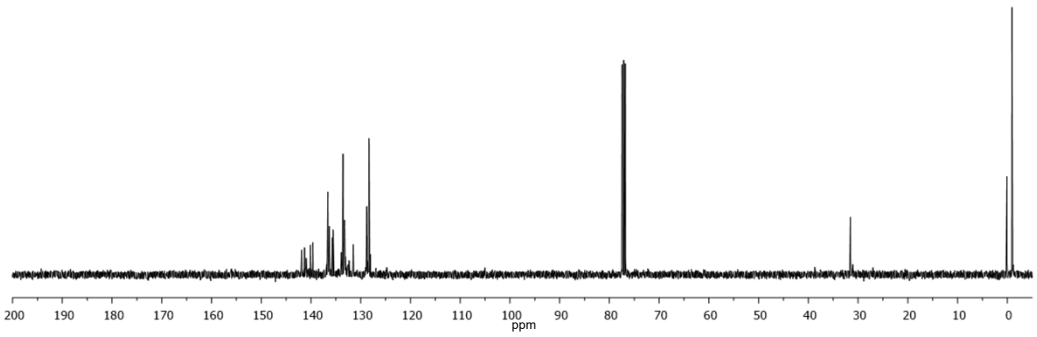

^{1}H NMR spectrum ($CDCl_3$) of compound **38**

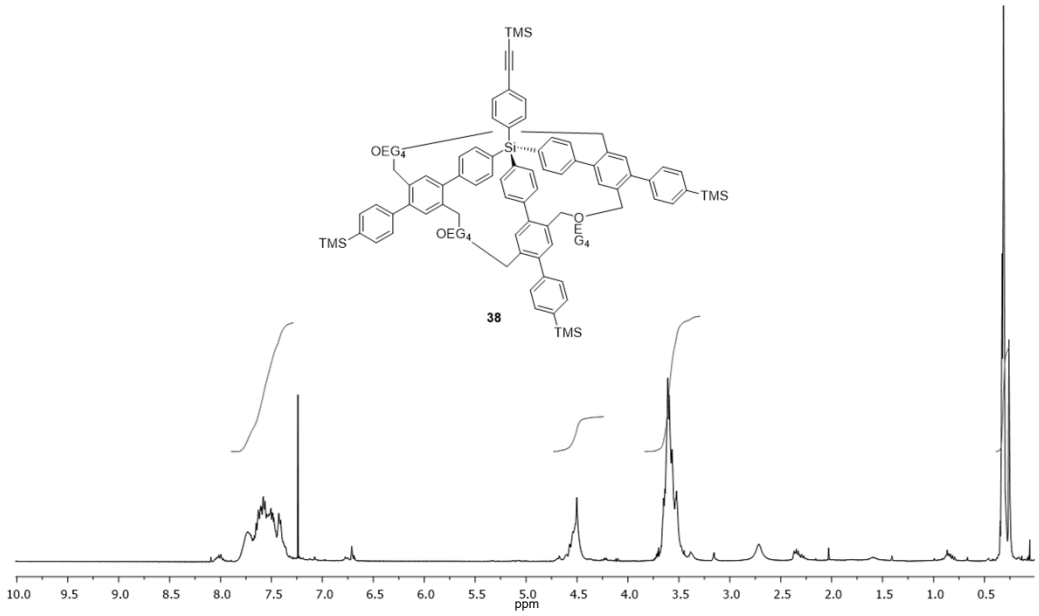

^{13}C NMR spectrum ($CDCl_3$) of compound **38**

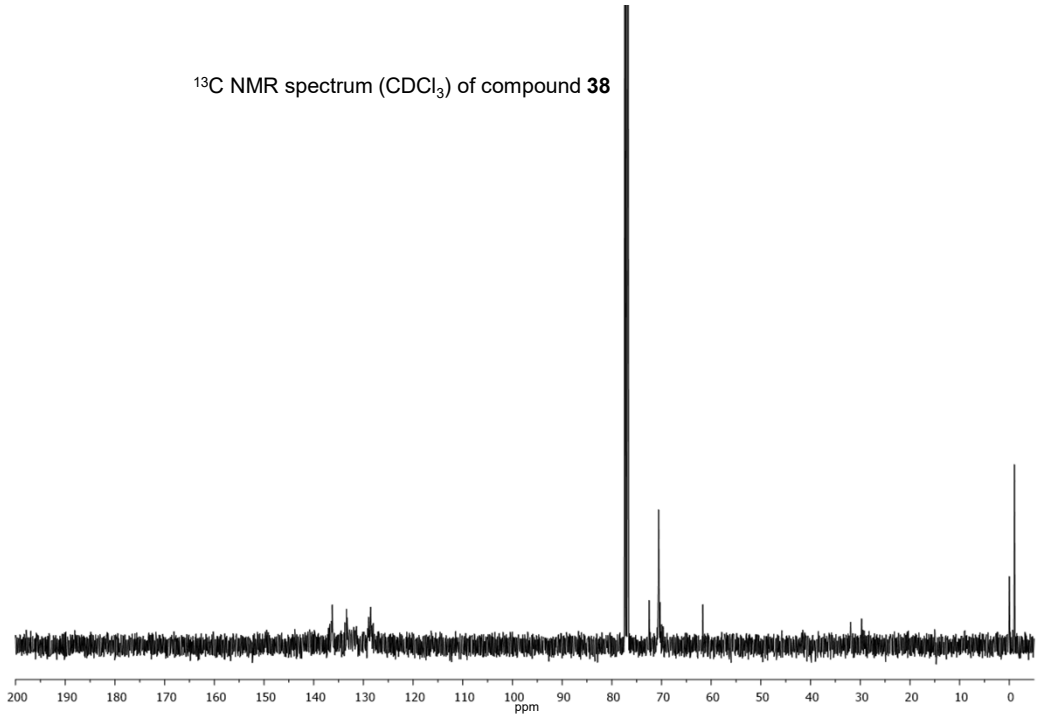

^{1}H NMR spectrum ($CDCl_3$) of compound **40**

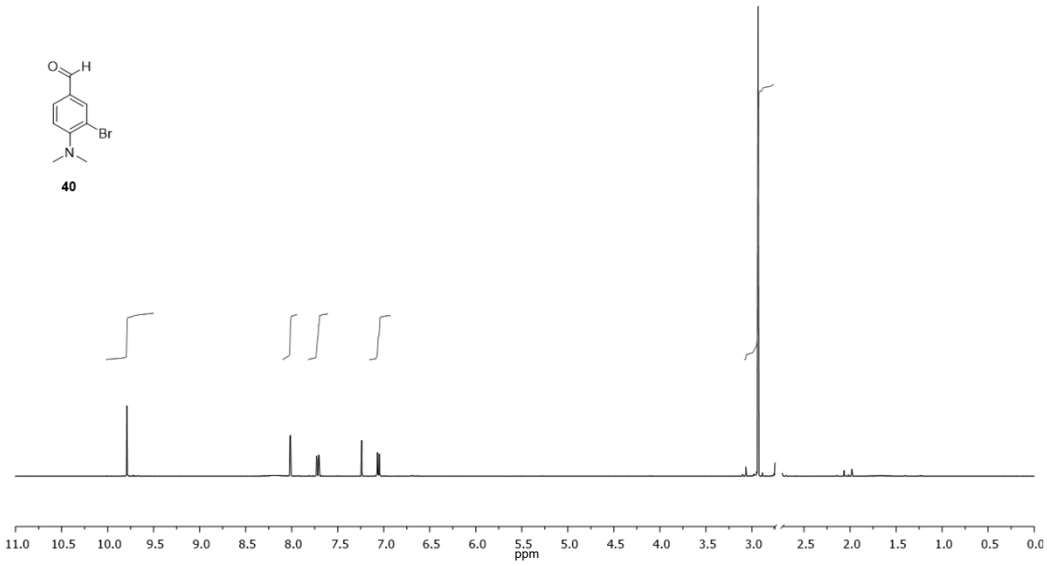

^{13}C NMR spectrum ($CDCl_3$) of compound **40**

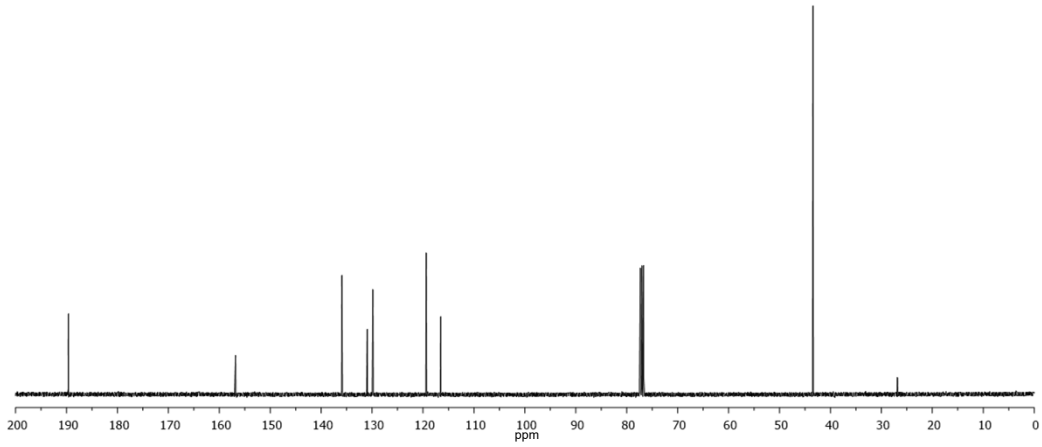

^{1}H NMR spectrum ($CDCl_3$) of compound **41**

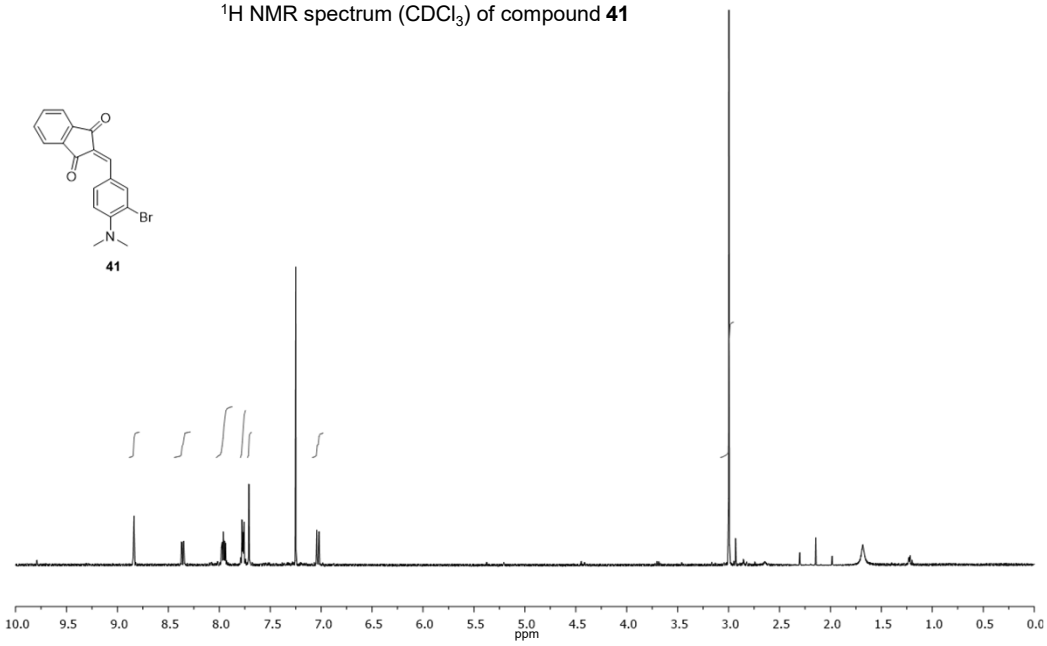

^{13}C NMR spectrum ($CDCl_3$) of compound **41**

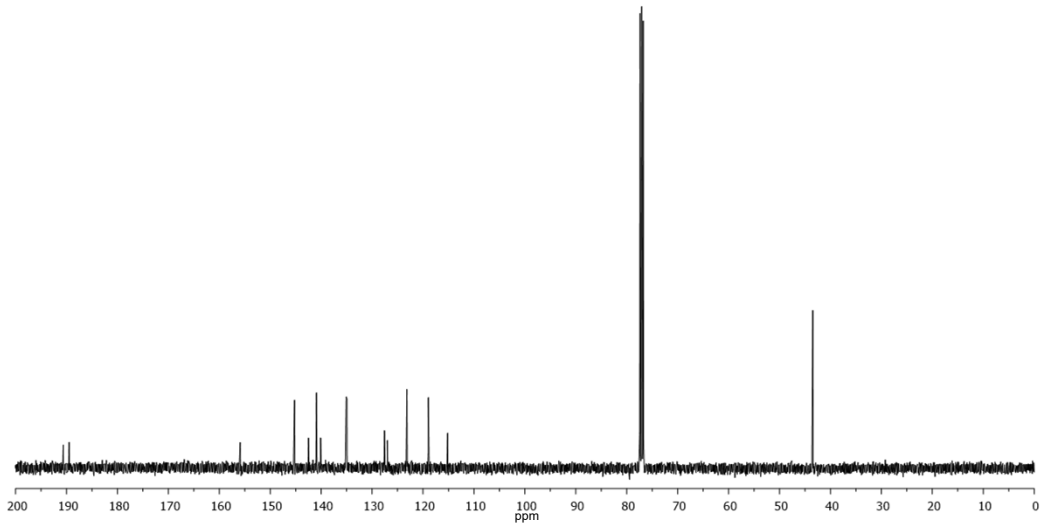

^{1}H NMR spectrum ($CDCl_3$) of compound **44**

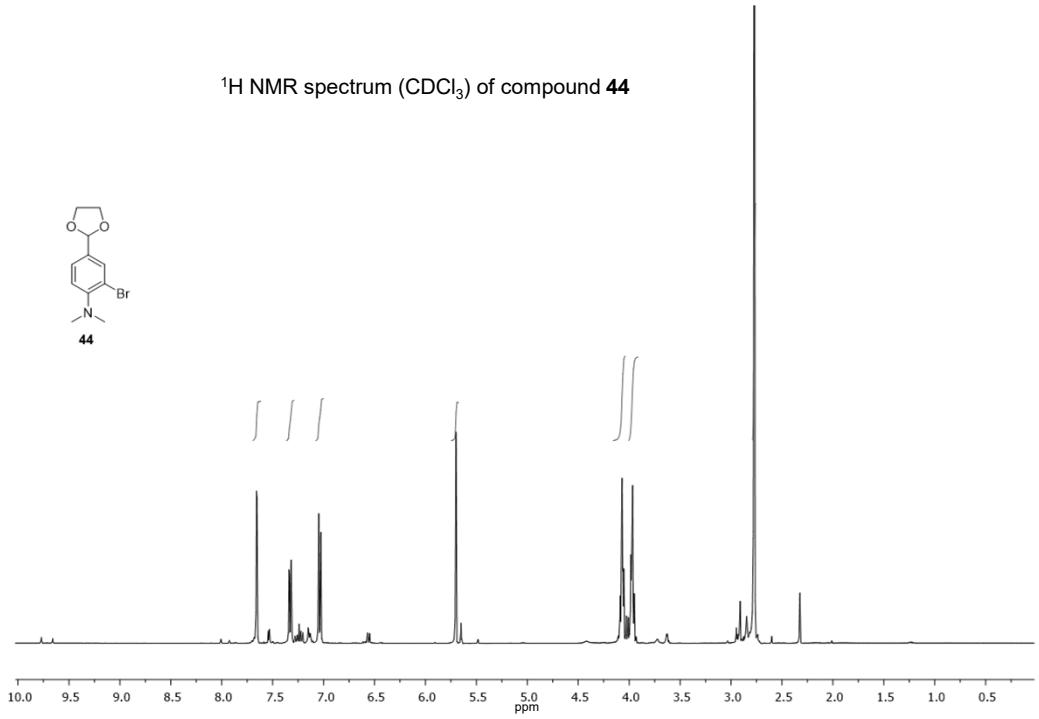

^{13}C NMR spectrum ($CDCl_3$) of compound **44**

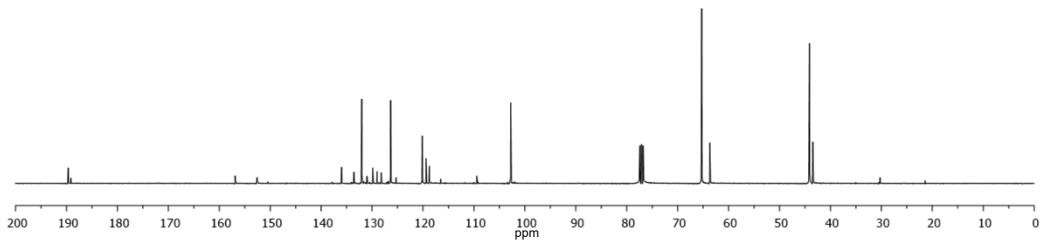

^{1}H NMR spectrum ($CDCl_3$) of compound **46**

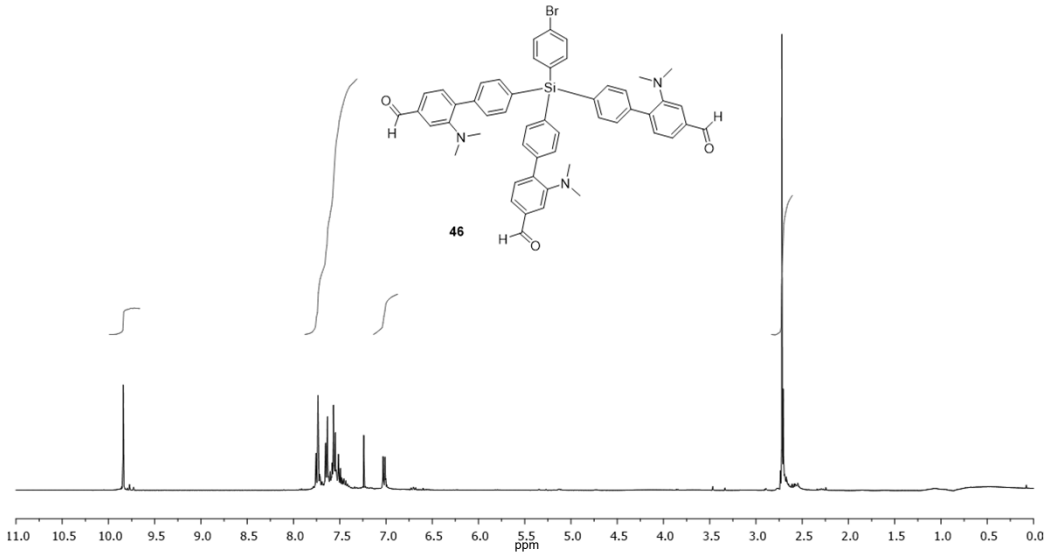

^{13}C NMR spectrum ($CDCl_3$) of compound **46**

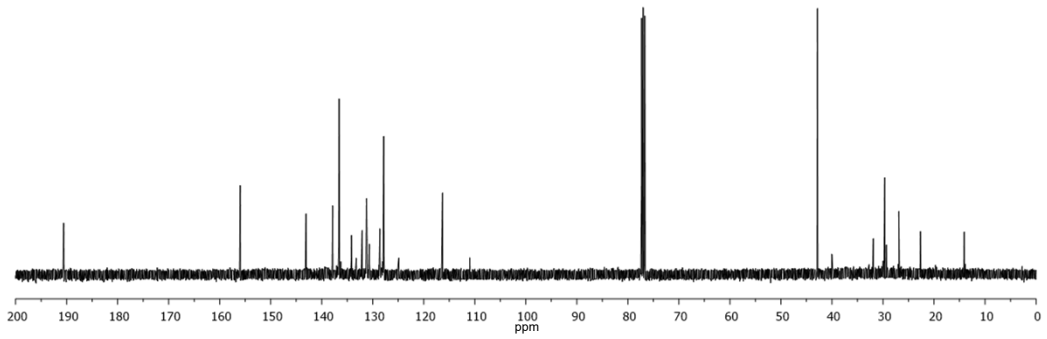

^{1}H NMR spectrum ($CDCl_3$) of compound **47**

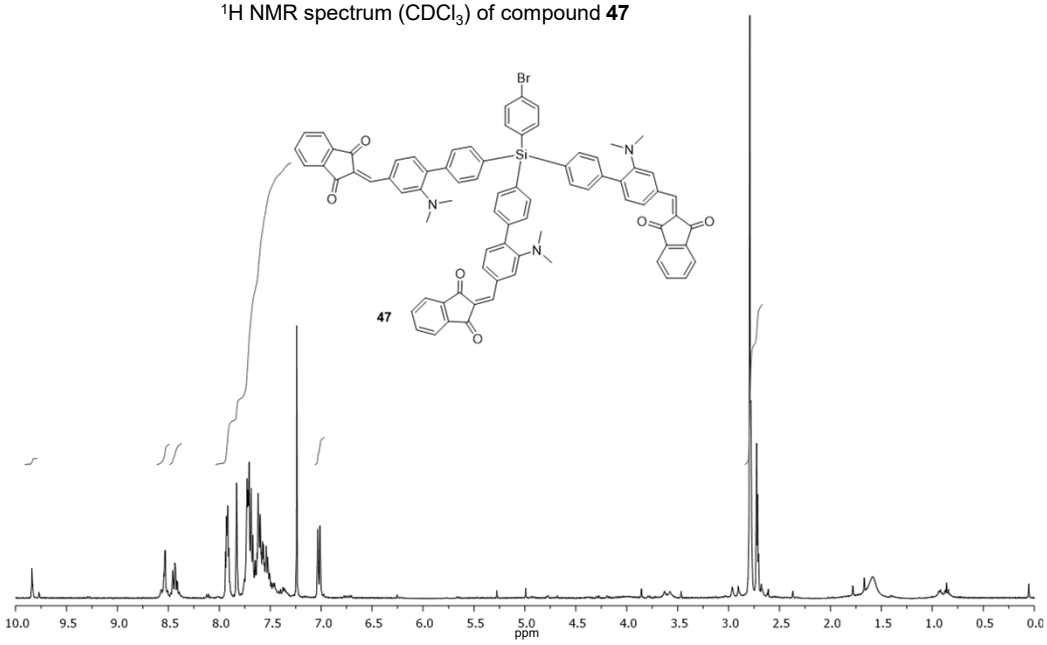

^{13}C NMR spectrum ($CDCl_3$) of compound **47**